8404561

Manesh, Abdulkarim Nick

STABILITY OF THE WORKING HIGHWALL IN A STRIP MINING OPERATION AND COMPARISON OF THE FAILURE IN A PHYSICAL MODEL WITH THAT OF A TWO-DIMENSIONAL FINITE ELEMENT ANALYSIS

The University of Oklahoma PH.D. 1983

University
Microfilms
International 300 N. Zeeb Road, Ann Arbor, MI 48106

PLEASE NOTE:

In all cases this material has been filmed in the best possible way from the available copy. Problems encountered with this document have been identified here with a check mark __√__.

1. Glossy photographs or pages _____
2. Colored illustrations, paper or print _____
3. Photographs with dark background __√__
4. Illustrations are poor copy _____
5. Pages with black marks, not original copy _____
6. Print shows through as there is text on both sides of page _____
7. Indistinct, broken or small print on several pages __√__
8. Print exceeds margin requirements _____
9. Tightly bound copy with print lost in spine _____
10. Computer printout pages with indistinct print _____
11. Page(s) __________ lacking when material received, and not available from school or author.
12. Page(s) __________ seem to be missing in numbering only as text follows.
13. Two pages numbered __________. Text follows.
14. Curling and wrinkled pages _____
15. Other ____

THE UNIVERSITY OF OKLAHOMA

GRADUATE COLLEGE

STABILITY OF THE WORKING HIGHWALL IN A STRIP MINING OPERATION AND COMPARISON OF THE FAILURE IN A PHYSICAL MODEL WITH THAT OF A TWO-DIMENSIONAL FINITE ELEMENT ANALYSIS

A DISSERTATION
SUBMITTED TO THE GRADUATE FACULTY
IN PARTIAL FULFILLMENT OF THE
REQUIREMENTS FOR THE
DEGREE OF
DOCTOR OF PHILOSOPHY

BY

ABDULKARIM NICK MANESH
NORMAN, OKLAHOMA

1983

STABILITY OF THE WORKING HIGHWALL IN A STRIP MINING OPERATION AND COMPARISON OF THE FAILURE IN A PHYSICAL MODEL WITH THAT OF A TWO-DIMENSIONAL FINITE ELEMENT ANALYSIS

A DISSERTATION

APPROVED FOR THE SCHOOL OF PETROLEUM AND GEOLOGICAL ENGINEERING

APPROVED BY

DISSERTATION COMMITTEE

ACKNOWLEDGEMENT

I owe much to my chairman, John D. Morris, who by his own example has shown the virtue of being honest in one's thinking, of clearly saying what you mean, and of giving argument for it. Of course, I alone am finally responsible for any wrong paths I may have taken.

I sincerely wish to thank the members of my dissertation committee at the University of Oklahoma, Dr. Jimmy Harp, Dr. Roy Knapp, Dr. Ronald Evans, Dr. Faruk Civan, and Dr. Luther White, for their continued support and encouragement while writing this paper, and to Dr. Thomas Murray for use of the equipment in Fears Structural Lab which was under his oversight.

I wish also to acknowledge Mr. Robert Arndt and Mrs. Gwen Williamson of the Oklahoma Mining and Mineral Resources Research Instiute for financial support to complete this project.

I would also like to thank my typist, Mrs. Norma Harris, for her skill and efficiency and for the deadlines she helped me to make even at the expense of her other obligations.

Perhaps, most importantly, I am indebted to my father, Ali, who left this world before witnessing this fruit of his struggle. And to my respected mother, Many, my wife Laila and my children Parjack and Parnian, who so lovingly and patiently waited, to them I owe more than I know to say.

TABLE OF CONTENTS

LIST OF FIGURES

LIST OF TABLES

ABSTRACT

This study is comprised of an analysis of slope stability in strip mines using a finite element model as well as a physical model. The physical model was designed to simulate typical rather than specific strip mine conditions in Oklahoma. The study includes the selection of the physical model material and the design of the loading apparatus based on dimensional analysis. The failure surface geometry and front surface displacements of the model when loaded were studied and comparisons have been made between the test results. The displacements represent the initial movement of the slope. It was found that the slope remains stable unless a failure surface appears which intersects the plane of weakness. In order to numerically model typical conditions in a strip mine, a two-dimensional plane strain analysis employing the finite element method was used and a simplified method for strip mine stability has been developed. The results obtained from this method were compared to the physical model. The failure surface geometry and the front surface displacement followed a pattern similar to that obtained by the experimental investigation.

Chapter 1

INTRODUCTION

1.1 Nature of the Problem

Oklahoma coal resourses have been estimated to be greater than seven billion short tons (Friedman, 1976). The coal deposits are primarily located in eastern Oklahoma and due to their shallow depth the extration is almost exclusively by surface mining methods.

The strip mining of Oklahoma coals continues to be of signficant interest. As with all forms of energy, the cost of coal is rising, and with that rise, deeper, less accessible coal deposits can be excavated. However, with the need for deeper strip mines comes an increased need for the understanding of slope stability and safety in order for mining to be economic. Because of the uncertainties and heterogeneties that exist in rock masses it is necessary to rely upon large facotrs of safety.

Traditional methods for the study of slope stability have been applied to caol mining operations similar to those in Oklahoma. In particular, the "equilibrium mehtod", which applies to consolidated and unconsolidated soil, has found some application. But it has been known since 1965 that "equilibrium mehtods" do not accurately model real physical situation in areas of overconsolidated and brittle rocks. Recently developed numerical techniques are capable of handling the problem but as yet have not been successfully applied to coal mines.

1.2 Approach to the Problem

The present study in an application of a geomechanical model and analytical procedure. The approach taken in the experimental work involves (1) development of a model material, (2) design and construction of the model based on dimensional analysis, (3) selection of the loading apparatus, (4) development of instrumentation, (5) loading of the model to failure, (6) analysis and discussion of the test results.

Before any model tests were conducted, a series of unconfined compressive strength tests were made on the model material in order to establish its mechanical properties. All model tests in this study were conducted using the same model material.

Several tests with different compressive strengths for the rock and the slope angles have been applied. The variables investigated in the study were face displacement of the slope, failure surface geometry, and surface distributed loading rate as a drag line load or other overburden geological loadings on the top of the working highwall. All model tests were loaded incrementally to failure and the failure surface for each test determined.

In the numerical part, the finite element method has been applied in order to predict stresses and displacements within a slope of a strip mine. The problem is analysed using two dimensional plane strain and assuming homogenous, isotropic, linear material properties.

1.3 Objective of the Investigation

The main objective of this investigation was to describe the problem of strip mine slope stability throughly, and to define the accuracy of the two-dimensional finite element analysis to determine the displacement pattern in the mass of a strip mine slope, by comparing computer results to the displacement measured in a physical model.

The second objective of this research is to add to the present knowledge of the failure mode and safe design of Oklahoma strip mines. The failure of a slope as a function of compressive strength of rock in a mining region and the geometry of a mine is also investigated. The compressive strength of the model material for each test was adapted based on dimensional analysis to a real rock, in order to establish a support for the finite element analysis.

The simplified approach as based on the finite element analysis will allow design of a safe and economical strip mine cross section without having to run a sophisticated finite element program.

Futhermore, since the failure mode and strength parameters computed from the analytical analysis agree reasonably well with the laboratory tests results, more confidence can be placed in the established approach for the safe design of strip mines in general and Oklahoma coal mines in particular.

1.4 Scope of the Study

In the stability analysis of slopes in soft rocks like the shales of Oklahoma, there are at present two basic lines of approach. The first one is the equilibrium method, which is basically an extension of soil mechanics theory. The second one is stress-strain analysis. The equilibrium method is also capable of predicting the approximate location of the ultimate failure surface, but satisfactory slope design should include magnitude of the displacement as well as failure. It would be desirable, therefore, to analyze the slope for deformation and safety by computing the stresses and displacements within the structure.

The availability of high-speed digital computers and the development of the finite element technique for analysis during the last two decades has made it possible to analyze problems involving much greater degrees of complexity than was formerly possible. Thus it is now feasible to solve slope stability problems involving complex boundary conditions in material with hetrogeneous properties.

The measured variation in displacement along a slope structure provides the engineer with an indication of the range of stress-strain concentrations that develop in a rock slope structure. In addition, in some cases, the strain variations may indicate that failure develops progressively across the slope mass from a particular point to another point.

The method of design used in this study based on finite elements are not only useful in straight forward slope design but also provide a method of solving complicated slope stability problems.

Chapter 2

LITERATURE SEARCH

2.1 Computerized Literary Search

For the purpose of this study a literature survey was performed by an extensive computer search of several pertinent available data bases, namely: NTIS(National Technical Information Service), SSIE(Smithsonian Science Information Exchange), C.D.A.(Comprehensive Dissertation Abstracts),GEOREF (Americal Geological Institute). The search was performed to provide historical literature applicable and pertinent to the problem under consideration. In addition to the computer search, a review of available journals and publication through the Engineering and the Geology Libraries at the University of Oklahoma was conducted.

The search has indicated that no strip mine slope stability studies have been conducted in the past which include both experimental and analytical approaches together, nor have efforts been made to prepare "a general design approach" based on finite element analysis.

There are some marginal studies that are related to the topic addressed in this research. These studies can be categorized in the following two groups:

- Stability of excavation, embankments, and open pit mines using equilibrium methods.
- Stability of excavations and open pit mines using finite element method.

2.2 Equilibrium Method

Equilibrium methods of slope stability analysis have been widely used for designing the slopes in soil or loose and weathered rocks. It has been found to be satisfactory and sufficiently simple to be employed for practical problems.

There are at present several methods of stability analysis in existence which apply the equilibrium principle. In general, most of these methods apply the technique of slices, Fellenius (1936), Taylor (1937), Bishop (1955), Janbu (1957), Chugaev (1964), Morgenstern and Price (1965), Spencer (1967), Skempton and Hutchinson (1969), and Sarama (1973), and Sarama (1979). In these methods, the available strength is computed on the basis of the Mohr-Coulomb failure criterion (Sarama, 1979). These methods mainly differ in the shape of the assumed slip surfaces and in the handling of the indeterminacy of the problem.

Charts for investigating the stability of homogeneous earth slopes based on equilibrium limit have been available for many years. The best known of these are Taylor's (1937), Bishop's (1957), Mongenstern's (1965), Spencer's (1967) and Janbu's (1954). Each of these charts has limitations. Taylor's charts do not take into account pore pressures and are based on total stresses. Bishop and Mongenstern's charts are based on effective stresses and are for a wider slope angle range (up to 34^0) than Bishop and Mongenstern's charts. Janbu's charts have greater range and the need for extensive interpolation and extrapolation has been removed. However, the charts are for toe circle failure only, and an iterative procedure is required to determine the factor of safety for a given slope. Also, no information is given on the location of the critical slip circles (Brian, 1978). Brian (1978), attempted to make stability charts for simple earth slopes. In this investigation the problem is reduced to finding a failure surface that gives a minimum stability number instead of searching for a failure surface that gives the minimum safety factor.

2.3 Two-Dimensional Finite Element Analysis

Among the studies conducted on homogeneous soil or rock excavations the following are mentioned:

Dunlop and Duncan (1968, 1969, 1970), Constantopoulos (1970), Duncan and Goodman (1968), Finn (1966, 1968), Bhattacharyya (1970), Pariseau (1970). In these studies generalized two-dimensional analysis was applied. Based on these articles it can be said that the behavior of excavations during construction may be reasonably well predicted by the finite element technique if appropriate physical model and material properties are employed (Desai & Christian, 1977). Since neither soil nor rock can sustain any appreciable tension, the solutions should be evaluated in the light of this fact. Zienkiewiex et al (1968) have suggested an approach to this problem. When tension greater than the tensile strength develops, an iterative process is performed in which the excess tensile stresses are relieved and redistributed to the adjacent elements.

Wang and Sun (1970) in a study of stability of pit slopes utilized a systematic analysis of pit slope structure by the stiffness matrix-method. The program can be used to calculate the magnitude of stress concentration at the toe and the stress distribution in any homogenous pit slope. In 1972, they developed a computer program to analyze pit slope stability by using the finite element method. A two-dimensional finite element stress analysis computer program using triangular elements for linear elastic analysis was used.

Pariseau (1972) described an elastic-plastic approach to the evaluation of slope stability for deep, open pit mines in order to calculate the stresses, strains and displacements. Results relating these parameters to the analysis of slope stability in an actual mine were discussed. He has indicated that both numerical analysis and field experinece shows that the geological structure has a pronounced influence on stability.

Wright (1974), superimposed the critical circular slip surface upon the finite element configuration of the slope and showed that the limiting equilibrium solution could then be applied. From the equilibrium solution, the mobilized shear strength along the circular slip surface was averaged and compared to the assigned value. This ratio was considered as the factor of safety against the sliding of a slope. The results exceeded the equilibrium limit by more than 20% for a homogeneous and normally consolidated slope and almost 100% for an overconsolidated clay.

Smithhan and Chen (1976) presented a plane-strain finite element progressive failure stress analysis of soil slopes throughout the entire range of loading up to the ultimate strength. Emphasis was placed on the effect of large soil deformation on the behavior of slopes, and the techniques to evaluate the overall stability of such slopes. As a conclusion it is mentioned that, the finite element large deformation analysis is found to be very useful when dealing with a progressive failure stress analysis of a natural slope.

Kawamoto and Takeda (1979) discussed how to take the pre-existing cracks and the developed cracks into account in the analysis of rock slopes without the modification of geometry of the finite element system. The effects of pre-existing cracks in the rock mass on the behavior of the rock slope have also been investigated.

Several publications show that the instability of slopes in stiff clays and shales often cannot be explained in terms of peak strength values determined by laboratory tests and equilibrium methods of stability analysis (Duncan and Dunlop, 1969). These papers include failures of excavations and natural slopes, and encompass failures during construction as well as many years later. Therefore, an effort is taken in this study to consider all phases of the problem which are realistic and characteristic of possible situations in the field. In the following chapters assumptions gained from scale model experiment which are more realistic with regard to the geometry of the failing rock mass and the mechanisms of failure will be discussed. Analysis based on those realistic assumptions lead to an improved method of strip mine slope analysis.

Chapter 3

Similitude Requirements

3.1 Introduction

In order to obtain experimental results of significance, both structure and rock properties have to be modelled according to the laws of similitude. A model is a device so related to a physical system that observations on the model may be used to accurately predict the performance of the physical system in the desired respect (Murphy, 1950). The physical system for which the predictions are to be made is called the prototype.

Most rock is difficult to cut or shape and the model size is usually restricted because of the capacity of testing machines. Obviously, the use of low strength synthetic materials, such as plasters, mortars, etc., that can be cast into the desired dimensions would simplify model testing. In general, the mechanical properties of synthetic materials must satisfy model-prototype requirements.

The purpose of the failure experiments is to obtain basic information about the behavior and failure modes of a slope model and therefore of the prototype. To overcome the obvious difficulties in simulating a prototype, there should first be a clear understanding of its relationship to the model (Rosenblad, 1970). The required relationships necessary to allow for prototype predictions from model tests can be accomplished by the theory of similitude which may be developed from dimensional analysis. Consideration of the dimensions in which each variable is expressed combined with the relationships that exist between the variables form the basis for dimensional analysis.

3.2 Selection of Variables

Before a dimensional analysis can be conducted a set of basic quantities must be selected and then the variables in the system can be defined in terms of the basic quantities used. These basic quantities are mass, length, and time or force, length and time. Newton's Second Law of Motion, F=Ma, relates these quantities. This relationship, expressed dimensionally is $F=MLT^{-2}$ and any one quantity may be described in terms of the other three.

The significant variables that affect the behavior of a slope in a strip mine can be grouped as: (1) stresses, (2) intact material properties (3) external loading, (4) geometry of the structure (Figure 3-1). The parameters can be related with a functional relationship.

$$\sigma_p=f(\gamma_p, L_p, E_p, a_p, b_p, q_{up}, S_p, T_p, \nu_p, \phi_p, f_p) \qquad (3.1)$$

where

σ_p = stress in the prototype

L_p = the height of slope structure

γ_p = Density

E_p = Modulus of elasticity

F_p = the external applied load to the slope structure

a_p = width of structure

b_p = length of the slope structure

q_{up} = Unconfined compressive strength

S_p = shear strength

T_p = tensile strength

ν_p = Poisson's ratio

ϕ_p = internal friction

Two of the variables ν , ϕ in equation (3.1) are dimensionless. Since, the Buckingham's π-theorom restrict the π terms in the functional relationship

$$\pi_1 = f\ (\pi_2, \pi_3, \pi_4 \text{-------} \pi_n) \qquad (3.2)$$

to dimensionless and independent variables, two π-terms are established with ν , ϕ

$\pi_1 = \nu$

$\pi_2 = \phi$

Therefore, ten variables remain in the dimensional analysis.

In order to check the total number of dimensionless products, the variables should be tabulated in terms of the basic dimensions of mass, length, and time.

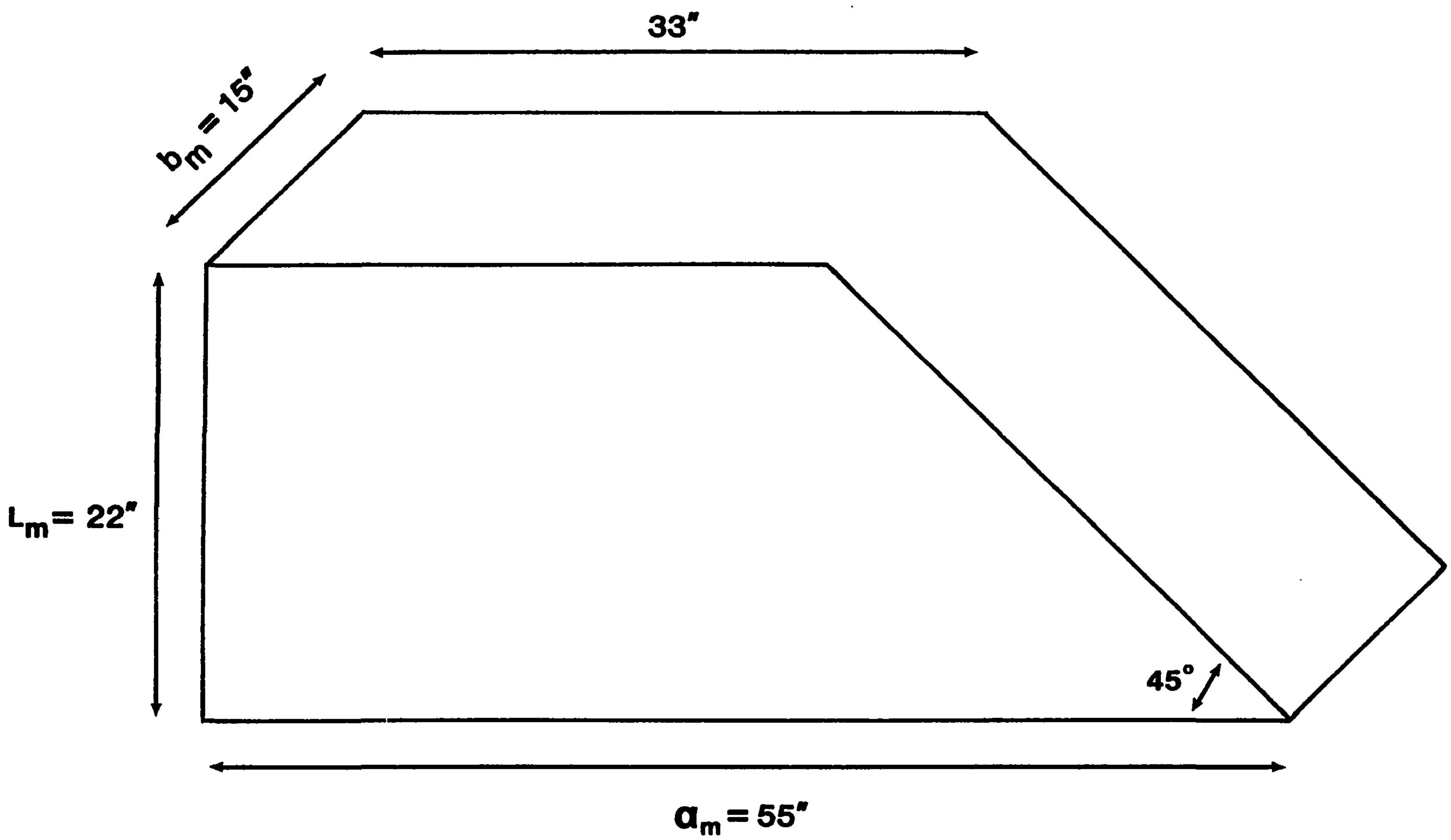

Figure 3-1, Model Dimensions

$$\begin{array}{c|cccccccccc} & \sigma_p & \gamma_p & L_p & E_p & F_p & S_p & T_p & q_{up} & a_p & b_p \\ \hline M & 1 & 1 & 0 & 1 & 1 & 1 & 1 & 1 & 0 & 0 \\ L & -1 & -2 & 1 & -1 & 1 & -1 & -1 & -1 & 1 & 1 \\ T & -2 & -2 & 0 & -2 & -2 & -2 & -2 & -2 & 0 & 0 \end{array}$$

The determinant formed from the first two rows of the eighth and ninth columns in the illustrated dimensional matrix is a nonzero matrix.

$$\begin{vmatrix} 1 & 0 \\ -1 & 1 \end{vmatrix} = 1-0 = 1>0$$

Note also that the determinant formed from any three columns in the large matrix is zero. For example when columns 6, 7, and 9 is taken.

$$\begin{vmatrix} 1 & 1 & 0 \\ -1 & -1 & 1 \\ -2 & -2 & 0 \end{vmatrix} = 0-2+0-0+2+0 = 0$$

Since all third-order determinants vanish the rank of the matrix is two. The rank of the matrix is instructive as seen in Buckingham's theorem. "The number of dimensionless products in a complete set is equal to the total number of variable minus the rank of the dimensional matrix " (Langhaar 1969). Hence the number of dimensionless products in a complete set is 10-2=8.

There are several methods for determining the set of π-terms. An unknown exponent is assigned to each of the 12 variables. Since each π-term must be dimensionless, the exponents of the L, M, T parameters must also be zero. Therefore, an equation is written so that the exponents of all dimensional variables containing a length dimension, L, after summation can be equated to zero. In the same way we can write equations for the other two basic parameters, M and T. Now there are three auxillary dimensional equations. Two dimensionless variables ϕ , ν have exponent one and there remain ten variables for which exponents must be determined.

Since there are 3 equations and 10 unknowns, arbitrary values should be assigned to seven of the unknowns. In general a value of 1 is assigned to one of the unknowns and the others will be zero. Substitution of these values into the three auxiliary equations allows the determination of each π-term. This process is repeated until all the π-terms are determined. For a complete description of this kind of analysis one can refer to many standard references (Murphy, 1950) (Langhaar, 1969).

Thus the developed π-terms are

$$\begin{array}{llll} \pi_1 = \nu & \pi_4 = \dfrac{\gamma L}{E} & \pi_7 = \dfrac{S}{E} & \pi_{10} = \dfrac{b}{L} \\ \pi_2 = \phi & \pi_5 = \dfrac{F}{EL^2} & \pi_8 = \dfrac{T}{E} & \\ \pi_3 = \dfrac{\sigma}{\gamma L} & \pi_6 = \dfrac{qu}{E} & \pi_9 = \dfrac{a}{L} & \end{array} \tag{3.3}$$

Replacing the subscripts p with m for model gives equivalent expressions for the π-terms for the model. The condition for model-prototype similitude is that the following equations should be satisfied:

$$
\begin{aligned}
&\nu_p = \nu_m && \frac{S_p}{E_p} = \frac{S_m}{E_m} \\
&\phi_p = \phi_m && \\
&\frac{\sigma_p}{\gamma_p L_p} = \frac{\sigma_m}{\gamma_m L_m} && \frac{T_p}{E_p} = \frac{T_m}{E_m} \\
&\frac{\gamma_p L_p}{E_p} = \frac{\gamma_m L_m}{E_m} && \frac{a_\rho}{L_p} = \frac{a_n}{L_m} \\
&\frac{F_p}{E_p L_p^2} = \frac{F_m}{E_m L_M^2} && \frac{b_p}{L_p} = \frac{b_m}{L_m} \\
&\frac{q_{up}}{E_p} = \frac{q_{um}}{E_m} &&
\end{aligned}
\qquad (3.4)
$$

From (3.4)

$$\frac{L_p}{L_m} = \frac{\gamma_m E_p}{\gamma_p E_m}$$

where L_p/L_m is the prototype-to-model scale ratio. Similarly

$$\frac{F_p}{F_m} = \frac{E_p L_p^2}{E_m L_m^2}$$

From equation 3.4 it can be seen, for example, that a mortar with an unconfined compressive strength of 55 psi and modulus of elasticity, $E_m = 2.2 \times 10^4$ psi is a representative of a prototype rock(shale, where $E_p = 0.75 \times 10^6$ psi) whose unconfined compressive strength is equal to 1875 psi, assuming Poisson's ratio for both is the same.

$$\frac{q_{up}}{0.75 \times 10^6} = \frac{55}{2.2 \times 10^4}, \quad q_{up} = 1875 \text{ psi.}$$

A synthetic model material able to satisfy all the requirements of equation (3.4) is probably not attainable. Usually some compromise is necessary and first consideration should be given to matching the more important properties.

Therefore, if the uniaxial compressive strength is considered to be the factor that will dominate failure in this study in the prototype, the relationship

$$\frac{q_{up}}{E_p} = \frac{q_{um}}{E_m}$$

should be satisfied and the other model strengths can be disregarded. Generally Poisson's ratio will have the least effect on model-prototype similitude (Obert, 1967). However it is possible for dimensionless quantities like Poisson's ratio, angle of friction and strain to be the same in the model as in the prototype (Erguvanli,1972).

Since gravity loading has a minimal effect upon the behavior of the modeling in this study, it has not been considered.

The dimensional analysis here is so general that not only can it be used for observing degrees of freedom and weak points of surface excavation in rock bodies but it is also applicable for quantitative evaluation of underground excavations and structures in different rocks.

Chapter 4

EXPERIMENTAL STUDY

4.1 Introduction

Failures that may occur in an open excavation in rock due to large overburden pressures or live equipment loading are as yet not completely understood. In the last two decades substantial progress has been made toward the understanding of the failures that occur in intact or weathered rocks due to excavation in highways or open pit mines. But there remains a serious lack of knowledge about failure surface extension and failure surface shape for different rocks. Among these over-consolidated clay, and stiff or fissured clay shales can be mentioned. As a result no reliable method of design for slopes consisting of such rocks under circumstances of practical importance exists.

Several investigators have concluded on the basis of failure problems for clay shales that the usual methods of strength testing and stability analysis are not suitable. This uncertainty created such a lack of confidence that in most critical cases engineers have suggested a high factor of safety, which sometimes goes beyond five yielding an obviously uneconomical design. "Because of contradictions between theory and observation, consistently reliable predictions of rock behavior will be the exception and not the rule, until we understand the failure mechanism of rock"

(Judd, 1969). To accomplish this purpose, a working highwall in a strip mine is modeled to examine the failure mechanism of the structure.

The model is not designed to simulate a specific prototype case in the field, but proposed to add to the present knowledge of the strength, behavior, failure of mine slopes as well as the effect of shape of the critical potential surface in loose and hard rock. Conclusions will be generalized as far as possible in order to obtain a reasonable design approach for Oklahoma mines located in clay, clay shale or hard rock.

4.2 Considered Mechanical Properties

A rock element is an assemblage of different minerals with strength resulting from the minerals plus the cementation type. Strength of a rock element is not only related to the weakest part of the rock matrix and the mineral components but also on the type of bond between the minerals. The critical height of slope is determined by the mechanical defects such as joints, faults and weakness planes as well. In present studies, a high vertical slope is thought to be safe if its intact unconfined compressive strength is high, (Terzaghi, 1962). However planes of weakness which are seldom considered introduce uncertainty. Furthermore, engineering constants such as Young's modulus and Poisson's ratio are unreliable due to rock anisotropy in that they change with load and direction within the rock (Wantland, 1963).

"Engineering observations have to be made on specified rocks and are frequently confined to a determination of uni-axial compressive strength and modulus" (Jaeger 1971). Both of these important mechanical properties of rock are considered in the physical model in this study.

4.3 Plane of Weakness

The plane of weakness in this experiment is a plane that seperates the coal layer from overlying rock. It has appreciably lower strength than the rock or the coal layer and constitutes the mechanical discontinuity in the slope structure.

Gouge, or some infilling material is frequently found at the sedimentary contact. The resistance to sliding along the plane is related to the thickness and type of material. Since the infilling material between two planes is quite wide the small surface asperities should have little influence on the shear resistance. Therefore, the plane of weakness in the model is assumed smooth and is covered with sand as infilling material.

4.4 Design of Loading Steel Frame

A steel frame with dimensions based on relationship (3.4) was made for use in this investigation. The steel frame dimensions are shown in table 4-1. The frame is made of 2 by 2 angles and tubes and braced by angles to prevent local displacements. Inside the frame are pieces of horizontal and vertical clear plexiglass plates with ½ inch thickness supported by the steel angles. The plexiglass sections can be individually removed from the steel frame for the purpose of cleaning or other adjustments. The advantage of plexiglass is its transparency which allows an analysis of the failure surface.

Table 4-1

Dimensions of Model (steel frame)

Prototype Dimensions	Relationship	Model Dimensions
$L_p = 90"$ $b_p = 61.375"$ $L_p/L_m = 49.1$	$\frac{L_p}{L_m} = \frac{b_p}{b_m}$ $49.1 = \frac{61.375"}{b_m}$	$L_m = 22"$ $b_m = 15"$
$a_p = 225.04$	$\frac{a_p}{a_m} = \frac{L_p}{L_m}$ $\frac{225.04}{a_m} = 49.1$	$a_m = 55"$

Miller and Hilts (1970), by gathering field data on open pit mine slope stability have obtained the following interesting conclusion:

"Cut slopes in moderately disturbed areas will be stable at the recommended slope angles until a cut is made through the coal at the toe of the slope. Where the coal seam is confined and loaded from above slope failure may not occur for several weeks following completion of the key cut in the coal."

In order to provide this condition the front edge of the box adjacent to the plane of weakness is extended ½ inch and it can be seen on Figure 4-1.

A plan view schematic drawing of the complete assembly is given in Figure 4-1 where each component is labled.

4.5 Model Material Control

The model material is an important part of a rock-like model development and must indicate the simulated properties of natural rock. A material that simulates rock in all of its physical properties may never be developed (Rosenblad,1970) but the material properties can be scaled in accordance with dimensional analysis to achieve simulitude requirements. In civil and mining engineering work, the strength and deformation properties are usually of most interest (Erguvanli,1972).

Unit weight was considered in order to check the uniformity checks were necessary for verifying the homogenous material prepartion technique.

Unit weight determinations were made on cored cylinders so that the volume of each cylinder was known.

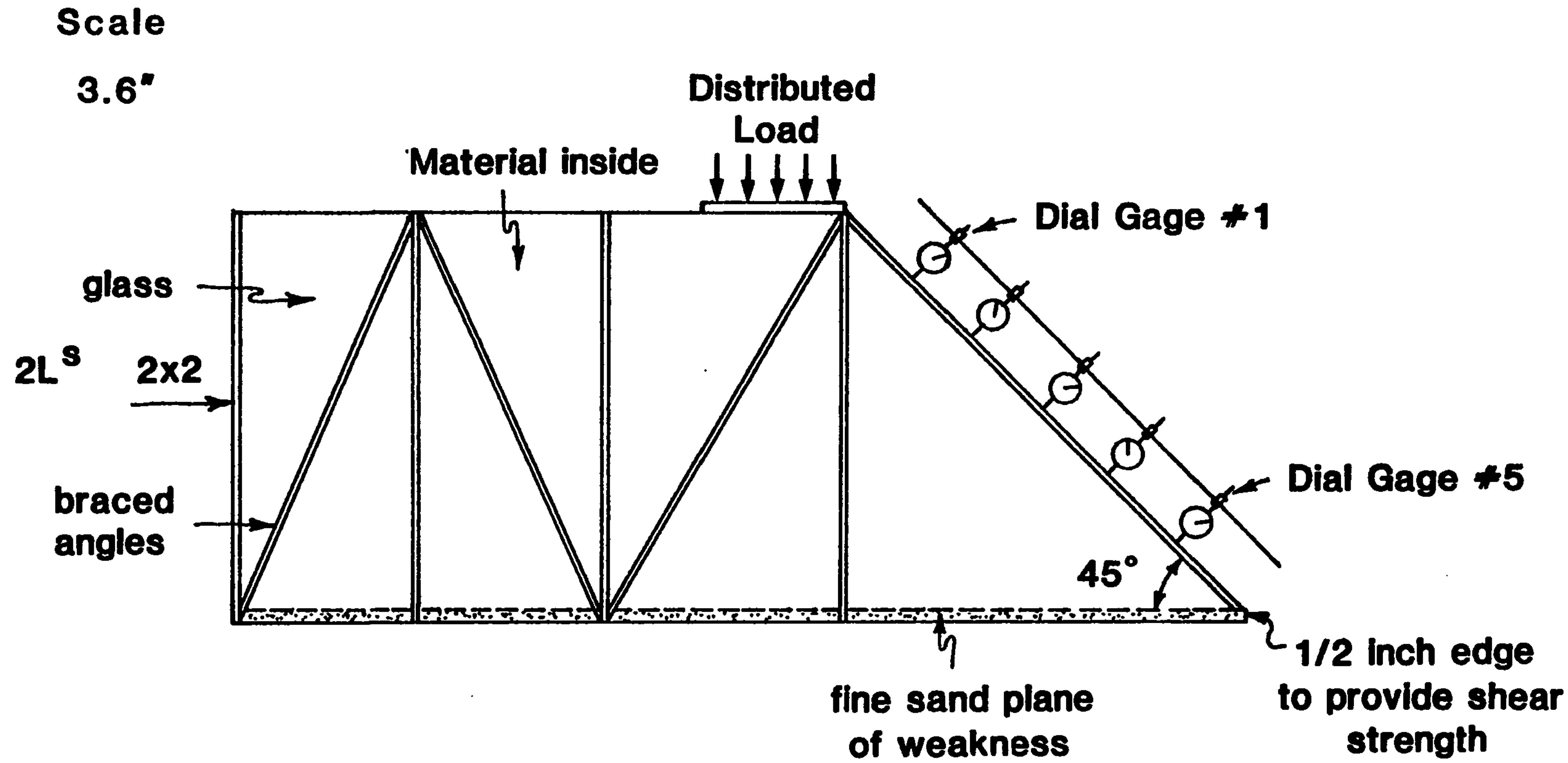

Figure 4-1,

A side view of the model

Unconfined Compressive Strength

Compressive strength is normally defined as the stress required to crush a cylindrical rock sample unconfined at its sides. Compressive failure in rock occurs through internal collapse of the rock structure due to compression of pore space resulting in grain fracture and movement along grain and crystal boundaries. The true compressive strength of a rock is therefore influenced by its internal structure. Harder rock reflects higher compressive strength. After grain and cementation fracturing of rock under compression, shear strength is expected to control the failure of rock.

The unconfined compression strength test was selected since it is the primary reflection of rock failure and it is a relatively routine test. Cylinders which were 6.2 inches in height and 3.0 inches in diameter were selected for use in obtaining the unconfined compressive strength. For each test of the model six specimens, three from each layer during the filling of the model were molded in brass molds. The brass molds are of the type used for making portland cement mortar test specimens. These kind of specimens require much less material and less preparation. Industrial oil was used in order to prohibit bonding of the brass mold to the model material.

The unconfined compression tests were conducted using a universal compressive strength machine. The unconfined compressive strength served two purposes: First, to determine if the material in question satisfied the upper strength limit requirement; second, to obtain the modulus of elasticity of the material by establishing the relationship between stress and strain.

4.6 Material Components

It is hard to find a good modeling mixture as cuttability and rigidity are mutually exclusive in most materials. Most of the materials used in previous studies have a ductile failure behaviro which does simulate a rock. Availability, workability, and reproducibility are important factors that have been considered.

A literature search revealed that various combinations of the following constituents have been tried as a model material: cement, sand, and water; sand, wax and mica; sand and clay; and plaster, neat or mixed with barite, lead oxide, mica, diatomite, kaolinite, or lime (Erguvanli, 1972). Since most engineering studies employ a combination of sand cement and water to model in situ rock, these materials were selected to be used in this project.

Rosenbald (1970) discussed four possible cementing agents which can be used to make model materials, portland cement, gypsum cement, natural cement, and pottery clay.

Both pottery clay and natural cement in the hardened form exhibit a brittle failure, which is undesirable in this case. Portland cement and gypsum cement have been used extensively in model work.

Two types of commercial sand were used in these tests. In test numbers 1 to 5 the first type of sand gave better relationships between stress and strain and as a result a better value for the modulus of elasticity.

Water was used in all mixes in order to hydrate the cement and make the mixture workable. Water was present in two forms, free and bonded. The free water provided a good workable mix. The free water for 2 tests indicated that because of evaporation intensity the material strength is increased very fast and cannot be controlled. The bonded water can be driven out only at temperature above 130°F. The Fears Structural Laboratory temperature during the tests was between 70° - 80° F.

4.7 Preparation of Model Material

The model material was made by mixing fine sand with cement and water. A concrete mixer machine with four cubic feet capacity was used to prepare the model material. The sand and cement were tumbled while dry in the mixer until the mixture was homogenous (about twenty minutes). Once the dry mix was homogenous, water was slowly added as tumbling continued. Mixing continued for about ten minutes after all water was added to ensure homogeneity. The water cement ratio used was 0.2 and cement to sand ratio used was between 1/14 up to 1/10. It was necessary during the wet mixing to break up large lumps of material with rod or by hand. The wet mix looks and feels like a damp, bulky fine sand, with no fluidity.

Before pouring the material in the steel box a thin layer of fine sand was spread on the bottom of the box in order to provide the friction between the model material and the bottom as a plane of weakness.

The wet material was placed in the box model in about 5 inch thick layers and each layer was compacted by 300 successive compaction rod blows spaced in a uniform pattern over the surface of the layer. The surface of each layer was scarified deeply after compaction and before adding material for the next layer to insure that there would be no continuous planes of weakness in the compacted material.

In this manner the box was completely filled and compacted to a level of ½ inch above the top of the box and the excess material was removed carefully with a sharp edged metal trowel.

From each layer 3 core samples were taken in order to monitor the compressive strength of the material. Cylindrical specimen molds were filled in layers with three layers per specimen. Specimens were rodded 24 times with a small diameter steel rod for compaction. After each mold was filled the excess material was scraped off with a metal trowel.

The sloping front of the model was clamped and covered with a sheet of thick plastic for a period of one or two days depending on the required compressive strength. The top level of slope was allowed to air dry except the section on which loading would occur, which was covered with a 1 inch steel plate 15 by 8 inches in dimension.

Since the prepared material does have a desirable modulus of elasticity, it deforms sufficiently under loading allowing the resulting deformation to be measured on an array of dial gages. In general, the modulus of elasticity of the cohesive material was required to be high enough to permit handling without breakage but low enough so that the material would fail in plane-strain compression with a loading apparatus of reasonable dimensions.

The maximum time spent on any preparation was 8 hous and the minimum time was 6 hours.

4.8 Instrumentation

The modulus of elasticity for the material used in each test was obtained from cylinders where the overall specimen deformation was used to determine the axial strain. The average strain of the core sample under compression was determined by measuring the relative displacement between two points and dividing by the initial distance between the points $(\varepsilon = \frac{\Delta H}{H})$. The displacement of points in the core sample relative to the base plate in the testing machine were measured using a dial gage on each side of the sample. Sulfur caps were mounted on the cylinders to make the ends planar. The caps affected the shape of the stress-strain curves significantly due to the inability to apply pre-loading on weak and brittle cylinders. The stress-strain curve for the gaged cylinders was used to represent the model material properties.

Dial gages were also used for measuring the deformation and behavior of the box and model material. Continuous load was maintained in the vertical direction and transfered to the upper surface by a 15 x 8 inch plate. Displacement between the upper surface and the base plate was measured to an accuracy of 0.001 inch.

The main purpose of tests #1 to #5 was to investigate the failure surface geometry of a working highwall slope under a distributed load. In addition the displacements of the slope surface itself were simultaneously studied. To accomplish this purpose a series of 5 dial gages for tests # 1 to #5 and 4 dial gages for the remaining tests were mounted parallel to the upstream face of the slope through a slot in the frame, to record the deformations of the upstream slope as loading progressed. Reading of the gages were taken after each increment of loading.

Displacement of the steel frame and the plexiglass plate was controlled by the use of the several dial gages mounted on the sides, Figure 4-2.

4.9 Testing Procedure

Following is a description of the testing procedure that was used for loading the slope model. Some modifications of the dimensions were used for tests #6 to #9. The tests varied from 4 to 6 hours in duration.

Once the required compressive strength had been reached as determined from the core samples, the model was loaded. The testing steps were as follows:

1. Compressive strength estimation were obtained by applying the load on 3 sulfur-capped core samples, and averaging their values.
2. Stress-strain relationships and consequently the modulii of elasticity were obtained by applying axial load to each of the 3 core samples.
3. Pre-loading was used to minimize end effects and to obtain a smooth stress-strain curve.
4. By a rough estimation, 1/6 of predicted strength was applied on the model as pre-loading.
5. The "zero" readings on all dial gages placed on the model were taken.
6. Two dial gages were situated at the top surface while 4

other dial gages monitored the lateral deformation of the box. For tests #1 to #5 five dial gages measured slope front displacements while four gages were employed in tests 6 to 9. Readings were taken after each increment of loading.

7. Each loading increment took approximately 30 seconds.
8. The axial loading was transferred to the model by a 8 x 15 x 1 inch steel plate for tests #1 to #5 and by a 5 x 15 x 1 inch steel plate for tests #6 to #9.
9. After noting the appearance time and nature of preliminary cracks the loading was continued to final failure.
10. Each test failure surface was traced on the plexiglass side in order to compare it with other tests.
11. Once failure is complete and final readings made, the model can be carefully unloaded for the next test.

It is possible to calculate the resulting displacement that has occured at different depths at the front face by comparing the differences between the first and final dial gage readings.

4.10 Presentation and Discussion of Model Test Data

From the data presented in tables 4-1 to 4-9 and Figures 4-1 to 4-12 in Appendix A the following outcomes may be drawn:

1. Experiments were performed to provide enough knowledge of strip mine slope behavior to accomplish this

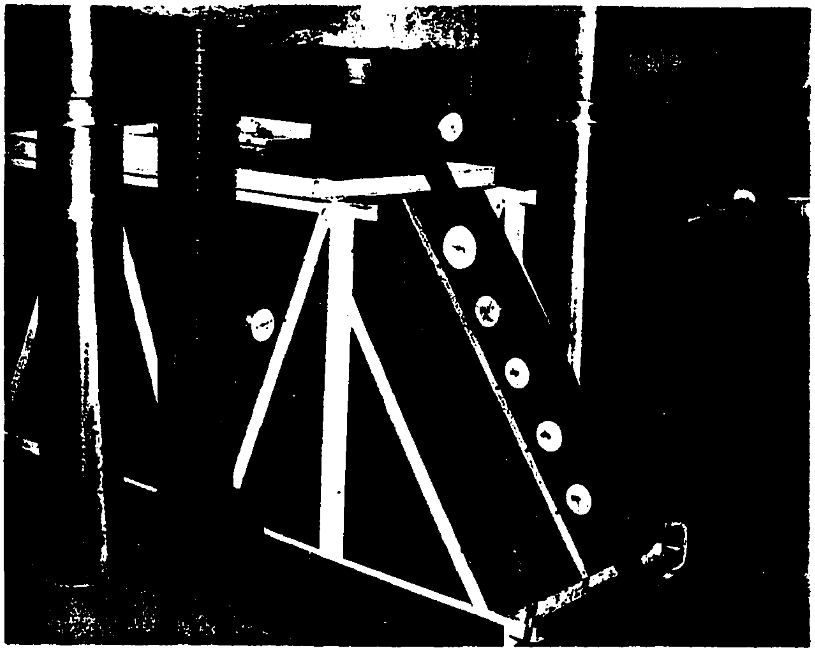

a) Model Instrumentation

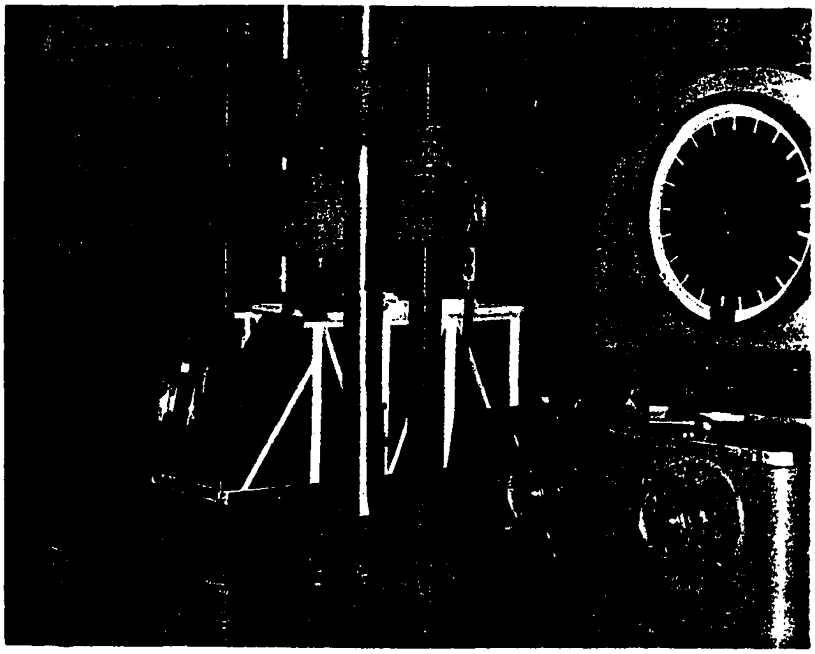

b) Loading Machine

Figure 4-2, An illustration of model instruments and loading equipment.

Table 4-2 Computation of modulus of elasticity of model for different tests (E = .75 X 10^6 psi for prototype shale rock)

	Model					Prototype
	Test No.	Modulus of Elasticity E, psi	Compressive Strength psi	Angle of Shear Failure ϕ	Unit Weight lb/ft^3 (wet)	Compressive Strength PSI
Slope $\alpha = 45^0$ (on plane of weakness)	1	$23.6X10^3$	26.0	35^0	135	826
	2	$25X10^3$	34.52	30^0	140	1052
	3	$28X10^3$	40.0	24^0	142	1205
	4	$44.6X10^3$	72.86	22^0	145	1226
	5	$54X10^3$	224.22	15^0	150	3114
Vertical Cut	6	$19X10^3$	23.0	34^0	136	907
	7	$25X10^3$	32.0	31^0	138	960
Slope α=26.5	8	$44.20 X10^3$	60.0	23^0	142	1016
	9	$42.16X10^3$	89.6	18^0	147	1593

purpose, the front face of the model which simulated a working high-wall was instrumented to measure face displacement.

2. The records of the front surface displacemnts are shown in Tables 4-1 to 4-9, Appendix A. Variation of displacement with depth at the front surface is plotted in Figure 4-3.
3. Observation during the experiment has proven that the tension crack first occurs on the top and then a crack appears in the middle and spreads upward toward the tension crack and finally downward to the plane of weakness.
4. The displacements present the initial movement of the material, which structure remains stable unless the failure surface appears and intersects the plane of weakness.
5. In mining, engineers should specify what location should be monitored. If there is not an accurate knowledge of the critical region, the area to be monitored could be extensive.

Displacement in the lower portion (Dial gage #4) is maximum and was increasing as cracking neared. This can possibly give warning of threatening failure in a strip mine slope.

In a mine the magnitude of face movement is totally unknow until an actual failure occurs. On the other hand stability analysis based on laboratory strength properties fail to provide satisfactory comparisons with slope behavior observed in the full-scale test cut at some mines. This is due to the presence of joints and fractures. However, knowing the most critical point based on the experiment in this study there is no need for overly sophisticated instruments to monitor the movements. Simple devices can be installed to predict the failure and to give an alarm of any movement.

6. Complete failure was clearly indicated by a sudden outward translation of the front surface and a corresponding settlement of the top surface of the model.
7. While making the sulfur caps it was discovered that the more brittle core samples failed due to the twisting necessary in the capping process. Such brittle materials require extreme care during test-preparation.
8. With increasing compressive strength, the curvature of the failure surface decreased for test #1 o #5. All the failure surfaces intercepted the plane of weakness somewhere near the toe of the slope.
9. Test #6 and #7 for a vertical cut and #8, #9 for a slope were carried out in order to see if this kind of loading and material modeling indicates well-known failure surface. Based on Figures 4-11 and 4-12 Appendix A, it can be seen that toe failure did not occur, indicating good agreement between theory and model.
10. In all the tests except #1 and #9 the initial crack appeared somewhere below the head of slide. This supports Peck's(1969) statement: "It does not necessarily imply that failure always starts at the head of a slide; there are undoubtedly several other forces to be considered".

11. The failure surface is not circular for loose rock when there is a restriction for the penetration of slip surface (plane of weakness) through a rigid stratum below.

By monitoring the excessive strip mine slope displacements during the operation with the knowledge of the most critical point of a working highwall (dial gage #4), the behavior of a potential failure can be predicted. This ensures that the slope is safe and may exhibit small movements within acceptable design. On the other hand it would also enable the mine operators to take steps to minimize production and equipment damages and danger to human life.

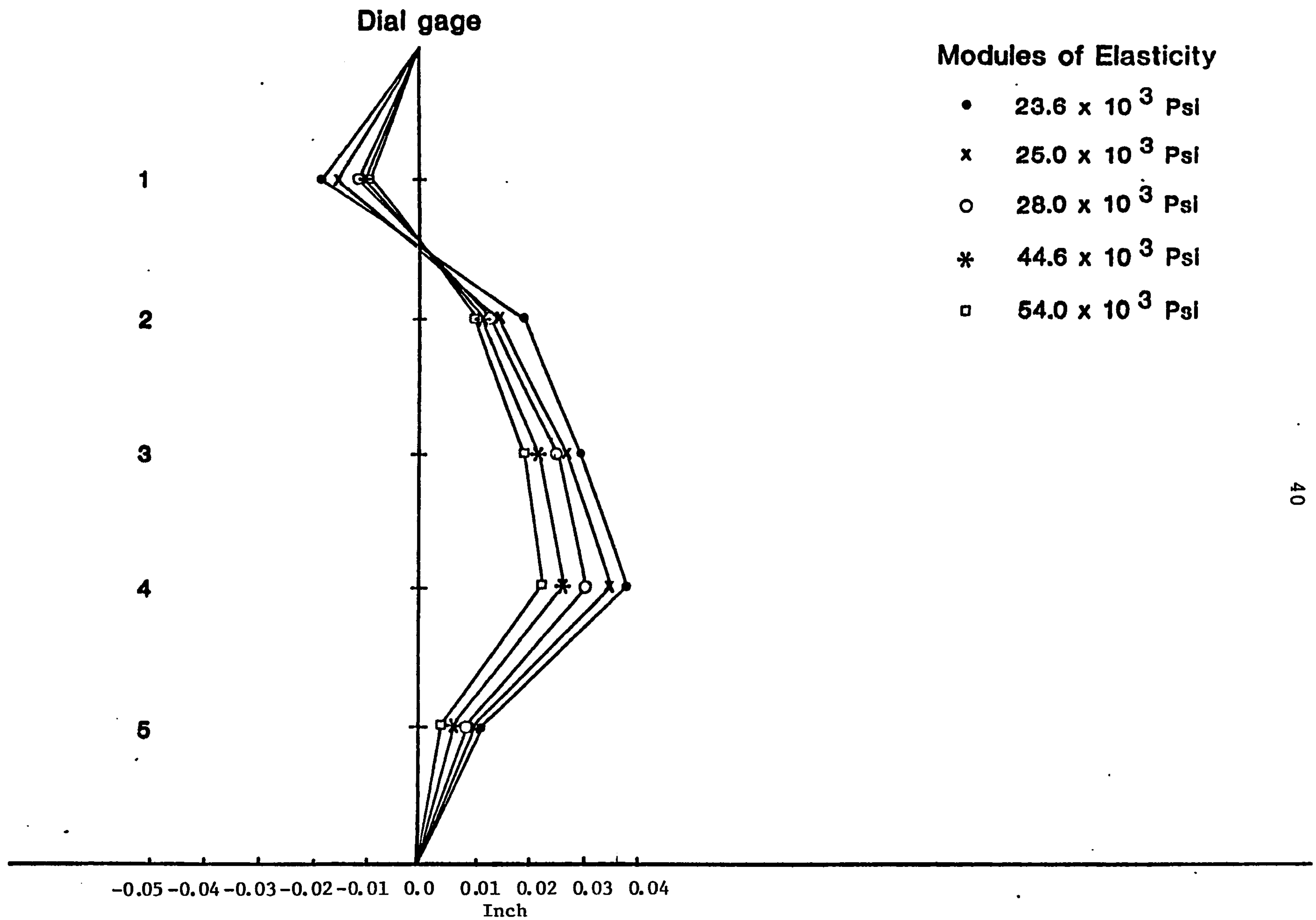

FIGURE 4-3 Maximum displacement at the front surface of physical model for different loading and material

Chapter 5

STABILITY OF SPOIL PILES AND UNCONSOLIDATED WORKING HIGHWALL

5.1 Introduction

One of the problems associated with coal strip mining is disposal or storage of a large volume of overburden waste material generated during the mining operation. This waste material is called spoil. Dumping or loose storage of spoil piles is a source of siltation, acid water runoff, and landslides. Several different regulations restrict the size and geometry of overburden storage areas in order to assure their stability. These regulations include: limiting the steepness of a natural slope upon which overburden can be placed; limiting the angle of the fill slope which is referred to as the "natural angle of repose" of the spoil.

Several investigations have illustrated that spoil failures occured in surface mines which were in agreement with regulations. However, the regulations are so general that in some cases interpretation of the regulations resulted in excessive costs, while simple analysis shows that a less extreme plan would yield sufficient stability with less mining cost for a particular region.

Both unconsolidated highwall (used here as a soft or fractured rock) and spoil consist of combination of coarse and fine material. Since stability analysis based on equilibrium methods are applicable as long as soft rock is considered, this chapter will include:

- A brief review of the equilibrium method
- A study of mechanisms involved in unconsolidated highwall and spoil failures.
- Some suggestions for modification of existing approaches based on the equilibrium method for spoil stability analysis.

Finally the purpose of this chapter is not to compute the stability of particular Oklahoma strip mines but to develop better approach on which to design such mines. Unfortunately, little or no research has been done in strip mine slope behavior which can be used as a basis for comparison . The stability hazard related to groundwater has not been reported in Oklahoma surface mine operations, but spoil failure has been seen in some mining sites (Figure 5-1).

5.2 Equilibrium Method

Most slope stability analysis methods employ the assumption of limit equilibrium where the soil is assumed to be in a state of plastic equilibrium. A cross section of unit thickness as a two-dimensional plane strain problem is assumed. A free body diagram of a soil mass, bounded by the top surface and the assumed failure surface is analysed using equations of statics. Strength parameters and pore pressure distribution are assigned to the cross section based on a combination of in situ and laboratory testing. The soil is usually considered to be homogenous in directions normal to the cross section.

The observation of many failed slopes resulted in the development of stability analysis procedures which considered circular or arc shaped failure surfaces, now known as the Swedish method. Swedish methods are divided into two groups. The first group is based on the assumption that the soil mass above the failure surfaces acts as a mass unit. The second group assumes the soil mass to be divided into a number of slices and the conditions of static equilibrium are applied to the individual slices and summed for the entire structure.

For the case of cohesive clay, application of the equilibrium method with a circular failure surface is widely recommended. It has been of proven value in the studies of soil and unconsolidated material. Therefore, it will be applicable to spoil stability of Oklahoma mines.

Slope stability analysis methods based on equilibrium method possess some of the following deficiencies:

1. The parameters of strength such as (C,ϕ) must be estimated or determined in the laboratory. In actual slopes, great uncertainty exists in this respect.
2. The safety factor is assumed to be the same at all points of the failure surface.

Figure 5-1. Slope failure in a strip mining located at eastern part of Oklahoma.

3. The Basic Equilibrium Method was applied on circular failure surfaces only. More recently, the slice procedure has been extended to failure surfaces which have no restrictions placed on their shape. The method is referred to as the Generalized Method of Slices.
   The experimental study discussed in the previous chapter provides a good support for the "Generalized Method of Slices".
4. The problem is statically indeterminate and cannot be solved without the deformation condition.
5. Equilibrium analysis will provide a valid indication of stability for large factors of safety but they are not capable of indicating which zones are most highly stressed. Analysis has shown that the elastic stress concentration around slopes may be large enough to cause local failure of the soil even when the factor of safety against catastrophic failure is as large as five (Dunlop and Duncan, 1970).
6. The Failure Criterion is not capable of accounting for the anisotropic behavior associated with the existence of planes of weakness (Hoek and Brown, 1980).

The study in the following sections is made to eliminate some of these deficiencies and to develope a reasonable approach applicable to the analysis of spoil and unconsolidated highwalls of strip mines.

5.3 Factor of safety

The factor of safety is commonly defined as the ratio of available shear strength of the soil to the shear resistance required to maintain equilibrium. The safety factor is then

$$F_S = \frac{\text{Shear strength available to resist sliding}}{\text{Shear stress mobilized along failure surface}}$$

and after rearranging this equation, one gets

$$\tau = \frac{1}{F_s} (C + \sigma \text{ tg } \phi) \qquad 5\text{-}1$$

where τ is the mobilized shear stress, C is the cohesion, ϕ is the angle of internal friction, and σ is the normal stress on the plane of failure resulting from the applied loads, and F_s is the safety factor with respect to shear strength. The factor of safety for a stable spoil or highwall must be at least equal to unity.

5.4 Determination of the Critical Slip Surface

The critical failure surface is the slip surface which has the lowest factor of safety. Since all other slip surfaces produce higher factors of safety, any method of analysis that does not determine the critical slip surface results in unsafe situations.

The experimental study discussed in the previous chapter indicated that the slip surface is not a circle for loose rock when there is a restriction for the penetration of the slip surface through a rigid stratum below. The effect of the shape of critical slip surfaces has already been shown to be of possible importance in computing factors of safety for homogenous simple slopes (Bell, 1968). The experimental results show that the slip surface can be divided into three zones, linear near the top, concave outward in the middle region, and a flat surface adjacent to the coal layer for the highwall, while coinciding with the original ground surface or the undistrubed underclay for spoil, as shown in Figures 5-2, 5-3.

In general, the slip surface can be considered as a composite of curved and flat surfaces.

Establishing the critical slip surface based on the equilibrium method is largely a trial and error process, accomplished by numerical or graphical methods. Because of the repetitive nature of the calculations it is possible to use computers to allow for more iteration in the analysis of complex failure surfaces. Several analytical methods have been developed but among them the Fellenius or the Simplified Bishop Method (1955) is recommended because of the error involved in this method is less than with other methods.

5.5 Indeterminacy

In the slope stability analysis which assumes circular arc shaped failure surfaces, the soil mass is divided into a number of slices. In order to determine shear strength for each slice, the normal stress must be known. For each slice in Figure 5-4, there are three equations of equilibrium and n unknowns. Clearly

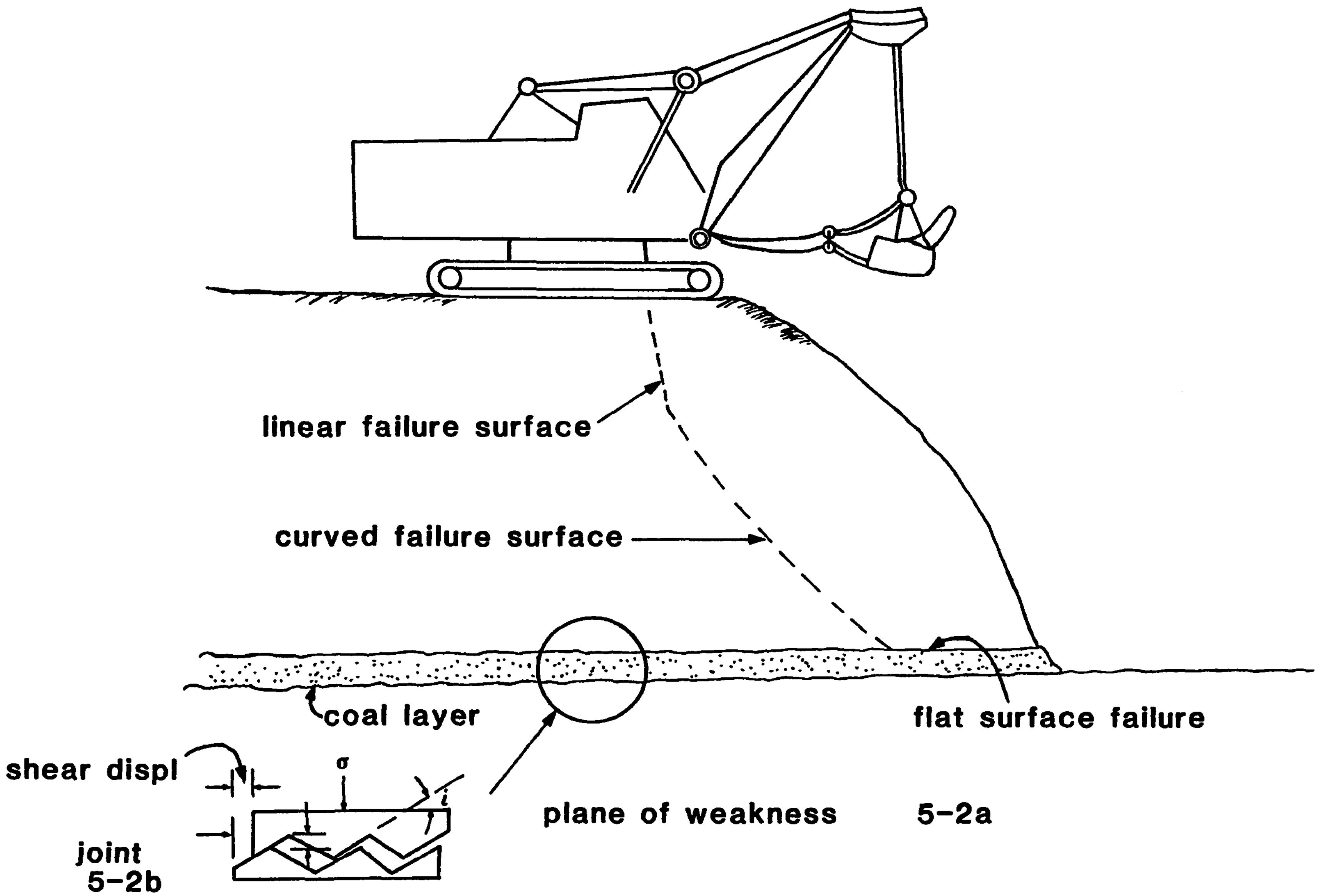

Figure 5-2, Expected slip surface in a strip mine.

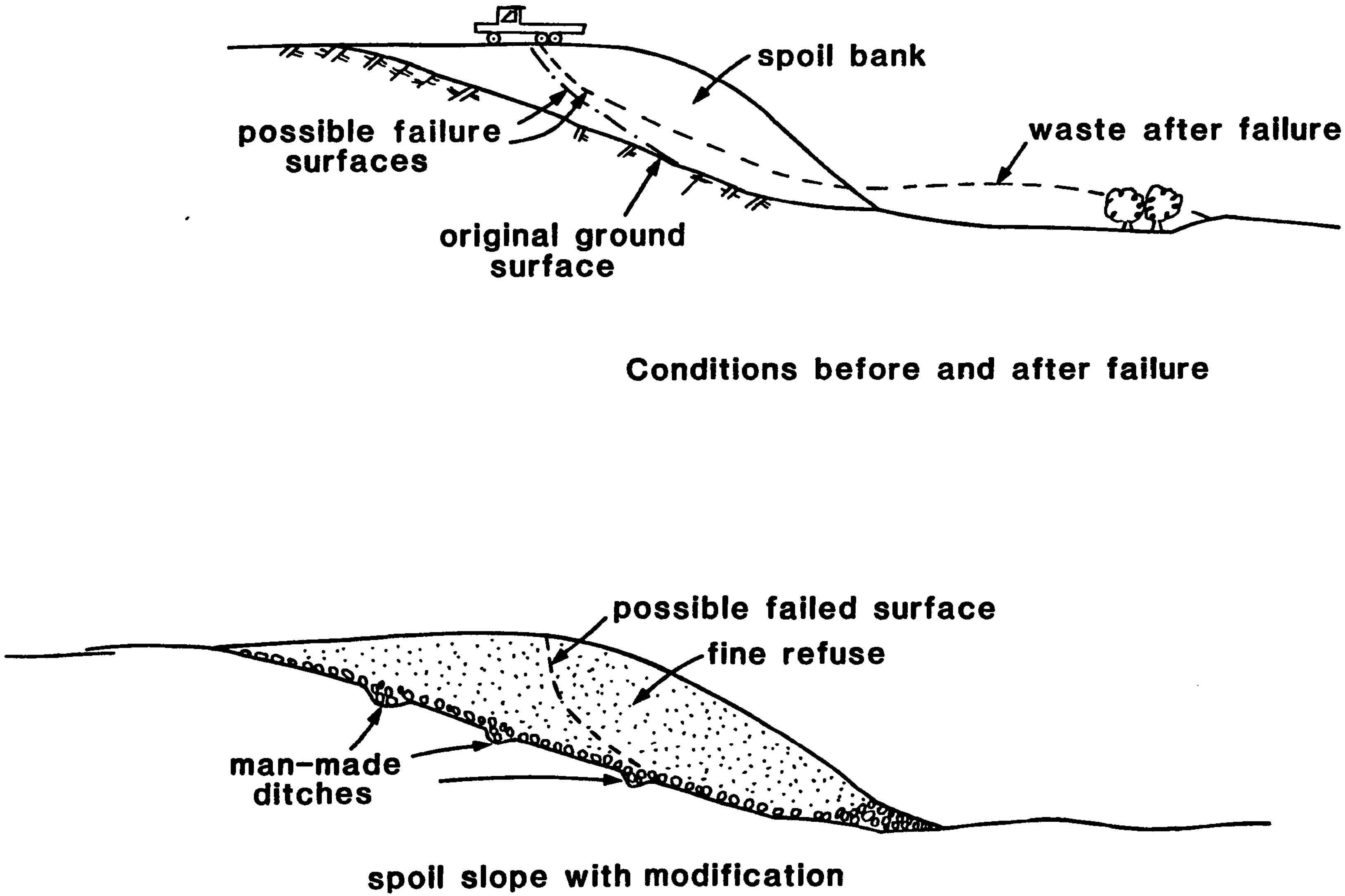

Figure 5-3, A typical cross section of a spoil bank.

the problem is statically indeterminate. The alternative is to employ assumptions in order to reduce the number of unknowns.

Bishop (1954), Janbu (1956), Mongenstern and Price (1975), Bell (1968) and others have attempted to develop a statically determinant procedure to determine the factor of safety for a sliding body. Each one has a set of particular assumptions and Bishop considers no external forces acting on the surface of the slope. Of these Janbu's and Bishops procedures are recommended in spoil slope analysis because they are less error prone.

It should be mentioned that there is considerable literature published on slope stability and its indeterminacy. The purpose of this section is not to present a comprehensive critique, but particular emphasis is placed on modification of the methods which are most applicable to the analysis of spoil and unconsolidated highwall throughout this research.

5.6 Plane Failure

One of the methods to store the waste from the first cut is to push it down the natural slope to form a sidehill bench which is called spoil bank. Figure 5-3, shows a typical cross section of a spoil bank.

There are two possible modes of failure for spoil banks; one involving plane failure surfaces which coincide with the

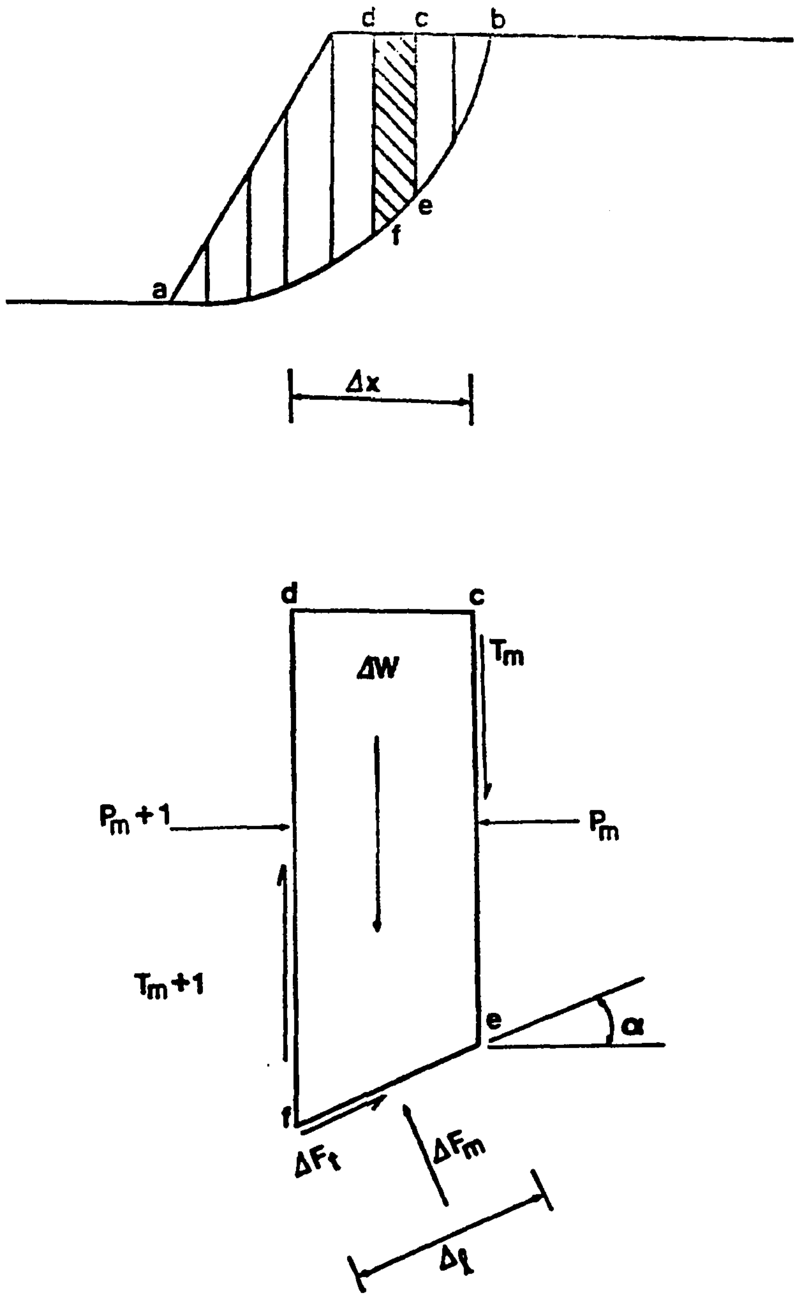

Bishop's assumption, no external forces on the face of the slope:

$$\Sigma(P_m - P_{m+1}) = 0$$
$$\Sigma(T_m - T_{m+1}) = 0$$

Figure 5-4, an illustration of indeterminacy of slice method.

original ground surface at the bottom of the fill, and the other involving circular or curved failure surfaces which lie entirely within the fill bench. The curved failure surface will be more critical if the shear strength of the spoil materials at the bottom are the same as the original ground surface. If the original ground surface is not cleaned of the organic material then the original ground surface is a plane of weakness and the plane failure is more critical. However, both modes of failure must be investigated and the one which gives the smaller safety factor will control the design.

The plane failure procedure has been utilized in analyizing the stability of surface mine spoil banks by Huang (1977). The analysis of plane failure with modification in Huang's approach in order to approximate reality in spoil bank stability is presented in this section.

Figure 5-5 illustrates the forces acting on a spoil bank. Huang established the following relationship for the factor of safety as

$$F = \frac{\bar{C}H\ CSC\alpha + (1-r_u)\ W \cos\alpha\ tg\,\bar{\phi}}{W \sin\alpha} \qquad 5\text{-}2$$

where

$\bar{C}$ is the effective cohesion of soil, H is the height, and H CSC α is the length of the failure plane and $\bar{\phi}$ is the effective angle of internal friction of soil. $\bar{N}$ is the effective force normal to the failure plane and W is the total weight of fill and r_u

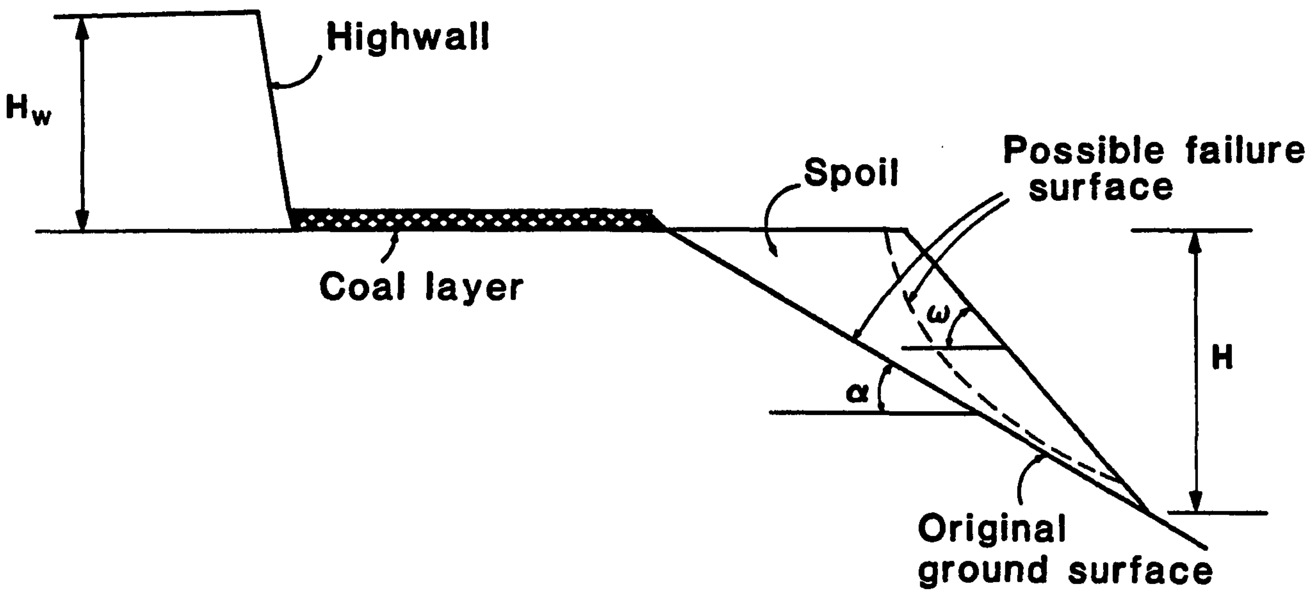

Cross section of a spoil bank
in a conventional contour mine

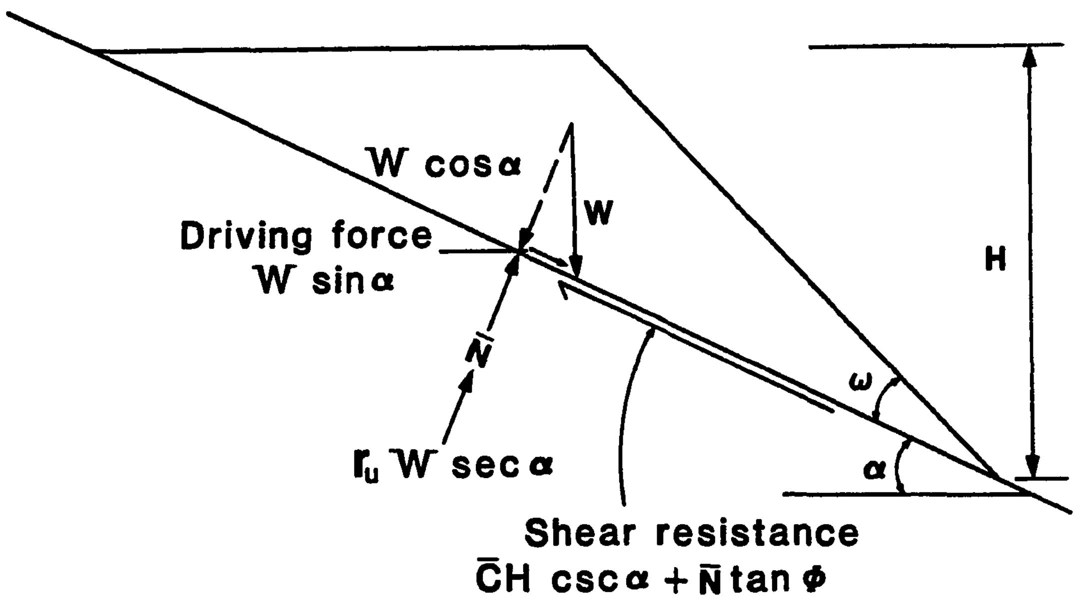

Figure 5-5, Forces on spoil bank. (HUANG, 1977) is the pore pressure ratio, which is a ratio between the pore pressure along the failure plance and the overburden pressure. For a derivation of relationship 5-2 the reader should consult Huang (1977).

The total weight of fill W can be written as

$$W = \tfrac{1}{2}\gamma H^2 \csc \omega \csc \alpha \sin(\omega - \alpha) \qquad 5\text{-}3$$

where

γ is the mass unit weight of fill.

Substituting W from Equation 5-3 into Equation 5-2, the safety factor is

$$F = 2 \sin\omega \csc\alpha \csc(\omega-\alpha) \left(\frac{\bar{C}}{\gamma H}\right) + (1-r_u) \tan\bar{\phi} \cot\alpha \qquad 5\text{-}4$$

If the interface of the original ground surface and the spoil or the interface of unconsolidated highwall and the coal layer is considered as a joint the $\bar{\phi}$ can be modified. Patten (1966) has reported that the roughness of joints can be taken into account by increasing the friction angle on the joint surface. If the discontinuity surface between the unconsolidated highwall and the coal layer or spoil and original ground surface is inclined at an angle i to the shear stress as shown in Figure 5-2, a relationship between the applied shear and normal stress can be written as:

$$\tau = \sigma \, tg(\phi + i) \qquad 5\text{-}5$$

Barton (1973) derived the following emprical equation:

$$\tau = \sigma \, tg \, (\phi + JRC \, . \, \log_{10} \frac{\sigma}{\sigma_i}) \qquad 5\text{-}6$$

Where JRC is a joint roughness coefficient which is between 5 and 20, and $\frac{\sigma}{\sigma_i}$ is effective normal stress to joint compressive strength ratio.

Barton's experiments were carried out at low normal stresses and his equation is applicable in the range $0.01 < \sigma/_{\sigma_i} < 0.3$. (Hoek and Bray, 1977) Since the normal stress in most rock slope stability problems falls within this range, the application of this equation is recommended.

By substituting the modified ϕ from Equation 5-6 into Equation 5-4, the safety factor is considered as:

$$F = 2 \, \mathrm{Sin} \, \omega \, \mathrm{CSC} \, \alpha \, \mathrm{CSC} \, (\omega - \alpha) \, (\frac{\overline{C}}{\gamma H}) + (1-r_u) \, tg \, (\overline{\phi} + JRC \log_{10} \frac{\sigma}{\sigma_i}) \, \mathrm{Cot}.\alpha \qquad 5\text{-}7$$

This equation is applicable when the original ground surface is covered by organic or loose materials with a lower shear strength as well as other similar cases.

If the original ground surface roughness is to be changed by man-made parallel ditches or if coarse refuse is deposited at the bottom of the fill as a blanket, the safety factor will be effectively modified. Experience indicates that the water within this coarse refuse drains freely thus the shear resistance will be increased.

If the interface between the unconsolidated highwall and the underlying coal layer is filled with a soft clay or fine material the method of analysis must be altered. Goodman(1970) showed experimental results which indicated that once the filling thickness exceeds the amplitude of the surface projections, the strength of the joint is controlled by the strength of the material.

Barton (1974) presented a comprehensive review of the shear strength of filled discontinuities and prepared a table for the shear strength values of the filled joints. If a major discontinuity with a significant thickness of infilling material is encountered in a mining excavation, the shear strength of the discontinuity should be taken as that for the infilling material. It is recommended that the shear strength of infilling material be determined in accordance with soil mechanics principles.

Appendix B shows application of a modified approach to spoil bank stability and a comparison with Huang's procedure.

5.7 Method of Slices

One of the most widely used methods for determining the factor of safety of a circular failure surface is the method of slices. This method permits the utilization of different values for C and ϕ for each slice. As previously discussed the indeterminacy is an important factor in this method.

Bishop (1955) extended the Slice Method by including the effect of forces between the slices (known as the Bishop Method of Slices). As mentioned before for each slice in Figure 5-4, there are three equations of equilibrium and more unknowns. Thus the problem is statically indeterminate. It is necessary to employ assumptions in order to reduce the number of unknowns. The force ΔW is assumed to act vertically through the center of the slice, while ΔF_m acts perpendicular to the base of the slice at the midpoint. ΔF_t is the shear force required to maintain equilibrium. Conversly if the resultants of the interslice forces are assumed to be equal and opposite they cancel one another, a situation handled by the Ordinary Method of Slices. Bishop expressed that the value of safety factor using the Ordinary Method of Slices is conservative when compared to the Bishop Method of Slices. By summing forces in a directional normal to the shear surface at the midpoint of each slice, the safety factor for the Ordinary Method of Slices becomes as:

$$F_s = \frac{\Sigma\{\bar{c}\Delta\ell + \left[(\Delta W + Q)\ \mathrm{Cos}\alpha - \Delta p \Delta\ell\right] \mathrm{tg}\bar{\phi}}{\Sigma\ (\Delta W + Q)\,\mathrm{Sin}\alpha}$$

where

W The total weight of the slice of soil

$\Delta\ell$ The length of the slice of soil

α The angle of inclination of slip surface

Δp The excess pore pressure

In the Bishop Method by considering the interslice forces, the expression for the safety factor is

$$F_s = \frac{\Sigma \{ \bar{c}\Delta\ell \text{Cos}\alpha + \left[(\Delta W + Q - \Delta p \Delta\ell \text{ Cos}\alpha) + (T_m - T_{m+1}) \right] tg\bar{\phi} \} \dfrac{1}{\text{Cos}\alpha + (tg\bar{\phi}\dfrac{\sin\alpha}{F_s})}}{\Sigma \Delta W \sin\alpha}$$

For the details of derivation the reader can refer to the given reference. Bishop assumes that if no external forces are present and the slope is stable, then

$$\Sigma(P_m - P_{m+1}) = 0$$

$$\Sigma(T_m - T_{m+1}) = 0$$

where

P_m, P_{m+1} - The resultants of the total horizontal forces, including the effect of seepage if present

T_m, T_{m+1} - The vertical shear forces on sections m and m+1 respectively

Bishop's method involves a lengthy process of determining the safety factor. An initial value is assumed for F_s by taking $(T_m - T_{m+1}) = 0$, then the values of $(T_m - T_{m+1})$ are adjusted to satisfy the condition such as $\Sigma(P_m - P_{m+1}) = 0$.

Bishop suggested that in most cases the factor of safety given by $(T_m - T_{m+1}) = 0$ is sufficiently accurate. This method is known as Bishop's Simplified Method and assumes that the interslice forces are horizontal. Wright (1973) has shown that the variation in F_s by either method is less than 6%.

Spencer (1967) expressed that the error involved in the Bishop Simplified Method is conservative.

Janbu (1954) applied the method of slices to limit equilibrium analysis in which composite or general failure surfaces were investigated. In this analysis he assumed the same assumptions employed in Bishop's Simplified Method. In Bishop's approach the moments are taken about a central location which is the center of the circular arc; whereas in Janbu's Method moments are taken about the midpoint of the base of each slice.

When the shape of the failure surface is not circular as a result of some structural feature such as the spoil waste and rock interface or loose highwall and coal layer interface, the conditions assumed in deriving the circular failure charts are no longer valid. Significant errors can arise from the application of the circular failure charts in such cases, particularly when low shear planar features such as spoil and original ground surface form part of failure surface. Consequently, a more accurate form of analysis must be used.

Janbu's Method of analysing non-circular failure is simple enough to permit the solution of strip mine problems by hand. The earthquake force can be taken as 0.05 times the weight of the slice and applied as a horizontal force at the centroid of each slice (Cowhered, 1977).

In appendix B a hypethetical problem is solved using various methods. Using Huang's approach, considering the plane of weakness as a joint, the safety factor is decreased and the modified procedure is more conservative.

5.8 Variational Method

The calculus of variations allows the determination of the critical sliding line without the necessity of estimating the slip surface shape. The method has been applied by Garber (1973), Biermatowski (1976), Revilla and Castillo (1977), Garber and Baker (1979).

The work in Appendix B is an extension of Revilla and Castillo (1977) research. The non-linear equations have been solved using numerical techniques in order to obtain the safety factor. Since their method is based on Janbu's method considering cohesive soils and since strip mine spoil is not a cohesive waste, the method is not recommended for the case under consideration.

Furthermore the approach is not applicable to cohesive highwalls since the external loading and plane of weakness is not included.

Chapter 6

AN ANALYSIS OF THE FAILURE OF OVERCONSOLIDATED AND BRITTLE ROCKS USING THE FINITE ELEMENT TECHNIQUE

6.1 Introduction

The fact that heavily overconsolidated, fissured clays and clay shales cannot be analysed by conventional methods has been mentioned before. It has been pointed out by Bishop (1976) that the error associated with conventional methods is related to the brittleness of this type of rock. Skempton (1965) and Bjerrum (1967) discussed the importance of the stress-strain characteristics of such rock. Furthermore, Duncan and Dunlop (1969) discussed the effect of initial stress conditions in overconsolidated clays and shales that may contribute to the slope stability of such rock. This study was performed using a plane strain formulation of the finite element technique.

Deformation and fracture in these rocks are related to the complex process of deformation due to loading and unloading in the past. The hysteresis loop formed in a loading-unloading cycle, (which in a sense is an indication that energy has been dissipated) cannot be justified for overconsolidated clay rock. It appears that the strain energy is stored in the rock, but at present there is no generalized model to explain the effect of this process adequately. Also the stress-strain relationships found in the laboratory do not include the type of elastic rebound that occurs at the site (Emery, 1966).

The model under consideration for simulation of a strip mine by the finite element method is based on the model suggested by Dunlop and Duncan for a slope but combined with a simplified approach for the plane of weakness.

6.2 Classification and Identification of Rock

Field investigation has shown that the rock which typically overlies coal layers in Oklahoma can be divided in three groups, clay, brittle shale and hard shale. Clay can be either cohesive normally consolidated clay or overconsolidated clay. Brittle shale can be weathered shale or overconsolidated clay shale. Hard shale includes both stiff fissured shale and intact shale free from joints and fissures. In occasional sections coal deposits may be covered by sandstone, limestone or varied rock types.

In the previous chapter it was mentioned that the equilibrium method can be applied to normally consolidated clay. This chapter includes the application of the finite element method to the analysis of a working highwall consisting of overconsolidated clay, clay shale and intact hard rock.

6.3 Initial Stresses

The most important factor affecting the behavior of an excavated slope is its initial stress state. These stresses might be measured but are usually estimated. The vertical stresses are assumed to be equal to the overburden pressure and the horizonal stresses are equal to K (earth pressure coefficient) times overburden pressure. For a normally consolidated rock, the value of K can be calculated from elasticity considerations $K = \frac{\nu}{(1-\nu)}$.

For an overconsolidated rock that has been under cyclic loading and unloading the difficulties in estimating the initial stresses are greater. In fact the erosion of overlying rock will increase the value of the earth pressure coefficient. The value of K is estimated using the following relationship for over-consolidated rock (Goodman, 1980)

$$K = K_o + \left[\left(K_o - \frac{\nu}{1-\nu}\right) \Delta Z \right] \cdot \frac{1}{Z} \qquad 6\text{-}1$$

where

K_o = initial value of earth pressure coefficient before unloading

Z_o = the depth before unloading

Δ_Z = the thickness of the removed overburden

ν = Poisson's ratio

The vertical and horizonal stresses can be calculated from following relationships

$$\sigma_y = \gamma Z - P_w \qquad 6\text{-}2$$

$$\sigma_x = K\sigma_y \qquad 6\text{-}3$$

In equations 6-2 and 6-3 γ is the unit weight of rock and P_w is the pore water pressure. For the cases where the rock is below ground water level, the saturated unit weight is considered.

6.4 Residual Stresses

In addition to the initial stress (gravitational stress) caused by rock loading from its own weight there are residual stresses which are due to the tectonic history of the rock formation. These stresses developed due to a variety of causes, including the shrinking earth's crust, plate collesions, mountain building, etc. The stress field in the earth's crust is so complicated that the rock mass seldom gives sufficient information to predict the stresses resulting from this past tectonic activity. However, the gravitational forces combined with horizontal residual forces can provide an important influence on the stability of deep strip mine slopes.

Jointed rocks and soft sedimentary rocks cannot long retain residual stresses because in the jointed rock the stress has been relieved by fracturing and in the sedimentary rock as well as igneous rocks (Piteau, 1970), can retain high residual stresses.

Near surface stress measurements in hard rock areas have in some cases shown that the horizontal stress component at the surface can be much greater than the vertical stress. At Grand Coulee Dam, Washington, the Bureau of Reclamation measured horizontal in situ stresses which were 6 times the lithostatic stress (Dodd, Anderson, 1971). High lateral stress in a mine near Barberton, Ohio also has been reported (Long, 1963).

It is important to mention that the residual lateral stress should not be confused by lateral stress due to overconsolidation. But, in general, in Oklahoma strip mines no residual stresses are expected due to the existance of relatively soft rock.

6.5 Creep

Creep is a time-dependent strain and can be expected on a slope where high stresses are concentrated for a long time (Murral, Misra, 1962).

In general, deformations due to time are negligible in hard rock excavations but for soft rocks such as shale and mudstone, creep deformations can be readily seen and may lead to failure within days (Piteau, 1970).

Creep is not an important factor in the stability of strip mine slopes since a working highwall is constantly being altered during the excavation operation.

6.6 Groundwater

The water pressure distribution depends on the geologic structure, the permeability and the storage capacity of the rock mass. Raising the watertable increases water pressure and consequently creates a possible failure condition. Instability related to groundwater pressures follows several different mechanisms that provide the condition of failure of the slope structure (Terzaghi, 1962, Muller, 1964, Serafin, 1968).

High storage capacity creates high hydrostatic pressures in the saturated rock mass. These hydrostatic pressures are both lateral and vertical and their intensity increases with depth.

Groundwater fluctuations (rises and drawdown in the water level), change the hydrostatic pressure. To model the fluctuating hydrostatic pressure, forces are calculated and applied to the nodal points of the elements. Both uplift and lateral forces should be calculated and applied to the nodal points of each element. The uplift force U is equal to

$$U = \gamma_w \cdot V_s - \gamma\left(\frac{V_v}{2}\right) \qquad 6\text{-}4$$

where γ_w is the unit weight of water, γ is the densitv of rock and V_s is the volume of solids in the element and V_v is the voids of the element (Efrossini, 1975).

The lateral forces are equal to the hydrostatic pressure times the length of the solid at the triangular element.

The rate of lowering of the groundwater level depends on the rate of excavation. Because of the higher rate of excavation in strip mining the equilibrium position can not be reached during the excavation operation. Therefore, in order to specify the groundwater boundary on the finite element model, field observation and measurement is necessary.

6.7 Dynamic Loading

The dynamic loading in slope structures is usually concentrated on exposed surfaces and the maximum seismic force produced should be evaluated under its most unfavorable orientation. The vibrational loading caused by the use of heavy construction equipment, i.e., drag line, can induce such a dynamic stress field, as can earthquakes and blasting.

In strip mining operations frequent blasting is required. No catastrophic failures have been reported to date in Oklahoma. It is reasonable to assume that the influence of blasting on slope stability results only in temporary deterioration of the rock properties.

To simulate the earthquake effect in a finite element model the horizontal forces can be introduced as nodal point forces. These new horizontal forces are equal to: (Efrossini, 1975)

$$F_H = (F_{HO})\ C + (F_V)\ C$$

where

F_H is the horizontal force including earthquake effect, and

F_{HO} is the horizontal force due to excavation, and

F_V is the vertical force due to excavation, and

C is the earthquake coefficient.

The earthquake coefficient can be obtained by dividing the measured acceleration by acceleration of gravity g.

Finally, the state of stress for each element after including dynamic loading, is calculated by adding the stress changes to the initial stress values.

6.8 Simulation of Excavation

The study of excavation was carried out by plane strain analysis which reduces a real three-dimensional problem to two-dimensions (Appendix C). A three-dimensional solution requires a much greater number of computations and is generally too expensive and complex to analyze. Such a simplification of the three-dimensional problem to a two-dimensional one is needed in order to achieve a strip mine analysis. The results of the two-dimensional analysis can then be interpreted in terms of their applicability to the actual three-dimensional geometry and excavation sequences.

The process of excavation was simulated by computing the forces acting on the excavated slope face and applying the opposite of these forces to the same surface on the nodal points, Figure 6-1. The final state of stress for each element was estimated by adding the stress variation due to excavation to the intial stress values.

It has been shown that for a homogenous, isotropic, linear elastic material the resulting stresses are independent of the excavation sequence, therefore analysis involving a single step of excavation or a number of steps should give the same results (Dunlop, 1970). Thus the single step approach for simulating the excavation of Oklahoma strip mines is suggested.

The displacements to be considered are those which are induced by the excavated rock. The load is applied as a concentrated force on related nodal points. Therefore it is an appropriate assumption to consider the initial displacements and strains to be equal to zero before application of loads. The displacements are obtained by standard structural methods.

Since shear strength is assumed to be constant in the structure, a constant modulus of elasticity can be applied in the analysis (Dunlop, 1969).

6.9 Boundary Condition

A trianglar finite element mesh is used for stress analysis. The structure is divided into a number of horizontal or inclined straight lines which are not permitted to intersect each other. The end points of each line are on the boundary of the structural model. Each line is further divided into a number of intervals of either equal or arbitrary length. Special attention was paid to insure that the lateral boundaries in this model were sufficiently distant from the slope face. Thus the boundary nodal points are considered as fixed boundary nodes. The nodal points along the bottom boundary were constrained from moving vertically, simulating the preexisting weakness plane between coal and rock. A typical mesh with numbering of nodal points, coordinates and elements is shown in figure 6-2.

Although the stress conditions in the region immediately adjacent to the slope and the front surface are considered to be of primary interest in this chapter, the failure surface, the movement of the front surface, as well as the displacements on the other boundaries will illustrate the importance of model simulation.

6.10 Failure and Safety Factor

For the case of constant modulus throughout the depth, if shear stress values are equal to the undrained shear

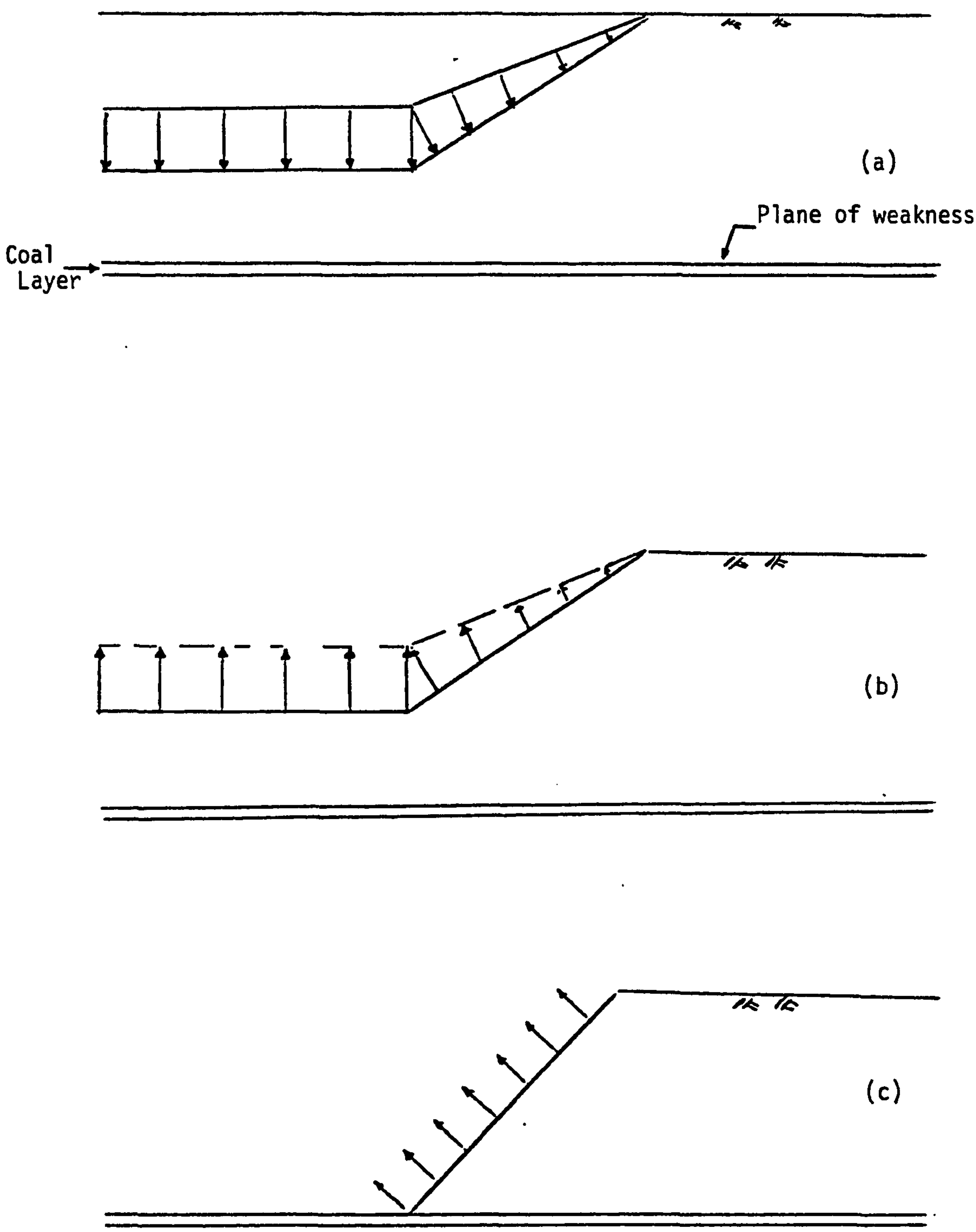

Figure 6-1 Analytic Simulation of Excavation

strength of the clay failure will occur. The undrained shear strength of the clay can be determined in the laboratory but the value can be assumed based on previous experiments.

There are several methods for determining the failure surface location. Brown and King (1966) have illustrated that the failure surface is made up of trajectories of maximum shear stress directions.

The factor of safety is defined as the ratio of the shear strength to the shear force along the failure surface. First it is required to calculate shear stress and normal stress at any point. Second, normal stresses and shear stresses along the failure surface may be obtained. Consider Figure 6-3, stresses σ_x, σ_y, τ_{xy} should be calculated by the numerical technique. Assume point A is on a line, tangent to the failure surface and σ_n normal stress and τ_{nm} shear stress at that surface. The angle θ is the angle between the tangent at A and the line normal to the x-axis. Then the normal and shear stress on the failure surface at point A can be determined by

$$\sigma_n = \tfrac{1}{2} (\sigma_x + \sigma_y) + \tfrac{1}{2} (\sigma_x - \sigma_y) \text{ Cos } 2\theta + \tau_{xy} \text{ Sin } 2\theta \qquad 6\text{-}3$$

$$\tau_{nm} = \tau_{xy} \text{ Cos } 2\theta - \tfrac{1}{2}(\sigma_x - \sigma_y) \text{ Sin } 2\theta \qquad 6\text{-}4$$

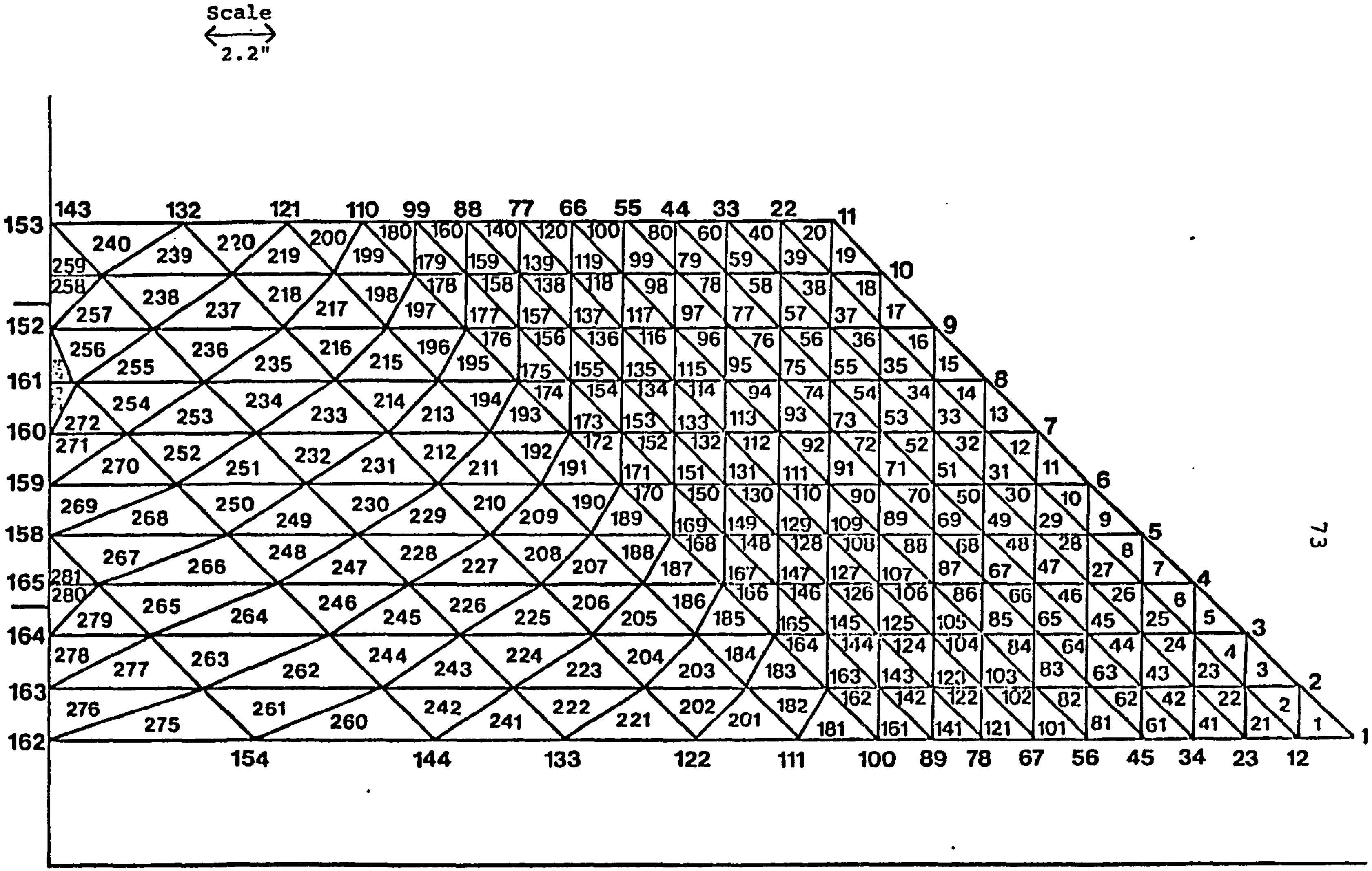

Figure 6-2, Slope structure for model and a real strip mine

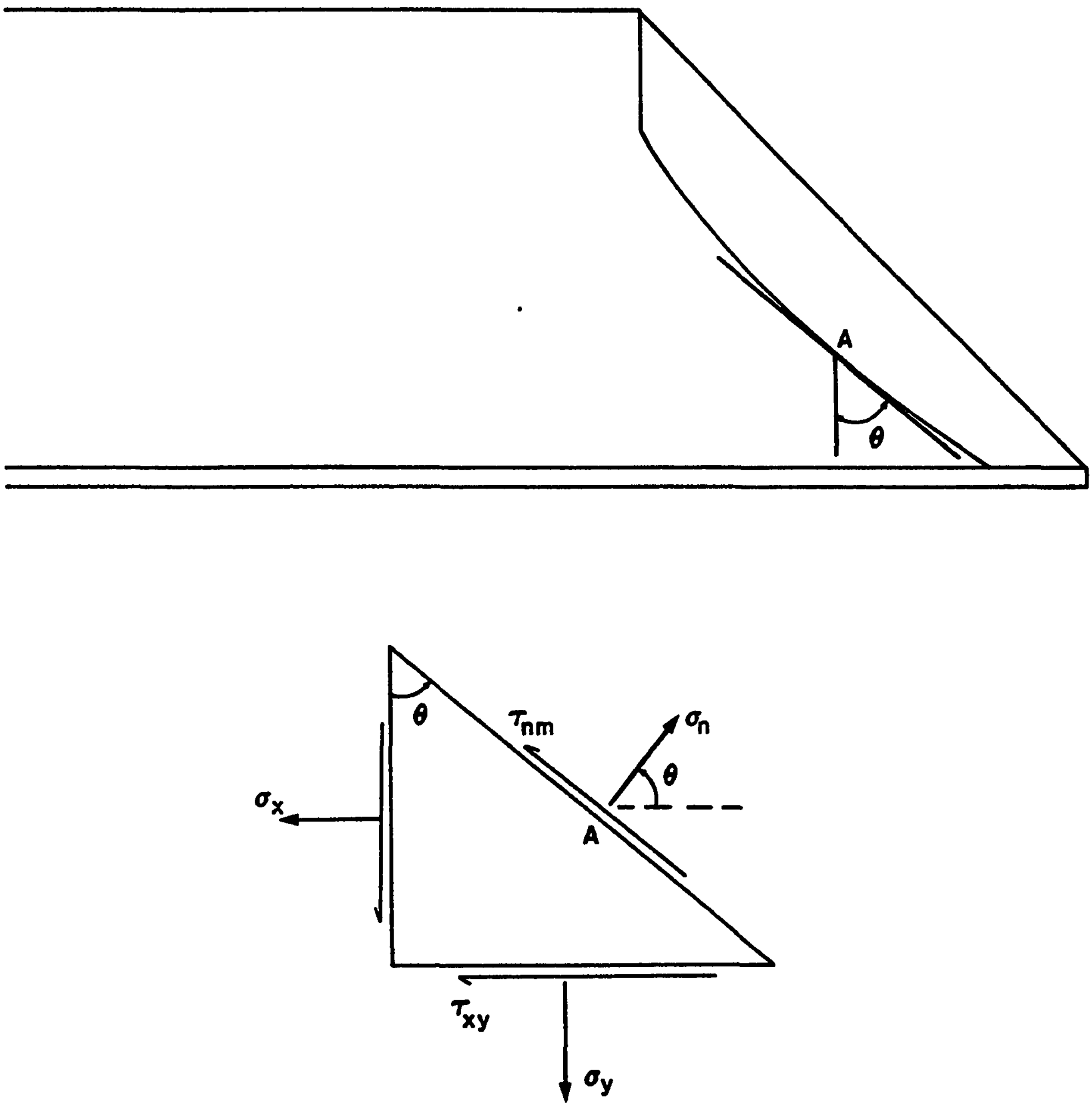

Figure 6–3, Stresses at a point on a Failure Surface.

Knowing the principal stresses from finite element analysis, the normal and shear stresses at every point along the failure surface can be determined by equations 6-3 and 6-4. Then by substituting σ_n in the Coulomb equation, the shear resistance can be obtained.

$$\tau = C + \sigma_n \operatorname{tg}\phi \qquad 6\text{-}5$$

C and ϕ are already defined. The total shear strength and total shear force are obtained by summing the shear strengths and shear stresses at all points along the failure surface. The factor of safety is defined as:

$$F_s = \frac{\Sigma(C + \sigma_n \operatorname{tg}\phi)\, dL}{\Sigma\tau_{mn}\, dL} \qquad 6\text{-}6$$

where dL is defined as an incremental length.

6.11 Stress Distribution Along the Plane of Weakness

Within an infilling material or in the vicinity of a shear zone the displacement related to reduction of shear strength combined with dilatory effects and secondary fractures can be observed. Finite element modeling and formulation for stress distribution along such a shear zone is not fully developed. Only a small number of contributions to the numerical analysis of the detailed behavior of rock joints in direct shear have been made. This can be related to the difficulties of specifying the constitutive laws for the behavior of rock materials and joints and evaluating the respective parameters. However, the existence of weak structural planes in a rock slope body, or in the rocks surrounding a mine excavation may play an all-important role in rock stability. In analytical computations for rock mechanics important research topics consist of simulating these weak planes and reflecting their mechanical non-linear properties (Jun, 1979). Of the few models describing the effect of weak planes, the following have some bearing on the problem under consideration:

Goodman (1974) suggested a joint element model with emphasis on mechanical non-linear properties of joints.

Ghaboussi et al (1973) explained slip elements that model rock joints, faults and interfaces with finite element analysis.

Byrne (1974) incorporated a transversely isotropic filling material in the joint element formulation.

Jun (1979) suggested an analytical model for the mechanical non-linear properties of the simulated joint planes based on in situ direct shear testing data.

Hously and Worth (1980) have suggested that the only appropriate constitutive relationship for an intensely sheared region is one involving no dilation.

Analytical results reported by Goodman and Dubios (1972) have illustrated that, for planar joints with low values of i (less than five), the dilatancy effects may not be large. For the case of the strip mines in Oklahoma the joint surfaces are mostly planar. It is sufficient to account for the joint roughness by adjusting the joint friction angle only and assuming that there is no dilatancy.

The simulation of the plane of weakness as a simplified method was performed in this study by considering the rock mass adjacent to the discontinuity as a continuum with fixed boundary conditions. The shear strength of the plane of weakness was calculated by Barton's equation. If the shear stress on the nodal points calculated by finite element representing the weakness plane is greater than the shear strength calculated from Barton's equation, then it is assumed that failure on the joints had accurred.

6.12 Coal Layer

Lateral elongation in the coal layer will generally occur throughout its full depth following completion of the key cut in the coal layer. As discussed in the chapter three the model is designed based on the fact that there is no key cut. Therefore, analysis of the coal layer is not an important subject in Oklahoma strip mines.

Attempts to understand the elastic and engineering properties of a coal layer are as yet quite basic and preliminary, and any conclusions are to be considered tentative. For example little is known concerning the stiffness and strength of coal. This section will review existing methods and propose extentions to be used in this analysis of the stability of the coal layer.

The application of the finite element technique to the coal layer requires detailed knowledge of the constitutive relations of the coal materials involved. Unfortunately, in the present state of knowledge, there is no generally accepted understanding of these relations. The determination of the compliances based on constitutive relations of coal in a laboratory shows considerable scatter. This should be expected for a heterogenous material such as coal that contains numerous bedding planes. Each bedding plane contains visible layers such as fusain or calcite that are oriented in the direction of the bedding planes.

Consequently in the past distribution of compliance values has been determined based on statistical analysis (Atkinson, 1976).

The compliance matrices include non-symmetry in the off-diagonal terms, indicating that the coal layer connot be considered as a single intact isotropic layer. The compliances obtained by loading normal to the bedding planes are different from those obtained by loading parallel to the bedding planes. The presence of the non-symmetry may therefore be related to the bedding planes (Atkinson, 1976) (Van, 1975).

Previous studies have neglected the non-symmetry of the compliance matrix, and a symmetric compliance matrix is assumed.

Finite element analysis programs require material property input in the stiffness matrix and this is possible if the compliance matrix is non-singular.

Inspection of a coal layer reveals the existance of horizontal bedding planes and two sets of vertical cracks called cleats which are nearly perpendicular to one another. It is reasonable to assume that the mechanical behavior of coal will be influenced by this orthogonal system and a transversely anisotropic or an orthotropic material model is a good approximation. The stiffness matrix based on a transversely anisotropic material model is arranged in Appendix C.

In the closed form solution the coal layer can be assumed to be formed of n laminae bonded together to make a laminate and to act as an integral structural element.

The stiffness of such a composite material configuration can be obtained from the properties of the constituent laminae by well known procedures. The coal laminate is assumed to consist of perfectly bonded orthotropic laminae, and infinitesimally thin bonds with no shear deformation. Consequently, the displacements are continuous across the laminae boundaries so that no laminae can slip relative to another. Therefore the coal layer laminates acts as a single layer with known special properties for each laminae. The assumptions require the determination of the mechanical properties of each bedding planes.

Appendix D includes the application of mechanics of composite material to the coal layer and with this approach the stresses, strains and occurance of failure in a coal layer can be predicted.

6.13 Output Discussion

In order to obtain information concerning the failure surface and movement of the model structure, a finite element mesh (Figure 6-2) with 281 triangle elements and 164 nodal points were analyzed. Both uniform and non-uniform meshes were used since the meshes can be made finer around the failure surface where high shear stress trajectories are expected. Based on observations from the physical model, the nodal points on the vertical boundaries far from the slope surface and the plane of weakness are constrained from moving in either direction. The assumed effective stress parameters of rock are $\nu = 0.2$ and $E = 54000$ Psi.

The behavior of the slope model subjected to four concentrated vertical loads on nodes number 11, 22, 33, 44 were analyzed in order to investigate the slip surface shape and the most critical displacement on the front surface of the slope. For each run the structure was subjected to four different concentrated loads of 5, 10, 20 and 30 kips and is treated similar to the problem discussed in the experimental chapter with the application of the theory of elasticity.

The movement of the nodal points on the front surface represents the displacement of the body. Like the physical model the external load was applied on the top surface and the displacement of the front surface was carefully studied.

The finite element solution gives the displacement of all the nodes within the slope structure but the displacement of the nodal points 1 to 11 located along the front surface are given more importance in this study. When the displacement for 1 to 11 were plotted, (figure 6-4) node number five was found to undergo the largest displacement. This node is therefore chosen as the reference from which the displacement data is presented in terms of the load-displacement curve.

Comparing the displacements for this model (figure 6-4) with the physical model (figure 4-3) it can be seen that the patterns of the variation of displacement with depth at the front surface are almost identical at all locations. The results indicate that the displacement of node number 1 is zero as expected due to its position on the boundary.

Yielding first occurs around the elements 18 and 36, then concurrently spreads upward toward the ground surface and downward to the plane of weakness. This is what has been seen in the physical model. Elements such as 80, 98, 116, 134 and 152 are located in the tension zone and it is in this region that a tension crack was noted in the experimental study before complete failure occured. As the loading was increased, more tension zones are developed farther from the slope surface and this also has been seen in the physical model. Therefore, in a real strip mine as the floor of excavation gets deeper (called loading) more cracks can be expected further from the excavation. Some individual elements close to the ground surface and adjacent to the front surface yield at very low load levels. This is due to local bulging that helps to reduce the potential yielding stresses. This should not be considered as a part of the failure surface but can be understood as a local collapse. Figures 6-5 and 6-6 show the failed elements that make up the failure surface for the model. When the failure surface from the experimental study (Figure 4-10-2, Appendix A) is compared to the failure surface obtained from the numerical study (Figures 6-5 and 6-6) good agreement is noted for hard rock. In general, the failure surface has minor changings for the variation of the applied loads.

The finite element program has been run for a working highwall with a 45^0 slope angle and 100 feet height. The vertical boundary is placed 250 feet away from the toe. The nodal points on the vertical boundary and the plane of weakness are constrained from moving in either direction.

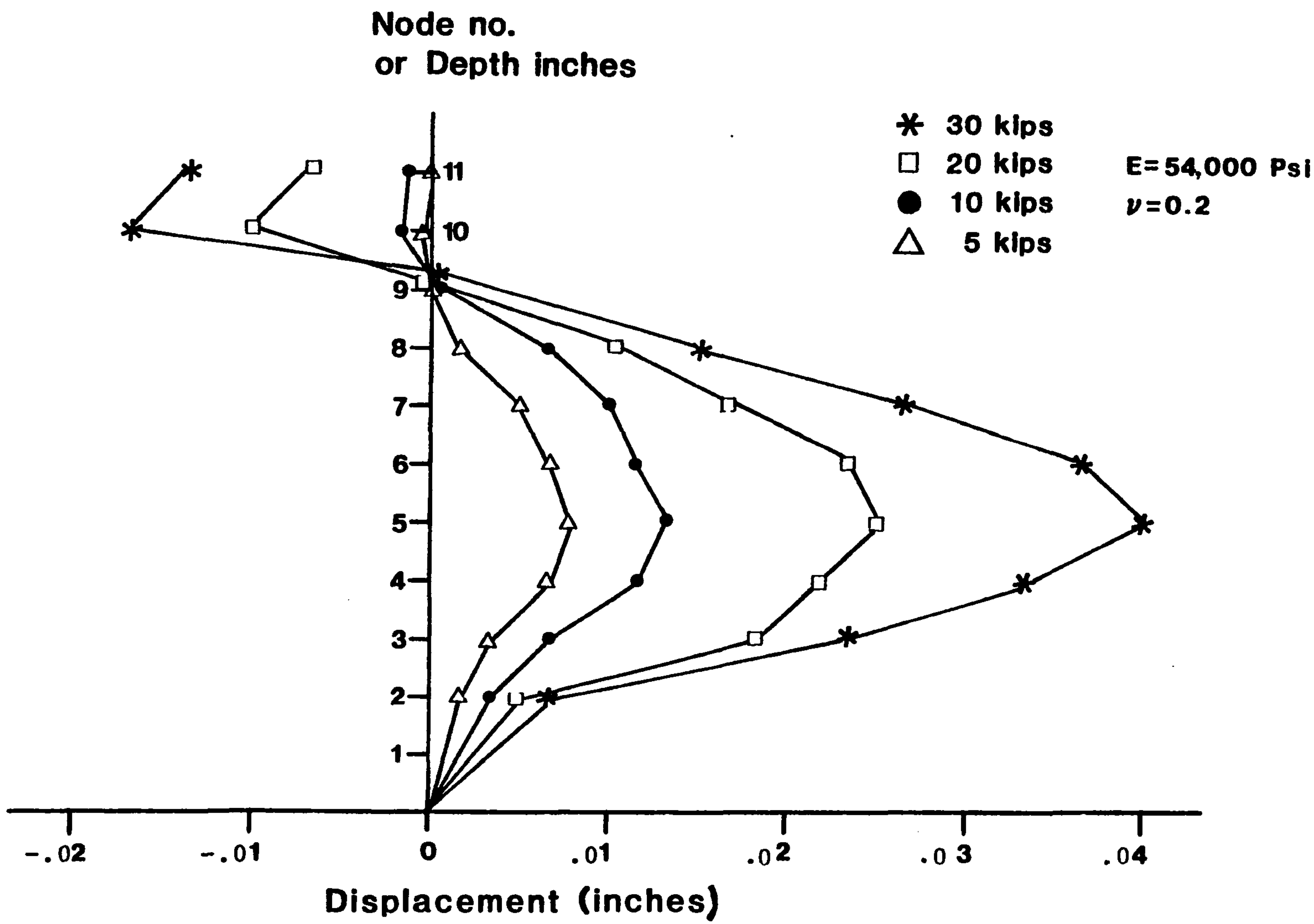

Figure 6-4, Maximum displacement at the front surface of model
(E=54000 Psi, ν=0.2)

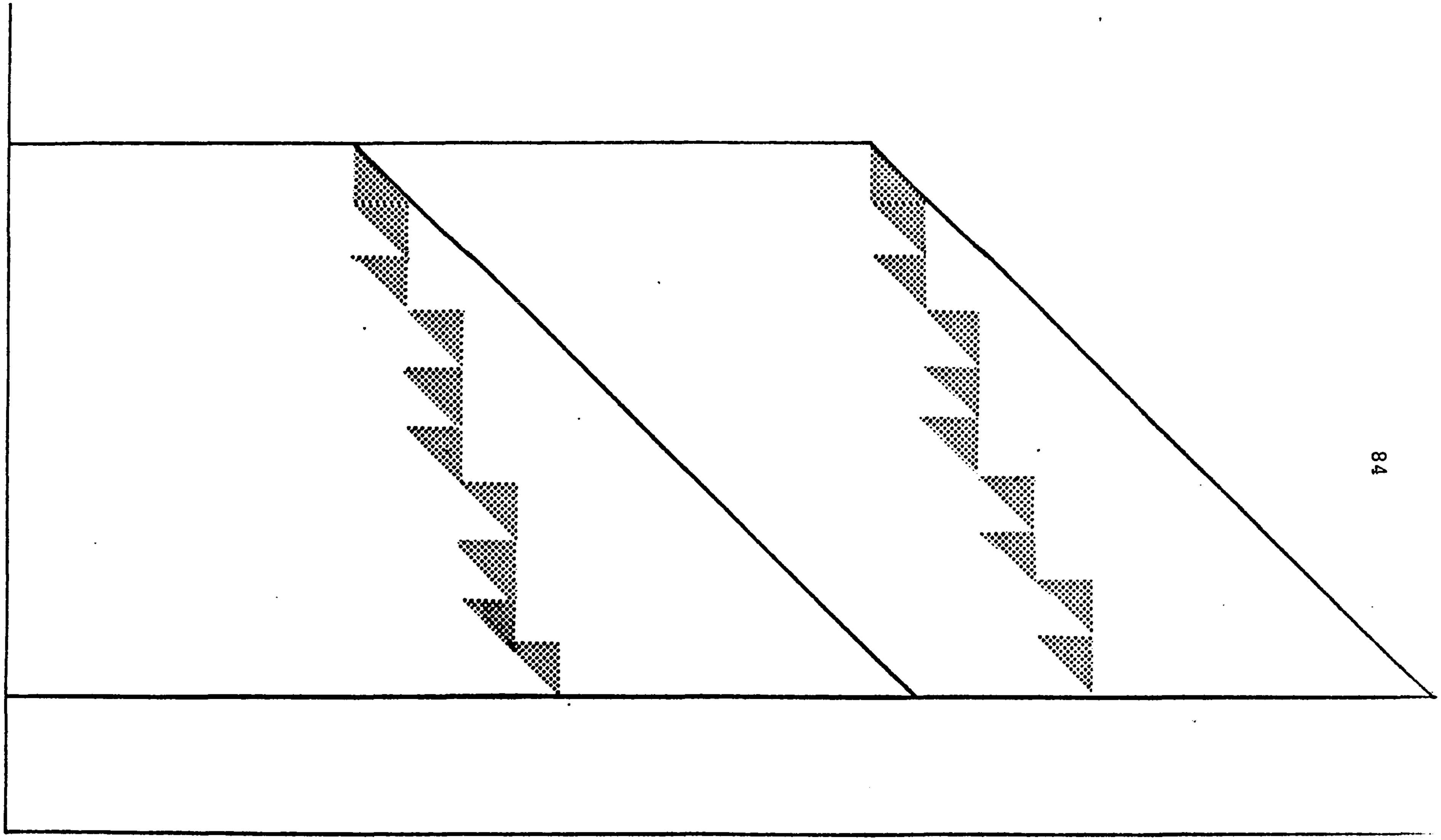

(a) Failure surface for model with 10 Kips Concentrated load on nodes 11, 22, 33, 44

$E = 0.54 \times 10^5$ Psi, $\nu = 0.2$

(b) Failure surface for model with 5 Kips Concentrated load on nodes 11, 22, 33, 44.

$E = 0.54 \times 10^5$ Psi, $\nu = 0.2$

Figure 6-5, Failure Surface For Finite Element Model

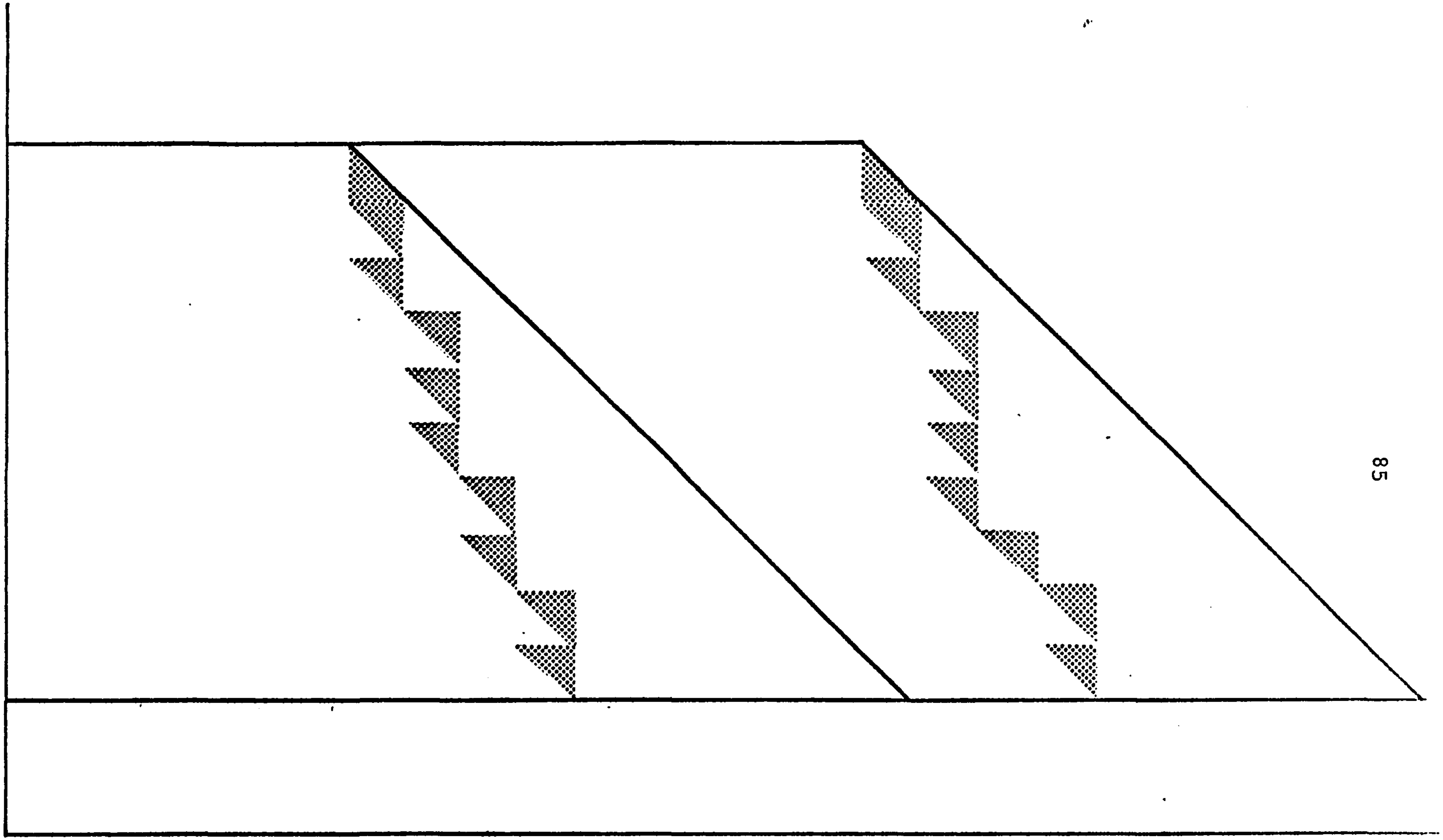

(a) Failure surface for model with 30 Kips concentrated load on nodes 11, 22, 33,44

$E = 0.54 \times 10^5$ Psi, $\nu = 0.2$

(b) Failure surface for model with 20 Kips. Concentrated load on nodes 11, 22, 33, 44

$E = 0.54 \times 10^5$, $\nu = 0.2$

Figure 6-6, Failure Surface For Model

First, the structure was considered as a normally consolidated rock and 30 kips concentrated load was applied on nodal points 11, 22, 33, 44. The lateral earth coefficient varies while other variables are constant. Of all the nodal points located along the front surface, number 5 has been found to undergo the largest displacemnt. Table 6-1, shows the variation of the maximum displacement at node number five for different lateral earth coefficients.

Figures 6-7 and 6-8, illustrate the possible failure surfaces for lateral earth coefficients 0.4 and 0.8. It can be said that by increasing the lateral earth coefficient, the failure surface for a working highwall moves toward the slope surface. In order to indicate the stress variation the structure is divided into six sections and tables 6-2 and 6-3 illustrate the maximum stress variation with changing lateral earth coefficient. It is concluded that variation of the lateral earth coefficient has a significant effect on the stress pattern of the slope. The principal stresses σ_x and τ_{xy} have been increased but σ_y was decreased. It is observed that excavation produces greater variations in the stresses at the lower part of the slope than the upper part and high stress concentration is located around the fixed boundary, node number one. The variation of stress σ_y is higher than the variation of stress σ_x and τ_{xy}.

Table 6-1, Maximum Displacement at Node Number 5 for Different Lateral Earth Coefficients, normally consolidated rock.

Case No.	K Lateral Earth Coefficient	γ, lb/ft^3 Density	ν Poisson's Ratio	E, Psi Modulus of Elasticity	Max. Displ. at Node No. 5, ft
1	0.4	160	0.2	0.75×10^6	0.8099×10^{-3}
2	0.5	160	0.2	0.75×10^6	0.1119×10^{-2}
3	0.6	160	0.2	0.75×10^6	0.14312×10^{-2}
4	0.7	160	0.2	0.75×10^6	0.17242×10^{-2}
5	0.8	160	0.2	0.75×10^6	0.20704×10^{-2}

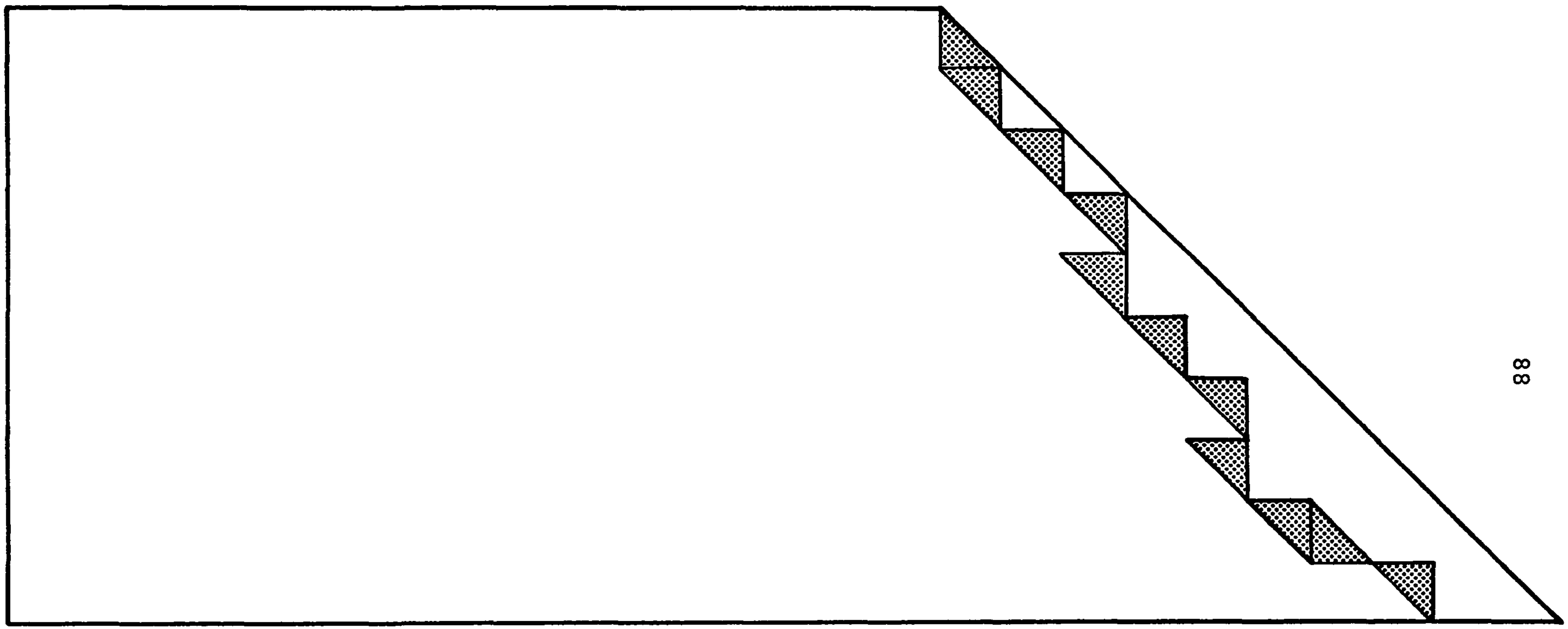

Figure 6-7, Failure surface for normally consolidated rock with 30 Kips concentrated load on nodes 11,12,33,44,

$E = 0.76 \times 10^6$ Psi, $\nu = 0.2$, $\gamma = 160$ Pcf, $K = 0.4$

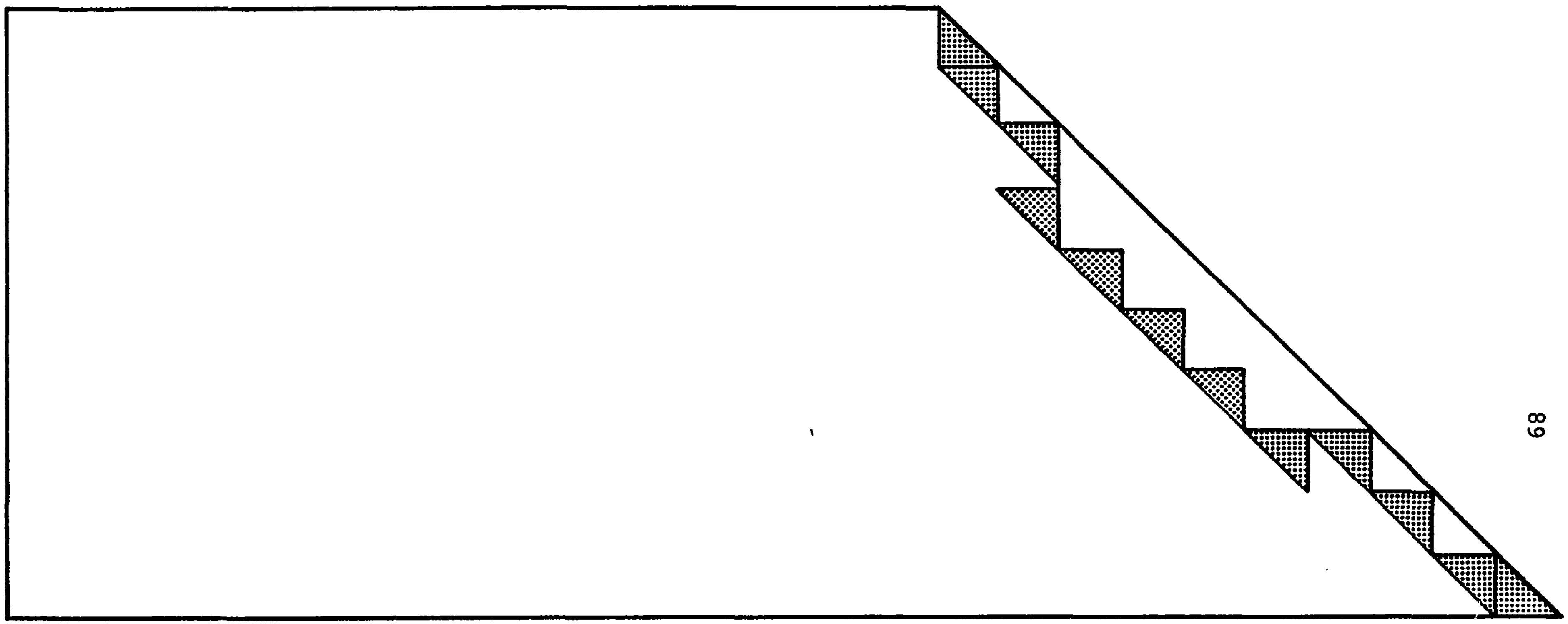

Figure 6-8, Failure surface for normally consolidated rock with 30 Kips concentrated load on nodes 11, 22, 33, 44,

$E = 0.76 \times 10^6$ Psi, $\nu = 0.2$, $\gamma = 160$ Pcf , $K = 0.8$

Table 6-2, Stress variation due to excavation in slope structure with K = 0.4, ν = 0.2, E = 0.75 X 10^6Psi, γ = 160 Pcf

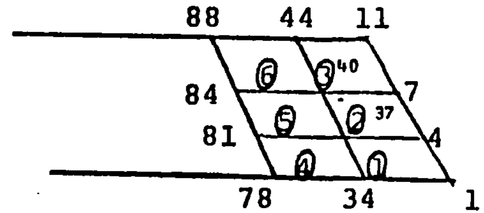

Section	1	2	3	4	5	6
TAU xy KSF	2.2	1.65	1.73	2.14	1.27	-1.16
SIGMA X KSF	2.14	1.46	-2.54	1.51	1.23	-1.27
SIGMA y KSF	8.29	5.38	-3.19	5.42	2.23	-2.61

Table 6-3, Stress variation due to excavation in slope structure with K = 0.8, ν = 0.2 E = 0.75 X 10^6Psi, γ = 160 PcF

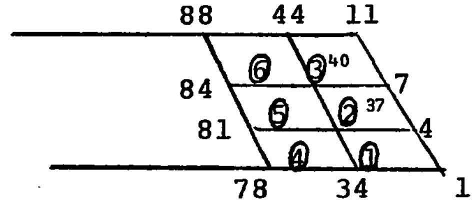

Section	1	2	3	4	5	6
TAU xy KSF	4.85	2.35	1.59	3.60	2.12	-1.38
SIGMA X KSF	3.75	3.55	2.08	2.47	2.40	1.62
SIGMA Y KSF	6.45	4.90	-3.16	5.37	2.22	-2.64

Also, the same structure was considered as an overconsolidated rock. Table 6-4 shows the variation of the maximum displacement at node number five with lateral earth coefficients greater than one.

Figure 6-9 and 6-10, illustrate the possible failed elements comprising the failure surfaces for lateral earth coefficents 3 and 5. It is seen that there is not any significant change in the possible failure surfaces. As a conclusion it can be said that in overconsolidated rock the failure surface undergoes very minor change with increasing lateral earth coefficient, while normally consolidated rock tends to fracture closer to slope surface.

Table 6-5 shows the variation of the maximum displacement at node number five with varying modulus of elasticity. In general, the modulus of elasticity of rock has a great effect on the front surface displacement. Increasing the modulus of elasticity of the rock material results in proportional adverse variation of the displacement of the slope front surface and minor effect on the highly stressed zone.

Table 6-6, illurstrates the effect of Poisson's ratio on displacement of node number five and stress in element number one. A change in Poisson's ratio affects the distribution of stresses, while magnitude of the horizontal stress shows more variation.

Table 6-4, Maximum displacement at node number five for different lateral earth coefficient, overconsolidated rock.

Case No.	K Lateral Earth Coefficient	δ lb/ft^3 Density	ν Poisson's Ratio	E,Psi Modulus of Elasticity	Max. Displ. at Node No.5, ft X 10^{-2}
1	2	160	0.2	0.76 X 10^6	0.587
2	3	160	0.2	0.76 X 10^6	0.904
3	4	160	0.2	0.76 X 10^6	1.220
4	5	160	0.2	0.76 X 10^6	1.537

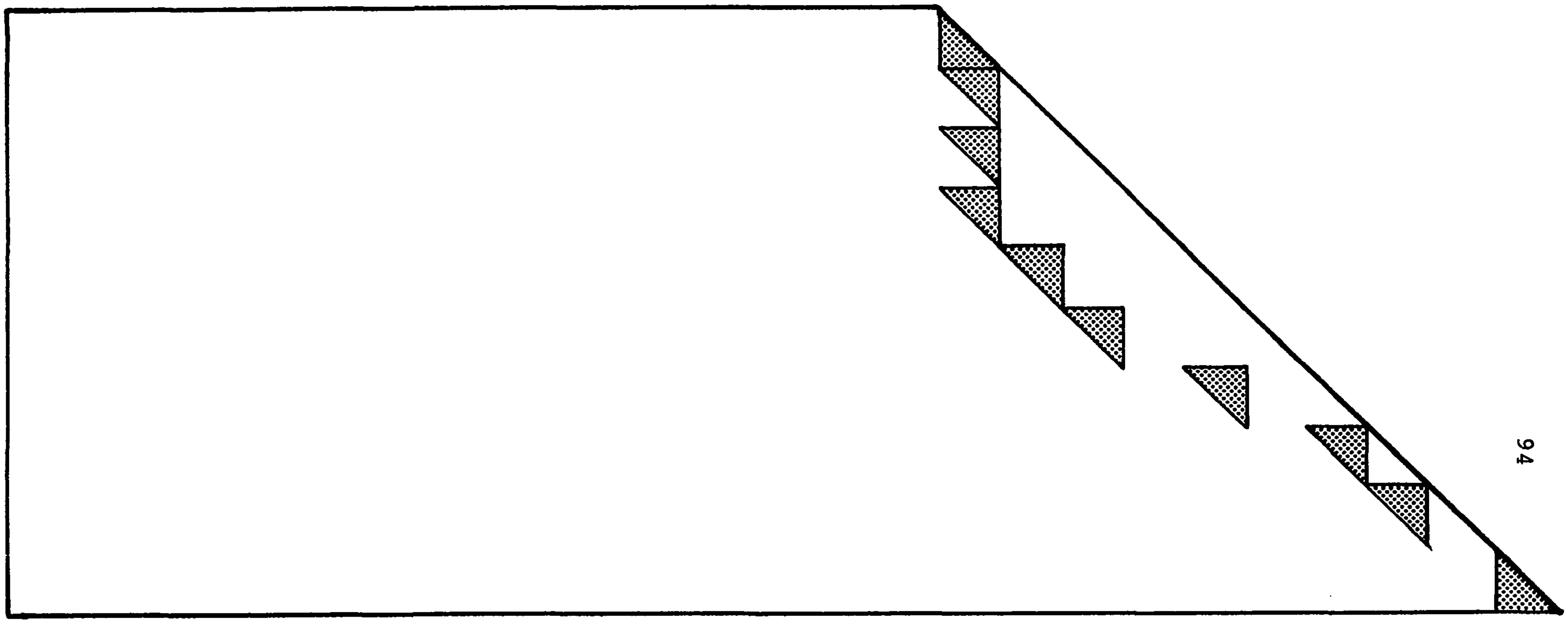

Figure 6- 9 Possible failure surface for overconsoiidated rock with 30 Kips concentrated load on nodes 11,22,33,44,and

$E = 0.76 \times 10^{6}$ Psi, $\nu = 0.2$, $\gamma = 160$ PCF, $K = 3.0$

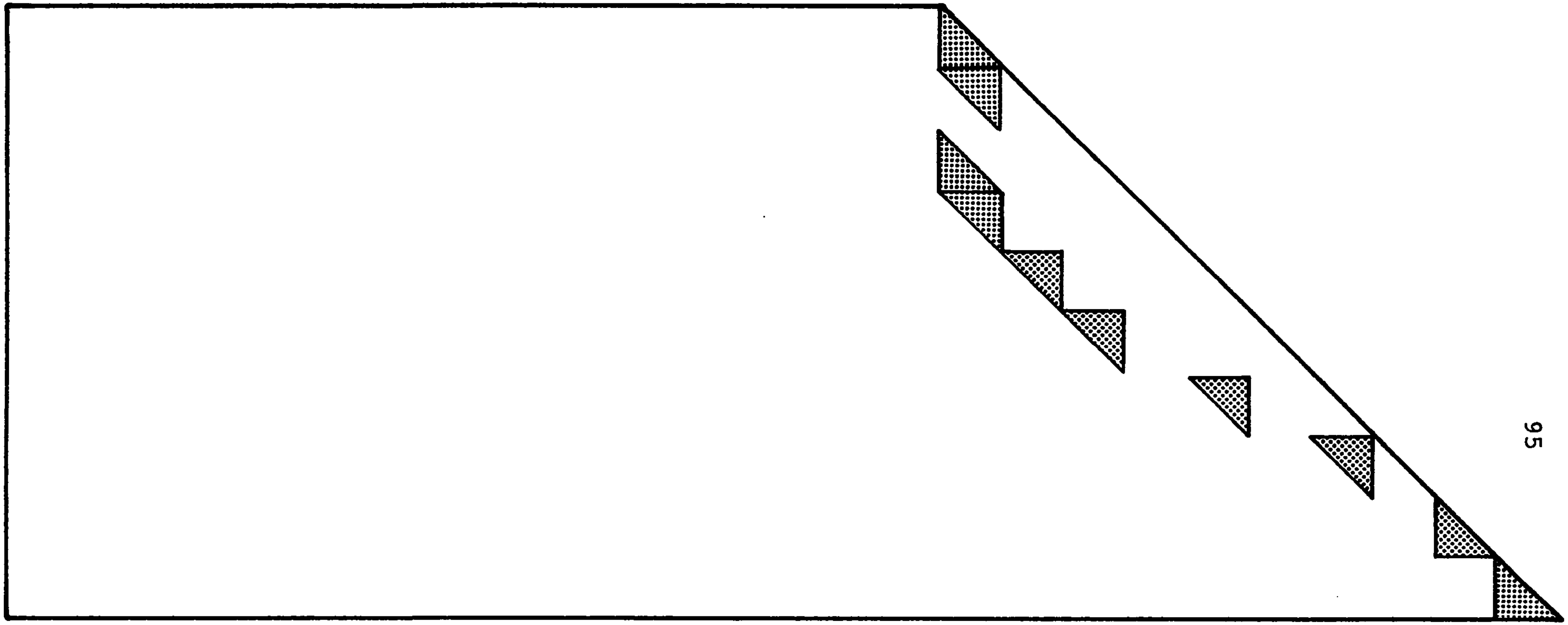

Figure 6-10 Possible fallure surface for overconsolidated rock with 30 Kips concentrated load on nodes 11, 22, 33, 44 and

$E = 0.76 \times 10^6$ Psi, $\nu = 0.2$, $\gamma = 160$ PcF, K= 5.0

TABLE 6-5

Maximum Displacement at node number 5 and variation of stress at element number one for different value of modulus of elasticity and K = 5, $\nu = 0.2$, $\gamma = 160\ lb/ft^3$

E, Modulus of Elasticity Psi	0.34×10^6	0.42×10^6	0.49×10^6	0.55×10^6	0.63×10^6
Displacement Feet	0.33×10^{-1}	0.27×10^{-1}	0.237×10^{-1}	0.207×10^{-1}	0.184×10^{-1}
σ_x KSF	-4.88	-4.88	-4.87	-4.87	-4.87
σ_y KSF	-19.52	-19.52	-19.51	-19.51	-19.51
τ_{xy} KSF	36.29	36.29	36.29	36.29	36.29

Table 6-6, Maximum displacement at node number 5 for different values of Poission's ratio and variation of stresses

$E = 0.34 \times 10^6$ Psi
$\gamma = 160$ lb/ft^2
$K = 5.0$

ν Poisson's ratio	0.15	0.25	0.30	0.35
Maximum Displacement at node No.5 feet	0.327×10^{-1}	0.335×10^{-1}	0.337×10^{-1}	0.337×10^{-1}
σ_x, KSF at element No. 1	-3.34	-6.79	-9.32	-12.98
σ_y, KSF at element No. 1	-18.96	-20.38	-21.76	-24.12
τxy, KSF at element No. 1	36.89	35.58	34.70	33.59

When comparing Tables 6-1 and 6-4, it is observed that using a higher lateral earth coefficient, (K = 5.0 instead of K = 0.4), results in considerable increase in the displacement along the slope surface.

The program has also been run for a strip mine with $\nu = 0.3$ and $E = 0.57 \times 10^5$ Psi, $\gamma = 160$ Pcf, K =5 and 100 feet height. Figures 6-11 and 6-12 show the possible failure surfaces and displacements at the front surface respectively. The maximum displacement at node number 5 is 0.205 feet. Comparing this case with the output in Table 6-5, it can be seen that in a strip mine slope with a very low modulus of elasticity, large displacement occurs with no important change to the failure surface while variation of σ_x is greater than the variation of the other two principal stresses. Appendix C lists the output for this case. The stress distribution shows a tension zone which starts from the ground surface under the concentrated loads and penetrates to a depth of one-third of the excavation height.

In general, it has been seen that the two-dimensional finite element method is able to simulate the geometry and loading system, while calculating the stresses and displacements, providing enough information in order to compare the failure surface pattern of a working highwall slope in a strip mine.

It indicates that such analysis can provide a good quantitative estimate of working highwall movements. The computed displacements are of the same order of magnitude as those reported from other field studies and observations.

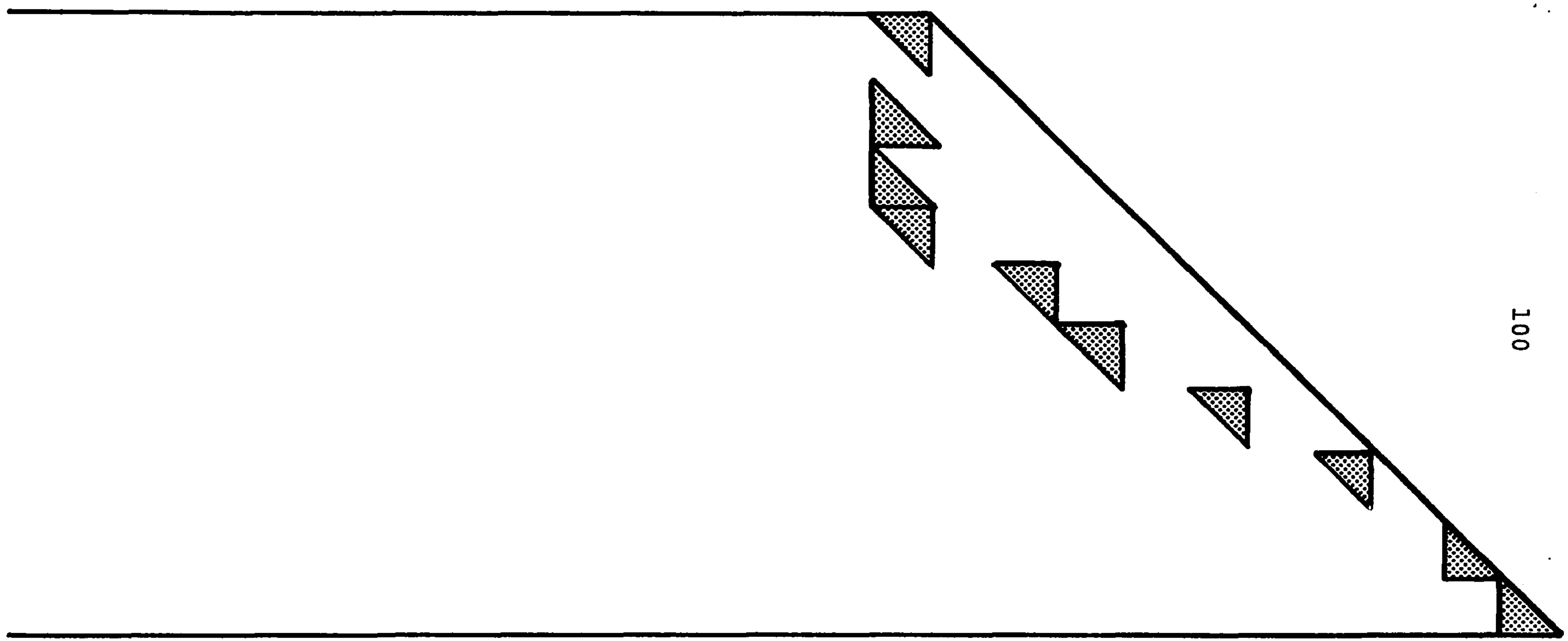

Figure 6-11, Possible failure surface for a strip mine with ν=.2, E=0.57 X 10^5 Psi, γ=160 Pcf, K= 5 and 100 feet height

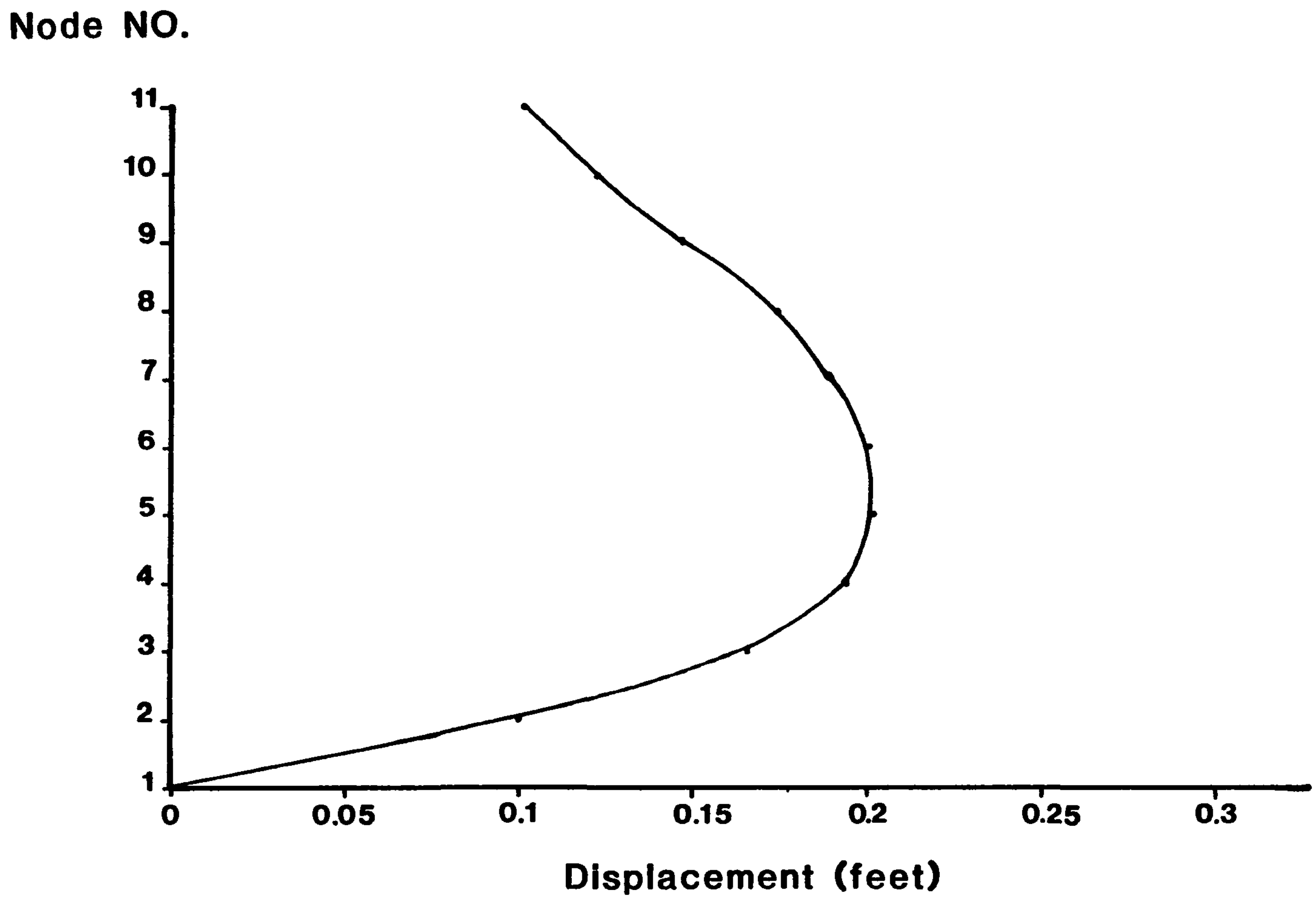

Figure 6-12, Maximum displacement at the front surface for astrip mine with

ν=0.3, E= 0.57 X 10^5 Psi, γ= 160 Pcf and 100 feet height

Chapter 7

SUMMARY AND CONCLUSION

7.1 Summary

An experimental investigation has been performed in order to study the failure and front surface displacement of a slope on a weak plane representing a strip mine. The study consists of the development of the model material and design of the loading apparatus based on dimensional analysis, and the development of instrumentation, interpretation and presentation of the test data.

The main objective of this study was to add to the present knowledge of the behavior and failure of a strip mine in general. The model was not designed to simulate a specific strip mine in Oklahoma.

A series of tests was conducted on the model. The failure surfaces of several slopes were observed and studied as a function of model geometry, unconfined compressive strength and the modulus of elasticity of the model material. A set of dial gages were installed at the front surface of the model for measuring the displacements of the front surface. Comparisons have been made between the test results by changing the mechanical properties of model material. The equilibrium method and its deficiencies have been discussed. In general this method (with some modifications) has been recommended for soil and loose rock. An example which included the plane of weakness has been solved.

Two-dimensional finite element analysis was employed for the parametric study and stability analysis of the physical model and working highwall of the strip mine. Formulation of the method, types of elements and loading condition for a strip mine were described. In applying this method to a strip mine analysis, the following assumptions and simplification were necessary:

1. The rock slope profile was considered normal to a hypothetical axis of the system while the top surface remains flat for a certain length. This implies that the stresses in the structure are principal stresses and plane strain conditions can be assumed.
2. The reduction of a real three-dimensional problem to a two dimensional one; the simulation of the three-dimensional condition is possible by applying lateral forces to the planar two-dimensional finite element to represent the horizontal gravitaional or tectonic forces.
3. The variation of stresses, due to excavation was estimated in the finite element model by applying the rock weight as a concentrated force on the nodal points of the finite element mesh acting at the front surface of slope.

4. The lateral earth coefficient, K, for a homogeneous, isotropic, elastic material has been taken greater than one in order to represent overconcolidated rock.

The importance of lateral earth coefficient for a normally consolidated and over-consolidated rock as well as other mechnical properties such as the modules of elasticity and Poisson's ratio and their effects on the failure surface, stresses and front surface displacement were investigated. Application of the elastic analysis approach using finite element and mechanics of composite material concepts to the stability of a coal layer was discussed and material properties in a stiffness matrix for transversely anisotropic and orthotropic material have been suggested.

The results obtained from the finite element analysis were compared to those from the physical model. The failure surface and the front surface displacements obtained from finite element analysis followed a pattern similar to that obtained by the experimental investigation, thereby establishing its reliability.

7.2 Conclusion

From the results of this study, the following conclusions can be drawn:

1. This study has presented a numerical approach to the strip mine stability problem. It is the first study to treat this problem in both a numerical and experimental framework.
2. Crack occurence and propagation was observed in the physical model by applying about two third of the final loading. This indicates that the highwall slope can remain stable until deep cracks occur. Thus, acoustic monitoring in a strip mine cannot be a reliable device. Appearance of shallow cracks may not be dangerous if the controlled loading does not exceed the ultimate strength of the rock mass.
3. For a strip mine slope in rock the shape of the most critical slip surface is not a circular arc as reported earlier by several investigators. The failure surface attains a linear shape as the compressive strength of the rock increases.
4. The failure surface was observed to develop first near a depth of one-half the excavation height. It then extended upward to the ground surface and downward to the plane of weakness and finally includes a portion of the plane of weakness.

5. The physical model showed that considerable outward displacement of the slope surface is possible during the period of loading, but as failure approached only minor displacement occured. Therefore, monitoring the slope displacements should be a part of the controlling process from the preliminary stage to the final stage of excavation.
6. The plane of weakness as an interface between the coal layer and the overlying soil used in the equilibrium method has an important effect on the computed safety factor.
7. The study has shown that the finite element method provides an appropriate technique for stability investigation of a strip mine excavated in hard rock. Figure 7-1, illustrates an agreement between physical and numerical model.
8. Analyses based on the use of isotropic linear elastic stress-strain characteristics has been found to be useful in obtaining significant information about the variation of stresses and displacements with depth, and finally for initial investigations of strip mine stability.
9. Brittle and overconsolidated clay and clay shale slopes can be modeled by the finite element method

and the coefficient of earth pressure, K, has a significant effect on the front surface movement, failure surface and shear stresses.

10. A simplified method for strip mine stability analysis using a numerical model based on finite elements has been presented.

11. Analyses based on experimental work and the finite element method show a slip surface of two-portions, a vertical tension zone immediately below the ground surface and a curve or a line extended to the plane of weakness, (Figure 7-2).

12. The maximum displacement occurs almost at the mid-point of the exposed slope (node number five) in a strip mine, (Figure 7-3). A comparison between the results obtained for a real strip mine, 100 feet height, with a different moduli of elasticity (75×10^4 psi and 56×10^3 psi) indicated that the range of displacements at node number five were 0.14 and 1.92 inches respectively.

13. Monitoring the displacements of the slopes is a difficult and important task, although of fundamental importance. Knowing the critical location and magnitude of displacements from finite element analysis, internal instruments for measuring

horizontal movements (such as deformation rods or any appropriate mechanical devices) can be installed.

14. Good agreement between the predicted failure surface by the finite element method and observed results of physical model tests was demonstrated, (Figure 7-4). This indicates the suitability of the approach applied in this study for making reasonably accurate evaluations of the failure surface and front surface displacements in a strip mine.

It is hoped that the results presented herein will help in a better understanding of the behavior and safe design of the strip mines of Oklahoma in the future.

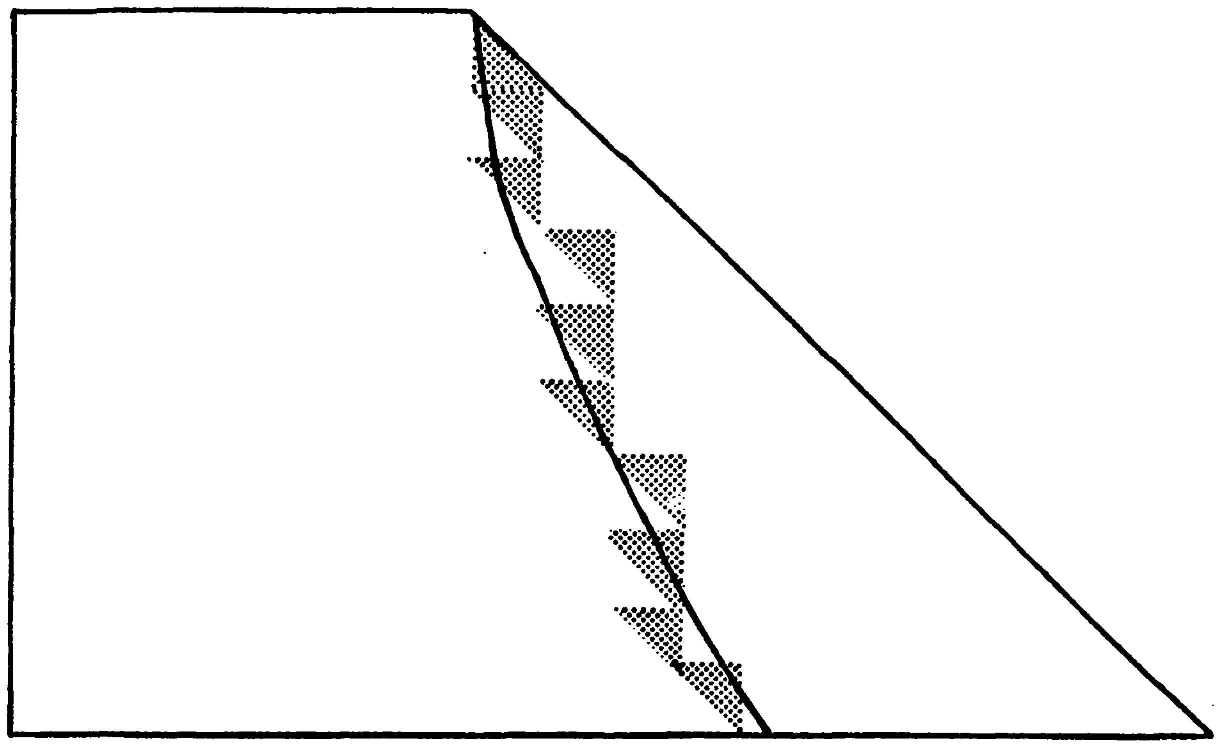

Figure 7-1 A comparison of failure surfaces of numerical model ($E = 54.0 \times 10^3$ psi, $\nu = 0.2$ and 10 kips concentrated load on nodal points 11, 22, 33, 44) with physical model (Test #5, $E = 54.0 \times 10^3$ psi, hard rock).

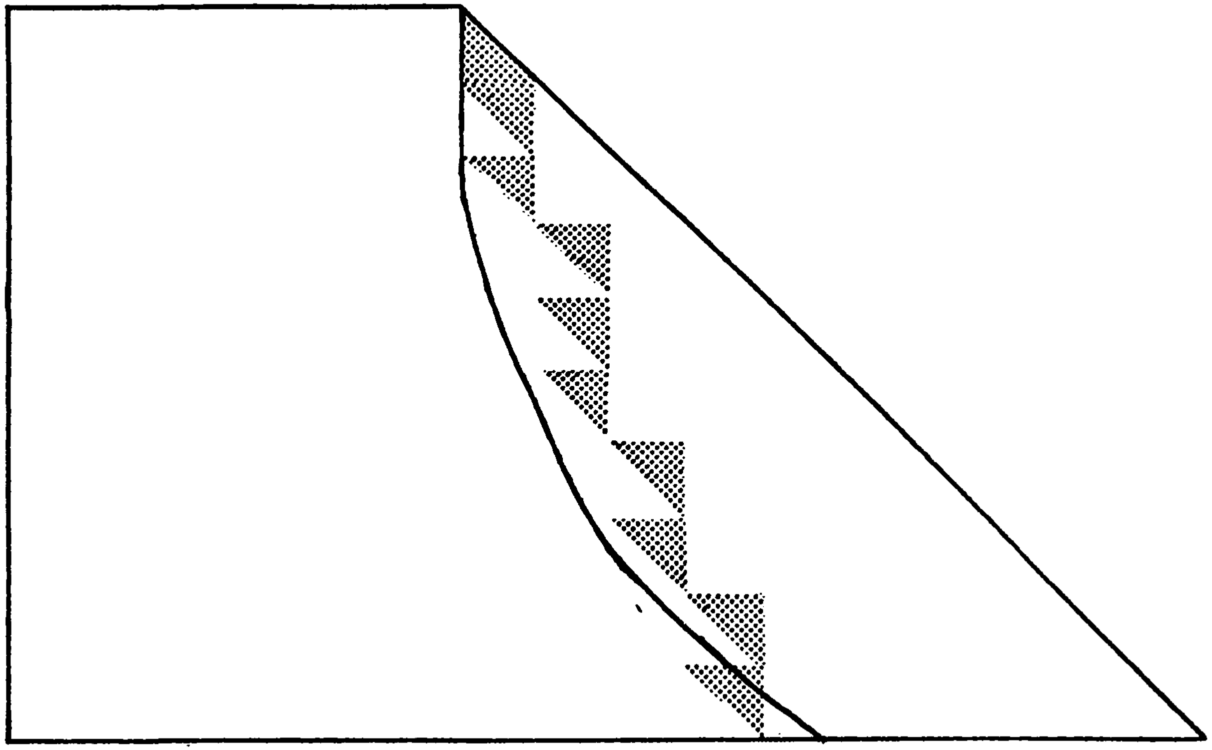

Figure 7- 2 A comparison of failure surfaces of numerical model ($E = 23.6 \times 10^3$, $\nu = 0.2$ and 5 kips concentrated load on nodal points 11, 22, 33, 44) with physical model (Test #1, $E = 23.6 \times 10^3$ psi, loose rock).

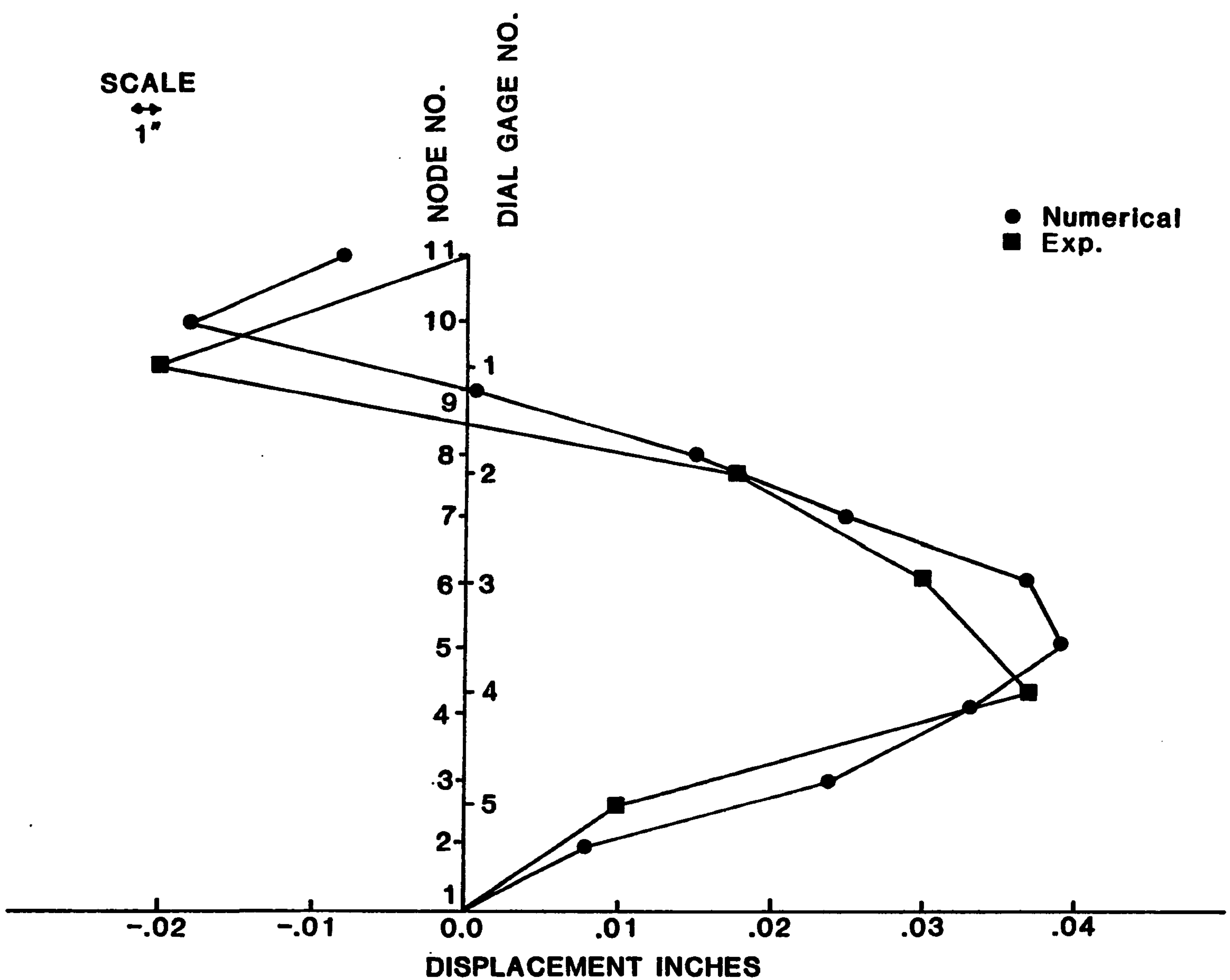

Figure 7-3 A comparison of front surface displacement for numerical model (E=54.x 10^3psi, ν=0.2 and 30 kips concentrated load on nodes No. 11, 22, 33, 44) with physical model (Test #1, E=23.6 x 10^3psi).

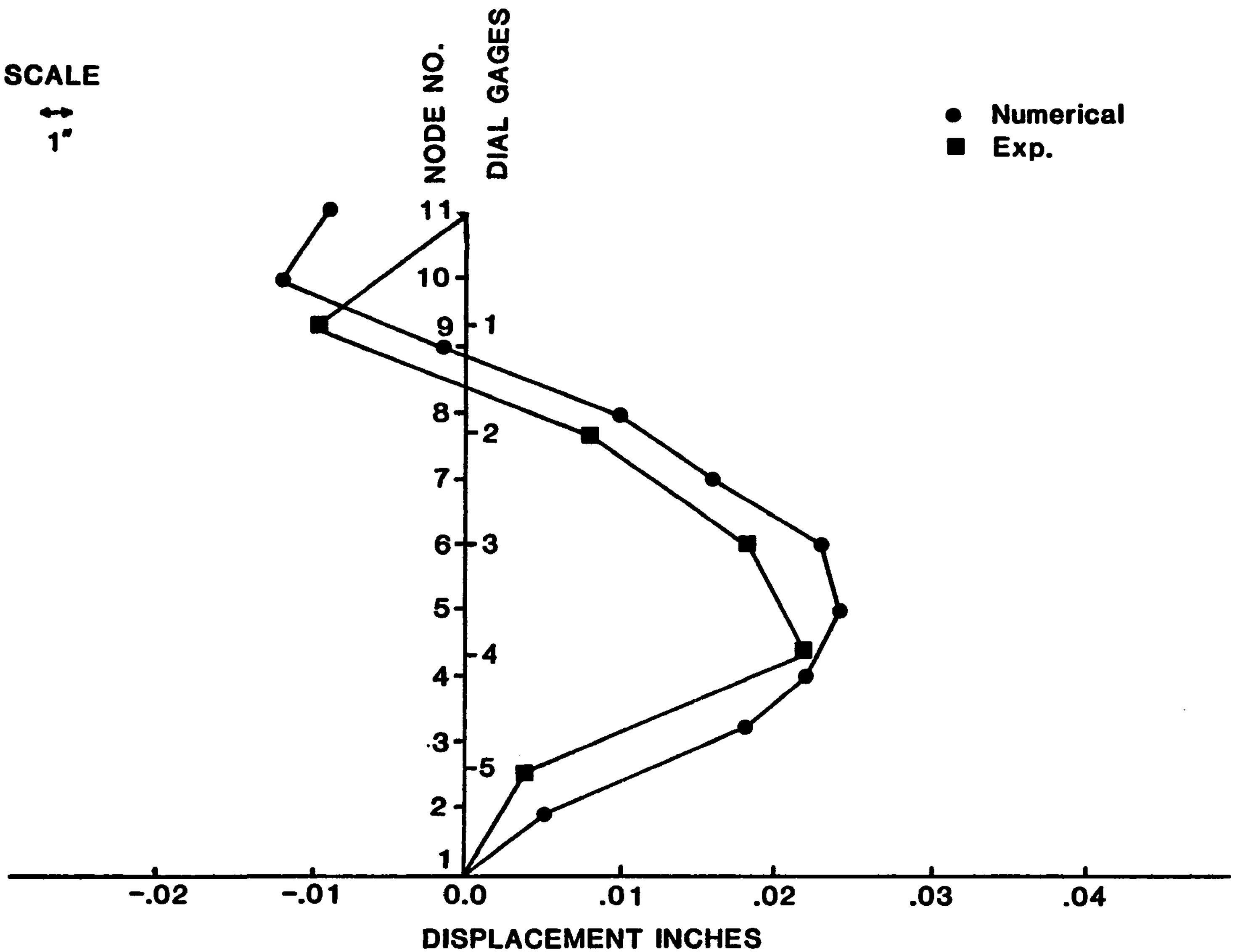

Figure 7-4 A comparison of pattern of front surface displacement of numerical model (E=54.0 x 10^3psi, ν=0.2 and 20 kips concentrated load on nodal points 11, 22, 33, 44) with physical model (Test #5, E=54.0 x 10^3psi).

REFERENCES

Atkinson, H. R. and Ko, Y. H., "Statistical Variations of the Compliance of Coal", Numerical Methods in Geomechanics, ASCE, 1976, pp. 367.

Barton, N. R., "Review of a New Shear Strength Criterion for Rock Joints:, Engineering Geology, Vol. 7, 1973, pp. 287-332.

Bell, M. J., "General Slope Stability Analysis", Journal of Soil Mechanics and Foundation Division, November, 1968, pp. 1253.

Bell, M. J., "Noncircular Sliding Surfaces", Journal of Soil Mechanics and Foundation Division, November , 1968, pp. 1253.

Bhattacharyya, K. K. and S. H. Boshkov, "Determination of the Stresses and the Displacement in Slopes by the Finite Element Method", Proceeding 2nd Cong. Int. Soc. Rock Mech., Belgrad, 1970, Vol. 3, pp. 339-344.

Bishop, A. W., "The Influence of Progressive Failure on the Choice of the Method of Stability Analysis", Journal of Geotechnique England, Vol. XXI, Number 2, June 1971, pp. 168-172.

Bishop, A. W., "The Use of Slip Circle in the Stability Analysis of Slopes", Geotechnique, London, England, Vol.5, No. 1, 1955, pp. 7-17.

Biernatowski, K., "Stability of Slopes in Variational and Probabilistic Solutions", European Conference on Soil Mechanics and Fundamental Engineering, Vienna, 1976.

Bjerrum, L., "Progressive Failure in Slopes of Overconsolidated Plastic Clay and Clay Shales Proceedings", Journal of the Soil Mechanics and Foundations Division, ASCE, Vol 93, No. SM5, September 1967, pp.1-49.

Brian F. Cousins, "Stability Charts for Simple Earth Slopes", Journal of the Geotechnical Engineering Division, Vol. 104, No. GT2, February 1978, pp. 13572.

Brown, C. B. and King, I. P., "Automatic Embankment Analysis: Equilibrium and Instability Conditions", Geotechnique, Vol. 16, No. 3, 1966, pp. 209-219.

Byrne, R. J., "Physical and Numerical Models in Rock and Soil Slope Stability", Ph.D. thesis, James Cook, University of North Queensland, 1974.

Chugdev, R. R., "Stability Analusis of Earth Slopes" USSR All Union Scientific Research Institute of Hufraulic Engineering, 1964. (Translated from Russian, Israel Program for Scientific Translation, Jerusalem, Israel, 1966).

Constantopoulos, I. V. and J. T. Christian and R. V. Whitman, "Initiation of Failure in Slopes in Over-Consolidated Clays and Clay Shales", U. S. Army Eng. Nucl. Cratering Group, NCG Tech. Rep. 29, Livermore, CA., November 1970.

Cowherd C. D., Proceedings of the Conference on Geotechnical Practice for Disposal of Solid Waste Material, Geotechnical Characteristics of Coal Mine Waste, American Society of Civil Engineers, 1977, pp. 384.

Desai, S. C. and Christian T. J., "Numerical Methods in Geotechnical Engineering", McGraw-Hill Book Co., 1977, pp. 543.

Dodds, J. S., Anderson, H. W., 1971, "Tectonic Stresses and Rock Stability, " 135h Symp. on Rock Mechanic, University Of Illinois, September 1971, pp. 171-182.

Duncan, J. M. and P. Dunlop, "Slopes in Stiff Fissured Clays and Shales", Journal Soil Mech. Found. Div. ASCE. Vol.95, No. SM2, March 1969, pp. 467-492.

Duncan, J. M. and R. E. Goodman, "Finite Element Analyses of Slopes In Jointed Rock", U. S. Army Eng. Water, W. Exp. Stn. Cont. Rep. S-68-3, Vicksburg, Miss., February 1968.

Dunlop, P. and J. M. Duncan and H. B. Seed, "Finite Element Analyses of Slopes in Soil", U. S. Army Eng. Water, W. Exp. Stn., Contr. Rep. S-68-6, Vicksburg, Miss., 1969.

Dunlop, P. and J. M. Duncan, "Development of Failure Around Excavated Slopes", J. Soil Mech. Found. Div. ASCE, Vol. 96, No. SM2, March 1970, pp. 471-493.

Emery, C. L., 1966, "Rock Mechanics in Open Pit Mining", Annual General Meeting of C.I.M.M., April 1966, pp.16.

Erguvanli A. Kand and Richard E. Goodman, "Applications of Models to Engineering Geology for Rock Excavations", Bulletin of the Association of Engineering Geologists, Vol. IX. No. 2, 1972, pp. 89-102.

Fellenius, W., "Calculation of the Stability of Earth Dams", Transactions 2nd Congress on Large Dams, Washington, D.C., Vol. 4, 1936, pp. 445-459.

Finn, W.D.L. and A. P. Traitskii, "Computation of Stresses and Strains in Dams Made of Local Materials, Earth Slopes, and Their Foundations, by the Finite Element Method", Hydrotech. Constru., No. 6, June 1968, pp. 492-499.

Finn, W.D.L., "Static and Dynamic Stresses in Slopes", Proc. 1st Congr. Int. Soc. Rock Mech. Lisbon, 1966, Vol.2, pp. 167-169.

Friedman, S. A., "Applied Coal Geology", Oklahoma's Geological Survey, January 1976, pp. 53.

Fumagalli, E., "Statical and Geomechanical Models", Springer, New York, New York, 1973.

Garlier, M. and Baker R., "Extreme-Value Problems of Limiting Equilibrium", Journal of the Geotechnical Eng. Division, Vol. 105, No. GT10, Oct. 1979, pp. 1155.

Garber, M., "Variational Method for Investigating the Stability of Slopes", Soil Mechanics Fdn. Eng., New York 10, No.1, 1973.

Garber, M. and Rafael Baker, "Extreme-Value Problems of Limiting Equilibrium", Journal of the Geotechnical Eng. Division, Vol. 105 No. GT10, October 1979, pp. 14901.

Gates, R. H., "Slope Analysis for Explosive Excavations", Proc. 13th Symp. Rock Mech. Stability Rock Slopes, University of Illinois, August-September 1971. pp. 243-268.

Ghaboussi, J. and E. Wilson and J. Isenberg, "Finite Element Analysis for Rock Joints and Interfaces", Journal of Soil Mech. and Found. Div. ASCE. 99, 1973.

Goodman, R. E. and J. Dubois, "Duplication of Dilatorncy In Analysis of Jointed Rocks", Journal of Soil Mechanics and Foundation Division ASCE. 98, 1972.

Goodman, R. E., "Methods of Geological Engineering In Discontinuous Rocks", Berkeley West Publishing Company, 1976.

Goodman, R. E., "The Deformability of Joints in Determination of the In-Situ Modules of Deformation of Rock", American Society for Testing and Materials Special Technical Publication, No. 477, 1970, pp 174-196.

Goodman, R. E., "The Mechanical Properties of Joints", Proc. 3rd Congress, Int. Soc. for Rock Mech. Denver, 1974.

Hoek, E. and Bray J., "Rock Slope Engineering", The Institution of Mining and Metallurgy, London, 1977.

Hoek, E. and Brown T. E., "Emprical Strength Criterion for Rock Masses", Journal of the Geotechnical Engineering Division, September 1980, pp. 1013.

Houlsby G. T. and Worth P.C., "Strain and Displacement Discontinuities in Soil", Journal of the Engineering Mechanics Division, Vol. 106, No. EM4. August 1980, pp. 753.

Huang, Y. H. Proceeding, Specialty Conference on Geotechnical Practice for Disposal of Solid Waste Materials Geotechnical Engineering Division, American Society of Civil Engineers, Ann Arbor, Michigan.

Hutchinson, J.N. and Somerville, S. H. and Petley, D. J., "A Landslide in Periglacially Distrubed Eturia Marl at Bury Hill, Staffordshire", The Quarterly Journal of Engineering Geology, Vol. 6 Nos. 3 & 4, 1973, pp. 377-404.

Jaeger, J. C., "Friction of Rocks and Stability of Rock Slopes", Journal of Geotechnique England, Vol 21, No. 2, 1971, pp. 97-134.

Janbu, N. "Application of Composite Slip Circles for Stability Analysis", Proc. European Conference on Stability of Earth Slopes. Stockholm, Vol. 3, 1954, Page 43-49.

Janbu, N., "Earth Pressures and Bearing Capacity Calculations by Generalized Procedure of Slices", Proceedings of the Fourth International Conference on Soil Mechanics and Foundation Engineering, Vol.2, 1956, pp. 207-212.

Janbu, N., "Stability Analysis of Slopes With Dimensionless Parameters", D. Sc. Thesis, Harvard Soil Mechanics Series No. 46, 1954.

Jones, M. R., "Mechanics of Composite Materials", McGraw-Hill Book Co., 1975.

Judd, Wm. R., "Statistical Methods to Compile and Correlate Rock Properties and Preliminary Results," Strain Distribution Around Underground Openings, Tech. Report No.2, Advanced Research Projects Ag., Dept. of Defence, pp. 109.

Jun HSU KE, "Non-linear Analysis of the Mechanical Properties of Joint and Weak Intercalation In Rock", Numerical Methods in Geomechanics, Aachen 1979, pp. 523.

Kalkani C. E., Proceedings, Sixteenth Symposium on Rock Mechanics, Two Dimensional Finite Element Analysis for the Design of Rock Slopes, 1977, pp.15.

Langhaar, H. L., "Dimensional Analysis and Theory of Models", John Wiley and Sons, Inc., New York (1969).

Long, A. E., 1963, "Open Pit Slope Stability Research," Mining Congress Journal, June 1963, pp. 68-71.

Miller, P. R. and D. E. Hilts Proceedings, Eleventh Symposium on Rock Mechanics, Experimental Open-Pit Mine Slope Stability Study, 1970, pp. 147.

Muller, L., "The Rock Slide in the Vajont Valley," Rock Mechanics and Eng. Geology, Vol. II/3-4, 1964, pp. 148-212.

Muller, L., John, K. W., 1963, "Recent Development of Stability Studies of Steep Rock Slopes in Europe," Transactions, Society of Mining Engineer, Vol. 226, Sept. 1963, p.6.

Murrel, S. A. Misra, A.K., 1962. "Time-dependent Strain on 'Creep' in Rocks and Similar Non-metallic Materials," Trans. Inst. Min. Metall., London, Vol. 71, 1962, pp. 353-378.

Mozgenstern, N. R. and Price, V. E., "The Analysis of the Stability of General Slip Surfaces", Geotechnique, London, England, Vol. 15, No.1, 1965, pp. 79-93.

Murphy, Glenn, "Similitude in Engineering", The Ronald Press Company, New York, 1950.

Obert, L. and duvall I. W., "Rock Mechanics and the Design of Structures in Rock", John Wiley and Sons, Inc., New York, 1967, pp. 399.

Pariseau, W. G. and B. Voight and H. D. Dahl, "Finite Element Analyses of Elastic-Plastic Problems in the Mechanics of Geologic Media", An Over-view, Proc. 2d Congr. Int. Soc. Rock Mech., Blegrade, 1970, Vol 2, pp. 311-323.

Parisea, W. G., "Elastic-Plastice Analysis of Pit Slope Stability", Proceedings, Symposium on Finite Element Method in Geotechnical Engineering, Vicksburg, Mississippi, May 1972.

Patton, F. D., "Multiple Modes of Shear Failure In Rock", Proc. 1st Int. Congress of Rock Mech. Lisleon 1966, Vol. 1, pp. 509-513.

Peck, B. R., "Stability of Natural Slopes, Stability and Performance of Slopes and Embankments", American Society of Civil Engineers, 1969, pp. 444.

Piteau, D. R., 1970, "Geological Factors Significant to the Stability of Slopes Cut in Rock," Proc. of the Symp. on Theor. Background to the Planning of Open Pit Mines, Johannesburg, September 1970, pp. 33-53.

Piteau, D. R., 1970, "Engineering Geology Contribution to the Study of Stability of Slopes in Rock with Particular Reference to De Beers Mine", Vol. I and II, July, 1970, pp. 222.

Prez, R.E. C., "Analysis of an Underground Opening in Jointed Rock", Ph.D. Thesis, University of Illinois, Urbana, Illinois, 1980.

Price, V. R., "The Role of Caol In Future U.S. Energy Development", Bulletin of the Association of Engineering Geologist Vol. XIII, No. 2, 1976.

Rajagopal, S. R., "On the Structural Characterization of Rocks", Ph.D. Thesis, University of California, Davis, California, 1971,pp. 266.

Revilla, J. and Castillo, E., "The Calculus of Variations Applied to Stability of Slope", Journal of Geotechnique, No. 1, 1977, pp. 1-11.

Rosenblad, L. J., "Geomechanics Model Study of the Failure Modes of Jointed Rock Mass", Ph.D. Thesis, University of Illinois, 1970.

Sarama K. Sarada, "Stability Analysis of Embankments and Slopes", Journal of the Geotechnical Engineering Division, Vol. 105, No. GT12. Dec. 1979, pp. 15068.

Sarama, S. K., "Stability Analysis of Embankments and Slopes", Geotechnique, London, England, Vol. 23, No.3, 1973, pp. 423-433.

Serafin, J. L., "Influence of Interstitial Water of the Behavior of Rock Mass," Rock Mechanics in Engineering Practice, Ed.O. C. Zienkiewiez and D.S. Stagg, John Wiley and Sons, 1968, pp. 55-97.

Skempton, A.W., "Long-term Stability of Clay Slopes", Geotechnique, Vol. 14, No. 2, 1964, pp. 77-102.

Snitbhan, N. and Chen W. F., "Finite Element Analysis of Large Deformation in Slopes", Numerical Methods in Geomechanics, Vol. II, June 1976, pp. 744-756.

Spencer, E., "A Method of Analysis of the Stability of Embankments Assuming Parallel Interslice Forces," Geotechnique, London, England, Vol. 17, No. 1, 1967, pp. 11-26.

Taylor, D. W., "Stability of Earth Slopes", Journal of the Boston Society of Civil Engineers, Vol. 24, No. 3, 1937, pp. 337-386.

Terzaghi, K., "Stability of Steep Slopes on Hard Unweathered Rock," Geotechnique, Vol. 12, No. 4, pp. 251-270, 1962.

Van Eeckhout, E. M. and S. S. Peng, "The Effect of Humidity on the Compliance of Coal Mine Shales," Int. J. Rock Mech. Min. Sci. and Geomech. Abstract, Vol.12, 1975, pp. 335-340.

Wang, F. D. and M. C. Sun, "Slope Stability Analysis by the Finite Element Stress Analysis and Limiting Equilibrium Method," U. S. Bur. Mines Rep. Invest. 7341, Washington, D. C., January 1970.

Wantland, D., "Geophysical Measurement of Rock Properties in Situ," Int. Symp. on the State of Stress in The Earth's Crust, Santa Monica, Calif., 1963.

Whitman, V. R. and Bouley A. W., "Use of Computers for Slope Stability Analysis, Stability and Performance of Slopes and Embankments," American Society of Civil Engineers, August 1969, pp. 519.

Wright, G. Stephen and Kulhawy H. Fred and Duncan M. James, "Accuracy of Equilibrium Slope Stability Analysis," Journal of the Soil Mechanics and Foundation Division, Vol. 99, No. SM10, October 1974, pp. 783-790.

Wu, T. H., "Soil Mechanics", Allyn and Bacon, Inc., Boston 1966, pp. 248-250.

Zienkiewiez, O. C. and S. Valiappan and I. P. King, "Stress Analysis of Rock as A No Tension Material," Geotechnique, Vol. 18, No. 1, March 1968, pp. 56-66.

Zook, L. R. and Bender E. R., "Landslide Problems of the Eastern Kentucky Coal Fields", Bulletin of the Association of Engineering Geologist, Vol. XII, No. 4, 1975.

Appendix A

Model Test Data

Table 4-1

Test #1

DATA: Front Surface Displacement

Max. Lateral Displacement of box, .012 inch

Load lb	Dial Gage #1 Reading	Dial Gage #2 Reading	Dial Gage #3 Reading	Dial Gage #4 Reading	Dial Gage #5 Reading	
0.0	0. 5872	0.5380	0.5180	0.40120	0.4360	
250	0. 5870	0.5389	0.5180	0.40120	0.4360	
500	0. 5741	0.5389	0.5180	0.40130	0.4460	
750	0.5639	0.5389	0.5181	0.40130	0.4460	
1000	0.5630	0.5380	0.5160	0.40122	0.4460	
1250	0 5624	0.5371	0.5151	0.40120	0.4460	
1500	0.5621	0.5365	0.5149	0.40119	0.4329	
1750	0.5620	0.5365	0.5144	0.40110	0.4329	
2000	0.5620	0.5351	0.5140	0.40110	0.4322	
2225	0.5619	0.5351	0.5130	0.40110	0.4319	
2500	0.5619	0.5350	0.5125	0.40100	0.4312	
2750	0.5618	0.5349	0.5120	0.40090	0.4315	
3000	0.5616	0.5345	0.5110	0.40095	0.4318	
3250	0.5612	0.5345	0.5110	0.4015	0.4322	CRACK
3500	0.5609	0.5340	0.5101	0.4030	0.4328	
3750	0.5600	0.5340	0.5110	0.4040	0.4331	
4000	0.5590	0.5350	0.5112	0.4055	0.4340	
4250	0.5585	0.5360	0.5115	0.4060	0.4355	
4500	0.5590	0.5380	0.5120	0.4075	0.4366	
4750	0.5605	0.5400	0.5130	0.4080	0.4380	
5000	0.5620	0.5430	0.5145	0.4086	0.4395	
5250	0.5635	0.5480	0.5160	0.4091	0.4410	
5500	0.5659	0.5540	0.5200	0.4100	0.4430	
5750	0.5670	0.5550	0.5360	0.4209	0.4450	
6000	0.5692	0.5560	0.5470	0.4382	0.4470	

Table 4-1-1

Test #1

DATA: Stress-Strain Relationship

LOAD lb.	PSI	Dial Gage #1 Reading	Dial Gage #2 Reading	Dial Gage #1 Displacement	Dial Gage #2 Displacement	ΔH AVE.inch.	$\varepsilon = \frac{\Delta H}{H}$
0.0	0.0	0.3441	0.6097	0.0	0.0	0.0	0.0
24	3.395	0.3450	0.6104	0.0009	0.0007	0.0008	0.000133
44	6.225	0.3461	0.6108	0.002	0.0011	0.00155	0.0002583
34	11.884	0.3482	0.6115	0.0041	0.0018	0.00295	0.000491
04	14.714	0.3491	0.6121	0.005	0.0024	0.0037	0.000617
24	17.540	0.3500	0.6130	0.0059	0.0033	0.0046	0.000766
44	20.373	0.3506	0.6136	0.0065	0.0039	0.0052	0.000866
54	26.032	0.3522	0.6142	0.0081	0.0045	0.0063	0.00105

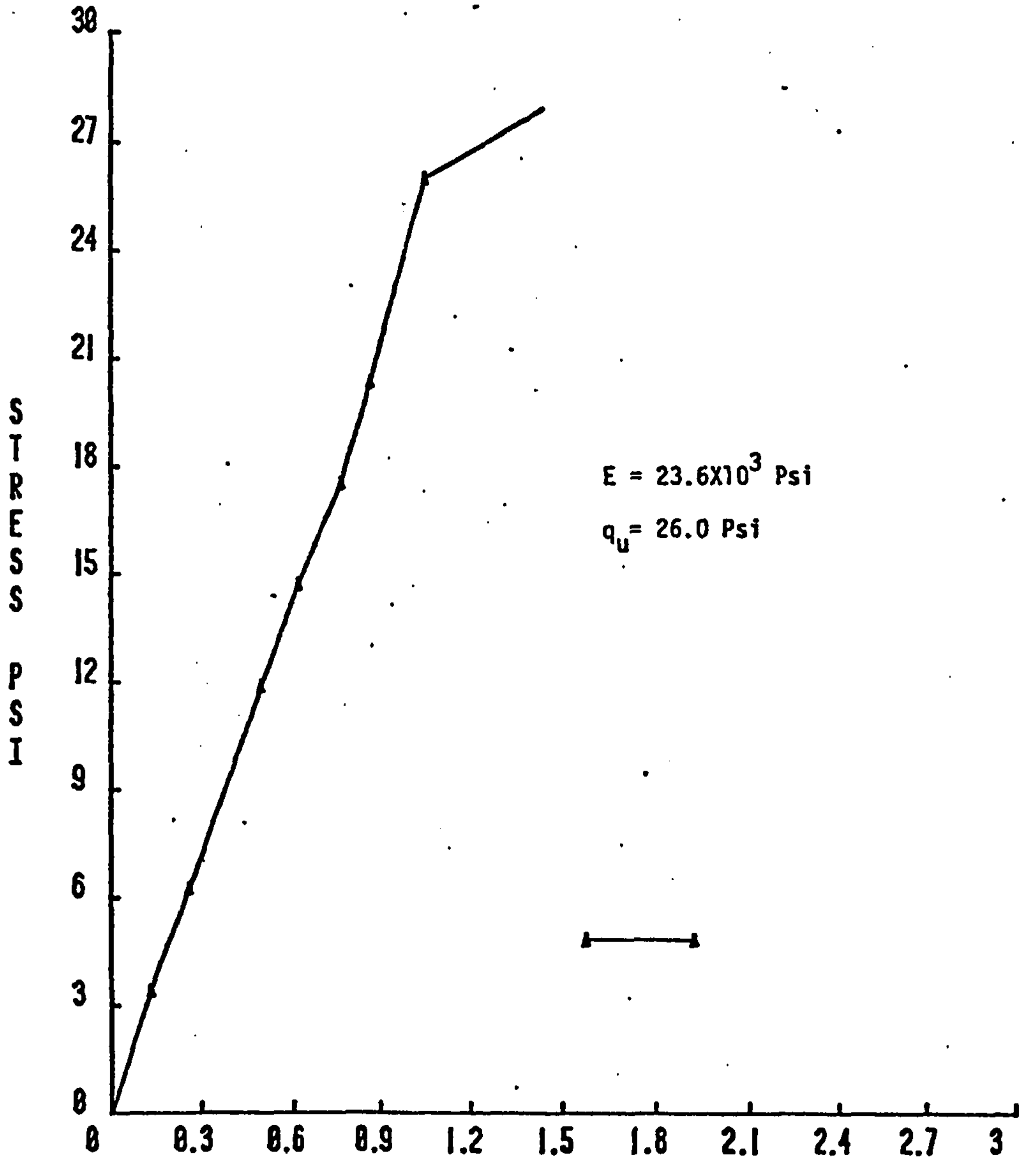

FIGURE 4-1: STRAIN (*10+3 IN/IN)

TEST # 1

TABLE 4-2

TEST #2

DATA: Front Surface Displacement
Max. Lateral Displace of box, .014 inch

Load lb.	Dial Gage #1 Reading	Dial Gage #2 Reading	Dial Gage #3 Reading	Dial Gage #4 Reading	Dial Gage #5 Reading	
0.0	0.3888	0.5480	0.3582	0.3289	0.3475	
500	0.3864	0.5450	0.3560	0.3280	0.3460	
1000	0.3860	0.5450	0.3565	0.3280	0.3455	
1500	0.3850	0.5450	0.3565	0.3280	0.3455	
2000	0.3849	0.5440	0.3560	0.3270	0.3450	
2500	0.3830	0.5430	0.3560	0.3260	0.3450	
3000	0.3810	0.5410	0.3540	0.3260	0.3450	
3500	0.3780	0.5380	0.3520	0.3250	0.3450	
4000	0.3740	0.5360	0.3510	0.3250	0.3450	
4500	0.3710	0.5340	0.3500	0.3250	0.3460	
5000	0.3680	0.5320	0.3499	0.3250	0.3488	
5500	0.3640	0.5310	0.3498	0.3270	0.3522	CRACK
6000	0.3610	0.5299	0.3500	0.3300	0.3580	
6500	0.3580	0.5290	0.3520	0.3340	0.3582	
7000	0.3560	0.5395	0.3680	0.3420	0.3560	
7500	0.3728	0.5620	0.3852	0.3639	0.3575	
8000						

TABLE 4-2-1

Test #2

DATA: Stress-Strain Relationship

LOAD Lb.	PSI	Dial Gage #1 Reading	Dial Gage #2 Reading	Dial Gage #1 Displacement	Dial Gage #2 Displacement	ΔH Ave.in	$\varepsilon = \frac{\Delta H}{H}$
0.0	0.0	0.2440	0.5098	0.0	0.0	0.0	0.0
24	3.375	0.2450	0.5103	0.001	0.005	0.00075	0.000125
44	6.225	0.2460	0.5109	0.002	0.0011	0.00155	0.000258
84	11.884	0.2480	0.5114	0.004	0.0016	0.0028	0.000467
104	14.714	0.2490	0.5120	0.005	0.0022	0.0036	0.00060
124	17.540	0.2499	0.5129	0.0059	0.0031	0.0045	0.00075
144	20.373	0.2505	0.5135	0.0065	0.0037	0.0048	0.0008
184	26.032	0.2520	0.5140	0.0080	0.0042	0.0061	0.001016
204	28.86	0.2530	0.5150	0.009	0.0052	0.0071	0.00118
224	31.692	0.2540	0.5154	0.010	0.0056	0.0078	0.00130
244	34.52	0.2550	0.5180	0.011	0.0082	0.0096	0.00160
284	40.181	0.2580	0.5195	0.014	0.0097	0.0118	0.00197

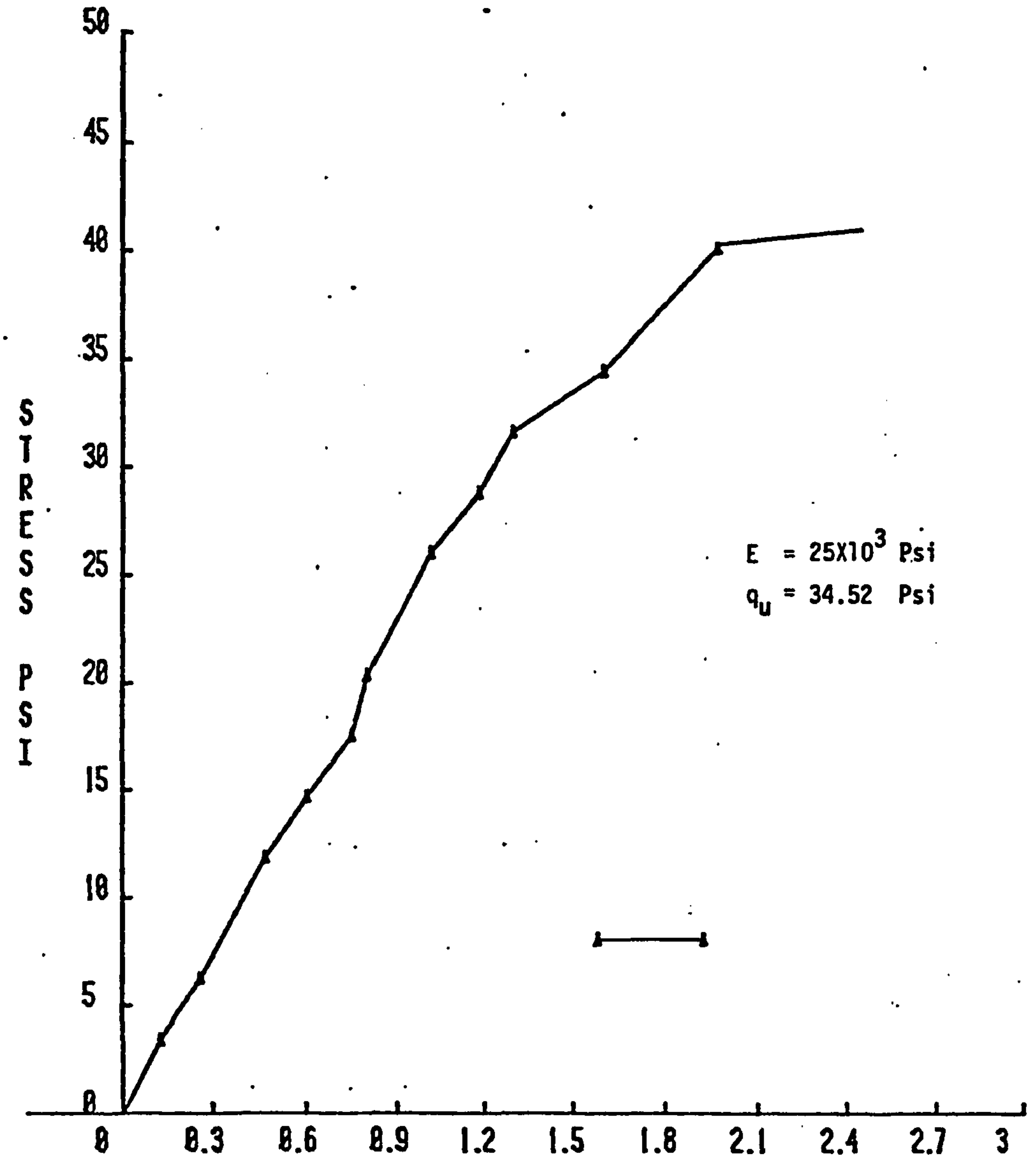

FIGURE 4-2: STRAIN (*10+3 IN/IN)

TEST # 2

TABLE 4-3-1

TEST #3

DATA: Stress-Strain Relationship

Load lb.	Dial Gage #1 Reading	Dial Gage #2 Reading	Dial Gage #3 Reading	Dial Gage #4 Reading	Dial Gage #5 Reading
14000	0.3170	0.5805	0.4055	0.4180	0.3455
14500	0.3175	0.5815	0.4160	0.4190	0.3470
15000	0.3185	0.5825	0.4250	0.4200	0.3470
15500	0.3195	0.5880	0.4350	0.4480	0.3565

TABLE 4-3

TEST #3

DATA: Front Surface Displacement
Max. Lateral Displacement of box, .016 inch

Load lb	Dial Gage #1 Reading	Dial Gage #2 Reading	Dial Gage #3 Reading	Dial Gage #4 Reading	Dial Gage #5 Reading	
0.0	0.3325	0.5750	0.4100	0.4180	0.3475	
500	0.3295	0.5880	0.4100	0.4200	0.3475	
1000	0.3275	0.5880	0.4100	0.4200	0.3475	
1500	0.3270	0.5880	0.4100	0.4200	0.3475	
2000	0.3270	0.5878	0.4100	0.4200	0.3474	
2500	0.3265	0.5875	0.4100	0.4200	0.3473	
3000	0.3260	0.5865	0.4090	0.4190	0.3472	
3500	0.3260	0.5865	0.4090	0.4190	0.3472	
4000	0.3255	0.5860	0.4085	0.4190	0.3470	
4500	0.3249	0.5853	0.4080	0.4180	0.3465	
5000	0.3245	0.5850	0.4075	0.4175	0.3465	
5500	0.3245	0.5850	0.4075	0.4170	0.3462	
6000	0.3240	0.5845	0.4070	0.4169	0.3455	
6500	0.3235	0.5842	0.4065	0.4165	0.3452	
7000	0.3230	0.5840	0.4064	0.4162	0.3450	
7500	0.3225	0.5835	0.4060	0.4150	0.3445	
8000	0.3220	0.5825	0.4055	0.4150	0.3441	
8500	0.3215	0.5820	0.4052	0.4150	0.3440	
9000	0.3210	0.5820	0.4050	0.4149	0.3440	
9500	0.3205	0.5815	0.4050	0.4149	0.3440	
10000	0.3195	0.5810	0.4050	0.4149	0.3440	
10500	0.3190	0.5805	0.4045	0.4149	0.3440	
11000	0.3180	0.5790	0.4030	0.4145	0.3440	
11500	0.3175	0.5790	0.4025	0.4145	0.3439	CRACK
12000	0.3170	0.5790	0.4025	0.4150	0.3441	
12500	0.3170	0.5790	0.4025	0.4152	0.3442	
13000	0.3170	0.5792	0.4030	0.4160	0.3450	
13500	0.3169	0.5800	0.4040	0.4180	0.3455	

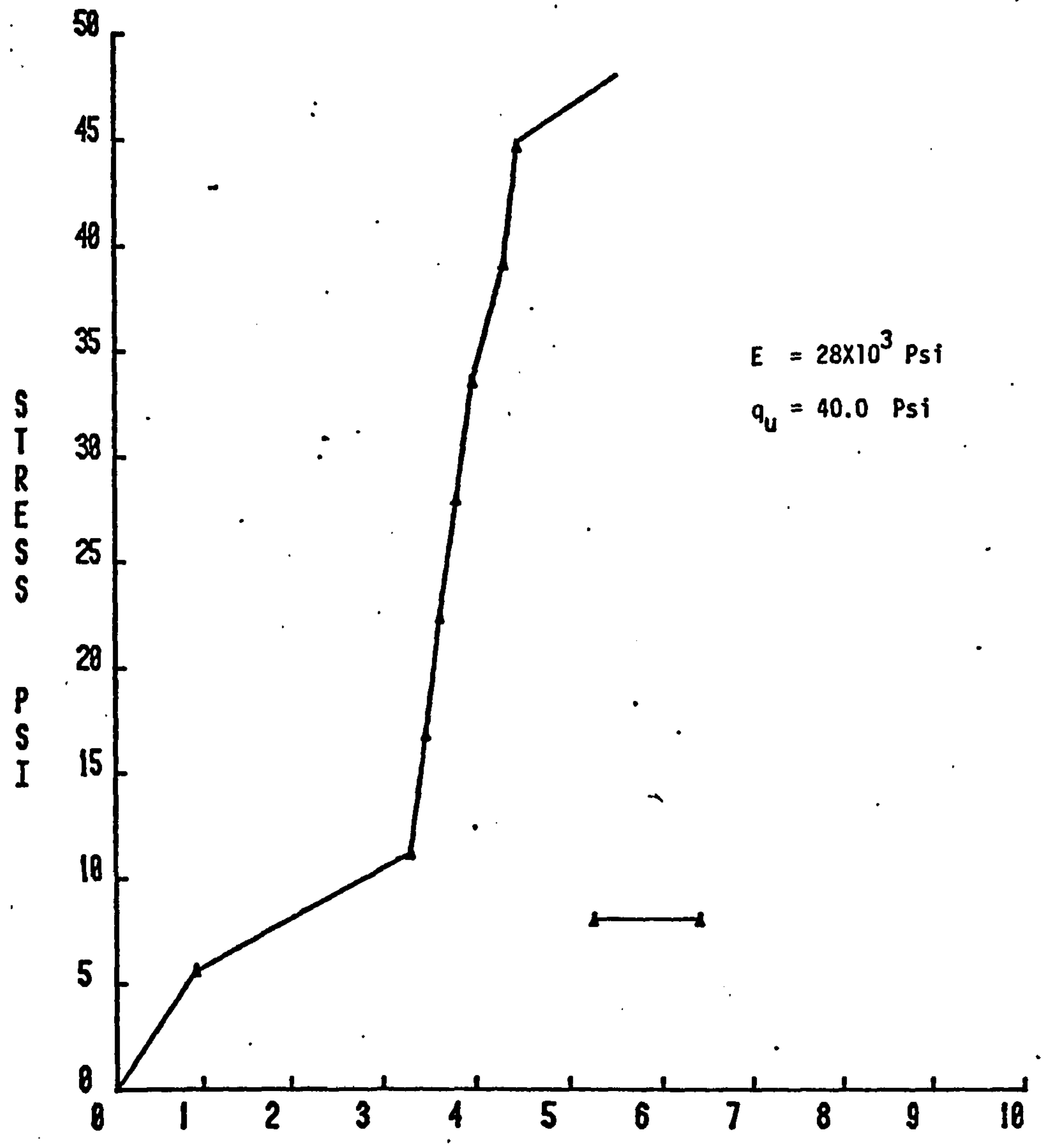

FIGURE 4-3:

TEST # 3

TABLE 4-3-2

DATA: Test #3 Sample #1

LOAD lb.	PSI	Dial Gage #1 Reading	Dial Gage #2 Reading	#1 Displacement	#2 Displacement	AV. ΔH	$\varepsilon = \frac{\Delta H}{H}$
0.0	0.0	0.6720	0.6891	0.0	0.0	0.0	0.0
50	5.61	0.6780	0.6945	0.006	0.0054	0.0057	0.00092
100	11.21	0.6920	0.7100	0.02	0.0209	0.0205	0.00348
150	16.82	0.6922	0.7120	0.0202	0.0229	0.0216	0.00348
200	22.42	0.6930	0.7131	0.021	0.024	0.0225	0.00363
250	28.03	0.6940	0.7144	0.022	0.0253	0.0236	0.00381
300	33.63	0.6950	0.7156	0.023	0.0265	0.0247	0.00398
350	39.24	0.6960	0.7169	0.024	0.0278	0.0267	0.00431
400	44.84	0.6980	0.7184	0.026	0.0293	0.0276	0.00445

TABLE 4-4

Test #4

DATA: Front Surface Displacement
Max. Lateral Displacement of box, .016 inch.

Load	Dial Gage #1 Reading	Dial gage #2 Reading	Dial Gage #3 Reading	Dial Gage #4 Reading	Dial Gage #5 Reading	
10.0	0.3842	0.4375	0.5896	0.5645	0.4595	
1000	0.3840	0.4360	0.5896	0.5645	0.4452	
2000	0.3835	0.4005	0.5896	0.5645	0.4451	
3000	0.3825	0.3555	0.5885	0.5630	0.4441	
4000	0.3820	0.3545	0.5879	0.5620	0.4432	
5000	0.3810	0.3535	0.5870	0.5610	0.4420	
6000	0.3800	0.3525	0.5860	0.5600	0.4410	
7000	0.3795	0.3515	0.5852	0.5590	0.4400	
8000	0.3775	0.3499	0.5850	0.5585	0.4399	
9000	0.3775	0.3496	0.5850	0.5583	0.4399	
10000	0.3760	0.3494	0.5849	0.5583	0.4399	
11000	0.3755	0.3490	0.5849	0.5583	0.4400	
12000	0.3740	0.3485	0.5848	0.5583	0.4409	
13000	0.3730	0.4485	0.5849	0.5589	0.4415	
14000	0.3715	0.4480	0.5849	0.5590	0.4430	
15000	0.3710	0.4480	0.5849	0.5600	0.4440	CRACK
16000	0.3690	0.4479	0.5850	0.5620	0.4465	
17000	0.3685	0.4479	0.5859	0.5630	0.4480	
18000	0.3675	0.4479	0.5865	0.5650	0.4510	
19000	0.3670	0.4479	0.5880	0.5675	0.4570	
20000	0.3660	0.4480	0.5900	0.5720	0.4650	
21000	0.3722	0.4485	0.6116	0.5905	0.4655	

TABLE 4-4-1

TEST #4

DATA: Stress-Strain Relationship

Load PSI	Load lb	Dial Gage #1 Reading	Dial Gage #2 Reading	#1 Displacement	#2 Displacement	ΔH AV	$\varepsilon = \frac{\Delta H}{H}$
0.0	0.0	0.4630	0.3880	- 0.0	0.00	0.00	0.00
11.21	100	0.4631	0.3960	0.0001	0.008	0.0041	0.00066
22.42	200	0.4650	0.3965	0.002	0.0085	0.0053	0.00085
33.63	300	0.4661	0.3970	0.0031	0.009	0.0061	0.00098
44.84	400	0.4685	0.3980	0.0055	0.010	0.0077	0.0012
56.05	500	0.4701	0.4000	0.0071	0.012	0.0096	0.0015
72.80	650	0.4800	0.4050	0.017	0.017	0.017	0.0027

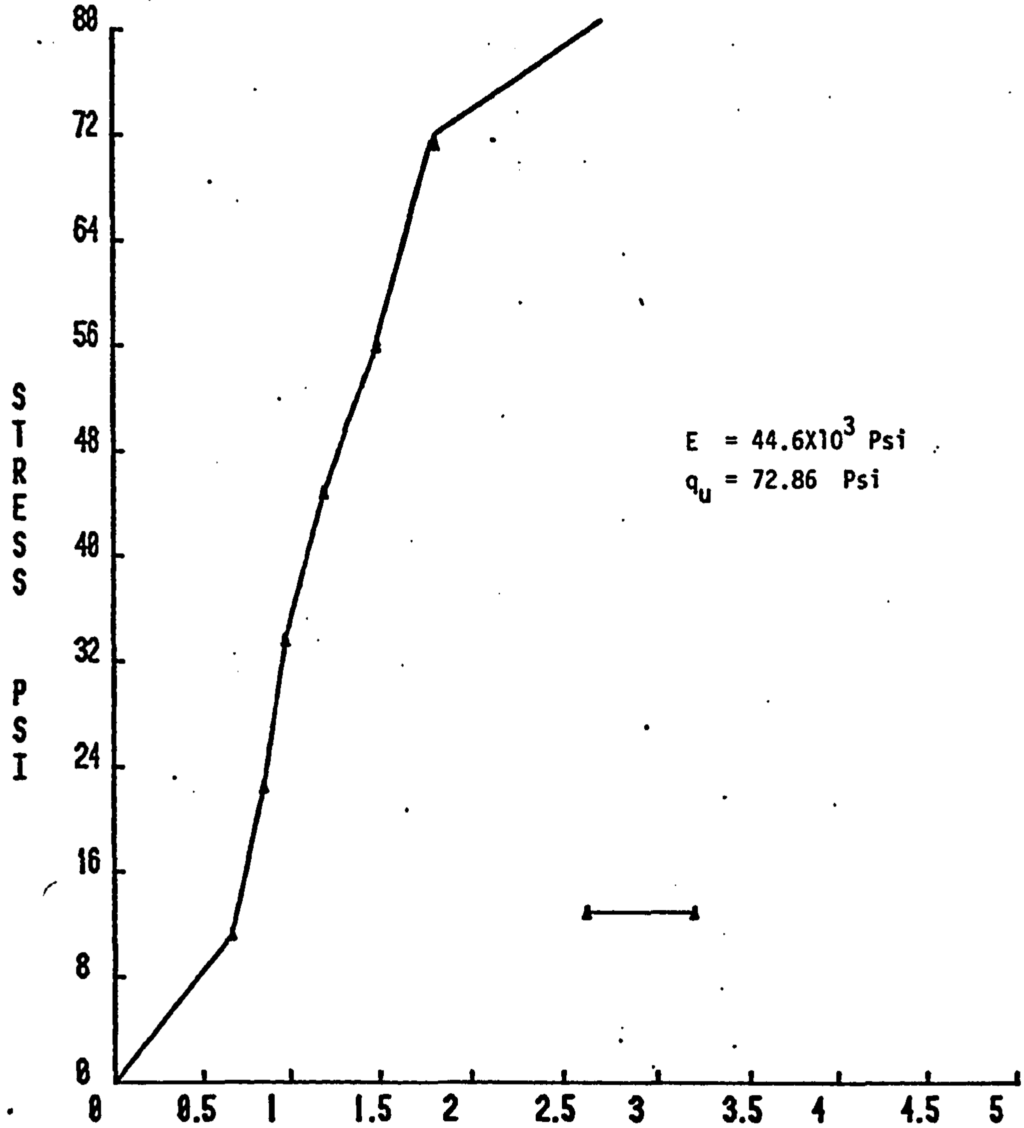

FIGURE 4-4: STRAIN (*10+3 IN/IN)

TEST # 4

TABLE 4-5

TEST #5

DATA: Front Surface Displacement
Max. Lateral Displacement of Box, .025 inch

Load lb	Dial Gage #1 Reading	Dial Gage #2 Reading	Dial Gage #3 Reading	Dial Gage #4 Reading	Dial Gage #5 Reading
0.0	0.2685	0.5260	0.4630	0.3699	0.4349
1000	0.2670	0.5260	0.4630	0.3699	0.4280
2000	0.2670	0.5260	0.4630	0.3699	0.4195
3000	0.2640	0.5260	0.4625	0.3675	0.4185
4000	0.2625	0.5260	0.4619	0.3690	0.4179
5000	0.2615	0.5260	0.4614	0.3685	0.4172
6000	0.2550	0.5260	0.4605	0.3680	0.4165
7000	0.2545	0.5240	0.4600	0.3675	0.4160
8000	0.2540	0.5240	0.4599	0.3672	0.4159
9000	0.2535	0.5240	0.4595	0.3670	0.4152
10000	0.2530	0.5240	0.4590	0.3665	0.4149
11000	0.2525	0.5240	0.4585	0.3663	0.4145
12000	0.2510	0.5225	0.4582	0.3660	0.4139
13000	0.2505	0.5225	0.4579	0.3655	0.4135
14000	0.2500	0.5215	0.4575	0.3652	0.4132
15000	0.2490	0.5213	0.4570	0.3602	0.4130
16000	0.2480	0.5213	0.4565	0.3601	0.4130
17000	0.2470	0.5213	0.4562	0.3600	0.4130
18000	0.2465	0.5212	0.4560	0.3600	0.4131
19000	0.2455	0.5213	0.4555	0.3600	0.4131
20000	0.2450	0.5212	0.4555	0.3650	0.4134
21000	0.2445	0.5212	0.4553	0.3650	0.4135
22000	0.2435	0.5170	0.4550	0.3650	0.4140
23000	0.2425	0.5170	0.4550	0.3651	0.4145
24000	0.2420	0.5170	0.4550	0.3652	0.4150
25000	0.2419	0.5170	0.4560	0.3660	0.4160
26000	0.2410	0.5170	0.4569	0.3670	0.4170
27000	0.2410	0.5172	0.4575	0.3680	0.4185

TABLE 4-5-1

TEST #5

DATA: Stress-Strain Relationship

Load lb	Dial Gage #1 Reading	Dial Gage #2 Reading	Dial Gage #3 Reading	Dial Gage #4 Reading	Dial Gage #5 Reading	
28000	0.2400	0.5180	0.4585	0.3699	0.4200	
29000	0.2400	0.5180	0.4595	0.3705	0.4210	
30000	0.2400	0.5189	0.4605	0.3719	0.4230	CRACK
31000	0.2395	0.5199	0.4615	0.3730	0.4245	
32000	0.2395	0.5199	0.4620	0.3735	0.4250	
33000	0.2395	0.5209	0.4630	0.3750	0.4262	
34000	0.2395	0.5209	0.4635	0.3760	0.4280	
35000	0.2395	0.5210	0.4649	0.3775	0.4295	
36000	0.2390	0.5220	0.4660	0.3790	0.4310	
37000	0.2399	0.5230	0.4680	0.3805	0.4330	
38000	0.2440	0.5260	0.4710	0.3830	0.4350	
39000	0.2460	0.5289	0.4730	0.3850	0.4360	
40000	0.2530	0.5340	0.4770	0.3885	0.4380	
41000	0.2585	0.5360	0.4810	0.3919	0.4389	

TABLE 4-5-2

TEST #5

DATA: Stress-Strain Relationship

Load lb	Load PSI	Dial Gage #1 Reading	Dial Gage #2 Reading	Dial Gage #1 Displacement	Dial Gage #2 Displacement	AVE. ΔH, in	$\varepsilon = \frac{\Delta H}{H}$
0.0	0.0	0.8660	0.5108	0.0	0.0	0.0	0.0
50	5.6	0.8700	0.5150	0.004	0.0042	0.0041	0.00066
100	11.21	0.8740	0.5156	0.008	0.0048	0.0064	0.00103
200	22.42	0.8743	0.5169	0.0083	0.0061	0.0072	0.00116
300	33.62	0.8760	0.5171	0.01	0.0063	0.0081	0.00131
400	44.84	0.8770	0.5183	0.011	0.0075	0.0093	0.0015
500	56.05	0.8775	0.5201	0.0115	0.0093	0.0104	0.00168
600	67.26	0.8785	0.5219	0.0125	0.0111	0.0118	0.0019
700	78.48	0.8800	0.5230	0.014	0.0122	0.0131	0.00211
800	89.68	0.8810	0.5245	0.015	0.0137	0.0144	0.00239
900	100.89	0.8820	0.5259	0.016	0.0151	0.0148	0.00239
1000	112.11	0.8830	0.5269	0.017	0.0161	0.0166	0.00268
1100	123.32	0.8845	0.5279	0.0185	0.0171	0.0178	0.00287
1200	134.53	0.8860	0.5291	0.020	0.0183	0.0192	0.0031
1300	145.74	0.8870	0.5300	0.021	0.0192	0.0201	0.00324
1400	156.95	0.8885	0.5309	0.0225	0.0201	0.0213	0.00344
1500	168.16	0.8890	0.5318	0.023	0.021	0.0225	0.00363
1600	179.37	0.8915	0.5329	0.0255	0.0221	0.0238	0.00384
1700	190.58	0.8940	0.5340	0.028	0.0232	0.0256	0.00413
1800	201.80	0.8959	0.5351	0.0299	0.0243	0.0271	0.00437
1900	213.00	0.8990	0.5361	0.033	0.0253	0.0292	0.00471
2000	224.22						

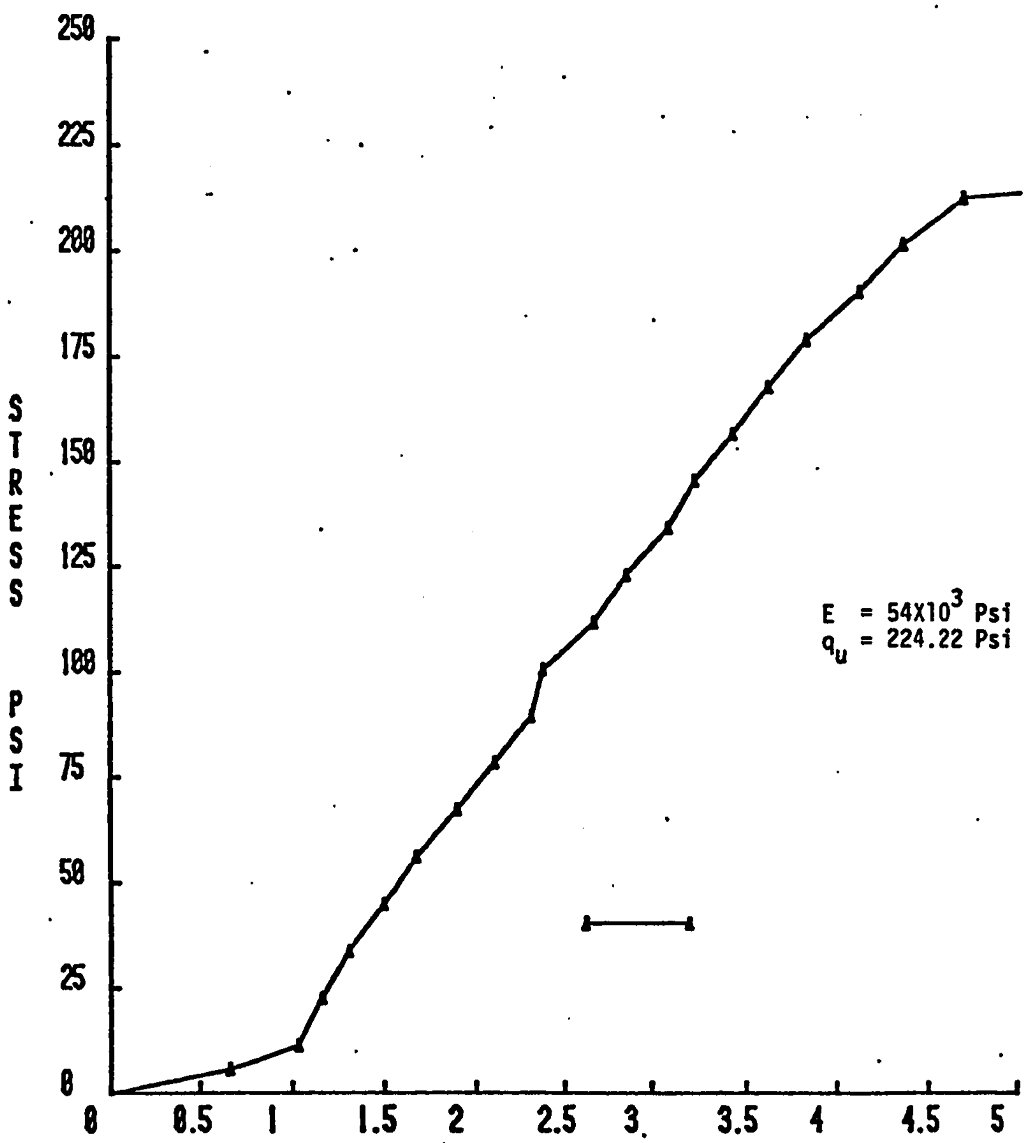

FIGURE 4-5: STRAIN (*10+3 IN/IN)

TEST # 5

TABLE 4-6

TEST #6

DATA: Vertical Cut, Front Surface Displacement
Max. Lateral Displacement of Box, .012 inch

Load	Dial Gage #1 Reading	Dial Gage #2 Reading	Dial Gage #3 Reading	Dial Gage #4 Reading	
0.0	0.4360	0.4655	0.3550	0.2260	
250	0.4360	0.4655	0.3550	0.2260	
500	0.4360	0.4655	0.3550	0.2260	
750	0.4360	0.4655	0.3550	0.2260	
1000	0.4360	0.4660	0.3550	0.2260	
1250	0.4360	0.4660	0.3555	0.2265	
1500	0.4365	0.4662	0.3555	0.2265	
1750	0.4375	0.4665	0.3555	0.2265	
2000	0.4390	0.4670	0.3565	0.2265	
2250	0.4400	0.4675	0.3580	0.2290	
2500	0.44100	0.4695	0.3585	0.2295	
2750	0.4420	0.4695	0.3585	0.2295	
3000	0.4440	0.4700	0.3600	0.2310	
3250	0.4450	0.4710	0.3600	0.2310	CRACK
3500	0.4455	0.4715	0.3610	0.2310	
3750	0.4475	0.4735	0.3620	0.2315	
4000	0.4490	0.4750	0.3630	0.2315	
4250	0.5500	0.4765	0.3645	0.2315	
4500	0.5550	0.4800	0.3680	0.2335	

TABLE 4-6-1

TEST #6

DATA: Stress-Strain Relationship

LOAD PSI	LOAD lb	Dial Gage #1 Reading	Dial Gage #2 Reading	Dial Gage #1 Displacement	Dial Gage #2 Displacement	Δ H AVE.	$\varepsilon = \frac{\Delta H}{H}$
0.0	0.0	0.2561	0.4437	0.0	0.0	0.0	0.0
11.88	84	0.2580	0.4450	0.0019	0.0013	0.0016	0.000267
14.71	104	0.2590	0.4460	0.0029	0.0023	0.0026	0.000433
17.54	124	0.2600	0.4470	0.0039	0.0033	0.0026	0.00060
20.37	144	0.2610	0.4480	0.0049	0.0043	0.0046	0.000770
23.20	164	0.2620	0.4490	0.0059	0.0053	0.0056	0.000903
26.032	184	0.2640	0.4550	0.0079	0.0113	0.0096	0.00160

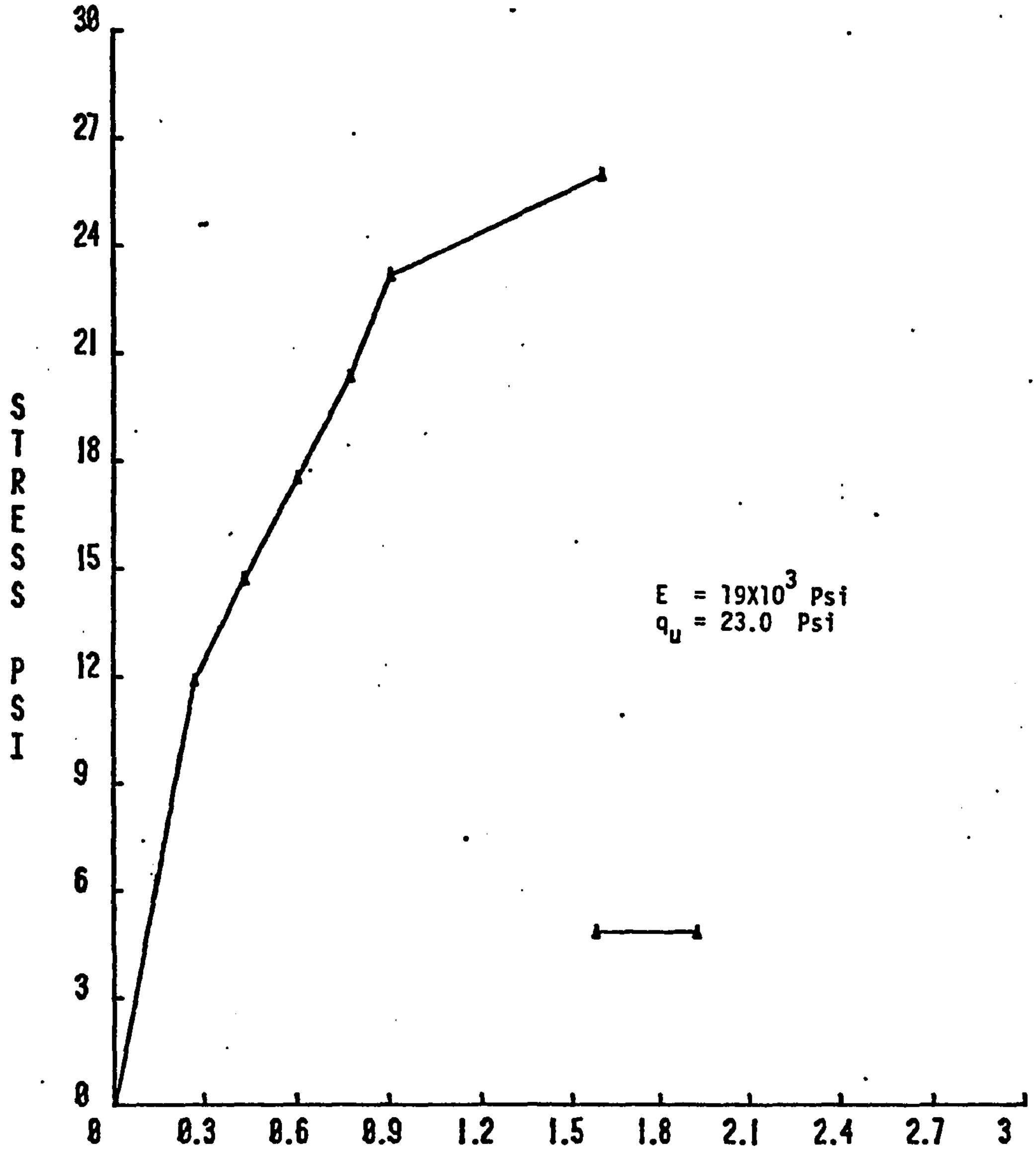

Figure 4-6: STRAIN (*10↑3 IN/IN)

TEST # 6

Table 4-7

DATA #7 Vertical cut, Front surface displacement
Maximum lateral displacement of box .015

BY

Load lb	Dial Gage Read. #1	#2	#3	#4	
0.0	0.400	0.2000	0.2475	0.3525	
500	0.4000	0.2000	0.2475	0.3525	
1000	0.4000	0.2000	0.2475	0.3525	
1500	0.4000	0.2000	0.2475	0.3525	
2000	0.4000	0.2000	0.2475	0.3520	
2500	0.4020	0.2000	0.2475	0.3515	
3000	0.4030	0.2009	0.2478	0.3505	
3500	0.4050	0.2010	0.2485	0.3500	
4000	0.4070	0.2020	0.2405	0.3519	
4500	0.4010	0.2090	0.2500	0.3470	crack
5000	0.4270	0.2180	0.2570	0.3480	
5500	0.4270	0.2195	0.2580	0.3480	
6000	0.4300	0.2220	0.2600	0.3480	
6500	0.4987	0.2430	0.2809	0.3698	

Table 4-7-1
Test #7

DATA Stress-strain relationship BY

Load lb	psi	Dial Gage #1 Read.	#2	Displ. #1	Displ. #2	Ave. ΔH	$\varepsilon = \frac{\Delta H}{H}$
0.0	0.0	0.2561	0.4437	0.0	0.0	0.0	0.0
84	11.88	0.2580	0.4450	0.0019	0.0013	0.0016	0.000267
104	14.71	0.2590	0.4460	0.0029	0.0023	0.0026	0.000433
124	17.54	0.2600	0.4470	0.0039	0.0033	0.0036	0.0006
144	20.37	0.2610	0.4480	0.0049	0.0043	0.0046	0.000767
164	23.20	0.2620	0.4481	0.0059	0.0044	0.0046	0.000767
184	26.03	0.2630	0.4490	0.0069	0.0053	0.0056	0.000933
204	28.86	0.2640	0.4500	0.0079	0.0063	0.0071	0.00118
224	31.67	0.2650	0.4501	0.0089	0.0064	0.0077	0.00128
244	34.52	0.2651	0.4510	0.0090	0.0073	0.0082	0.00137

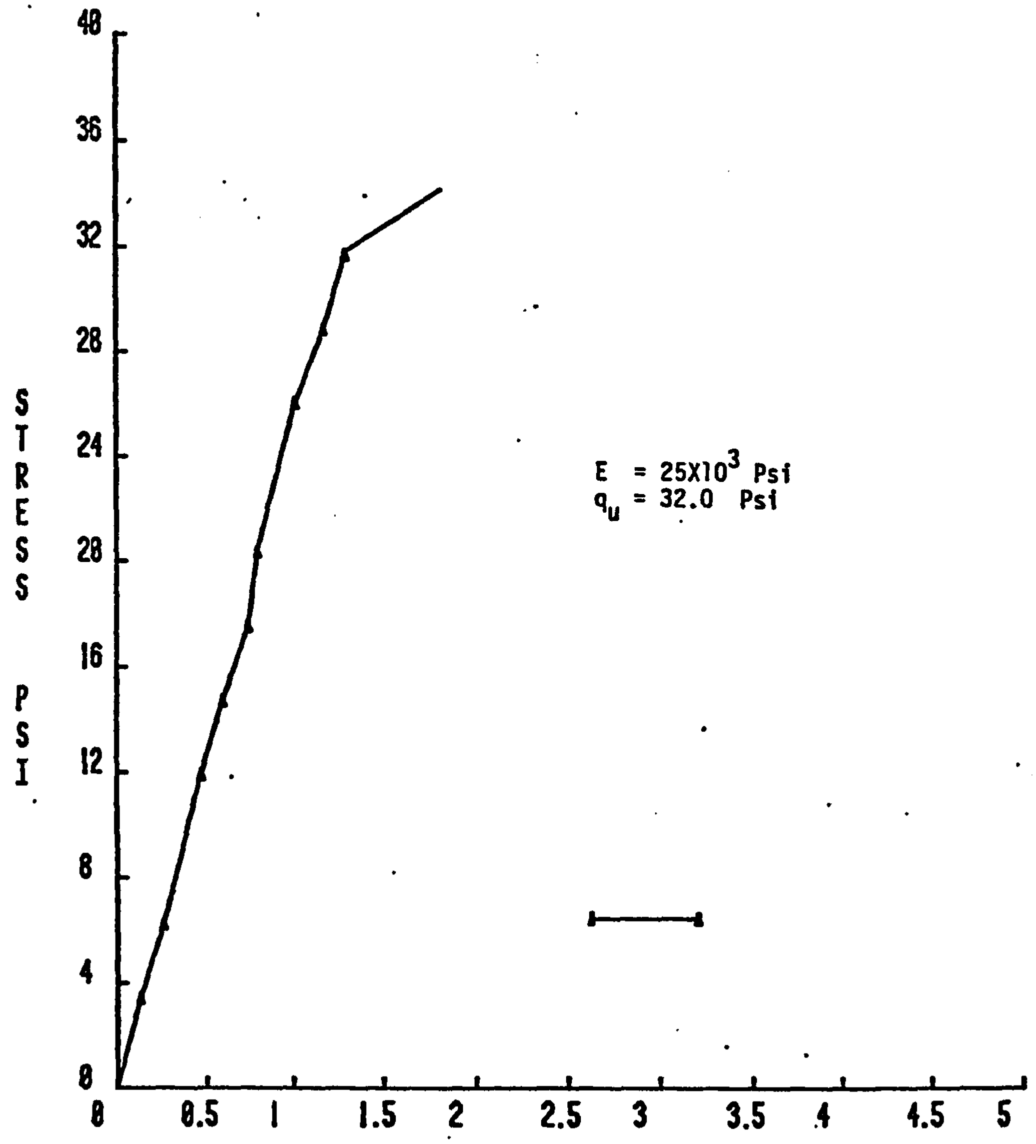

Figure 4-7: STRAIN (*10-3 IN/IN)

TEST # 7

Table 4-8
Test #8

DATA Front surface displacment
Maximum lateral displacement of box .014 inch

BY

Load lb.	Dial Gage #1	#2	#3	#4	
0.0	0.2000	0.1700	0.3520	0.5775	
500	0.2010	0.1700	0.3520	0.5775	
1000	0.2010	0.1700	0.3520	0.5775	
1500	0.2010	0.1700	0.3520	0.5774	
2000	0.2009	0.1699	0.3518	0.5774	
2500	0.2008	0.1697	0.3516	0.5772	
3000	0.2006	0.1694	0.3514	0.5770	
3500	0.2003	0.1691	0.3511	0.5768	
4000	0.2002	0.1687	0.3507	0.5762	
4500	0.2001	0.1685	0.3504	0.5760	
5000	0.2007	0.1683	0.3503	0.5758	crack
5500	0.2010	0.1700	0.3502	0.5756	
6000	0.2036	0.1710	0.3500	0.5752	
6500	0.2050	0.1730	0.3520	0.5760	
7000	0.2090	0.1750	0.3550	0.5800	
7500	0.2160	0.1800	0.3600	0.6000	
8000	0.2198	0.1920	0.3750	0.6780	

Table 4-8-1

DATA Test #8, stress-strain relationship

Load per lb		#1	#2	#1	#2	Ave ΔH	$\epsilon = \frac{\Delta H}{H}$
0.0	0.0	0.5151	0.6110	0.0	0.0	0.0	0.0
4.48	40	0.5157	0.6119	0.0006	0.009	0.0085	0.000121
8.97	80	0.5165	0.6125	0.0014	0.0015	0.00145	0.000233
13.45	120	0.5172	0.6130	0.0021	0.0020	0.00205	0.00033
17.93	160	0.5175	0.6136	0.0024	0.0026	0.0025	0.000403
22.42	200	0.5179	0.6142	0.0028	0.0032	0.0030	0.000484
26.91	240	0.5188	0.6149	0.0032	0.0029	0.0035	0.000581
31.39	280	0.5189	0.6155	0.0038	0.0045	0.0041	0.000661
35.87	320	0.5195	0.6160	0.0044	0.005	0.0047	0.000758
40.36	360	0.5201	0.6166	0.0050	0.0056	0.0053	0.000854
44.84	400	0.5209	0.6172	0.0058	0.0062	0.0060	0.000968
49.33	440	0.5215	0.6178	0.0064	0.0068	0.0066	0.00106
53.81	480	0.5224	0.6187	0.0073	0.0077	0.0075	0.00121
60.00	535	0.5238	0.6196	0.00869	0.00867	0.00868	0.00140

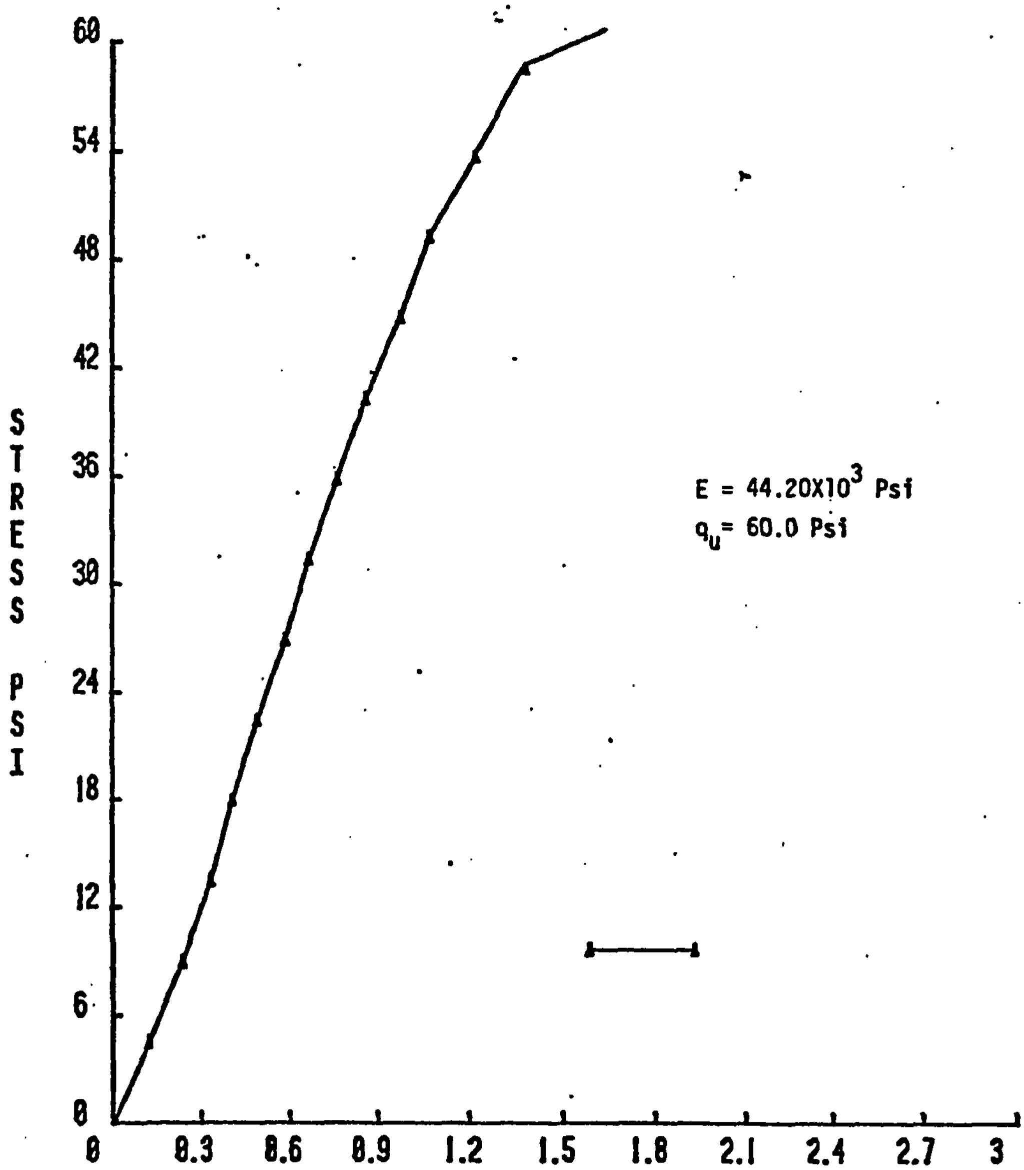

FIGURE 4-8: STRAIN (*10+3 IN/IN)

TEST # 8

Table 4-9

DATA Test #9 Front Surface Displacement
Maximum Lateral Displacement of box, 0.017 inch

Load	Dial Gage #1	#2	#3	#4	
0.0	0.5210	0.4000	0.3456	0.5100	
1000	0.5219	0.4005	0.3459	0.5100	
2000	0.5219	0.4005	0.3459	0.5100	
3000	0.5214	0.4001	0.3459	0.5100	
4000	0.5209	0.4000	0.3455	0.5100	
5000	0.5205	0.3995	0.3453	0.5100	
6000	0.5200	0.3990	0.3450	0.5100	
7000	0.5190	0.3970	0.3430	0.5070	
8000	0.5180	0.3965	0.3520	0.5055	
9000	0.5180	0.3960	0.3414	0.5049	
10000	0.5175	0.3960	0.3410	0.5040	
11000	0.5175	0.3960	0.3410	0.5042	
12000	0.5175	0.3957	0.3408	0.5040	
13000	0.5172	0.3954	0.3418	0.5040	
14000	0.5171	0.3955	0.3404	0.5040	
15000	0.5171	0.3951	0.3402	0.5030	
16000	0.5172	0.3951	0.3401	0.5031	
17000	0.5175	0.3951	0.3402	0.5031	crack
18000	0.5185	0.3960	0.3409	0.5032	
19000	0.5200	0.3970	0.3410	0.5040	
20000	0.5220	0.4000	0.3430	0.5050	
21000	0.5240	0.4060	0.3450	0.5080	

Table 4-9-1

DATA Test #9, Stress-strain relationship

	Load lb	Dial Gage #1 Read.	Dial Gage #2 Read.	Displ. #1	Displ. #2	Ave. ΔH	$\varepsilon = \frac{\Delta H}{H}$
0.0	0.0	0.4890	0.2225	0.0	0.0	0.0	0.0
11.21	100	0.4075	0.2300	0.0085	0.0075	0.008	0.00129
22.42	200	0.4990	0.2311	0.0100	0.0086	0.0093	0.0015
33.63	300	0.5000	0.2310	0.011	0.0095	0.0103	0.00166
0.84	400	0.5015	0.2335	0.0125	0.0110	0.0117	0.00188
56.05	500	0.5025	0.2350	0.0135	0.0124	0.0130	0.0021
67.26	600	0.5035	0.2371	0.0145	0.0146	0.01455	0.00234
78.47.	700	0.5052	0.2304	0.0162	0.0169	0.0165	0.0027
89.68	800	0.5080	0.2400	0.0190	0.0180	0.0185	0.00298

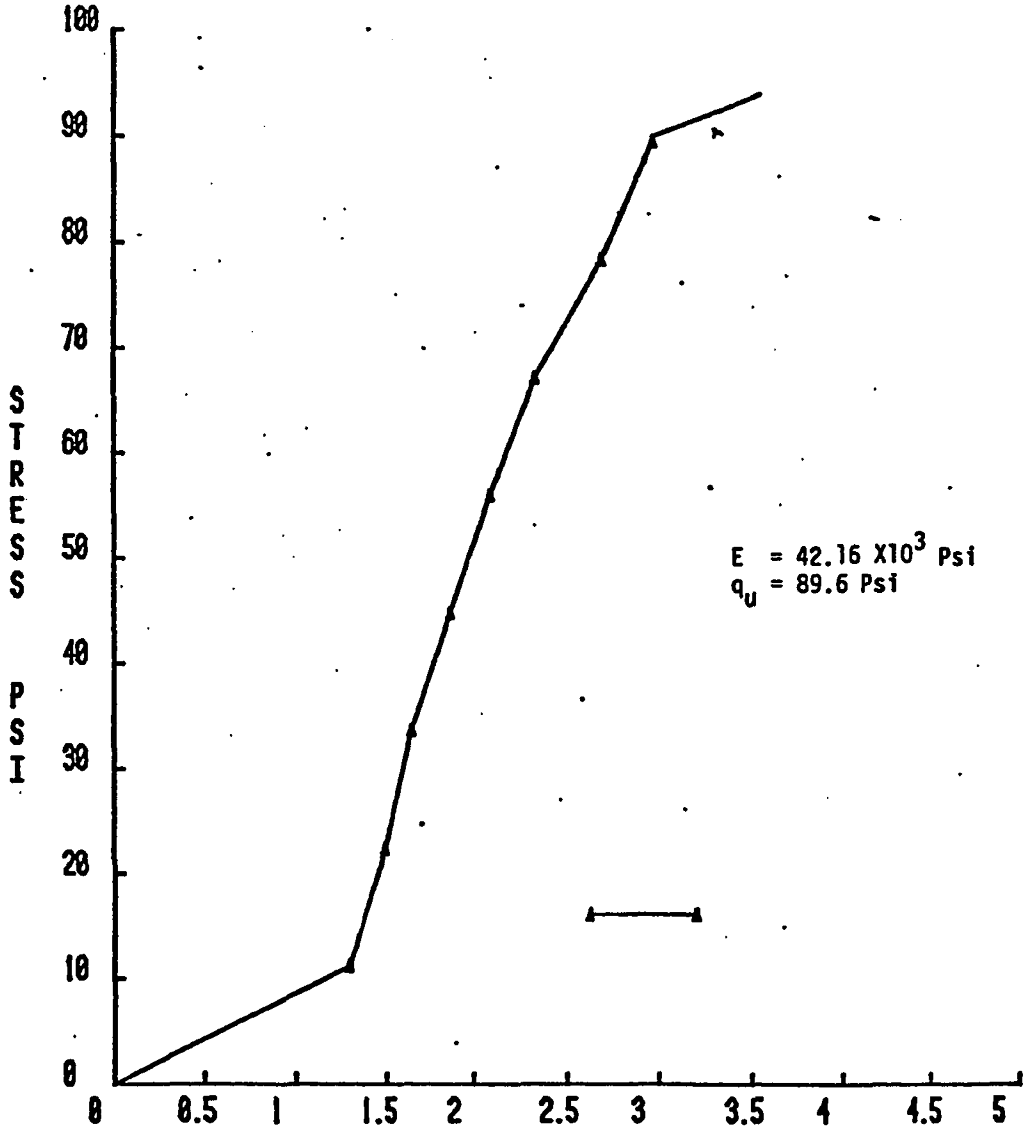

FIGURE 4-9: STRAIN (*10+3 IN/IN)

TEST # 9

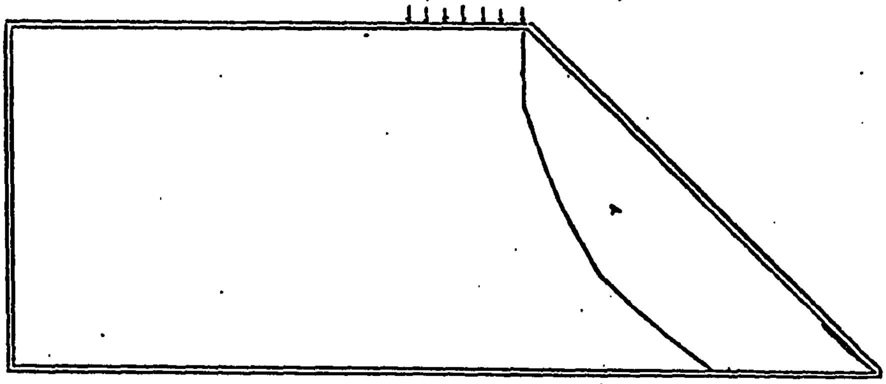

Test #1

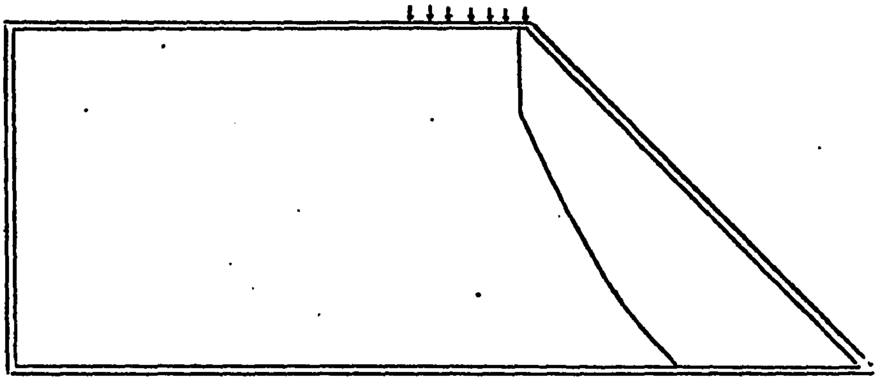

Test #2

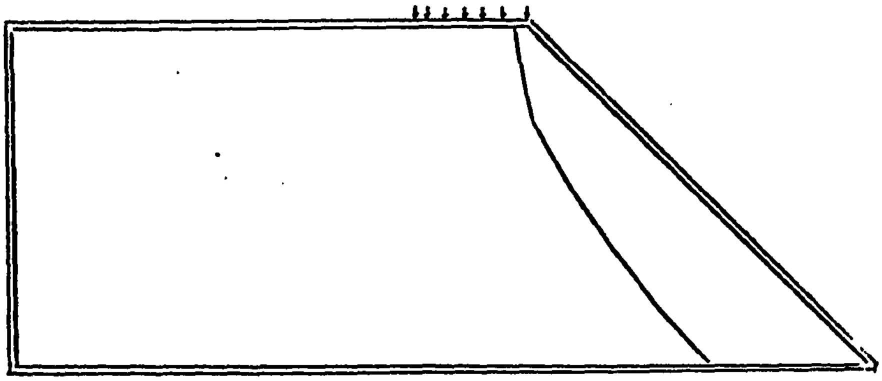

Test #3

Figure 4-10-1, illustration of failure surface for slope model

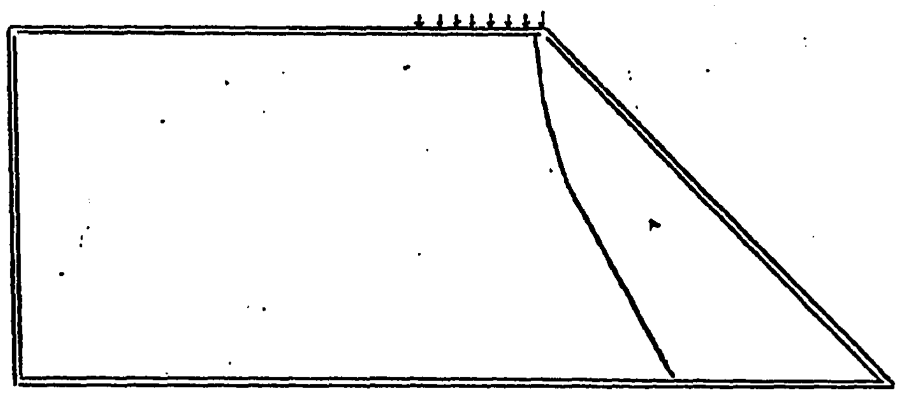

Test #4

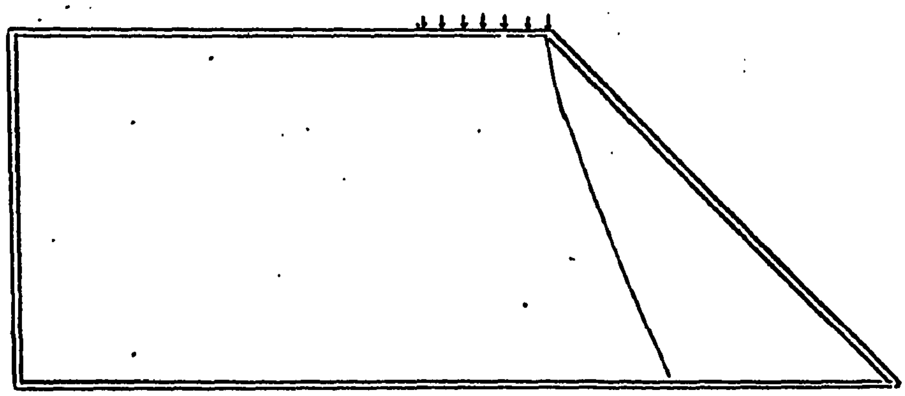

Test #5

Figure 4-10-2, illustration of failure surface for slope model

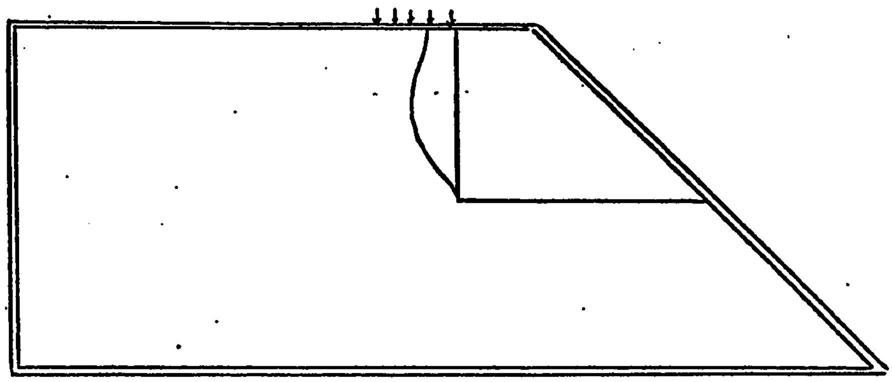

Test #6

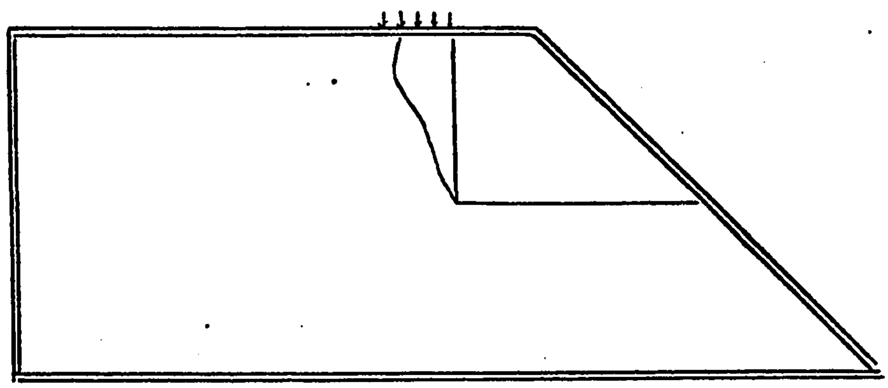

Test #7

Figure 4-11, illustration of failure surface for a vertical cut

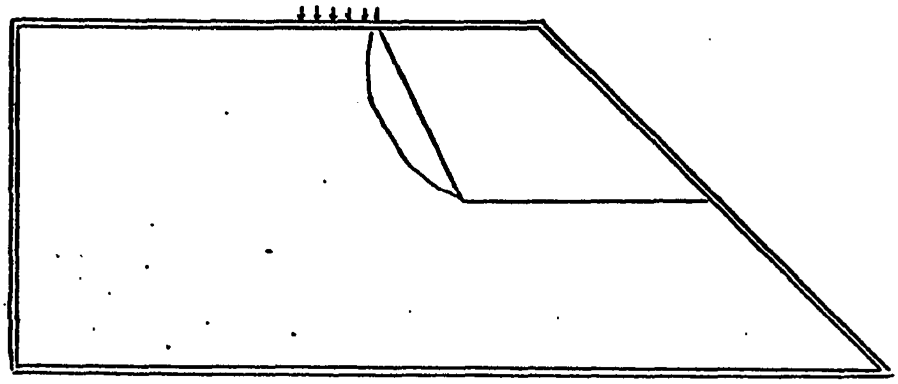

Test #8

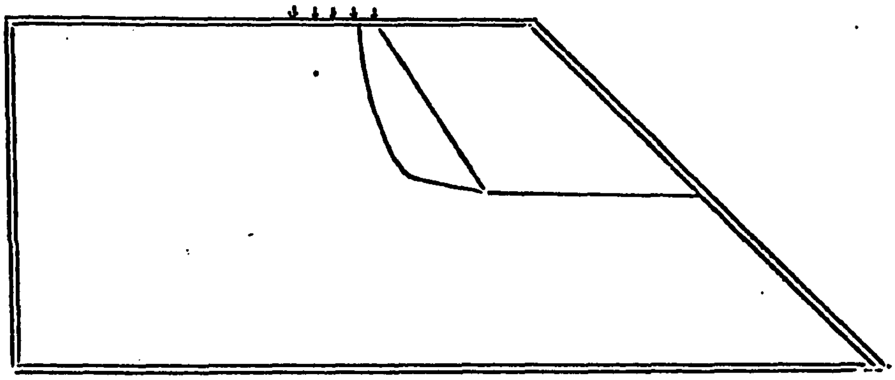

Test #9

Figure 4-12, illustration of failure surface for a slope (α=55^{o})

APPENDIX B

Solution of a Sample Problem by Equilibrium Methods and Application of the Varitional Method

Determine the factor of safety of the spoil bank with $H = 40$ ft., $\omega = 36^0$ and $\alpha = 20^0$.

The spoil slope has the following characteristics:

For fill material $\bar{C} = 200$ psf, $\bar{\phi} = 30^0$, $r_u = 0.05$

and $\gamma = 125$ pcf

For interface material $\bar{c} = 160$ psf, $\bar{\phi} = 24^0$ and $r_u = 0.1$

First consider plan failure using Equation 5-4,

$$F_s = 2 \sin \omega \csc \alpha \csc(\omega - \alpha)\left(\frac{c}{\gamma H}\right) + (1 - r_u) \tan \bar{\phi} \cot \alpha$$

$$F_s = 2 \sin 36 \csc 20 \csc (36 - 20)\left(\frac{160}{125 \times 40}\right) +$$

$$(1 - .05) \tan 24 \cot 20^0 = 1.56$$

The interface roughness, JRC coefficient is taken to be equal to five, because of poor workmanship in preparing the natural ground surface. Therefore, the plane of weakness is assumed smooth and nearly planar. Now using Equation 5-7,

$$F_s = 2 \sin 36^0 \csc 20 \csc (36 - 20) \left(\frac{160}{125 \times 40}\right) +$$

$$(1 - .05) \tan (24 + 5 \log_{10} 0.2) \cot 20^0 = 1.39$$

For circular failure, using the charts based on the simplified Bishop Method, Haung has obtained a minimum safety factor equal to 1.38.

Janbu's method of analysing non-circular failure is applied and after 4 iterations the convergence is obtained. The initial value of F_s was assumed to be 1.00 and the final value of the safety factor was 1.28.

The following table summarizes the safety factors obtained from different methods.

Plane Failure	Modified Plane Failure	Bishop's Method	Janbru's Method
1.56	1.39	1.38	1.28

Variational Method:

Determination of the safety factor for cohesive soils based on Janbu's method is from

$$F_s = \frac{\Sigma_{i=1}^{n} c \ \Delta x_i (1 + \tan^2 \alpha_i)}{\Sigma_{i=1}^{n} \Delta w_i \tan \alpha_i} \quad . \tag{1}$$

Where c is cohesion, Δw_i the weight of i^{th} slice, α_i the inclinations of the sliding curve and Δx_i the width of the i^{th} slice.

The factor of safety is expressed as a quotient of two integrals:

$$S = \frac{\int_{x_0}^{x_1} F\ (x,\ y,\ y')\ dx}{\int_{x_0}^{x_1} G\ (x,\ y,\ y')\ dx} \tag{2}$$

Thus the determination of the safety factor of a spoil slope coincides with the problem of determining the minimum value which takes functions (2). Castillo and Revilla have proven that the form of Euler's equation applicable for this problem is:

$$\frac{\int_{x_0}^{x_1} F\ (s,\ y,\ y')\ dx}{\int_{x_0}^{x_i} G\ (x,\ y,\ y')\ dx} = \frac{\frac{\partial F}{\partial y} - \frac{d}{dx}\ (\frac{\partial F}{\partial y'})}{\frac{\partial G}{\partial y} - \frac{d}{dx}\ (\frac{\partial G}{\partial y'})} \tag{3}$$

Therefore the curve which gives the minimum safety factor will have to satisfy this integro-differential equation.

Now let the width of the slices reduce to zero and $f = f(x)$ and $y = y(x)$ be the equations of the curves representing the slope profile and the sliding curves, respectively, Figure 1-B.

Now the substitution of

$$\Delta w_i = \gamma (y - f)\ \Delta x \tag{4}$$

into equation (1) gives

$$S = \frac{\int_{x_o}^{x_1} C\ (1 + y'^2)\ dx}{\int_{x_o}^{x_1} \gamma(y - f(x))y'dx} \tag{5}$$

where γ is the unit weight of the soil and x_o and x_1 are the abscissas of the two points where the sliding line intersects the slope profile.

The method is applied to an exponential slope that indicates a spoil slope. The spoil slope profile can be assumed as

$$f = H(e^{x/H_1} - 1) \tag{6}$$

H and H_1 are constants, Figure 1-B

The Euler equation for (S) is

$$S = \frac{2cy''}{\gamma f'} \tag{7}$$

Thus

$$y' = \frac{-\gamma S}{2c} f + B \tag{8}$$

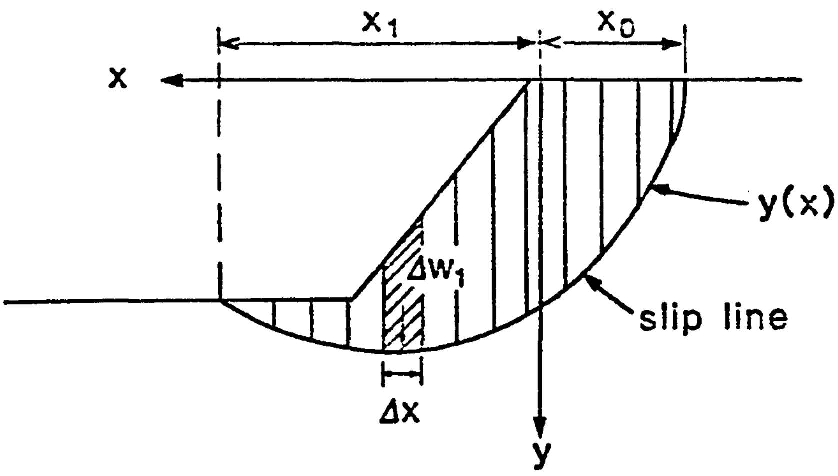

Figure 1, Slope profile and diagram used in Janleu's method.

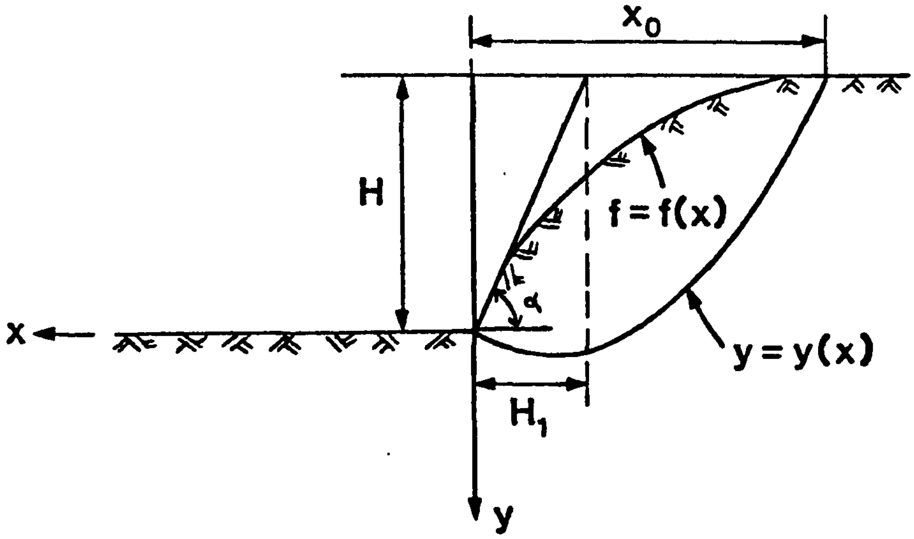

Figure 1-B, Geometrical definition of an exponential slope.
(Revilla and Castillo, 1977)

and its general solution is

$$y = -\frac{S\gamma}{2c} H H_1 e^{x/H_1} + \frac{S\gamma}{2c} Hx + Bx + D \tag{9}$$

using

$$G = \frac{\gamma H}{2c}$$

leads to

$$y = GH_1Se^{x/H_1} + (B + GS) c + D \tag{10}$$

This curve must pass throught the points (0,0), thus

$$D = G_1H_1S$$

and the problem must satisfy the following transversality condition

$$y'^2 - 2y'f' - 1 \,\Big|_{x = x_0} = 0 \tag{11}$$

For the details of the formulation the reader can refer to Revilla and Castillo (1977).

We now have equation (5) and (10) and (11) which have three unknown (S, x_0, B). However, the equations are non-linear.

A hypotical problem is analyzed with the following parameters

C lb/ft^2	H ft	H' ft	ϕ	γ lb/ft^3	F_s
600	14	5	0.0	120	.76
700	14	5	0.0	120	0.91
800	14	5	0.0	120	1.07
900	14	5	0.0	120	1.22
1000	14	5	0.0	120	1.40

and for each corresponding cohesion the safety factor in the last column is obtained.

The effect of cohesion on the safety factor is obvious. With decreasing cohesion the safety factor approaches to zero.

This proves that the variational method based on Janbu's method cannot be applied to non-cohesive spoil slopes of strip mines.

The following computer program is arranged to solve the non-linear equation by employing the numerical method.

```
$JOB
      DIMENSION S(10),B(5),XO(5),X(30)
      COMMON N
      COMMON /OTHERS/D,V,H1,C,IZ
C     C=COHESION OF SOIL POUND PER SQUARE FT
C     D=DENSITY OF SOIL POUND PER CUBIC FT
C     HI IS A CONSTANT  IN FEET
C     V=HEIGHT OF SPOIL SLOPE IN FEET
C     NUMBER OF SUBINTERVALS
      N=500
      READ(5,1)C,D,H1,V
    1 FORMAT(4F8.2)
C     X(1)=SF
C     X(2)=B
C     X(3)=XO
C     ESTIMATE THE VALUES FOR UNKNOWNS
      X(1)=3.
      X(2)=21.
      X(3)=33.
C     IZ IS THE NUMBER OF ITERATIONS
      IZ=30
      CALL NONLIN(3,5,IZ,2,X,.001)
C     3 IS THE NUMBER OF EQUATION
C     5 IS THE NUMBER OF DIGIT NUMBERS
C     2 IS THE OUTPUT FORMAT
C     .001 IS THE PERCISION OF THE CALCULATION
      WRITE(6,3)C,D,H1,V
    3 FORMAT(5X,'COHESION OF SOIL=',F6.2,15X,'DENSITY OF SOIL=',F6.2,15X
     *,'H1=',F6.2,15X,'HEIGHT OF SPOIL SLOPE =',F6.2,/)
      WRITE(6,2)X(1),X(2),X(3)
    2 FORMAT(5X,'SAFETY FACTOR=',F6.2,15X,'CONSTANT=',F6.2,15X,'XO=',F6.
     *2)
C     SUBROUTINE AUXFCN SOLVES THE INTEGRALS BY NUMERICALS METHOD
      STOP
      END
C     SUBROUTINE NONLIN IS WRITTEN BY DR. KEN BROWN IN THE NUMERICAL
C     SOLUTION OF ALGEBRIC EQUATION,1968

        SUBROUTINE NONLIN(N,NUMSIG,MAXIT,IPRINT,X,EPS)
        REAL      X(30),PART(30),TEMP(30),COL(30,31),RELCON,F
     & ,FACTOR,HOLD,H,FPLUS,DERMAX,TEST
        DIMENSION ISUB(30),LOOKUP(30,30)
        IFLAG=0.
        DELTA=1.E-7
        RELCON=10.E+0**(-NUMSIG)
        JTEST=1
        IF(IPRINT.EQ.1)PRINT 48
 48     FORMAT(1H1)
        DO 700 M=1,MAXIT
        IQUIT=0
        FMAX=0
        M1=M-1
        IF(IPRINT.NE.1)GO  TO 9
        PRINT  49,M1,(X(I),I=1,N)
 49     FORMAT(I5,3E18.8/(E23.8,2E18.8))
  9     DO 10 J=1,N
 10     LOOKUP(1,J)=J
        DO 500 K=1,N
        IF(K-1)134,134,131
 131    KMIN=K-1
```

```
      CALL BACK(KMIN,N,X,ISUB,COE,LOOKUP)
134   CALL AUXFCN(X,F,K)
      FMAX=AMAX1(FMAX,ABS(F))
      IF(ABS(F).GE.EPS) GO TO 1345
      IQUIT=IQUIT+1
      IF(IQUIT.NE.N)GO TO 1345
      GO TO 725
1345  FACTOR=0.001E+00
135   ITALLY=0
      DO 200 I=K,N
      ITEMP=LOOKUP(K,I)
      HOLD=X(ITEMP)
      PREC=5.E-4
      ETA=FACTOR*ABS(HOLD)
      H=AMIN1(FMAX,ETA)
      IF(H.LT.PREC) H=PREC
      X(ITEMP)=HOLD+H
      IF(K-1)161,161,151
151   CALL BACK (KMIN,N,X,ISUB,COE,LOOKUP)
161   CALL AUXFCN(X,FPLUS,K)
      PART(ITEMP)=(FPLUS-F)/H
      X(ITEMP)=HOLD
      IF(ABS(PART(ITEMP)).LT.DELTA) GO TO 190
      IF(ABS(F/PART(ITEMP)).LE.1.E+15)GO TO 200
190   ITALLY=ITALLY+1
200   CONTINUE
      IF(ITALLY.LE.N-K) GO TO 202
      FACTOR=FACTOR*10.0E+00
      IF (FACTOR.GT.11.) GO TO 775
      GO TO 135
202   IF(K.LT.N) GO TO 203
      IF(ABS(PART(ITEMP)).LT.DELTA) GO TO 775
      COE(K,N+1)=0.0E+00
      KMAX=ITEMP
      GO TO 500
203   KMAX=LOOKUP(K,K)
      DERMAX=ABS(PART(KMAX))
      KPLUS=K+1
      DO 210 I=KPLUS,N
      JSUB=LOOKUP(K,I)
      TEST=ABS(PART(JSUB))
      IF(TEST.LT.DERMAX) GO TO 209
      DERMAX=TEST
      LOOKUP(KPLUS,I)=KMAX
      KMAX=JSUB
      GO TO 210
209   LOOKUP(KPLUS,I)=JSUB
210   CONTINUE
      IF(ABS(PART(KMAX)).EQ.0.0)GO TO 775
      ISUB(K)=KMAX
      COE(K,N+1)=0.0E+00
      DO 220 J=KPLUS,N
      JSUB=LOOKUP(KPLUS,J)
      COE(K,JSUB)=-PART(JSUB)/PART(KMAX)
      COE(K,N+1)=COE(K,N+1)+PART(JSUB)*X(JSUB)
220   CONTINUE
500   COE(K,N+1)=(COE(K,N+1)-F)/PART(KMAX)+X(KMAX)
      X(KMAX)=COE(N,N+1)
      IF(N.EQ.1) GO TO 610
      CALL BACK(N-1,N,X,ISUB,COE,LOOKUP)
```

```
610     IF(M-1) 650,650,625
625     DO 630 I=1,N
        IF(ABS(TEMP(I)-X(I)).GT.ABS(X(I))*RELCON) GO TC 649
630     CONTINUE
        JTEST=JTEST+1
        IF(JTEST-3)650,725,725
649     JTEST=1
650     DO 660 I=1,N
660     TEMP(I)=X(I)
700     CONTINUE
        PRINT 1753
1753    FORMAT(/'NO CONVERGENCE.MAX NUMBER OF ITERATIONS USED.')
        IF(IPRINT.NE.1)GO TO 800
        PRINT 1763
1763    FORMAT('FUNCTION VALUES AT THE LAST APPROXIMATION FOLLOW:'/)
        IFLAG=1
        GO TO 7777
725     IF(IPRINT.NE.1) GO TO 800
7777    DO 750 K=1,N
        CALL AUXFCN(X,PART(K),K)
750     CONTINUE
        IF(IFLAG.NE.1)GO TO 8777
        PRINT 7788,(PART(K),K=1,N)
7788    FORMAT(3E20.8)
        GO TO 800
8777    PRINT 751
751     FORMAT(//'CONVERGENCE HAS BEEN ACHIEVED.THE FUNCTION VALUES')
        PRINT 7515,(PART(K),K=1,N)
7515    FORMAT('AT THE FINAL APPROXIMATION FOLLOW:'//(3E20.8))
        GO TO 800
775     PRINT 752
752     FORMAT(//'MODIFIED JACOBIAN IS SINGULAR.TRY A DIFFERENT')
        PRINT 7525
7525    FORMAT('INITIAL APPROXIMATION.')
800     MAXIT=M1+1
        RETURN
        END

        SUBROUTINE BACK(KMIN,N,X,ISUB,COE,LOOKUP)
        DIMENSION  X(30),COE(30,31),ISUB(30),LOOKUP(30,30)
      COMMON /OTHERS/D,V,H1,C,IZ
        DO 200 KK=1,KMIN
        KM=KMIN-KK+2
        KMAX=ISUB(KM-1)
        X(KMAX)=0.0E+00
        DO 100 J=KM,N
        JSUB=LOOKUP(KM,J)
        X(KMAX)=X(KMAX)+COE(KM-1,JSUB)*X(JSUB)
100     CONTINUE
        X(KMAX)=X(KMAX)+COE(KM-1,N+1)
200     CONTINUE
        RETURN
        END

      SUBROUTINE AUXFCN(X,Y,K)
      DIMENSION X(3),R(500),P(500)
      COMMON N
      COMMON /OTHERS/D,V,H1,C,IZ
      N=500
      G=(D*V)/(2.*C)
```

```
      GO TO (1,2,3),K
    1 FO=C+C*X(2)**2
      FN=C*(1.+((-G*X(1)*EXP(X(3)/H1))+(G*X(1)+X(2)))**2)
      RR=0.0
      M=N-1
      DO 4 I=1,M
      Q=(X(3)/N)*I
      R(I)=C*(1.+((-G*X(1)*EXP(Q/H1))+(G*X(1)+X(2)))**2)
      R(I)=RR+R(I)
      RR=R(I)
    4 CONTINUE
      RR=2.*RR
      H11=FO+FN+RR
      H11=(X(3)/(2.*N))*H11
      FO=D*X(2)
      FN=D*(-G*H1*X(1)*EXP(X(3)/H1)+G*X(1)*X(3)+X(2)*X(3)+G*H1*X(1)-V*EX
     *P(X(3)/H1)+V)*(-G*EXP(X(3)/H1)+G*X(1)+X(2))
      PP=0.0
      M=N-1
      DO 5 J=1,M
      Q=(X(3)/N)*J
      P(J)=D*(-G*H1*X(1)*EXP(Q/H1)+G*X(1)*X(3)+X(2)*X(3)+G*H1*X(1)-V*EXP
     *(Q/H1)+V)*(-G*EXP(Q/H1)+G*X(1)+X(2))
      P(J)=PP+P(J)
      PP=P(J)
    5 CONTINUE
      PP=2.*PP
      H2=FO+FN+PP
      H2=(X(3)/(2.*N))*H2
      Y=X(1)*H2-H11
      RETURN
    2 Y=(-G*X(1)*EXP(X(3)/H1)+(G*X(1)+X(2)))**2-2.*(-G*X(1)*EXP(X(3)/H1)
     *+(G*X(1)+X(2)))*V/H1*EXP(X(3)/H1)-1.
      RETURN
    3 Y=V*(EXP(X(3)/H1)-1.)+G*H1*X(1)*EXP(X(3)/H1)-(G*X(1)+X(2))*X(3)+G*
     *H1*X(1)
      RETURN
      END
```

```
$EXEC
 COHESION OF SOIL=900.00              DENSITY OF SOIL=130.00              H1= -

 SAFETY FACTOR=  1.11            CONSTANT=  2.17                XO= 18.64

STATEMENTS EXECUTED=  244511

CORE USAGE       OBJECT CODE=   10224 BYTES,ARRAY AREA=   11908 BYTES,TOTAL AREA AVA

DIAGNOSTICS        NUMBER OF ERRORS=       0, NUMBER OF WARNINGS=       0, NUMBER OF

COMPILE TIME=     0.09 SEC,EXECUTION TIME=     4.74 SEC,     22.04.24    MONDAY
```

Appendix C

Finite Element Formulation and Computer Program

Finite Element Formulation For Rock As
A Linear Material

In this section, the standard finite element technique is described and then an appropriate stiffness martix for a particular rock is suggested.

Triangular Finite Element

The basis of the finite element analysis is subdividing a continuum into an assemblage of discrete pieces called finite elements, the vertices of which are called "nodal points", Figure C-1. Triangular elements are the simplest to use because if made small enough, they give results comparable to results obtained with more elaborate quadrilateral elements.

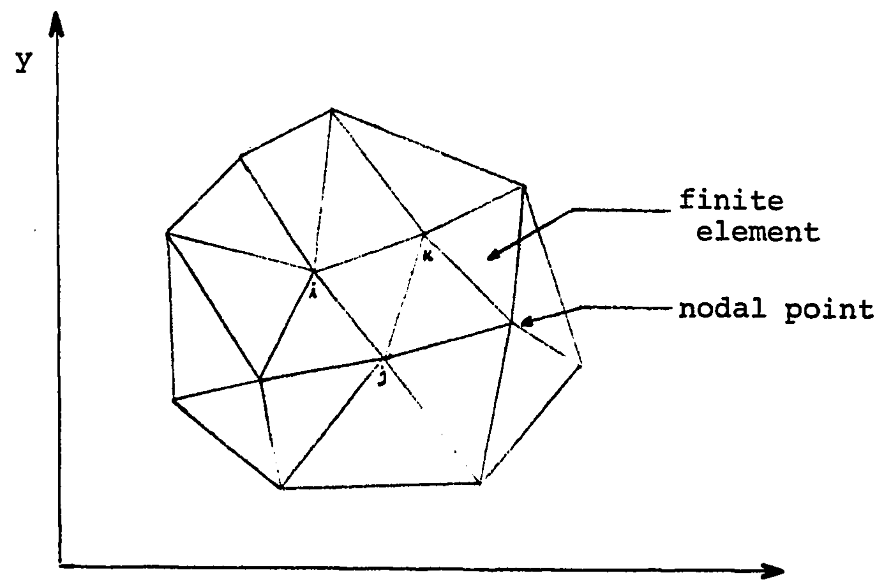

Figure C-1. A continuum divided into triangular elements.

Elemental Stiffness Formulation

Consider a triangle element of Figure C-1 with a constant thickness h and the local coordinates as shown in Figure C-2.

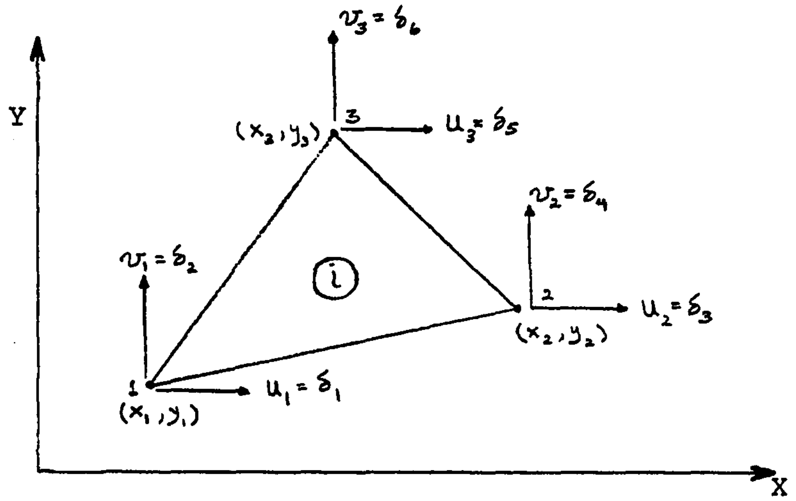

Figure C-2. The three-noded triangular element, local system.

Suitable displacement functions have been shown to be the linear polynomials

$$U_i(x,y) = a_1 + a_2x + a_3y \qquad (1\text{-a})$$

$$V_i(x,y) = a_4 + a_5x + a_6y \qquad (1\text{-b})$$

where U (x,y) and V(x,y) are the x and y components of displacement within the element. Let the element nodal displacement vector δ_i be defined as

$$\delta_i = \begin{Bmatrix} \delta_1 \\ \delta_2 \\ \delta_3 \\ \delta_4 \\ \delta_5 \\ \delta_6 \end{Bmatrix} = \begin{Bmatrix} U_1 \\ V_1 \\ U_2 \\ V_2 \\ U_3 \\ V_3 \end{Bmatrix} \qquad (2)$$

Thus the element has 6 degrees of freedom. The displacement functions can be written in matrix form as

$$\begin{Bmatrix} U_i(x,y) \\ V_i(x,y) \end{Bmatrix} = \begin{bmatrix} 1 & x & y & 0 & 0 & 0 \\ 0 & 0 & 0 & 1 & x & y \end{bmatrix} \begin{Bmatrix} a_1 \\ a_2 \\ a_3 \\ a_4 \\ a_5 \\ a_6 \end{Bmatrix}$$

Where $a_1 \; . \; . \; . \; a_6$ are constants that depend on the geometry and nodal displacement of the element. The nodal displacement vector is

$$\begin{Bmatrix} U & (x,y) \\ V & (x,y) \end{Bmatrix} = \begin{bmatrix} N \end{bmatrix}_i \quad \begin{Bmatrix} a \end{Bmatrix}_i \qquad (3)$$

where

$$\underset{2x6}{\begin{bmatrix} N \end{bmatrix}_i} = \begin{bmatrix} 1 & x & y & 0 & 0 & 0 \\ 0 & 0 & 0 & 1 & x & 6 \end{bmatrix}$$ Shape function matrix

and

$$\begin{Bmatrix} a \end{Bmatrix}^T = \begin{bmatrix} a_1 & a_2 & a_3 & a_4 & a_5 & a_6 \end{bmatrix}$$ Generalized Coordinates Vector

Equations (1-a) and (1-b) are admissable functions and so satisfy the definition of completeness.

If $a_2 = a_3 = a_5 = a_6 = 0$, then

$$U_i \; (x,y) = a_1$$

$$V_i \; (s,y) = a_4$$

which represents the rigid body displacements. For a plane elasticity problem the strain-displacement relationship is

$$\varepsilon_{xx} = \frac{\partial u}{\partial x} + \tfrac{1}{2}\left(\frac{\partial^2 u}{\partial x^2} + \frac{\partial^2 v}{\partial x^2}\right) \qquad \text{strain in x-direction}$$

$$\varepsilon_{yy} = \frac{\partial v}{\partial y} + \tfrac{1}{2}\left(\frac{\partial^2 u}{\partial y^2} + \frac{\partial^2 v}{\partial y^2}\right) \qquad \text{strain in y-direction}$$

$$\gamma_{xy} = \frac{\partial u}{\partial y} + \frac{\partial v}{\partial x} + \frac{\partial u}{\partial x}\frac{\partial u}{\partial y} + \frac{\partial v}{\partial x}\frac{\partial v}{\partial y} \qquad \text{shear strain in x-y plane}$$

Considering only first order (linear) terms and neglecting the second order changes in the displacements these simplify to

$$\varepsilon_{xx} = \frac{\partial U(x,y)}{\partial x} \tag{4-a}$$

$$\varepsilon_{yy} = \frac{\partial V(x,y)}{\partial y} \tag{4-b}$$

$$\gamma_{xy} = \frac{\partial U(x,y)}{\partial y} + \frac{\partial V(x,y)}{\partial x} \tag{4-c}$$

The strain field is found by differentiating equations (1-a) and (1-b) according to the definitions of strain:

$$\varepsilon_{xx} = a_2$$

$$\varepsilon_{yy} = a_6$$

$$\gamma_{xy} = a_3 + a_5$$

Therefore, the strain components in the element are constant. The linearity of U (x,y) and V(x,y) ensures compatibility between the sides of adjoining elements.

Substituting element nodal coordinate values in Equations (1-a) and (1-b) we obtain

$$\begin{Bmatrix} U_1 \\ V_1 \\ U_2 \\ V_2 \\ U_3 \\ V_3 \end{Bmatrix} = \begin{bmatrix} 1 & x_1 & y_1 & 0 & 0 & 0 \\ 0 & 0 & 0 & 1 & x_1 & y_1 \\ 1 & x_2 & y_2 & 0 & 0 & 0 \\ 0 & 0 & 0 & 1 & x_2 & y_2 \\ 1 & x_3 & y_3 & 0 & 0 & 0 \\ 0 & 0 & 0 & 1 & x_3 & y_3 \end{bmatrix} \begin{Bmatrix} a_1 \\ a_2 \\ a_3 \\ a_4 \\ a_5 \\ a_6 \end{Bmatrix}$$

If we take the local coordinate system origin at node 1 and specify the coordinates of nodes 2 and 3 with respect to node 1, then $x_1 = 0$, $y_1 = 0$, which reduces the previous equation to:

$$\begin{Bmatrix} U_1 \\ V_1 \\ U_2 \\ V_2 \\ U_3 \\ V_3 \end{Bmatrix} = \begin{bmatrix} 1 & 0 & 0 & 0 & 0 & 0 \\ 0 & 0 & 0 & 1 & 0 & 0 \\ 1 & x_2 & y_2 & 0 & 0 & 0 \\ 0 & 0 & 0 & 1 & x_2 & y_2 \\ 1 & x_3 & y_3 & 0 & 0 & 0 \\ 0 & 0 & 0 & 1 & x_3 & y_3 \end{bmatrix} \begin{Bmatrix} a_1 \\ a_2 \\ a_3 \\ a_4 \\ a_5 \\ a_6 \end{Bmatrix}$$

or

$$\{\delta\}_i = [A]_i \{a\}_i \qquad (5)$$

where

$$\underset{6\times 6}{[A]_i} = \begin{bmatrix} 1 & 0 & 0 & 0 & 0 & 0 \\ 0 & 0 & 0 & 1 & 0 & 0 \\ 1 & x_2 & y_2 & 0 & 0 & 0 \\ 0 & 0 & 0 & 1 & x_2 & y_2 \\ 1 & x_3 & y_3 & 0 & 0 & 0 \\ 0 & 0 & 0 & 1 & x_3 & y_3 \end{bmatrix} \qquad (6)$$

From equation (5)

$$\{a\}_i = [A^{-1}]_i \{\delta\}_i \tag{7}$$

Inversion of $[A]$ is always possible because

$$\det.[A] = -\left\{\det.\begin{bmatrix} 1 & x_1 & y_1 \\ 1 & x_2 & y_2 \\ 1 & x_3 & y_3 \end{bmatrix}\right\}^2$$

by the Laplace expansion and the quantity

$$\det.\begin{bmatrix} 1 & x_1 & y_1 \\ 1 & x_2 & y_2 \\ 1 & x_3 & y_3 \end{bmatrix}$$

is twice the area of the element. A routine calculation gives

$$\underset{6 \times 6}{[A^{-1}]_i} = \frac{1}{\Delta}\begin{bmatrix} \Delta & 0 & 0 & 0 & 0 & 0 \\ y_2 - y_3 & 0 & y_3 & 0 & -y_2 & 0 \\ x_3 - x_2 & 0 & -x_3 & 0 & x_2 & 0 \\ 0 & \Delta & 0 & 0 & 0 & 0 \\ 0 & y_2 - y_3 & 0 & y_3 & 0 & -y_2 \\ 0 & x_3 - x_2 & 0 & -x_3 & 0 & x_2 \end{bmatrix}$$

in which

$\Delta = 2$ (area of the element triangle) $= X_2\ Y_3 - X_3\ Y_2$

substituting equation (7) into equation (3) gives the displacement fields in terms of the element nodal displacement vector:

$$\begin{Bmatrix} U_i(x,y) \\ V_i(x,y) \end{Bmatrix} = \begin{bmatrix} N \end{bmatrix}_i \begin{Bmatrix} a \end{Bmatrix}_i = \begin{bmatrix} N \end{bmatrix} \begin{bmatrix} A^{-1} \end{bmatrix}_i \begin{Bmatrix} \delta \end{Bmatrix}_i \qquad (9)$$

Now, the strain vector, $\{\varepsilon\}_i$ can be computed from the displacement field given by equation (9):

$$\{\varepsilon\}_i = \begin{Bmatrix} \varepsilon_x \\ \varepsilon_y \\ \gamma_{xy} \end{Bmatrix} = \begin{Bmatrix} U_x \\ U_y \\ U_y + V_x \end{Bmatrix} = \begin{bmatrix} \frac{\partial}{\partial x} & 0 \\ 0 & \frac{\partial}{\partial y} \\ \frac{\partial}{\partial y} & \frac{\partial}{\partial x} \end{bmatrix} \begin{Bmatrix} U_i(x,y) \\ V_i(x,y) \end{Bmatrix}$$

or

$$\{\varepsilon\}_i = \begin{bmatrix} B \end{bmatrix} \begin{bmatrix} A^{-1} \end{bmatrix}_i \{\partial\}_i \qquad (10)$$

where

$$\underset{3X6}{\begin{bmatrix} B \end{bmatrix}}_i = \begin{bmatrix} \frac{\partial}{\partial x} & 0 \\ 0 & \frac{\partial}{\partial y} \\ \frac{\partial}{\partial y} & \frac{\partial}{\partial x} \end{bmatrix} \qquad \underset{2x6}{\begin{bmatrix} N \end{bmatrix}}_i = \begin{bmatrix} 0 & 1 & 0 & 0 & 0 & 0 \\ 0 & 0 & 0 & 0 & 0 & 1 \\ 0 & 0 & 1 & 0 & 1 & 0 \end{bmatrix}$$

The stress compontents in the element can be derived using the material constitutive relationships expressing stress components in terms of strain components given in equation (10). This relationship can be expressed as:

$$\{\sigma\} = [D]\{\varepsilon\}_i = [D][B][A^{-1}]_i\{\delta\}_i \tag{11}$$

where

$$\underset{3x1}{\{\sigma\}_i} = \begin{Bmatrix} \sigma_x \\ \sigma_y \\ \sigma_{xy} \end{Bmatrix}$$

and $\underset{3x3}{[D]_i}$ is elasticity matrix of the element.

<u>Element Stress-Strain Relationships</u>

The stress-strain relations for a Hookian material are

$$\begin{bmatrix} \sigma_{xx} \\ \sigma_{yy} \\ \tau_{xy} \end{bmatrix} = \begin{bmatrix} C_{11} & C_{12} & C_{13} \\ C_{21} & C_{22} & C_{23} \\ C_{31} & C_{32} & C_{33} \end{bmatrix} \begin{bmatrix} \varepsilon_{xx} \\ \varepsilon_{yy} \\ \gamma_{xy} \end{bmatrix}$$

For an isotropic rock in plane strain

$$[C] = \frac{E}{(1+\nu)\ (1-2\nu)} \begin{bmatrix} 1-\nu & \nu & 0 \\ \nu & 1-\nu & 0 \\ 0 & 0 & \frac{1-2\nu}{2} \end{bmatrix}$$

or

$$[D] = \mu \begin{bmatrix} 1 & D_{12} & 0 \\ D_{12} & 1 & 0 \\ 0 & 0 & D_{33} \end{bmatrix}$$

where E is the modulus of elasticity, ν is Poisson's ratio and

$$\mu = \frac{E(1-\nu)}{(1+\nu)(1-2\nu)}$$

$$D_{12} = \frac{\nu}{1-\nu}$$

$$D_{33} = \frac{1-2\nu}{2(1-\nu)}$$

In order to account for the coal layer that has parallel texture a transversely anisotropic elastic stress-strain relationship is suggested.

$$[D] = \begin{bmatrix} \frac{E_1(1-\eta\nu_2^2)}{(1+\nu_1)(1-\nu_1-2\eta\nu_2^2)} & \frac{E_1\nu_2}{1-\nu_1 2\eta\nu_2^2} & 0 \\ \frac{E_1\nu_2}{1-\nu_1-2\eta\nu_2^2} & \frac{E_2(1-\nu_1)}{1-\nu_1-2\eta\nu_2^2} & 0 \\ 0 & 0 & 2G_2 \end{bmatrix}$$

or

$$[D] = \begin{bmatrix} D_{11} & D_{12} & 0 \\ D_{12} & D_{22} & 0 \\ 0 & 0 & D_{33} \end{bmatrix} \qquad (12)$$

with $\eta = \frac{E_1}{E_2}$. The x is oriented parallel but the y axis is orthogonal to the texture. The Young's moduli E_1 and E_2 are valid for compression normal and parallel to the texture, respectively. Poisson's ratio ν_2 is the strain parallel to the texture in orthogonal compression, and ν_1 is for strain parallel to texture in parallel compression, which is also perpendicular to the strain.

This rock model has already been applied to regularly jointed rock. This model gives useful results in a rock with the series of discontinuitites that represents a direction of latent cleavity due to bedding or schistosity. Substituting the elements of matrices $\left[D\right]_i$ (for isotropic) and $\left[B\right]_i$ into Equation (11) we obtain:

$$\left\{\sigma\right\}_i = \begin{pmatrix} 0 & \mu & 0 & 0 & 0 & \mu D_{12} \\ 0 & \mu D_{12} & 0 & 0 & 0 & \mu \\ 0 & 0 & \mu D_{33} & 0 & \mu D_{33} & 0 \end{pmatrix} \left[A^{-1}\right]_i \left\{\delta\right\}_i \qquad (13)$$

in which the first and fourth column elements are zero since they represent zero stresses due to rigid body displacements.

As in the previous finite element formulations, for some given loading (in x-y plane) on the element, we can formulate the total potential energy expression generalized element stiffness matrix, $\bar{K}_i$ as

$$\left[\bar{K}\right]_i = \iiint_{V_i} \left[B\right]_i^T \left[D\right]_i \left[B\right]_i \, dv_i = h \iint_{A_i} \left[B\right]_i^T \left[D\right]_i \left[B\right]_i \, da_i \qquad (14)$$

where A_i represents the area of the i^{th} element and h is the thickness (constant) of the element. On carrying the multiplication and integration over A_i, we arrive at the matrix $\left[\bar{K}\right]_i$ for isotropic and transversely anistropic materials respectively in the forms:

$$\left[\bar{K}\right]_i = \frac{h\Delta\mu}{2}\begin{bmatrix} 0 & 0 & 0 & 0 & 0 & 0 \\ 0 & 1 & 0 & 0 & 0 & D_{12} \\ 0 & 0 & D_{33} & 0 & D_{33} & 0 \\ 0 & 0 & 0 & 0 & 0 & 0 \\ 0 & 0 & D_{33} & 0 & D_{33} & 0 \\ 0 & D_{12} & 0 & 0 & 0 & 1 \end{bmatrix} \tag{15-a}$$

$$\left[\bar{K}\right]_i = \frac{h\Delta}{2}\begin{bmatrix} 0 & 0 & 0 & 0 & 0 & 0 \\ 0 & D_{11} & 0 & 0 & 0 & D_{12} \\ 0 & 0 & D_{33} & 0 & D_{33} & 0 \\ 0 & 0 & 0 & 0 & 0 & 0 \\ 0 & 0 & D_{33} & 0 & D_{33} & 0 \\ 0 & D_{12} & 0 & 0 & 0 & D_{22} \end{bmatrix} \tag{15-b}$$

The equilibrium equation of the element is:

$$\left\{F\right\}_i = \left[K\right] \left\{\delta\right\}_i \tag{16}$$

where

$$\left[K\right]_i = \left[A^{-1}\right]_i^T \left[\bar{K}\right]_i \left[A^{-1}\right]_i \tag{17}$$

is the element stiffness matrix. By Equations (7) and (17) we may rewrite Equation (16) in the form

$$\left\{F\right\}_i = \left[A^{-1}\right]_i^T \left[\bar{K}\right]_i \left[A^{-1}\right] \left[\delta\right]_i = \left[A^{-1}\right]_i^T \left[\bar{K}\right]_i \left\{a\right\}_i \tag{18}$$

Multiplication of $\left[A^{-1}\right]_i^T$ and $\left[K\right]_i$ for isotropic and transversely anisotropic respectively yields the matrices

$$\left[A^{-1}\right]_i^T\left[\bar{K}\right]_i = \frac{h\mu}{2}\begin{bmatrix} 0 & (y_2 - y_3) & D_{33}(X_3 - X_2) & 0 & D_{33}(X_3 - X_2) & D_{12}(y_2 - y_3) \\ 0 & D_{12}(X_3 - X_2) & D_{33}(y_2 - y_3) & 0 & D_{33}(y_2 - y_3) & (X_3 - X_2) \\ 0 & y_3 & -D_{33}X_2 & 0 & -D_{33}X_3 & D_{12}y_3 \\ 0 & -D_{12}X_3 & D_{33}y_3 & 0 & D_{33}y_3 & -X_3 \\ 0 & -y_2 & D_{33}X_2 & 0 & D_{33}X_2 & -D_{12}y_2 \\ 0 & D_{12}X_2 & -D_{33}Y_2 & 0 & -D_{33}y_2 & X_2 \end{bmatrix} \quad (19\text{-a})$$

For isotropic

$$\left[A^{-1}\right]_i^T\left[\bar{K}\right]_i = \frac{h}{2}\begin{bmatrix} 0 & D_{11}(y_2 - y_3) & D_{33}(X_3 - X_2) & 0 & D_{33}(X_3 - X_2) & D_{12}(y_2 - y_3) \\ 0 & D_{12}(X_3 - X_2) & D_{33}(y_2 - y_3) & 0 & D_{33}(y_2 - y_3) & D_{22}(X_3 - X_2) \\ 0 & D_{11}y_3 & -D_{33}X_3 & 0 & -D_{33}X_3 & D_{12}y_3 \\ 0 & -D_{12}X_3 & D_{33}y_3 & 0 & D_{33}y_3 & -D_{22}X_3 \\ 0 & -D_{11}y_2 & D_{33}X_2 & 0 & D_{33}X_2 & -D_{12}y_2 \\ 0 & D_{12}X_2 & -D_{33}y_2 & 0 & -D_{33}y_2 & D_{22}X_2 \end{bmatrix} \quad (19\text{-b})$$

For transversely anisotropic

Each column of matrices (19-a) and (19-b) satisfies the conditions

$$\Sigma F_x = \text{Row (1)} + \text{Row (3)} + \text{Row (5)} = 0$$

$$\Sigma F_y = \text{Row (2)} = \text{Row (4)} + \text{Row (6)} = 0$$

The zeros in the first and fourth columns of the matrice (19-a) and (19-b) represents nodal forces induced by unit values of a_1 and a_4 which correspond to rigid body translations in the X and y directions, respectively.

Definition of the element stiffness matrix Equation (17) then yields,

$$\left[K\right]_i = \left[A^{-1}\right]_i^T \left[\bar{K}\right]_i \left[A^{-1}\right]_i$$

which, after substitution will give the element stiffness matrix for isotropic and transversely anisotropic rock respectively.

Subroutine TES performs this function in the computer program listed in the following section of this appendix.

$$
[K]_i = \frac{h\mu}{2\Delta}
\left[\begin{array}{c|c|c|c|c|c}
\begin{array}{l}(y_2 - y_3)^2\\ + D_{33}(x_3 - x_2)^2\end{array} &
\begin{array}{l}D_{12}(x_3 - x_2)(y_2 - y_3)\\ + D_{33}(x_3 - x_2)(y_2 - y_3)\end{array} &
\begin{array}{l}y_3(y_2 - y_3)\\ - D_{33}x_3(x_3 - x_2)\end{array} &
\begin{array}{l}D_{33}y_3(x_3 - x_2)\\ - D_{12}x_3(y_2 - y_3)\end{array} &
\begin{array}{l}- y_2(y_2 - y_3)\\ + D_{33}x_2(x_3 - x_2)\end{array} &
\begin{array}{l}- D_{33}y_2(x_3 - x_2)\\ + D_{12}x_2(y_2 - y_3)\end{array} \\ \hline
\begin{array}{l}D_{12}(x_3 - x_2)(y_2 - y_3)\\ + D_{33}(y_2 - y_3)(x_3 - x_2)\end{array} &
\begin{array}{l}D_{33}(y_2 - y_3)^2\\ + (x_3 - x_2)^2\end{array} &
\begin{array}{l}D_{12}y_3(x_3 - x_2)\\ - D_{33}x_3(y_2 - y_3)\end{array} &
\begin{array}{l}D_{33}y_3(y_2 - y_3)\\ - x_3(x_3 - x_2)\end{array} &
\begin{array}{l}- D_{12}y_2(x_3 - x_2)\\ + D_{33}x_2(y_2 - y_3)\end{array} &
\begin{array}{l}- D_{33}y_2(y_2 - y_3)\\ + x_2(x_3 - x_2)\end{array} \\ \hline
\begin{array}{l}y_3(y_2 - y_3)\\ - D_{33}x_3(x_3 - x_2)\end{array} &
\begin{array}{l}- D_{33}x_3(y_2 - y_3)\\ + D_{12}y_3(x_3 - x_2)\end{array} &
y_3^2 + D_{33}x_3^2 &
- (D_{12} + D_{33})x_3y_3 &
\begin{array}{l}- y_3y_2\\ - D_{33}x_3x_2\end{array} &
\begin{array}{l}D_{33}x_3x_2\\ + D_{12}x_2y_3\end{array} \\ \hline
\begin{array}{l}- D_{12}x_3(y_2 - y_3)\\ + D_{33}y_3(x_3 - x_2)\end{array} &
\begin{array}{l}D_{33}y_3(y_2 - y_3)\\ - x_3(x_3 - x_2)\end{array} &
- (D_{12} + D_{33})x_3y_3 &
D_{33}y_3^2 + x_3^2 &
\begin{array}{l}D_{12}x_3y_2\\ + D_{33}x_2y_3\end{array} &
\begin{array}{l}- D_{33}y_3y_2\\ - x_3x_2\end{array} \\ \hline
\begin{array}{l}-y_2(y_2 - y_3)\\ + D_{33}x_2(x_3 - x_2)\end{array} &
\begin{array}{l}D_{33}x_2(y_2 - y_3)\\ - D_{12}y_2(x_3 - x_2)\end{array} &
\begin{array}{l}- y_2y_3\\ - D_{33}x_2x_3\end{array} &
\begin{array}{l}D_{33}x_2y_3\\ + D_{12}x_3y_2\end{array} &
y_2^2 + D_{33}x_2^2 &
\begin{array}{l}- (D_{12} + D_3)\\ x_2y_2\end{array} \\ \hline
\begin{array}{l}D_{12}x_2(y_2 - y_3)\\ - D_{33}y_2(x_3 - x_2)\end{array} &
\begin{array}{l}- D_{33}y_2(y_2 - y_3)\\ + x_2(x_3 - x_2)\end{array} &
\begin{array}{l}D_{12}x_2y_3\\ + D_{33}x_3y_2\end{array} &
\begin{array}{l}- D_{33}y_2y_3\\ - x_2x_3\end{array} &
- (D_{12} + D_{33})x_2y_2 &
D_{33}y_2^2 + x_2^2
\end{array}\right]
$$

(20-a) Element Stiffness Matrix for isotropic material

$$
[K] = \frac{h}{2\Delta}
\begin{bmatrix}
D_{11}(y_2 - y_3)^2 + D_{33}(x_3 - x_2)^2 & D_{33}(x_3 - x_2)(y_2 - y_3) + D_{12}(y_2 - y_3)(x_3 - x_2) & D_{11}(y_2 - y_3)\,y_3 - D_{33}(x_3 - x_2)\,x_3 & D_{33}(x_3 - x_2)\,y_3 - D_{12}(y_2 - y_3)\,x_3 & -D_{11}(y_2 - y_3)\,y_2 + D_{33}(x_3 - x_2)\,x_2 & -D_{33}(x_3 - x_2)\,y_2 + D_{12}(y_2 - y_3)\,x_2 \\
D_{12}(x_3 - x_2)(y_2 - y_3) + D_{33}(y_2 - y_3)(x_3 - x_2) & D_{33}(y_2 - y_3)^2 + D_{22}(x_3 - x_2)^2 & D_{12}(x_3 - x_2)\,y_3 - D_{33}(y_2 - y_3)\,x_3 & D_{33}(y_2 - y_3)\,y_3 - D_{22}(x_3 - x_2)\,x_3 & -D_{12}(x_3 - x_2)\,y_2 + D_{33}(y_2 - y_3)\,x_2 & -D_{33}(y_2 - y_3)\,y_2 + D_{22}(x_3 - x_2)\,x_2 \\
D_{11}y_3(y_2 - y_3) - D_{33}x_3(x_3 - x_2) & -D_{33}x_3(y_2 - y_3) + D_{12}y_3(x_3 - x_2) & D_{11}y_3^2 + D_{33}x_3^2 & -D_{33}x_3y_3 - D_{12}y_3x_3 & -D_{11}y_3y_2 - D_{33}x_3x_2 & D_{33}x_3y_2 + D_{12}y_3x_2 \\
-D_{12}x_3(y_2 - y_3) + D_{33}y_3(x_3 - x_2) & D_{33}y_3(y_2 - y_3) - D_{22}x_3(x_3 - x_2) & -D_{12}x_3y_3 - D_{33}y_3x_3 & D_{33}y_3^2 + D_{22}x_3^2 & D_{12}x_3y_2 + D_{33}y_3x_2 & -D_{33}y_3y_2 - D_{22}x_3x_2 \\
-D_{11}y_2(y_2 - y_3) + D_{33}x_2(x_3 - x_2) & D_{33}x_2(y_2 - y_3) - D_{12}y_2(x_3 - x_2) & -D_{11}y_2y_3 - D_{33}x_2x_3 & D_{33}x_2y_3 + D_{12}y_2x_3 & D_{11}y_2^2 + D_{33}x_2^2 & -D_{33}x_2y_2 - D_{12}y_2x_2 \\
D_{12}x_2(y_2 - y_3) - D_{33}y_2(x_3 - x_2) & D_{33}y_2(y_2 - y_3) + D_{22}x_2(x_3 - x_2) & D_{12}x_2y_3 + D_{33}y_2x_3 & -D_{33}y_2y_3 - D_{22}x_2x_3 & -(D_{12} + D_{33})\,x_2y_2 & D_{33}y_2^2 + D_{22}x_2^2
\end{bmatrix}
$$

(20-b) Element Stiffness Matrix for Transversely Isotropic Material

Assemblage of the Structural Stiffness Matrix

To solve the problem, it is necessary to combine the individual element stiffness matrices $\left[K \right]_i$ and the individual load matrices $\left\{ F \right\}_i$ to form the structural stiffness matrix $\left[K \right]$ and the structural load matrix $\left\{ F \right\}$, respectively.

All of the cited references on finite element analysis contains the process of assemblage.

The matrices $\left\{ F \right\}$ and $\left[K \right]$ connected with the structural system are related by the equation

$$\left\{ F \right\} = \left[K \right] \left\{ \delta \right\}$$

where $\left\{ F \right\}$ is the structural load matrix, $\left[K \right]$ as defined before and $\left\{ \delta \right\}$ in the structural nodal displacement matrix. Solution of this force-displacement equation gives the unknown nodal displacements $\left\{ \delta \right\}$.

The entire computational process for an elastic analysis is diagramatically represented in Figure C-3.

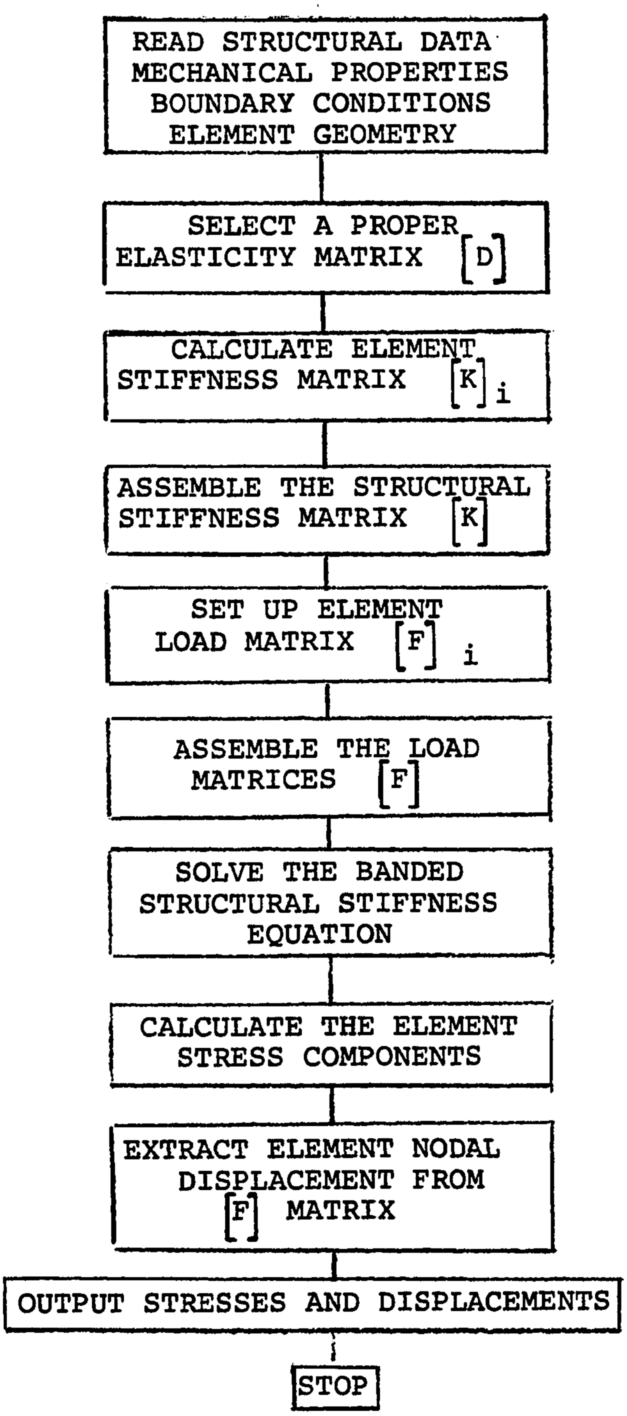

Figure C-3. FLOWCHART FOR FINITE ELEMENT PROGRAM

```
$JOB
      DIMENSION S(910,26),F(910,1),NFREE(910),NCOD(52),CM(910,1)
      DIMENSION ES(6,6),EF(6),IE(3),PX(3),PY(3),X(3),Y(3)
      DIMENSION SIGMA(3),ICR(6)
      DIMENSION INFMT(12),OUTFMT(12)
      DIMENSION IPCONE(20),IPCON(20),PCONQ(20),NCODE(886)
C=====================================================
C     THIS PROGRAM HAS BEEN WRITTEN BASED ON THE COURSE CONTENT OF CE
C     6763 AND HAS BEEN MODIFIED FOR ANALYSIS OF JOINTED BLOCKY ROCKS IN
C     1979. THE PROGRAM HAS BEEN ADJUSTED TO ANALYSE A STRIP MINE AND TO
C     CALCULATE STRESSES AND DISPLACEMENTS OF A CONTINUOUS MEDIA.
C     THE PROGRAM CAN SOLVE EITHER A PLANE STRESS OR PLANE STRAIN PROBLEM
C     FOR ANY GIVEN NODAL FORCES AND PRESCRIBED DISPLACEMENTS.
C     ANALYSIS IS PERFORMED BY THE FINITE ELEMENT METHOD.MAKING USE OF
C     LINEAR TRIANGULAR ELEMENTS.
C     BY COMBINING FOUR TRIANGULAR ELEMENTS IT BECOMES POSSIBLE TO USE
C     QUADRILATERAL ELEMENTS AND TO OBTAIN MORE ACCURATE RESULTS.
C=====================================================
C
C
C
C S-IS THE STRUCTURAL STIFFNESS MATRIX
C F-IS THE STRUCTURAL LOAD MATRIX
C NFREE-IS THE FREE NODES VECTOR
C NCOD-IS THE CONSTRAIND NODES VECTOR
C CM- IS THE VECTOR THAT REPLACES THE LOAD VECTOR F WHICH
C  WILL BE DESTRYED TO CONTAIN THE NODAL DISPLACEMENTS.
C  THE REASON THAT WE KEEP THE LOAD VECTOR, BECAUSE WE
C  GOING TO USE IT IN THE ENERGY CALCULATION
C ES-IS THE ELEMENT STIFFNESS MATRIX
C EF-IS THE ELEMENT LOAD VECTOR
C IE-IS THE VECTOR OF THE ELEMENT NODES INDEX
C P(X),P(Y)-ARE THE BOUNDARY TRACTIONS IN X AND DIRECTIONS RESPECTIVELY
C X,Y-ARE THE X AND Y COORDINATES OF EACH NODE TO BE CALCULATED
C  FROM CERTAIN FIXED GLOBAL COORDINATES
C SIGMA-IS THE STRESS VECTOR
C ICR- IS THE VECTOR OF ROW AND COLUMN INDICIES. THIS VECTOR
C    TAKES CARE OF FINDING THE ROWS AND COLUMNS IN THE STRUCTURAL
C    STIFFNESS MATRIX THAT CORRESPOND TO THE ROWS AND COLUMNS
C    OF THE ELEMENT STIFFNESS MATRIX UNDER CONSIDERATION
C NTE=NO OF TOTAL ELEMENTS
C NTD=NO OF TOTAL NODAL DISPLACEMENTS
C NTF=NO OF TOTAL FREE NODAL DISPLACEMENTS
C NCD=NO OF CONSTRAINED NODAL DISPLACEMENTS
C NB=BAD WIDTH OF THE S MATRIX
C NLC=NO OF LOADING CONDITIONS
C POISSIONS RATIO=NU,NO OF ELEMENT NODAL DISPL=NEND
C CODE NUMBER, CODE 0=PLANE STRAINE,CODE 1= PLANE STRESS
C NEND= NUMBER OF ELEMENT NODAL DISPLACEMENTS
C NPCONE- IS THE NUMBER OF PARTIALLY CONSTRAINED ELEMENT
C NPCON-IS THE NUMBER OF PARTIALLY CONSTRAINED NODES
C IPCONE-IS THE INDEX VECTOR OF PARTIALLY CONSTRAINED ELEMENTS
C IPCON-IS THE INDEX VECTOR OF PARTIALLY CONSTRAINED NODES
C PCONQ-IS THE INDEX VECTOR OF PARTIALLY CONSTRAINED QUANTITIES
      INTEGER CODE
      REAL NU,MU
      NU=.2
      E=8208.
C
C READ STRUCTURAL DATA
```

```
C
      READ (5,700) NTE,NTD,NCD,CODE,NB,NTF,NEND,NLC
  700 FORMAT(8I5)
C
C READ CONSTRAINED NODAL DISPL NUMBERS
C
      READ(5,702) (NCOD(I),I=1,9)
      READ(5,702) (NCOD(I),I=10,18)
      READ(5,702) (NCOD(I),I=19,27)
      READ(5,702) (NCOD(I),I=28,36)
      READ(5,702) (NCOD(I),I=37,45)
      READ(5,702) (NCOD(I),I=46,52)
 702  FORMAT(9I5)
C
C
C NCODE=0 FOR ELEMENT WITHOUT SPECIAL DISPLACEMENT
C NCODE=1 FORE ELEMENT WITH SPECIAL DISPLACEMENT
C INITIALIZED NCODE AS 0
C
      DO 998 K=1,NTE
      NCODE(K)=0.
  998 CONTINUE
          READ (5,933) NPCONE,NPCON
  933 FORMAT (2I5)
C
C WRITE INPUT DATA
C
      WRITE (6,800)
  800 FORMAT (1H1,1X,10HINPUT DATA/)
      PRINT 935,NPCONE,NPCON
 935  FORMAT (1H0,5X,7HNPCONE=,I5,5X,6HNPCON=,I5)
      IF (NPCONE)941,951,941
  941 DO 999 K=1,NPCONE
      READ (5,980) IPCONE(K)
  980 FORMAT (I5)
C
C MAKE NCODE=1 FOR ELEMENT WITH SPECIAL DISPLACEMENT
C
      J=IPCONE(K)
      NCODE(J)=1.
  999 CONTINUE
      PRINT 936
  936 FORMAT (1H0,5X,'INDEX VECTOR OF PARTIALLY CONSTRAINED ELEMENTS')
      PRINT 937,(IPCONE(K),K=1,NPCONE)
  937 FORMAT (1H0,5X,10I5)
C
      READ (5,702) (IPCON(K),K=1,NPCON)
      READ (5,950) (PCONQ(K),K=1,NPCON)
  950 FORMAT (6F10.5)
      PRINT 926
  926 FORMAT (1H0,5X,'INDEX VECTOR OF PARTIALLY CONSTRAINED NODES')
      PRINT 937,(IPCON(K),K=1,NPCON)
      PRINT 927
  927 FORMAT (1H0,5X,'INDEX VECTOR OF PARTIALLY CONSTRAINED QUANTITIES'
      DO 949 K=1,NPCON
      PRINT 932,K,PCONQ(K)
  932 FORMAT (1H0,5X,6HPCONQ(,I3,'3H)',E20.8)
  949 CONTINUE
  951 WRITE (6,801)
  801 FORMAT (1H0,2X,3HNTE,3X,3HNTD,2X,3HNCD,1X,4HCODE,3X,2HNB,2X,3HNTF
```

```
     11X,4HNEND,2X,3HNLC/)
      WRITE (6,700) NTE,NTD,NCD,CODE,NB,NTF,NEND,NLC
      WRITE (6,802)
  802 FORMAT(1H0,1X,31HCONSTRAINED NODAL DISPL NUMBERS/)
      WRITE (6,702) (NCOD(I),I=1,NCD)
      READ(5,703)INFMT
      READ (5,703) OUTFMT
  703 FORMAT(6X,12A4)
C
C INITIAL REWIND TO ASSURE PROPER TAPE POSITION
C
      REWIND 1
      WRITE (6,803)
  803 FORMAT(1H0,1X,12HELEMENT DATA/)
C
C NE=ELEMENT NUMBER
C IE=ELEMENT NODE INDICIES (NODE NUMBERS) TO BE READ IN COUNTER
C COUNTER CLOCKWISE DIRECTION
C READ NE,IE,X,Y,ELEMENTWISE,INTO TAPE 1
C
      DO 10 N=1,NTE
      READ (5,INFMT) NE,IE(1),IE(2),IE(3),X(1),X(2),X(3),Y(1),Y(2),Y(3)
C
C WRITE OUT FROM TAPE 1
C
      WRITE(6,OUTFMT) NE,IE(1),IE(2),IE(3),X(1),X(2),X(3),Y(1),Y(2),Y(
C
C MODIFY COORDINATES X AND Y SO THAT X(1)=Y(1)=0
C
      DO 155 I=2,3
      X(I)=X(I)-X(1)
      Y(I)=Y(I)-Y(1)
  155 CONTINUE
      X(1)=0.
      Y(1)=0.
   10 WRITE(1) NE,IE(1),IE(2),IE(3),X(1),X(2),X(3),Y(1),Y(2),Y(3)
C WRITE END OF FILE TO MARK THE END OF VALID INFORMATION
      END FILE 1
      REWIND 1
C
C SELECT A PROPER ELASTICITY MATRIX
C
      IF (CODE.EQ.0) GO TO 15
      MU=E/(1.-NU**2)
      D12=NU
      D33=(1.-NU)/2.
      GO TO 16
   15 MU=E*(1.-NU)/((1.+NU)*(1.-2.*NU))
      D12=NU/(1.-NU)
      D33=(1.-2.*NU)/(2.*(1.-NU))
C
   16 K=0
      DO 17 I=1,NTD
      DO 18 J=1,NCD
      IF(I.EQ.NCOD(J)) GO TO 17
   18 CONTINUE
      K=K+1
      NFREE(K)=I
   17 CONTINUE
C
```

```
C ZERO STRUCTURAL STIFFNESS AND LOAD MATRICES, S AND F
C
      DO 19 I=1,NTF
      DO 20 J=1,NLC
      F(I,J)=0.
   20 CONTINUE
      DO 21 K=1,NB
      S(I,K)=0.
   21 CONTINUE
   19 CONTINUE
C
C CALCULATE ELEMENT STIFFNESS MATRIX-ES (ELEMENTWISE)
C AND CONSTRUCT THE STRUCTURAL MATRIX S
C
      NL=1
      DO 23 N=1,NTE
C
C STEP 1 - READ THE ELEMENT DATA FROM TAPE 1
C
         READ (1) NE,IE(1),IE(2),IE(3),X(1),X(2),X(3),Y(1),Y(2),Y(3)
C
         DO 24 L=1,2
         ICR(L)=(IE(1)-1)*2+L
      ICR(L+2)=(IE(2)-1)*2+L
      ICR(L+4)=(IE(3)-1)*2+L
   24 CONTINUE
C STEP 2 - CALL TWO DIMENSIONAL ELEMENT STIFFNESS SUBROUTINE
C
      CALL TES(ES,X,Y,D12,D33,MU,NEND,EF,N,ICR,NPCON,NPCONE,IPCON,FCON
     1NCODE)
C
C STEP 3 - STUFF ES INTO S MATRIX BY CALLING STIFFNESS
C          ASSEMBLING SURROUTINE WITH THE AID OF ICR(I)
C ICR-INDEX MATRIX TO KEEP TRACK OF COLUMNS AND ROWS OF S
      CALL ASSEMS(ES,S,NFREE,NTF,NEND,ICR,NB,121)
      IF (NCODE(N))961,23,961
  961 DO 966 L=1,2
      ICR(L)=(IE(1)-1)*2+L
      ICR(L+2)=(IE(2)-1)*2+L
      ICR(L+4)=(IE(3)-1)*2+L
  966 CONTINUE
      CALL ASSEMF(EF,F,EFREE,NTF,NEND,NL,ICR,NB)
   23 CONTINUE
C
C REWIND TAPE 1 FOR LATER USE
C
      REWIND 1
C
C CALCULATE ELEMENT LOAD MATRICES-EF, AND CONSTRUCT THE
C STRUCTURAL LOAD MATRIX - F, FOR NO OF LOADING CONDITIONS
C
      DO 25 NL=1,NLC
C
C FOR EACH LOADING, READ THE NO OF LOADED ELEMENTS - LE
C
      READ (5,709) LE
  709 FORMAT(52X,I5)
      PRINT 333,LE
  333 FORMAT(1H0,5X,'NO. OF LOADED ELEMENTS LE=',I3)
      IF(LE.EQ.0) GO TO 30
```

```
C
C INPUT DATA ON EACH OF THE LOADED ELEMENTS
      DO 26 N=1,LE
      READ(5,710) NE,IE(1),IE(2),IE(3),X(1),X(2),X(3),Y(1),Y(2),Y(3)
  710 FORMAT(4I5,6F10.0)
      PRINT,NE,IE(1),IE(2),IE(3),X(1),X(2),X(3),Y(1),Y(2),Y(3)
      DO 27 I=1,NEND
      EF(I)=0.
   27 CONTINUE
      READ(5,711) (PX(I),PY(I),I=1,3)
  711 FORMAT(6X,6F10.3)
C
C SET UP EF MATRIX DUE TO BOUNDARY TRACTIONS, PX(I) AND PY(I)
C
      CALL EBL(EF,X,Y,PX,PY)
      DO 28 L=1,2
      ICR(L)=(IE(1)-1)*2+L
      ICR(L+2)=(IE(2)-1)*2+L
      ICR(L+4)=(IE(3)-1)*2+L
   28 CONTINUE
C
C STUFF EF  NTC-F
C
      CALL ASSEMF(EF,F,NFREE,NTF,NEND,NL,ICR,NB)
   26 CONTINUE
C
C NNC-NO OF NODAL CONCENTRATED LOADS (STRUCTURAL)
C
30    READ(5,712) NNC
  712 FORMAT(52X,I5)
      PRINT 444 ,NNC
  444 FORMAT(1H0,5X,'NO. OF CONCENTRATED NODAL LOADS NNC=',I3)
      IF (NNC.EQ.0) GO TO 25
      DO 32 N=1,NNC
      READ(5,713) NN,P
  713 FORMAT(6X,I5,F10.3)
      PRINT 555,NN,P
  555 FORMAT(1H0,5X,'AT THE NODAL POINT NN=',I3,5X,'THERE IS A LOAD P=
     1F10.3)
      DO 31 L=1,NTF
      IF (NN.EQ.NFREE(L)) GO TO 33
31     CONTINUE
  33  NN=L
      F(NN,NL)=F(NN,NL)+P
   32 CONTINUE
   25 CONTINUE
C
C SOLVE THE SYSTEM OF BANDED STRUCTURAL STIFFNESS EQUATIONS
C
      CALL SOLVE (S,F,NTF,NB,NLC)
C
C OUTPUT NODAL DISPLACEMENTS
C
      WRITE(6,806)
806    FORMAT(1H0,55X,19HNODAL DISPLACEMENTS/)
      DO 38 NL=1,NLC
      WRITE(6,815) NL
      WRITE(6,807)  (NFREE(I),F(I,NL) ,I=1,NTF)
  807 FORMAT(I4,50X,E17.6)
38    CONTINUE
```

```
C  STENY= STRAIN ENERGY
C  PTENT= PCTENTIAL ENERGY
C
       STENY=0.
       PTENY=0.
       DO 55 NL=1,NLC
       DO 56 I=1,NTF
       STENY=STENY+(F(I,NL)*CM(I,NL))/2.
 56    CONTINUE
C
C  SINCE QUARTER OF THE DISK IS ANALIZED MULTIPLY STENY BY 4
C
       STENY=4.*STENY
       PTENY=-STENY
       WRITE(6,820)
 820   FORMAT(1H0,1X,12HLOADING COND,8X,5HSTENY,10X,5HPTENY/)
       WRITE (6,821) NL,STENY,PTENY
 821   FORMAT(7X,I3,5X,E15.5,2X,E15.5)
 55    CONTINUE
       STOP
       END

       SUBROUTINE TES(ES,X,Y,D12,D33,U,NEND,EF,N,ICR,NPCON,NPCONE,IPCON
      1PCONQ,NCODE)
C
C CALCULATE THE ELEMENT STIFFNESS MATRIX .OUTPUT-ES
       DIMENSION ES(6,6),X(3),Y(3)
       DIMENSION EF(6),ICR(6),IPCON(20),PCONQ(20),NCODE(886)
       DO 150 I=1,NEND
       EF(I)=0.
       DO 151 J=1,NEND
       ES(I,J)=0.
 151   CONTINUE
 150    CONTINUE
C
C INPUT ES MATRIX (FACTOR H IS REMOVED)
C
       DEL=X(2)*Y(3)-X(3)*Y(2)
       C=U/(2.*DEL)
       X32=X(3)-X(2)
       Y23=Y(2)-Y(3)
        ES(1,1)=C*(Y23**2+D33*X32**2)
       ES(2,1)=C*(D12*X32*Y23+D33*Y23*X32)
       ES(3,1)=C*(Y(3)*Y23-D33*X(3)*X32)
       ES(4,1)=C*(-D12*X(3)*Y23+D33*Y(3)*X32)
       ES(5,1)=C*(-Y(2)*Y23+D33*X(2)*X32)
       ES(6,1)=C*(D12*X(2)*Y23-D33*Y(2)*X32)
       ES(2,2)=C*(D33*Y23**2+X32**2)
       ES(3,2)=C*(-D33*X(3)*Y23+D12*Y(3)*X32)
       ES(4,2)=C*(D33*Y(3)*Y23-X(3)*X32)
       ES(5,2)=C*(D33*X(2)*Y23-D12*Y(2)*X32)
       ES(6,2)=C*(-D33*Y(2)*Y23+X(2)*X32)
       ES(3,3)=C*(Y(3)**2+D33*X(3)**2)
       ES(4,3)=C*(-(D12+D33)*X(3)*Y(3))
       ES(5,3)=C*(-Y(2)*Y(3)-D33*X(2)*X(3))
       ES(6,3)=C*(D12*X(2)*Y(3)+D33*X(3)*Y(2))
       ES(4,4)=C*(D33*Y(3)**2+X(3)**2)
       ES(5,4)=C*(D33*X(2)*Y(3)+D12*X(3)*Y(2))
       ES(6,4)=C*(-D33*Y(2)*Y(3)-X(2)*X(3))
       ES(5,5)=C*(Y(2)**2+D33*X(2)**2)
```

```
      ES(6,5)=C*(-(D12+D33)*X(2)*Y(2))
      ES(6,6)=C*(D33*Y(2)**2+X(2)**2)
C USE SYMMETRY
      M=NEND-1
      DO 156 I=1,M
      K=I+1
      DO 157 J=K,NEND
      ES(I,J)=ES(J,I)
  157 CONTINUE
156   CONTINUE
C IF ELEMENT HAS A PRESCRIEED QUANTITY MODIFY ES AND EF
      IF(NCODE(N))100,200,100
100   DO 191 I=1,6
      DO 192 J=1,NPCON
      IF (ICR(I)-IPCON(J))192,193,192
192   CONTINUE
      GO TO 191
  193 DO 194 K=1,6
      EF(K)=EF(K)-ES(K,I)*PCONQ(J)
      ES(K,I)=0.
      ES(I,K)=0.
  194 CONTINUE
      ES(I,I)=1.
      EF(I)=PCONQ(J)
  191 CONTINUE
  200 RETURN
      END

      SUBROUTINE ASSEMS(ES,S,NFREE,NTF,NEND,ICR,NB,NTT)
C
C   TUFF ES MATRICES INTO THE S MATRIX (FREE NODAL DISPL ONLY)
C  OUTPUT - S MATRIX
C
      DIMENSION S(910,28),NFREE(NTF)
      DIMENSION ES(6,6),ICR(6)
C
C   LACE ZERO IN ICR(I) IF CONSTRAINED DISPLACEMENTS
C
      DO 202 K=1,NEND
      DO 203 L=1,NTF
      IF (ICR(K).EQ.NFREE(L)) GO TO 204
  203 CONTINUE
      ICR(K)=0.
      GO TO 202
  204 ICR(K)=L
  202 CONTINUE
C
C
C  FIND ROWS IN THE BANDED S MATRIX
C
      DO 205 K=1,NEND
      II=ICR(K)
      IF (II.EQ.0) GO TO 205
      DO 206 M=1,NEND
C
C  FIND COLUMNS IN THE BANDED S MATRIX
C
      IF (ICR(M).EQ.0) GO TO 206
      JJ=ICR(M)+1-II
      IF (JJ.LT. 1) GO TO 206
```

```
      S(II,JJ)=S(II,JJ)+ES(K,M)
  206 CONTINUE
  205 CCNTINUE
      RETURN
      END

      SUBROUTINE  EBL(EF,X,Y,PX,PY)
C
C CONVERT THE  ELEMENT  BOUNDARY TRACTIONS INTO THE ELEMENT  NODAL
C  FORCES-EF
C
      DIMENSION  EF(6),X(3),Y(3),PX(3),PY(3)
C
C  LET  PX(1)=PX23......PX(3)=PX12,  ETC.
C
      DEL=X(2)*Y(3)-X(3)*Y(2)
C
C ORDER I,J,K IN  THE  CYCLIC  ORDER  OF 1  ,2,3,1  AND SET  UF EF(I)
      DO 171 I=1,3
       J=(I-(I/3)*3)+1
      K=((I+1)-((I+1)/3)*3)+1
       A=SQRT((X(J)-X(K))**2+(Y(J)-Y(K))**2)
      B=DEL+0.5*(Y(J)-Y(K))*(X(J)+X(K))+0.5*(X(K)-X(J))*(Y(K)+Y(J))
C
      C=0.5*(Y(K)*(X(K)+X(J))-X(K)*(Y(K)+Y(J)))
C
      D=0.5*(-Y(J)*(X(K)+X(J))+X(J)*(Y(K)+Y(J)))
      EF(1)=EF(1)+B*A*PX(I)/DEL
       EF(2)=EF(2)+B*A*PY(I)/DEL
      EF(3)=EF(3)+C*A*PX(I)/DEL
      EF(4)=EF(4)+C*A*PY(I)/DEL
      EF(5)=EF(5)+D*A*PX(I)/DEL
      EF(6)=EF(6)+D*A*PY(I)/DEL
171    CCNTINUE
      RETURN
      END

       SUBRCUTINE ASSEMF (EF,F,NFREE,NTF,NEND,NL,ICR,NB)
C
C ASSEMBLE  EF INTO  F  AND OUTPUT F
C
      DIMENSION  F(NTF,1),NFREE(NTF)
      DIMENSION EF(6),ICR(6)
C
C FIND ROWS IN  UNBANDED STRUCTURAL STIFFNESS EQUATIONS
C PLACE ZERO IN ICR(I) IF  CONSTRAINED NODAL DISPLACEMENTS
C
      DO  222  K=1,NEND
      DO 223  L=1,NTF
      IF (ICR(K).EQ.NFREE(L)) GO  TO 224
223   CONTINUE
      ICR(K)=0
      GC  TC  222
 224   ICR(K)=L
222    CONTINUE
C
C  FIND ROWS  IN  BANDED  F  MATRIX
C
      DO 225 K=1,NEND
       II=ICR(K)
```

```
      IF (II.EQ.0) GO TO 225
         F(II,NL)=F(II,NL)+EF(K)
  225    CONTINUE
         RETURN
         END
      SUBROUTINE SOLVE(A,B,NN,MM,LC)
C
C     SOLUTION OF SYMMETRIC BAND EQUATIONS
C     A=MATRIX,STORED AS BAND
C     B=INPUT AS FORCE VECTOR, OUTPUT AS SOLUTION VECTOR
C     NN=NUMBER OF EQUATIONS
C     MM=BAND WIDTH, LC=WIDTH OF B
C     C
C     C-VECTOR DOES NOT ACCEPT VARIABLE DIMENSION, THEREFORE IT MUST
C       BE DIMENSIONED FOR EACH PROBLEM WITH NB-DIMENSION
C
      DIMENSION A(910,28),B(910,1),C(24)
      N=0
  100 N=N+1
C
C     REDUCE N TH EQUATION
C     DIVIDE RIGHT SIDE BY DIAGONAL ELEMENT
C
      DO 5 M=1,LC
    5 B(N,M)=B(N,M)/A(N,1)
C     CHECK FOR LAST EQUATION
      IF (N-NN)150,300,150
C
C     DIVIDE N TH EQUATION BY DIAGONAL ELEMENT
C
  150 DO 200 K=2,MM
      C(K)=A(N,K)
  200 A(N,K)=A(N,K)/A(N,1)
C
C     REDUCED REMAINING EQUATIONS
C
      DO 260 L=2,MM
      I=N+L-1
      IF(NN-I) 260,240,240
  240 J=0
      DO 250 K=L,MM
      J=J+1
  250 A(I,J)=A(I,J)-C(L)*A(N,K)
      DO 6 M=1,LC
    6 B(I,M)=B(I,M)-C(L)*B(N,M)
  260 CONTINUE
      GO TO 100
C
C     BACK SUBSTITUTION
  300 N=N-1
C
C     CHECK FOR FIRST EQUATION
C
      IF(N) 350,500,350
C
C     CALCULATE UNKNOWN B(N)
C
  350 DO 400 K=2,MM
      L=N+K-1
```

```
      IF(NN-L) 400,370,370
  370 DO 7 M=1,LC
    7 B(N,M)=B(N,M)-A(N,K)*B(L,M)
  400 CONTINUE
      GO TO 300
  500 RETURN
      END

      SUBROUTINE STRESS(EF,X,Y,MU,D12,D33,SIGMA,NEND)
C
C COMPUTE ELEMENT STRESS COMPONENTS, OUTPUT-SIGMA(I)
C
      DIMENSION EF(6),X(3),Y(3),SIGMA(3)
      DIMENSION A(6,6),DB(3,6),DBA(3,6)
      REAL MU
C
C ZERO A,DB,DBA,SIGMA MATRICES
C
      DO 400 I=1,3
      SIGMA(I)=0.
      K=I+3
      DO 401 J=1,NEND
      A(I,J)=0.
      A(K,J)=0.
      DB(I,J)=0.
      DBA(I,J)=0.
  401 CONTINUE
  400 CONTINUE
C
C INPUT DB MATRIX
C
      DB(1,2)=MU
      DB(1,6)=MU*D12
      DB(2,2)=DB(1,6)
      DB(2,6)=DB(1,2)
      DB(3,3)=MU*D33
      DB(3,5)=DB(3,3)
C
C INPUT A INVERSE MATRIX
C
      DEL=X(2)*Y(3)-X(3)*Y(2)
      A(1,1)=1.
      A(2,1)=(Y(2)-Y(3))/DEL
      A(3,1)=(X(3)-X(2))/DEL
      A(4,2)=1.
      A(5,2)=A(2,1)
      A(6,2)=A(3,1)
      A(2,3)=Y(3)/DEL
      A(3,3)=-X(3)/DEL
      A(5,4)=A(2,3)
      A(6,4)=A(3,3)
      A(2,5)=-Y(2)/DEL
      A(3,5)=X(2)/DEL
      A(5,6)=A(2,5)
      A(6,6)=A(3,5)
C
C FORM DBA MATRIX
C
      DO 405 I=1,3
      DO 406 J=1,NEND
```

```
      DO 407 K=1,NEND
      DBA(I,J)=DBA(I,J)+DB(I,K)*A(K,J)
  407 CONTINUE
  406 CONTINUE
  405 CONTINUE
C
C COMPUTE SIGMA
C
      DO 408 I=1,3
      DO 409 J=1,NEND
      SIGMA(I)=SIGMA(I)+DBA(I,J)*EF(J)
  409 CONTINUE
  408 CONTINUE
      RETURN
      END

$EXEC
```

INPUT DATA

NPCONE= 0 NPCON= 0

NTC	NTD	NCD	CODE	NE	NTF	NENC	NLC
281	322	52	0	24	270	6	1

CONSTRAINED NODAL DISPL NUMBERS

2	24	46	68	90	112	134	156	178
200	222	244	266	288	308	324	326	328
330	316	318	320	382	304	306	286	1
23	45	67	89	111	133	155	177	199
221	243	265	287	307	323	325	327	329
315	317	319	321	303	305	285		

ELEMENT DATA

1	1	2	12	250.0000	240.0000	240.0000	0.0000	10.0000	0.0000
2	2	13	12	240.0000	230.0000	240.0000	10.0000	10.0000	0.0000
3	2	3	13	240.0000	230.0000	230.0000	10.0000	20.0000	10.0000
4	3	14	13	230.0000	220.0000	230.0000	20.0000	20.0000	10.0000
5	3	4	14	230.0000	220.0000	220.0000	20.0000	30.0000	20.0000
6	4	15	14	220.0000	210.0000	220.0000	30.0000	30.0000	20.0000
7	4	5	15	220.0000	210.0000	210.0000	30.0000	40.0000	30.0000
8	5	16	15	210.0000	200.0000	210.0000	40.0000	40.0000	30.0000
9	5	6	16	210.0000	200.0000	200.0000	40.0000	50.0000	40.0000
10	6	17	16	200.0000	190.0000	200.0000	50.0000	50.0000	40.0000
11	6	7	17	200.0000	190.0000	190.0000	50.0000	60.0000	50.0000
12	7	18	17	190.0000	180.0000	190.0000	60.0000	60.0000	50.0000
13	7	8	18	190.0000	180.0000	180.0000	60.0000	70.0000	60.0000
14	8	19	18	180.0000	170.0000	180.0000	70.0000	70.0000	60.0000
15	8	9	19	180.0000	170.0000	170.0000	70.0000	80.0000	70.0000
16	9	20	19	170.0000	160.0000	170.0000	80.0000	80.0000	70.0000
17	9	10	20	170.0000	160.0000	160.0000	80.0000	90.0000	80.0000
18	10	21	20	160.0000	150.0000	160.0000	90.0000	90.0000	80.0000
19	10	11	21	160.0000	150.0000	150.0000	90.0000	100.0000	90.0000
20	11	22	21	150.0000	140.0000	150.0000	100.0000	100.0000	90.0000
21	12	13	23	240.0000	230.0000	230.0000	0.0000	10.0000	0.0000
22	13	24	23	230.0000	220.0000	230.0000	10.0000	10.0000	0.0000
23	13	14	24	230.0000	220.0000	220.0000	10.0000	20.0000	10.0000
24	14	25	24	220.0000	210.0000	220.0000	20.0000	20.0000	10.0000
25	14	15	25	220.0000	210.0000	210.0000	20.0000	30.0000	20.0000
26	15	26	25	210.0000	200.0000	210.0000	30.0000	30.0000	20.0000
27	15	16	26	210.0000	200.0000	200.0000	30.0000	40.0000	30.0000
28	16	27	26	200.0000	190.0000	200.0000	40.0000	40.0000	30.0000
29	16	17	27	200.0000	190.0000	190.0000	40.0000	50.0000	40.0000
30	17	28	27	190.0000	180.0000	190.0000	50.0000	50.0000	40.0000
31	17	18	28	190.0000	180.0000	180.0000	50.0000	60.0000	50.0000
32	18	29	28	180.0000	170.0000	180.0000	60.0000	60.0000	50.0000
33	18	19	29	180.0000	170.0000	170.0000	60.0000	70.0000	60.0000
34	19	30	29	170.0000	160.0000	170.0000	70.0000	70.0000	60.0000
35	19	20	30	170.0000	160.0000	160.0000	70.0000	80.0000	70.0000
36	20	31	30	160.0000	150.0000	160.0000	80.0000	80.0000	70.0000
37	20	21	31	160.0000	150.0000	150.0000	80.0000	90.0000	80.0000
38	21	32	31	150.0000	140.0000	150.0000	90.0000	90.0000	80.0000
39	21	22	32	150.0000	140.0000	140.0000	90.0000	100.0000	90.0000
40	22	33	32	140.0000	130.0000	140.0000	100.0000	100.0000	90.0000

41	23	24	34	230.0000	220.0000	220.0000	0.0000	10.0000	0.0000
42	24	35	34	220.0000	210.0000	220.0000	10.0000	10.0000	0.0000
43	24	25	35	220.0000	210.0000	210.0000	10.0000	20.0000	10.0000
44	25	36	35	210.0000	200.0000	210.0000	20.0000	20.0000	10.0000
45	25	26	36	210.0000	200.0000	200.0000	20.0000	30.0000	20.0000
46	26	37	36	200.0000	190.0000	200.0000	30.0000	30.0000	20.0000
47	26	27	37	200.0000	190.0000	190.0000	30.0000	40.0000	30.0000
48	27	38	37	190.0000	180.0000	190.0000	40.0000	40.0000	30.0000
49	27	28	38	190.0000	180.0000	180.0000	40.0000	50.0000	40.0000
50	28	39	38	180.0000	170.0000	180.0000	50.0000	50.0000	40.0000
51	28	29	39	180.0000	170.0000	170.0000	50.0000	60.0000	50.0000
52	29	40	39	170.0000	160.0000	170.0000	60.0000	60.0000	50.0000
53	29	30	40	170.0000	160.0000	160.0000	60.0000	70.0000	60.0000
54	30	41	40	160.0000	150.0000	160.0000	70.0000	70.0000	60.0000
55	30	31	41	160.0000	150.0000	150.0000	70.0000	80.0000	70.0000
56	31	42	41	150.0000	140.0000	150.0000	80.0000	80.0000	70.0000
57	31	32	42	150.0000	140.0000	140.0000	80.0000	90.0000	80.0000
58	32	43	42	140.0000	130.0000	140.0000	90.0000	90.0000	80.0000
59	32	33	43	140.0000	130.0000	130.0000	90.0000	100.0000	90.0000
60	33	44	43	130.0000	120.0000	130.0000	100.0000	100.0000	90.0000
61	34	35	45	220.0000	210.0000	210.0000	0.0000	10.0000	0.0000
62	35	46	45	210.0000	200.0000	210.0000	10.0000	10.0000	0.0000
63	35	36	46	210.0000	200.0000	200.0000	10.0000	20.0000	10.0000
64	36	47	46	200.0000	190.0000	200.0000	20.0000	20.0000	10.0000
65	36	37	47	200.0000	190.0000	190.0000	20.0000	30.0000	20.0000
66	37	48	47	190.0000	180.0000	190.0000	30.0000	30.0000	20.0000
67	37	38	48	190.0000	180.0000	180.0000	30.0000	40.0000	30.0000
68	38	49	48	180.0000	170.0000	180.0000	40.0000	40.0000	30.0000
69	38	39	49	180.0000	170.0000	170.0000	40.0000	50.0000	40.0000
70	39	50	49	170.0000	160.0000	170.0000	50.0000	50.0000	40.0000
71	39	40	50	170.0000	160.0000	160.0000	50.0000	60.0000	50.0000
72	40	51	50	160.0000	150.0000	160.0000	60.0000	60.0000	50.0000
73	40	41	51	160.0000	150.0000	150.0000	60.0000	70.0000	60.0000
74	41	52	51	150.0000	140.0000	150.0000	70.0000	70.0000	60.0000
75	41	42	52	150.0000	140.0000	140.0000	70.0000	80.0000	70.0000
76	42	53	52	140.0000	130.0000	140.0000	80.0000	80.0000	70.0000
77	42	43	53	140.0000	130.0000	130.0000	80.0000	90.0000	80.0000
78	43	54	53	130.0000	120.0000	130.0000	90.0000	90.0000	80.0000
79	43	44	54	130.0000	120.0000	120.0000	90.0000	100.0000	90.0000
80	44	55	54	120.0000	110.0000	120.0000	100.0000	100.0000	90.0000
81	45	46	56	210.0000	200.0000	200.0000	0.0000	10.0000	0.0000
82	46	57	56	200.0000	190.0000	200.0000	10.0000	10.0000	0.0000
83	46	47	57	200.0000	190.0000	190.0000	10.0000	20.0000	10.0000
84	47	58	57	190.0000	180.0000	190.0000	20.0000	20.0000	10.0000
85	47	48	58	190.0000	180.0000	180.0000	20.0000	30.0000	20.0000
86	48	59	58	180.0000	170.0000	180.0000	30.0000	30.0000	20.0000
87	48	49	59	180.0000	170.0000	170.0000	30.0000	40.0000	30.0000
88	49	60	59	170.0000	160.0000	170.0000	40.0000	40.0000	30.0000
89	49	50	60	170.0000	160.0000	160.0000	40.0000	50.0000	40.0000
90	50	61	60	160.0000	150.0000	160.0000	50.0000	50.0000	40.0000
91	50	51	61	160.0000	150.0000	150.0000	50.0000	60.0000	50.0000
92	51	62	61	150.0000	140.0000	150.0000	60.0000	60.0000	50.0000
93	51	52	62	150.0000	140.0000	140.0000	60.0000	70.0000	60.0000
94	52	63	62	140.0000	130.0000	140.0000	70.0000	70.0000	60.0000
95	52	53	63	140.0000	130.0000	130.0000	70.0000	80.0000	70.0000
96	53	64	63	130.0000	120.0000	130.0000	80.0000	80.0000	70.0000
97	53	54	64	130.0000	120.0000	120.0000	80.0000	90.0000	80.0000
98	54	65	64	120.0000	110.0000	120.0000	90.0000	90.0000	80.0000
99	54	55	65	120.0000	110.0000	110.0000	90.0000	100.0000	90.0000
100	55	66	65	110.0000	100.0000	110.0000	100.0000	100.0000	90.0000

101	56	57	67	200.0000	190.0000	190.0000	0.0000	10.0000	0.0000
102	57	68	67	190.0000	180.0000	190.0000	10.0000	10.0000	0.0000
103	57	58	68	190.0000	180.0000	180.0000	10.0000	20.0000	10.0000
104	58	69	68	180.0000	170.0000	180.0000	20.0000	20.0000	10.0000
105	58	59	69	180.0000	170.0000	170.0000	20.0000	30.0000	20.0000
106	59	70	69	170.0000	160.0000	170.0000	30.0000	30.0000	20.0000
107	59	60	70	170.0000	160.0000	160.0000	30.0000	40.0000	30.0000
108	60	71	70	160.0000	150.0000	160.0000	40.0000	40.0000	30.0000
109	60	61	71	160.0000	150.0000	150.0000	40.0000	50.0000	40.0000
110	61	72	71	150.0000	140.0000	150.0000	50.0000	50.0000	40.0000
111	61	62	72	150.0000	140.0000	140.0000	50.0000	60.0000	50.0000
112	62	73	72	140.0000	130.0000	140.0000	60.0000	60.0000	50.0000
113	62	63	73	140.0000	130.0000	130.0000	60.0000	70.0000	60.0000
114	63	74	73	130.0000	120.0000	130.0000	70.0000	70.0000	60.0000
115	63	64	74	130.0000	120.0000	120.0000	70.0000	80.0000	70.0000
116	64	75	74	120.0000	110.0000	120.0000	80.0000	80.0000	70.0000
117	64	65	75	120.0000	110.0000	110.0000	80.0000	90.0000	80.0000
118	65	76	75	110.0000	100.0000	110.0000	90.0000	90.0000	80.0000
119	65	66	76	110.0000	100.0000	100.0000	90.0000	100.0000	90.0000
120	66	77	76	100.0000	90.0000	100.0000	100.0000	100.0000	90.0000
121	67	68	78	190.0000	180.0000	180.0000	0.0000	10.0000	0.0000
122	68	79	78	180.0000	170.0000	180.0000	10.0000	10.0000	0.0000
123	68	69	79	180.0000	170.0000	170.0000	10.0000	20.0000	10.0000
124	69	80	79	170.0000	160.0000	170.0000	20.0000	20.0000	10.0000
125	69	70	80	170.0000	160.0000	160.0000	20.0000	30.0000	20.0000
126	70	81	80	160.0000	150.0000	160.0000	30.0000	30.0000	20.0000
127	70	71	81	160.0000	150.0000	150.0000	30.0000	40.0000	30.0000
128	71	82	81	150.0000	140.0000	150.0000	40.0000	40.0000	30.0000
129	71	72	82	150.0000	140.0000	140.0000	40.0000	50.0000	40.0000
130	72	83	82	140.0000	130.0000	140.0000	50.0000	50.0000	40.0000
131	72	73	83	140.0000	130.0000	130.0000	50.0000	60.0000	50.0000
132	73	84	83	130.0000	120.0000	130.0000	60.0000	60.0000	50.0000
133	73	74	84	130.0000	120.0000	120.0000	60.0000	70.0000	60.0000
134	74	85	84	120.0000	110.0000	120.0000	70.0000	70.0000	60.0000
135	74	75	85	120.0000	110.0000	110.0000	70.0000	80.0000	70.0000
136	75	86	85	110.0000	100.0000	110.0000	80.0000	80.0000	70.0000
137	75	76	86	110.0000	100.0000	100.0000	80.0000	90.0000	80.0000
138	76	87	86	100.0000	90.0000	100.0000	90.0000	90.0000	80.0000
139	76	77	87	100.0000	90.0000	90.0000	90.0000	100.0000	90.0000
140	77	88	87	90.0000	80.0000	90.0000	100.0000	100.0000	90.0000
141	78	79	89	180.0000	170.0000	170.0000	0.0000	10.0000	0.0000
142	79	90	89	170.0000	160.0000	170.0000	10.0000	10.0000	0.0000
143	79	80	90	170.0000	160.0000	160.0000	10.0000	20.0000	10.0000
144	80	91	90	160.0000	150.0000	160.0000	20.0000	20.0000	10.0000
145	80	81	91	160.0000	150.0000	150.0000	20.0000	30.0000	20.0000
146	81	92	91	150.0000	140.0000	150.0000	30.0000	30.0000	20.0000
147	81	82	92	150.0000	140.0000	140.0000	30.0000	40.0000	30.0000
148	82	93	92	140.0000	130.0000	140.0000	40.0000	40.0000	30.0000
149	82	83	93	140.0000	130.0000	130.0000	40.0000	50.0000	40.0000
150	83	94	93	130.0000	120.0000	130.0000	50.0000	50.0000	40.0000
151	83	84	94	130.0000	120.0000	120.0000	50.0000	60.0000	50.0000
152	84	95	94	120.0000	110.0000	120.0000	60.0000	60.0000	50.0000
153	84	85	95	120.0000	110.0000	110.0000	60.0000	70.0000	60.0000
154	85	96	95	110.0000	100.0000	110.0000	70.0000	70.0000	60.0000
155	85	86	96	110.0000	100.0000	100.0000	70.0000	80.0000	70.0000
156	86	97	96	100.0000	90.0000	100.0000	80.0000	80.0000	70.0000
157	86	87	97	100.0000	90.0000	90.0000	80.0000	90.0000	80.0000
158	87	98	97	90.0000	80.0000	90.0000	90.0000	90.0000	80.0000
159	87	88	98	90.0000	80.0000	80.0000	90.0000	100.0000	90.0000
160	88	99	98	80.0000	70.0000	80.0000	100.0000	100.0000	90.0000

161	89	90	100	170.0000	160.0000	160.0000	0.0000	10.0000	0.0000
162	90	101	100	160.0000	150.0000	160.0000	10.0000	10.0000	0.0000
163	90	91	101	160.0000	150.0000	150.0000	10.0000	20.0000	10.0000
164	91	102	101	150.0000	140.0000	150.0000	20.0000	20.0000	10.0000
165	91	92	102	150.0000	140.0000	140.0000	20.0000	30.0000	20.0000
166	92	103	102	140.0000	130.0000	140.0000	30.0000	30.0000	20.0000
167	92	93	103	140.0000	130.0000	130.0000	30.0000	40.0000	30.0000
168	93	104	103	130.0000	120.0000	130.0000	40.0000	40.0000	30.0000
169	93	94	104	130.0000	120.0000	120.0000	40.0000	50.0000	40.0000
170	94	105	104	120.0000	110.0000	120.0000	50.0000	50.0000	40.0000
171	94	95	105	120.0000	110.0000	110.0000	50.0000	60.0000	50.0000
172	95	106	105	110.0000	100.0000	110.0000	60.0000	60.0000	50.0000
173	95	96	106	110.0000	100.0000	100.0000	60.0000	70.0000	60.0000
174	96	107	106	100.0000	90.0000	100.0000	70.0000	70.0000	60.0000
175	96	97	107	100.0000	90.0000	90.0000	70.0000	80.0000	70.0000
176	97	108	107	90.0000	80.0000	80.0000	80.0000	80.0000	70.0000
177	97	98	108	90.0000	80.0000	80.0000	80.0000	90.0000	80.0000
178	98	109	108	80.0000	70.0000	80.0000	90.0000	90.0000	80.0000
179	98	99	109	80.0000	70.0000	70.0000	90.0000	100.0000	90.0000
180	99	110	109	70.0000	60.0000	70.0000	100.0000	100.0000	90.0000
181	100	101	111	160.0000	150.0000	145.0000	0.0000	10.0000	0.0000
182	101	112	111	150.0000	135.0000	145.0000	10.0000	10.0000	0.0000
183	101	102	112	150.0000	140.0000	135.0000	10.0000	20.0000	10.0000
184	102	113	112	140.0000	125.0000	135.0000	20.0000	20.0000	10.0000
185	102	103	113	140.0000	130.0000	125.0000	20.0000	30.0000	20.0000
186	103	114	113	130.0000	115.0000	125.0000	30.0000	30.0000	20.0000
187	103	104	114	130.0000	120.0000	115.0000	30.0000	40.0000	30.0000
188	104	115	114	120.0000	105.0000	115.0000	40.0000	40.0000	30.0000
189	104	105	115	120.0000	110.0000	105.0000	40.0000	50.0000	40.0000
190	105	116	115	110.0000	95.0000	105.0000	50.0000	50.0000	40.0000
191	105	106	116	110.0000	100.0000	95.0000	50.0000	60.0000	50.0000
192	106	117	116	100.0000	85.0000	95.0000	60.0000	60.0000	50.0000
193	106	107	117	100.0000	90.0000	85.0000	60.0000	70.0000	60.0000
194	107	118	117	90.0000	75.0000	85.0000	70.0000	70.0000	60.0000
195	107	108	118	90.0000	80.0000	75.0000	70.0000	80.0000	70.0000
196	108	119	118	80.0000	65.0000	75.0000	80.0000	80.0000	70.0000
197	108	109	119	80.0000	70.0000	65.0000	80.0000	90.0000	80.0000
198	109	120	119	70.0000	55.0000	65.0000	90.0000	90.0000	80.0000
199	109	110	120	70.0000	60.0000	55.0000	90.0000	100.0000	90.0000
200	110	121	120	60.0000	45.0000	55.0000	100.0000	100.0000	90.0000
201	111	112	122	145.0000	135.0000	125.0000	0.0000	10.0000	0.0000
202	112	123	122	135.0000	115.0000	125.0000	10.0000	10.0000	0.0000
203	112	113	123	135.0000	125.0000	115.0000	10.0000	20.0000	10.0000
204	113	124	123	125.0000	105.0000	115.0000	20.0000	20.0000	10.0000
205	113	114	124	125.0000	115.0000	105.0000	20.0000	30.0000	20.0000
206	114	125	124	115.0000	95.0000	105.0000	30.0000	30.0000	20.0000
207	114	115	125	115.0000	105.0000	95.0000	30.0000	40.0000	30.0000
208	115	126	125	105.0000	85.0000	95.0000	40.0000	40.0000	30.0000
209	115	116	126	105.0000	95.0000	85.0000	40.0000	50.0000	40.0000
210	116	127	126	95.0000	75.0000	85.0000	50.0000	50.0000	40.0000
211	116	117	127	95.0000	85.0000	75.0000	50.0000	60.0000	50.0000
212	117	128	127	85.0000	65.0000	75.0000	60.0000	60.0000	50.0000
213	117	118	128	85.0000	75.0000	65.0000	60.0000	70.0000	60.0000
214	118	129	128	75.0000	55.0000	65.0000	70.0000	70.0000	60.0000
215	118	119	129	75.0000	65.0000	55.0000	70.0000	80.0000	70.0000
216	119	130	129	65.0000	45.0000	55.0000	80.0000	80.0000	70.0000
217	119	120	130	65.0000	55.0000	45.0000	80.0000	90.0000	80.0000
218	120	131	130	55.0000	35.0000	45.0000	90.0000	90.0000	80.0000
219	120	121	131	55.0000	45.0000	35.0000	90.0000	100.0000	90.0000
220	121	132	131	45.0000	25.0000	35.0000	100.0000	100.0000	90.0000

221	122	123	133	125.0000	115.0000	100.0000	0.0000	10.0000	0.0000
222	123	134	133	115.0000	90.0000	100.0000	10.0000	10.0000	0.0000
223	123	124	134	115.0000	105.0000	90.0000	10.0000	20.0000	10.0000
224	124	135	134	105.0000	80.0000	90.0000	20.0000	20.0000	10.0000
225	124	125	135	105.0000	95.0000	80.0000	20.0000	30.0000	20.0000
226	125	136	135	95.0000	70.0000	80.0000	30.0000	30.0000	20.0000
227	125	126	136	95.0000	85.0000	70.0000	30.0000	40.0000	30.0000
228	126	137	136	85.0000	60.0000	70.0000	40.0000	40.0000	30.0000
229	126	127	137	85.0000	75.0000	60.0000	40.0000	50.0000	40.0000
230	127	138	137	75.0000	50.0000	60.0000	50.0000	50.0000	40.0000
231	127	128	138	75.0000	65.0000	50.0000	50.0000	60.0000	50.0000
232	128	139	138	65.0000	40.0000	50.0000	60.0000	60.0000	50.0000
233	128	129	139	65.0000	55.0000	40.0000	60.0000	70.0000	60.0000
234	129	140	139	55.0000	30.0000	40.0000	70.0000	70.0000	60.0000
235	129	130	140	55.0000	45.0000	30.0000	70.0000	80.0000	70.0000
236	130	141	140	45.0000	20.0000	30.0000	80.0000	80.0000	70.0000
237	130	131	141	45.0000	35.0000	20.0000	80.0000	90.0000	80.0000
238	131	142	141	35.0000	10.0000	20.0000	90.0000	90.0000	80.0000
239	131	132	142	35.0000	25.0000	10.0000	90.0000	100.0000	90.0000
240	132	143	142	25.0000	0.0000	10.0000	100.0000	100.0000	90.0000
241	133	134	144	100.0000	90.0000	75.0000	0.0000	10.0000	0.0000
242	134	145	144	90.0000	65.0000	75.0000	10.0000	10.0000	0.0000
243	134	135	145	90.0000	80.0000	65.0000	10.0000	20.0000	10.0000
244	135	146	145	80.0000	55.0000	65.0000	20.0000	20.0000	10.0000
245	135	136	146	80.0000	70.0000	55.0000	20.0000	30.0000	20.0000
246	136	147	146	70.0000	45.0000	55.0000	30.0000	30.0000	20.0000
247	136	137	147	70.0000	60.0000	45.0000	30.0000	40.0000	30.0000
248	137	148	147	60.0000	35.0000	45.0000	40.0000	40.0000	30.0000
249	137	138	148	60.0000	50.0000	35.0000	40.0000	50.0000	40.0000
250	138	149	148	50.0000	25.0000	35.0000	50.0000	50.0000	40.0000
251	138	139	149	50.0000	40.0000	25.0000	50.0000	60.0000	50.0000
252	139	150	149	40.0000	15.0000	25.0000	60.0000	60.0000	50.0000
253	139	140	150	40.0000	30.0000	15.0000	60.0000	70.0000	60.0000
254	140	151	150	30.0000	5.0000	15.0000	70.0000	70.0000	60.0000
255	140	141	151	30.0000	20.0000	5.0000	70.0000	80.0000	70.0000
256	141	152	151	20.0000	0.0000	5.0000	80.0000	80.0000	70.0000
257	141	142	152	20.0000	10.0000	0.0000	80.0000	90.0000	80.0000
258	142	153	152	10.0000	0.0000	0.0000	90.0000	90.0000	80.0000
259	142	143	153	10.0000	0.0000	0.0000	90.0000	100.0000	90.0000
260	144	145	154	75.0000	65.0000	40.0000	0.0000	10.0000	0.0000
261	145	155	154	65.0000	30.0000	40.0000	10.0000	10.0000	0.0000
262	145	146	155	65.0000	55.0000	30.0000	10.0000	20.0000	10.0000
263	146	156	155	55.0000	20.0000	30.0000	20.0000	20.0000	10.0000
264	146	147	156	55.0000	45.0000	20.0000	20.0000	30.0000	20.0000
265	147	157	156	45.0000	10.0000	20.0000	30.0000	30.0000	20.0000
266	147	148	157	45.0000	35.0000	10.0000	30.0000	40.0000	30.0000
267	148	158	157	35.0000	0.0000	10.0000	40.0000	40.0000	30.0000
268	148	149	158	35.0000	25.0000	0.0000	40.0000	50.0000	40.0000
269	149	159	158	25.0000	0.0000	0.0000	50.0000	50.0000	40.0000
270	149	150	159	25.0000	15.0000	0.0000	50.0000	60.0000	50.0000
271	150	160	159	15.0000	0.0000	0.0000	60.0000	60.0000	50.0000
272	150	151	160	15.0000	5.0000	0.0000	60.0000	70.0000	60.0000
273	151	161	160	5.0000	0.0000	0.0000	70.0000	70.0000	60.0000
274	151	152	161	5.0000	0.0000	0.0000	70.0000	80.0000	70.0000
275	154	155	162	40.0000	30.0000	0.0000	0.0000	10.0000	0.0000
276	155	163	162	30.0000	0.0000	0.0000	10.0000	10.0000	0.0000
277	155	156	163	30.0000	20.0000	0.0000	10.0000	20.0000	10.0000
278	156	164	163	20.0000	0.0000	0.0000	20.0000	20.0000	10.0000
279	156	157	164	20.0000	10.0000	0.0000	20.0000	30.0000	20.0000
280	157	165	164	10.0000	0.0000	0.0000	30.0000	30.0000	20.0000

```
281 157 158 165   10.0000    0.0000    0.0000   30.0000   40.0000   30.0000

    NO. OF LOADED ELEMENTS LE=  0

    NO. OF CONCENTRATED NODAL LOADS NNC= 13

    AT THE NODAL POINT NN= 44      THERE IS A LOAD P=   -30.000

    AT THE NODAL POINT NN= 66      THERE IS A LOAD P=   -30.000

    AT THE NODAL POINT NN= 88      THERE IS A LOAD P=   -30.000

    AT THE NODAL POINT NN= 21      THERE IS A LOAD P=    22.000

    AT THE NODAL POINT NN= 19      THERE IS A LOAD P=    43.000

    AT THE NODAL POINT NN= 17      THERE IS A LOAD P=    87.000

    AT THE NODAL POINT NN= 15      THERE IS A LOAD P=   130.000

    AT THE NODAL POINT NN= 13      THERE IS A LOAD P=   173.000

    AT THE NODAL POINT NN= 11      THERE IS A LOAD P=   217.000

    AT THE NODAL POINT NN=  9      THERE IS A LOAD P=   260.000

    AT THE NODAL POINT NN=  7      THERE IS A LOAD P=   303.000

    AT THE NODAL POINT NN=  5      THERE IS A LOAD P=   347.000

    AT THE NODAL POINT NN=  3      THERE IS A LOAD P=   390.000

                                                     NODAL DISPLACEMENTS

LOADING COND=   1
  3                                                    0.841762E-01
  4                                                   -0.255309E-01
  5                                                    0.128828E 00
  6                                                   -0.336846E-01
  7                                                    0.152390E 00
  8                                                   -0.341257E-01
  9                                                    0.161406E 00
 10                                                   -0.307359E-01
 11                                                    0.159473E 00
 12                                                   -0.259338E-01
 13                                                    0.149403E 00
 14                                                   -0.214778E-01
 15                                                    0.134114E 00
 16                                                   -0.186045E-01
 17                                                    0.116334E 00
 18                                                   -0.181596E-01
 19                                                    0.994929E-01
 20                                                   -0.206784E-01
 21                                                    0.898328E-01
 22                                                   -0.251202E-01
 25                                                    0.648932E-01
 26                                                   -0.131299E-01
 27                                                    0.105067E 00
 28                                                   -0.165204E-01
```

29	0.127888E 00
30	-0.192321E-01
31	0.137783E 00
32	-0.177668E-01
33	0.137805E 00
34	-0.159710E-01
35	0.130597E 00
36	-0.151132E-01
37	0.118794E 00
38	-0.160106E-01
39	0.105082E 00
40	-0.190583E-01
41	0.929496E-01
42	-0.234206E-01
43	0.849975E-01
44	-0.297157E-01
47	0.525044E-01
48	-0.647532E-02
49	0.876989E-01
50	-0.928371E-02
51	0.108795E 00
52	-0.991052E-02
53	0.118688E 00
54	-0.988917E-02
55	0.119855E 00
56	-0.104006E-01
57	0.114646E 00
58	-0.121942E-01
59	0.105436E 00
60	-0.155823E-01
61	0.948381E-01
62	-0.200657E-01
63	0.854738E-01
64	-0.252923E-01
65	0.796109E-01
66	-0.291433E-01
69	0.438288E-01
70	-0.253669E-02
71	0.745323E-01
72	-0.369321E-02
73	0.935834E-01
74	-0.439352E-02
75	0.102956E 00
76	-0.553290E-02
77	0.104671E 00
78	-0.773070E-02
79	0.100789E 00
80	-0.112243E-01
81	0.934995E-01
82	-0.156811E-01
83	0.850705E-01
84	-0.204997E-01
85	0.777426E-01
86	-0.242853E-01
87	0.737956E-01
88	-0.255607E-01
91	0.373864E-01
92	-0.203541E-03
93	0.641873E-01
94	-0.487305E-03

95	0.811397E-01
96	-0.143401E-02
97	0.896940E-01
98	-0.346861E-02
99	0.915428E-01
100	-0.673267E-02
101	0.885323E-01
102	-0.109510E-01
103	0.826163E-01
104	-0.155045E-01
105	0.758121E-01
106	-0.192717E-01
107	0.700008E-01
108	-0.208152E-01
109	0.666858E-01
110	-0.179154E-01
113	0.323612E-01
114	0.108866E-02
115	0.557654E-01
116	0.114779E-02
117	0.706762E-01
118	-0.112947E-03
119	0.782610E-01
120	-0.273230E-02
121	0.800018E-01
122	-0.643428E-02
123	0.775582E-01
124	-0.106297E-01
125	0.726968E-01
126	-0.143803E-01
127	0.672411E-01
128	-0.164759E-01
129	0.628110E-01
130	-0.155049E-01
131	0.593721E-01
132	-0.133767E-01
135	0.282610E-01
136	0.169756E-02
137	0.486755E-01
138	0.178865E-02
139	0.616563E-01
140	0.263161E-03
141	0.682353E-01
142	-0.259007E-02
143	0.697534E-01
144	-0.621026E-02
145	0.677281E-01
146	-0.977367E-02
147	0.637726E-01
148	-0.122775E-01
149	0.596152E-01
150	-0.126466E-01
151	0.559715E-01
152	-0.114208E-01
153	0.520338E-01
154	-0.102921E-01
157	0.247796E-01
158	0.167542E-02
159	0.425354E-01
160	0.186197E-02

161	0.537358E-01
162	0.209119E-03
163	0.593550E-01
164	-0.255584E-02
165	0.606397E-01
166	-0.568346E-02
167	0.589900E-01
168	-0.829275E-02
169	0.558743E-01
170	-0.953305E-02
171	0.527464E-01
172	-0.924673E-02
173	0.493208E-01
174	-0.846698E-02
175	0.449802E-01
176	-0.849254E-02
179	0.217283E-01
180	0.181058E-02
181	0.371100E-01
182	0.168263E-02
183	0.467063E-01
184	0.684038E-04
185	0.514708E-01
186	-0.234174E-02
187	0.525733E-01
188	-0.474535E-02
189	0.512917E-01
190	-0.637231E-02
191	0.487889E-01
192	-0.690093E-02
193	0.464254E-01
194	-0.639927E-02
195	0.428511E-01
196	-0.692163E-02
197	0.384408E-01
198	-0.698236E-02
201	0.189966E-01
202	0.164940E-02
203	0.322629E-01
204	0.145785E-02
205	0.404504E-01
206	0.448446E-04
207	0.444930E-01
208	-0.184473E-02
209	0.454769E-01
210	-0.349135E-02
211	0.444814E-01
212	-0.443659E-02
213	0.422277E-01
214	-0.461408E-02
215	0.404636E-01
216	-0.560944E-02
217	0.367288E-01
218	-0.545735E-02
219	0.321960E-01
220	-0.577770E-02
223	0.153882E-01
224	0.136780E-02
225	0.259363E-01
226	0.124731E-02

227	0.323781E-01
228	0.322766E-03
229	0.355793E-01
230	-0.784202E-03
231	0.364289E-01
232	-0.170184E-02
233	0.357189E-01
234	-0.233808E-02
235	0.339442E-01
236	-0.298151E-02
237	0.315009E-01
238	-0.326776E-02
239	0.278676E-01
240	-0.379786E-02
241	0.233512E-01
242	-0.453993E-02
245	0.114019E-01
246	0.116136E-02
247	0.191046E-01
248	0.133334E-02
249	0.237602E-01
250	0.102959E-02
251	0.259874E-01
252	0.495743E-03
253	0.264320E-01
254	-0.816532E-04
255	0.255348E-01
256	-0.651031E-03
257	0.236548E-01
258	-0.110089E-02
259	0.207380E-01
260	-0.174192E-02
261	0.169297E-01
262	-0.258481E-02
263	0.127684E-01
264	-0.317722E-02
267	0.762955E-02
268	0.114809E-02
269	0.126227E-01
270	0.167931E-02
271	0.152983E-01
272	0.162940E-02
273	0.162786E-01
274	0.131372E-02
275	0.159485E-01
276	0.938436E-03
277	0.144893E-01
278	0.605027E-03
279	0.117976E-01
280	0.100307E-03
281	0.821071E-02
282	-0.616528E-03
283	0.439066E-02
284	-0.626017E-03
289	0.477267E-02
290	0.131309E-02
291	0.716640E-02
292	0.158066E-02
293	0.817957E-02
294	0.148086E-02

295	0.817671E-02
296	0.131714E-02
297	0.717689E-02
298	0.121386E-02
299	0.471545E-02
300	0.818294E-03

		SIGMA X	SIGMA Y	SIGMA XY
LOADING COND= 1	NO OF ELEMT= 1	-0.58210E 01	-0.23284E 02	0.28788E 02
LOADING COND= 1	NO OF ELEMT= 2	0.11765E 02	-0.18888E 02	0.24547E 02
LOADING COND= 1	NO OF ELEMT= 3	0.12900E 02	-0.14349E 02	0.17625E 02
LOADING COND= 1	NO OF ELEMT= 4	0.16983E 02	-0.13328E 02	0.16680E 02
LOADING COND= 1	NO OF ELEMT= 5	0.18112E 02	-0.88146E 01	0.10998E 02
LOADING COND= 1	NO OF ELEMT= 6	0.18788E 02	-0.86456E 01	0.11091E 02
LOADING COND= 1	NO OF ELEMT= 7	0.19723E 02	-0.49049E 01	0.63695E 01
LOADING COND= 1	NO OF ELEMT= 8	0.18921E 02	-0.51055E 01	0.70276E 01
LOADING COND= 1	NO OF ELEMT= 9	0.19682E 02	-0.20624E 01	0.29827E 01
LOADING COND= 1	NO OF ELEMT= 10	0.17900E 02	-0.25078E 01	0.40108E 01
LOADING COND= 1	NO OF ELEMT= 11	0.18506E 02	-0.81738E-01	0.55928E 00
LOADING COND= 1	NO OF ELEMT= 12	0.15896E 02	-0.73443E 00	0.17898E 01
LOADING COND= 1	NO OF ELEMT= 13	0.16355E 02	0.11038E 01	-0.97372E 00
LOADING COND= 1	NO OF ELEMT= 14	0.13176E 02	0.30896E 00	0.31589E 00
LOADING COND= 1	NO OF ELEMT= 15	0.13482E 02	0.15331E 01	-0.17286E 01
LOADING COND= 1	NO OF ELEMT= 16	0.97710E 01	0.60540E 00	-0.53421E 00
LOADING COND= 1	NO OF ELEMT= 17	0.96916E 01	0.10877E 01	-0.16043E 01

```
 LOADING COND=  1
NO OF ELEMT=   18        0.55981E 01    0.14297E-01   -0.97383E 00

 LOADING COND=  1
NO OF ELEMT=   19        0.55800E 01   -0.58167E-01   -0.12815E 00

 LOADING COND=  1
NO OF ELEMT=   20        0.40223E 01   -0.44759E 00    0.50569E 00

 LOADING COND=  1
NO OF ELEMT=   21       -0.29936E 01   -0.11974E 02    0.22193E 02

 LOADING COND=  1
NO OF ELEMT=   22        0.83050E 01   -0.51498E 01    0.19918E 02

 LOADING COND=  1
NO OF ELEMT=   23        0.85523E 01   -0.81604E 01    0.15701E 02

 LOADING COND=  1
NO OF ELEMT=   24        0.13094E 02   -0.70251E 01    0.14818E 02

 LOADING COND=  1
NO OF ELEMT=   25        0.12572E 02   -0.51129E 01    0.10586E 02

 LOADING COND=  1
NO OF ELEMT=   26        0.15144E 02   -0.47198E 01    0.10557E 02

 LOADING COND=  1
NO OF ELEMT=   27        0.15621E 02   -0.28117E 01    0.67259E 01

 LOADING COND=  1
NO OF ELEMT=   28        0.15623E 02   -0.28113E 01    0.72198E 01

 LOADING COND=  1
NO OF ELEMT=   29        0.16028E 02   -0.11931E 01    0.38436E 01

 LOADING COND=  1
NO OF ELEMT=   30        0.14584E 02   -0.14541E 01    0.46326E 01

 LOADING COND=  1
NO OF ELEMT=   31        0.15296E 02   -0.20542E 00    0.17686E 01

 LOADING COND=  1
NO OF ELEMT=   32        0.13472E 02   -0.66126E 00    0.26754E 01

 LOADING COND=  1
NO OF ELEMT=   33        0.12677E 02    0.15611E 00    0.42032E 00

 LOADING COND=  1
NO OF ELEMT=   34        0.11312E 02   -0.43494E 00    0.12721E 01

 LOADING COND=  1
NO OF ELEMT=   35        0.11390E 02   -0.12440E 00   -0.26741E 00

 LOADING COND=  1
NO OF ELEMT=   36        0.85503E 01   -0.83433E 00    0.22363E 00

 LOADING COND=  1
NO OF ELEMT=   37        0.85780E 01   -0.72391E 00   -0.30131E 00
```

```
 LOADING COND=  1
NO OF ELEMT=   38       0.60530E 01    -0.13551E 01    -0.57373E-02

 LOADING COND=  1
NO OF ELEMT=   39       0.58094E 01    -0.23296E 01     0.47721E 00

 LOADING COND=  1
NO OF ELEMT=   40       0.39040E 01    -0.28060E 01    -0.35870E 00

 LOADING COND=  1
NO OF ELEMT=   41      -0.14764E 01    -0.59055E 01     0.17956E 02

 LOADING COND=  1
NO OF ELEMT=   42       0.64358E 01    -0.39274E 01     0.16609E 02

 LOADING COND=  1
NO OF ELEMT=   43       0.63738E 01    -0.41752E 01     0.13657E 02

 LOADING COND=  1
NO OF ELEMT=   44       0.10470E 02    -0.31513E 01     0.13092E 02

 LOADING COND=  1
NO OF ELEMT=   45       0.10590E 02    -0.26682E 01     0.98058E 01

 LOADING COND=  1
NO OF ELEMT=   46       0.12455E 02    -0.22020E 01     0.98309E 01

 LOADING COND=  1
NO OF ELEMT=   47       0.12620E 02    -0.15438E 01     0.66990E 01

 LOADING COND=  1
NO OF ELEMT=   48       0.13095E 02    -0.14251E 01     0.70960E 01

 LOADING COND=  1
NO OF ELEMT=   49       0.13238E 02    -0.85239E 00     0.42894E 01

 LOADING COND=  1
NO OF ELEMT=   50       0.12738E 02    -0.57739E 00     0.48662E 01

 LOADING COND=  1
NO OF ELEMT=   51       0.12830E 02    -0.60881E 00     0.24984E 01

 LOADING COND=  1
NO OF ELEMT=   52       0.11620E 02    -0.91136E 00     0.30798E 01

 LOADING COND=  1
NO OF ELEMT=   53       0.11644E 02    -0.81519E 00     0.12574E 01

 LOADING COND=  1
NO OF ELEMT=   54       0.98925E 01    -0.12530E 01     0.16229E 01

 LOADING COND=  1
NO OF ELEMT=   55       0.58864E 01    -0.12773E 01     0.49156E 00

 LOADING COND=  1
NO OF ELEMT=   56       0.79063E 01    -0.17718E 01     0.60620E 00

 LOADING COND=  1
NO OF ELEMT=   57       0.78153E 01    -0.21439E 01     0.28633E 00
```

LOADING COND=	NO OF ELEMT=			
1	58	0.59581E 01	-0.26082E 01	-0.20648E 00
1	59	0.59432E 01	-0.26678E 01	0.29455E 00
1	60	0.41960E 01	-0.31046E 01	-0.58632E 00
1	61	-0.57836E 00	-0.23135E 01	0.14989E 02
1	62	0.52970E 01	-0.84461E 00	0.14192E 02
1	63	0.50798E 01	-0.17134E 01	0.11906E 02
1	64	0.86390E 01	-0.82365E 00	0.11607E 02
1	65	0.85440E 01	-0.12038E 01	0.89570E 01
1	66	0.10458E 02	-0.72530E 00	0.90413E 01
1	67	0.10414E 02	-0.90102E 00	0.64491E 01
1	68	0.11161E 02	-0.71440E 00	0.67552E 01
1	69	0.11123E 02	-0.86324E 00	0.44161E 01
1	70	0.11001E 02	-0.89384E 00	0.47808E 01
1	71	0.10949E 02	-0.11031E 01	0.28210E 01
1	72	0.10154E 02	-0.13017E 01	0.30688E 01
1	73	0.10100E 02	-0.15192E 01	0.16053E 01
1	74	0.88470E 01	-0.18325E 01	0.16384E 01
1	75	0.87865E 01	-0.20742E 01	0.77892E 00
1	76	0.73047E 01	-0.24447E 01	0.41933E 00
1	77	0.73035E 01	-0.24615E 01	0.24024E 00

```
 LOADING COND=   1
NO OF ELEMT=    78        0.59175E 01   -0.28073E 01   -0.52654E 00

 LOADING COND=   1
NO OF ELEMT=    79        0.59786E 01   -0.25627E 01    0.11106E 00

 LOADING COND=   1
NO OF ELEMT=    80        0.54021E 01   -0.27068E 01   -0.13169E 01

 LOADING COND=   1
NO OF ELEMT=    81       -0.46476E-01   -0.18590E 00    0.12786E 02

 LOADING COND=   1
NO OF ELEMT=    82        0.45366E 01    0.95986E 00    0.12344E 02

 LOADING COND=   1
NO OF ELEMT=    83        0.42237E 01   -0.29151E 00    0.10443E 02

 LOADING COND=   1
NO OF ELEMT=    84        0.73215E 01    0.48292E 00    0.10325E 02

 LOADING COND=   1
NO OF ELEMT=    85        0.70921E 01   -0.43440E 00    0.81188E 01

 LOADING COND=   1
NO OF ELEMT=    86        0.89540E 01    0.31066E-01    0.82262E 01

 LOADING COND=   1
NO OF ELEMT=    87        0.87776E 01   -0.67469E 00    0.60523E 01

 LOADING COND=   1
NO OF ELEMT=    88        0.96618E 01   -0.45365E 00    0.62522E 01

 LOADING COND=   1
NO OF ELEMT=    89        0.95148E 01   -0.10416E 01    0.42906E 01

 LOADING COND=   1
NO OF ELEMT=    90        0.96133E 01   -0.10170E 01    0.44403E 01

 LOADING COND=   1
NO OF ELEMT=    91        0.94956E 01   -0.14879E 01    0.28153E 01

 LOADING COND=   1
NO OF ELEMT=    92        0.89786E 01   -0.16171E 01    0.26075E 01

 LOADING COND=   1
NO OF ELEMT=    93        0.88969E 01   -0.19437E 01    0.16200E 01

 LOADING COND=   1
NO OF ELEMT=    94        0.79351E 01   -0.21842E 01    0.13454E 01

 LOADING COND=   1
NO OF ELEMT=    95        0.79314E 01   -0.21592E 01    0.60096E 00

 LOADING COND=   1
NO OF ELEMT=    96        0.67015E 01   -0.25067E 01    0.10925E 00

 LOADING COND=   1
NO OF ELEMT=    97        0.68273E 01   -0.20033E 01   -0.12376E-01
```

```
 LOADING COND=  1
NO OF ELEMT=   98        0.55677E 01   -0.23182E 01    -0.87236E 00

 LOADING COND=  1
NO OF ELEMT=   99        0.60074E 01   -0.55907E 00    -0.49095E 00

 LOADING COND=  1
NO OF ELEMT=  100        0.61205E 01   -0.53081E 00    -0.22705E 00

 LOADING COND=  1
NO OF ELEMT=  101        0.24821E 00    0.59286E 00     0.11068E 02

 LOADING COND=  1
NO OF ELEMT=  102        0.39875E 01    0.19277E 01     0.10859E 02

 LOADING COND=  1
NO OF ELEMT=  103        0.36140E 01    0.43344E 00     0.91982E 01

 LOADING COND=  1
NO OF ELEMT=  104        0.63407E 01    0.11151E 01     0.91873E 01

 LOADING COND=  1
NO OF ELEMT=  105        0.60325E 01   -0.11774E 00     0.73051E 01

 LOADING COND=  1
NO OF ELEMT=  106        0.77926E 01    0.32228E 00     0.73956E 01

 LOADING COND=  1
NO OF ELEMT=  107        0.75432E 01   -0.67532E 00     0.55502E 01

 LOADING COND=  1
NO OF ELEMT=  108        0.84604E 01   -0.44601E 00     0.56302E 01

 LOADING COND=  1
NO OF ELEMT=  109        0.82669E 01   -0.12201E 01     0.39755E 01

 LOADING COND=  1
NO OF ELEMT=  110        0.84701E 01   -0.11693E 01     0.39475E 01

 LOADING COND=  1
NO OF ELEMT=  111        0.83389E 01   -0.16939E 01     0.25926E 01

 LOADING COND=  1
NO OF ELEMT=  112        0.79574E 01   -0.17893E 01     0.23764E 01

 LOADING COND=  1
NO OF ELEMT=  113        0.79147E 01   -0.19600E 01     0.14065E 01

 LOADING COND=  1
NO OF ELEMT=  114        0.70886E 01   -0.21666E 01     0.98010E 00

 LOADING COND=  1
NO OF ELEMT=  115        0.71817E 01   -0.17942E 01     0.46706E 00

 LOADING COND=  1
NO OF ELEMT=  116        0.59976E 01   -0.20903E 01    -0.12338E 00

 LOADING COND=  1
NO OF ELEMT=  117        0.63631E 01   -0.56807E 00    -0.21666E 00
```

```
 LOADING COND=  1
NO OF ELEMT=  118      0.55859E 01   -0.10474E 01   -0.30385E 00

 LOADING COND=  1
NO OF ELEMT=  119      0.57917E 01   -0.22444E 00   -0.23377E 00

 LOADING COND=  1
NC OF ELEMT=  120      0.62466E 01   -0.11072E 00    0.10805E 00

 LOADING COND=  1
NC OF ELEMT=  121      0.38704E 00    0.15482E 01    0.96653E 01

 LOADING COND=  1
NO OF ELEMT=  122      0.35621E 01    0.23419E 01    0.96044E 01

 LOADING COND=  1
NO OF ELEMT=  123      0.31553E 01    0.71463E 00    0.81115E 01

 LOADING COND=  1
NO OF ELEMT=  124      0.55799E 01    0.13208E 01    0.81473E 01

 LOADING COND=  1
NC OF ELEMT=  125      0.52352E 01   -0.58187E-01    0.65142E 01

 LOADING COND=  1
NO OF ELEMT=  126      0.68589E 01    0.34776E 00    0.65578E 01

 LOADING COND=  1
NO OF ELEMT=  127      0.65853E 01   -0.74699E 00    0.49773E 01

 LOADING COND=  1
NO OF ELEMT=  128      0.74606E 01   -0.52817E 00    0.49471E 01

 LOADING COND=  1
NC OF ELEMT=  129      0.72656E 01   -0.13081E 01    0.35445E 01

 LOADING COND=  1
NO OF ELEMT=  130      0.74785E 01   -0.12549E 01    0.33761E 01

 LOADING COND=  1
NO OF ELEMT=  131      0.73791E 01   -0.16523E 01    0.22441E 01

 LOADING COND=  1
NC OF ELEMT=  132      0.70365E 01   -0.17380E 01    0.19177E 01

 LOADING COND=  1
NC OF ELEMT=  133      0.70606E 01   -0.16418E 01    0.11291E 01

 LOADING COND=  1
NO OF ELEMT=  134      0.62947E 01   -0.18332E 01    0.69702E 00

 LOADING COND=  1
NO OF ELEMT=  135      0.64933E 01   -0.10387E 01    0.34081E 00

 LOADING COND=  1
NC OF ELEMT=  136      0.55544E 01   -0.12735E 01    0.11664E 00

 LOADING COND=  1
NC OF ELEMT=  137      0.57086E 01   -0.41663E 00   -0.59789E-01
```

LOADING COND= 1
NO OF ELEMT= 138 0.55697E 01 -0.46635E 00 0.92773E-01

LOADING COND= 1
NO OF ELEMT= 139 0.56493E 01 -0.14812E 00 -0.82348E-01

LOADING COND= 1
NO OF ELEMT= 140 0.60168E 01 -0.56252E-01 0.31239E 00

LOADING COND= 1
NO OF ELEMT= 141 0.42760E 00 0.17104E 01 0.84746E 01

LOADING COND= 1
NO OF ELEMT= 142 0.32103E 01 0.24061E 01 0.84968E 01

LOADING COND= 1
NO OF ELEMT= 143 0.27945E 01 0.74256E 00 0.71382E 01

LOADING COND= 1
NO OF ELEMT= 144 0.49597E 01 0.12839E 01 0.71773E 01

LOADING COND= 1
NO OF ELEMT= 145 0.46120E 01 -0.10684E 00 0.57473E 01

LOADING COND= 1
NO OF ELEMT= 146 0.60749E 01 0.25887E 00 0.57341E 01

LOADING COND= 1
NO OF ELEMT= 147 0.58125E 01 -0.79060E 00 0.43740E 01

LOADING COND= 1
NO OF ELEMT= 148 0.65920E 01 -0.59572E 00 0.42526E 01

LOADING COND= 1
NO OF ELEMT= 149 0.64284E 01 -0.12501E 01 0.30625E 01

LOADING COND= 1
NO OF ELEMT= 150 0.65946E 01 -0.12085E 01 0.28149E 01

LOADING COND= 1
NO OF ELEMT= 151 0.65477E 01 -0.13961E 01 0.16737E 01

LOADING COND= 1
NO OF ELEMT= 152 0.62121E 01 -0.14800E 01 0.15377E 01

LOADING COND= 1
NO OF ELEMT= 153 0.63002E 01 -0.11274E 01 0.91044E 00

LOADING COND= 1
NO OF ELEMT= 154 0.57412E 01 -0.12671E 01 0.66704E 00

LOADING COND= 1
NO OF ELEMT= 155 0.59270E 01 -0.52391E 00 0.45329E 00

LOADING COND= 1
NO OF ELEMT= 156 0.52300E 01 -0.69816E 00 0.37964E 00

LOADING COND= 1
NO OF ELEMT= 157 0.52934E 01 -0.44455E 00 0.16402E-01

```
 LOADING COND=   1
NO OF ELEMT=   158        0.54289E 01   -0.41066E 00    0.46171E 00

 LOADING COND=   1
NO OF ELEMT=   159        0.55422E 01    0.42422E-01    0.19963E 00

 LOADING COND=   1
NO OF ELEMT=   160        0.56057E 01    0.58308E-01    0.21166E 00

 LOADING COND=   1
NO OF ELEMT=   161        0.41281E 00    0.16512E 01    0.74311E 01

 LOADING COND=   1
NO OF ELEMT=   162        0.29041E 01    0.22741E 01    0.74862E 01

 LOADING COND=   1
NO OF ELEMT=   163        0.24989E 01    0.65314E 00    0.62499E 01

 LOADING COND=   1
NO OF ELEMT=   164        0.44281E 01    0.11354E 01    0.62716E 01

 LOADING COND=   1
NO OF ELEMT=   165        0.41037E 01   -0.16204E 00    0.50165E 01

 LOADING COND=   1
NO OF ELEMT=   166        0.53886E 01    0.15918E 00    0.49477E 01

 LOADING COND=   1
NO OF ELEMT=   167        0.51613E 01   -0.75021E 00    0.37770E 01

 LOADING COND=   1
NO OF ELEMT=   168        0.58196E 01   -0.58563E 00    0.35990E 01

,LOADING COND=   1
NO OF ELEMT=   169        0.57024E 01   -0.10544E 01    0.25935E 01

 LOADING COND=   1
NO OF ELEMT=   170        0.58106E 01   -0.10274E 01    0.23346E 01

 LOADING COND=   1
NO OF ELEMT=   171        0.58151E 01   -0.10094E 01    0.15598E 01

 LOADING COND=   1
NO OF ELEMT=   172        0.55542E 01   -0.10747E 01    0.13267E 01

 LOADING COND=   1
NO OF ELEMT=   173        0.56492E 01   -0.69472E 00    0.81115E 00

 LOADING COND=   1
NO OF ELEMT=   174        0.54220E 01   -0.75151E 00    0.69106E 00

 LOADING COND=   1
NO OF ELEMT=   175        0.55768E 01   -0.13212E 00    0.65350E 00

 LOADING COND=   1
NO OF ELEMT=   176        0.52102E 01    0.45152E 00   -0.87344E 00

 LOADING COND=   1
NO OF ELEMT=   177        0.51379E 01    0.10256E 00    0.54642E 00
```

LOADING COND= 1
NO OF ELEMT= 178 0.52844E 01 0.19918E 00 0.31576E 00

LOADING COND= 1
NO OF ELEMT= 179 0.52359E 01 0.50917E-02 0.84738E-01

LOADING COND= 1
NO OF ELEMT= 180 0.53476E 01 0.33019E-01 0.17353E 00

LOADING COND= 1
NO OF ELEMT= 181 0.37606E 00 0.15042E 01 0.64968E 01

LOADING COND= 1
NO OF ELEMT= 182 0.25486E 01 0.19671E 01 0.61497E 01

LOADING COND= 1
NO OF ELEMT= 183 0.21930E 01 0.54499E 00 0.54240E 01

LOADING COND= 1
NO OF ELEMT= 184 0.38511E 01 0.57976E 00 0.50979E 01

LOADING COND= 1
NO OF ELEMT= 185 0.35564E 01 -0.19901E 00 0.42906E 01

LOADING COND= 1
NO OF ELEMT= 186 0.46549E 01 0.21463E 00 0.39802E 01

LOADING COND= 1
NO OF ELEMT= 187 0.44349E 01 -0.66527E 00 0.31597E 01

LOADING COND= 1
NO OF ELEMT= 188 0.50060E 01 -0.29546E 00 0.28854E 01

LOADING COND= 1
NO OF ELEMT= 189 0.48829E 01 -0.79162E 00 0.21270E 01

LOADING COND= 1
NO OF ELEMT= 190 0.50199E 01 -0.54961E 00 0.19455E 01

LOADING COND= 1
NO OF ELEMT= 191 0.50136E 01 -0.57480E 00 0.13145E 01

LOADING COND= 1
NO OF ELEMT= 192 0.48636E 01 -0.52425E 00 0.12766E 01

LOADING COND= 1
NO OF ELEMT= 193 0.49682E 01 -0.10587E 00 0.74602E 00

LOADING COND= 1
NO OF ELEMT= 194 0.46415E 01 -0.32032E 00 0.90947E 00

LOADING COND= 1
NO OF ELEMT= 195 0.45613E 01 -0.64127E 00 0.91309E 00

LOADING COND= 1
NO OF ELEMT= 196 0.50281E 01 -0.32247E 00 0.67400E 00

LOADING COND= 1
NO OF ELEMT= 197 0.51280E 01 0.77267E-01 0.23228E 00

LOADING COND= 1 NO OF ELEMT= 198	0.50145E 01	-0.14553E 00	0.39940E 00
LOADING COND= 1 NO OF ELEMT= 199	0.50623E 01	0.45765E-01	0.91757E-01
LOADING COND= 1 NO OF ELEMT= 200	0.50202E 01	-0.84929E-01	0.18979E 00
LOADING COND= 1 NO OF ELEMT= 201	0.31186E 00	0.12474E 01	0.52628E 01
LOADING COND= 1 NO OF ELEMT= 202	0.21061E 01	0.16077E 01	0.46164E 01
LOADING COND= 1 NO OF ELEMT= 203	0.18138E 01	0.43868E 00	0.43244E 01
LOADING COND= 1 NO OF ELEMT= 204	0.31447E 01	0.89643E 00	0.37878E 01
LOADING COND= 1 NO OF ELEMT= 205	0.28947E 01	-0.10360E 00	0.33566E 01
LOADING COND= 1 NO OF ELEMT= 206	0.37799E 01	0.38310E 00	0.29450E 01
LOADING COND= 1 NO OF ELEMT= 207	0.35968E 01	-0.34943E 00	0.24476E 01
LOADING COND= 1 NO OF ELEMT= 208	0.41063E 01	0.22949E-01	0.21830E 01
LOADING COND= 1 NO OF ELEMT= 209	0.40187E 01	-0.32706E 00	0.17119E 01
LOADING COND= 1 NO OF ELEMT= 210	0.42422E 01	-0.12574E 00	0.15845E 01
LOADING COND= 1 NO OF ELEMT= 211	0.42288E 01	-0.17941E 00	0.11896E 01
LOADING COND= 1 NO OF ELEMT= 212	0.43218E 01	-0.12758E 00	0.11461E 01
LOADING COND= 1 NO OF ELEMT= 213	0.43049E 01	-0.19512E 00	0.84604E 00
LOADING COND= 1 NO OF ELEMT= 214	0.43750E 01	-0.94852E-01	0.79495E 00
LOADING COND= 1 NO OF ELEMT= 215	0.44123E 01	0.54364E-01	0.60229E 00
LOADING COND= 1 NO OF ELEMT= 216	0.45878E 01	-0.53430E-01	0.58198E 00
LOADING COND= 1 NO OF ELEMT= 217	0.46131E 01	0.47727E-01	0.33695E 00

```
LOADING COND=  1
NO OF ELEMT=  218        0.46572E 01   -0.74950E-01    0.36052E 00

LOADING COND=  1
NO OF ELEMT=  219        0.46802E 01    0.17004E-01    0.11834E 00

LOADING COND=  1
NO OF ELEMT=  220        0.45354E 01    0.44769E-01    0.15347E 00

LOADING COND=  1
NO OF ELEMT=  221        0.26479E 00    0.10592E 01    0.38995E 01

LOADING COND=  1
NO OF ELEMT=  222        0.16391E 01    0.13959E 01    0.31272E 01

LOADING COND=  1
NO OF ELEMT=  223        0.14166E 01    0.50573E 00    0.31522E 01

LOADING COND=  1
NO OF ELEMT=  224        0.24541E 01    0.94941E 00    0.25471E 01

LOADING COND=  1
NO OF ELEMT=  225        0.22638E 01    0.18791E 00    0.24316E 01

LOADING COND=  1
NO OF ELEMT=  226        0.30208E 01    0.50739E 00    0.19906E 01

LOADING COND=  1
NO OF ELEMT=  227        0.29105E 01    0.66047E-01    0.18372E 01

LOADING COND=  1
NO OF ELEMT=  228        0.33952E 01    0.29914E 00    0.15515E 01

LOADING COND=  1
NO OF ELEMT=  229        0.33355E 01    0.60452E-01    0.13683E 01

LOADING COND=  1
NO OF ELEMT=  230        0.36458E 01    0.24171E 00    0.11817E 01

LOADING COND=  1
NO OF ELEMT=  231        0.36015E 01    0.64695E-01    0.98774E 00

LOADING COND=  1
NO OF ELEMT=  232        0.38368E 01    0.24507E 00    0.84015E 00

LOADING COND=  1
NO OF ELEMT=  233        0.38123E 01    0.13687E 00    0.69625E 00

LOADING COND=  1
NO OF ELEMT=  234        0.41009E 01    0.18288E 00    0.53719E 00

LOADING COND=  1
NO OF ELEMT=  235        0.40698E 01    0.58570E-01    0.46019E 00

LOADING COND=  1
NO OF ELEMT=  236        0.43039E 01    0.78194E-01    0.33307E 00

LOADING COND=  1
NO OF ELEMT=  237        0.42751E 01   -0.36766E-01    0.25735E 00
```

LOADING COND= 1
NO OF ELEMT= 238 0.43934E 01 0.42034E 00 0.14093E 00

LOADING COND= 1
NO OF ELEMT= 239 0.42605E 01 -0.11128E 00 0.24205E-01

LOADING COND= 1
NO OF ELEMT= 240 0.45109E 01 0.57636E 00 -0.18953E 00

LOADING COND= 1
NO OF ELEMT= 241 0.26176E 00 0.10471E 01 0.26093E 01

LOADING COND= 1
NO OF ELEMT= 242 0.13265E 01 0.13979E 01 0.20005E 01

LOADING COND= 1
NO OF ELEMT= 243 0.11483E 01 0.68483E 00 0.20759E 01

LOADING COND= 1
NO OF ELEMT= 244 0.20612E 01 0.77782E 00 0.15782E 01

LOADING COND= 1
NO OF ELEMT= 245 0.19888E 01 0.48825E 00 0.16752E 01

LOADING COND= 1
NO OF ELEMT= 246 0.25877E 01 0.61237E 00 0.13413E 01

LOADING COND= 1
NO OF ELEMT= 247 0.25385E 01 0.41551E 00 0.13294E 01

LOADING COND= 1
NO OF ELEMT= 248 0.29179E 01 0.58834E 00 0.11069E 01

LOADING COND= 1
NO OF ELEMT= 249 0.28697E 01 0.39539E 00 0.99495E 00

LOADING COND= 1
NO OF ELEMT= 250 0.31512E 01 0.60530E 00 0.82033E 00

LOADING COND= 1
NO OF ELEMT= 251 0.30987E 01 0.39542E 00 0.66323E 00

LOADING COND= 1
NO OF ELEMT= 252 0.34558E 01 0.45282E 00 0.46607E 00

LOADING COND= 1
NO OF ELEMT= 253 0.34310E 01 0.35327E 00 0.36732E 00

LOADING COND= 1
NO OF ELEMT= 254 0.41263E 01 0.36625E 00 0.14947E-01

LOADING COND= 1
NO OF ELEMT= 255 0.41495E 01 0.45878E 00 0.40092E 00

LOADING COND= 1
NO OF ELEMT= 256 0.37089E 01 0.79545E 00 0.59659E 00

LOADING COND= 1
NO OF ELEMT= 257 0.36716E 01 0.64623E 00 -0.78497E-02

LOADING COND= 1
NO OF ELEMT= 258 0.40043E 01 0.10011E 01 -0.21410E 00

LOADING COND= 1
NO OF ELEMT= 259 0.40043E 01 0.10011E 01 -0.21410E 00

LOADING COND= 1
NO OF ELEMT= 260 0.29938E 00 0.11975E 01 0.16323E 01

LOADING COND= 1
NO OF ELEMT= 261 0.13292E 01 0.65306E 00 0.59467E 00

LOADING COND= 1
NO OF ELEMT= 262 0.13902E 01 0.89710E 00 0.14126E 01

LOADING COND= 1
NO OF ELEMT= 263 0.19698E 01 0.87859E 00 0.85452E 00

LOADING COND= 1
NO OF ELEMT= 264 0.19470E 01 0.78755E 00 0.12017E 01

LOADING COND= 1
NO OF ELEMT= 265 0.22278E 01 0.91871E 00 0.94396E 00

LOADING COND= 1
NO OF ELEMT= 266 0.21905E 01 0.76940E 00 0.94298E 00

LOADING COND= 1
NO OF ELEMT= 267 0.22164E 01 0.87586E 00 0.92768E 00

LOADING COND= 1
NO OF ELEMT= 268 0.21929E 01 0.78167E 00 0.58574E 00

LOADING COND= 1
NO OF ELEMT= 269 0.26181E 01 0.65453E 00 0.16606E 00

LOADING COND= 1
NO OF ELEMT= 270 0.26386E 01 0.73659E 00 0.30604E 00

LOADING COND= 1
NO OF ELEMT= 271 0.28670E 01 0.71675E 00 0.18657E 00

LOADING COND= 1
NO OF ELEMT= 272 0.28049E 01 0.46799E 00 -0.35099E 00

LOADING COND= 1
NO OF ELEMT= 273 0.00000E 00 0.00000E 00 0.00000E 00

LOADING COND= 1
NO OF ELEMT= 274 0.00000E 00 0.00000E 00 0.00000E 00

LOADING COND= 1
NO OF ELEMT= 275 0.00000E 00 0.00000E 00 0.00000E 00

LOADING COND= 1
NO OF ELEMT= 276 0.00000E 00 0.00000E 00 0.00000E 00

LOADING COND= 1
NO OF ELEMT= 277 0.00000E 00 0.00000E 00 0.00000E 00

```
 LOADING COND=  1
NO OF ELEMT=  278       0.00000E 00    0.00000E 00    0.00000E 00

 LOADING COND=  1
NO OF ELEMT=  279       0.00000E 00    0.00000E 00    0.00000E 00

 LOADING COND=  1
NO OF ELEMT=  280       0.00000E 00    0.00000E 00    0.00000E 00

 LOADING COND=  1
NO OF ELEMT=  281       0.00000E 00    0.00000E 00    0.00000E 00

 LOADING COND          STENY          PTENY

       1         0.14100E 01     -0.14100E 01

STATEMENTS EXECUTED= 1571576

CORE USAGE       OBJECT CODE=   21448 BYTES,ARRAY AREA=  117576 BYTES,TOTAL AREA AV

DIAGNOSTICS          NUMBER OF ERRORS=       0, NUMBER OF WARNINGS=      0, NUMBER C

COMPILE TIME=     0.18 SEC,EXECUTION TIME=    11.32 SEC,     21.13.21    TUESDAY

        C$BTCHEND
```

APPENDIX D

Application Of Mechanics Of Composite Material To A Coal Layer

In order to analyse the problem a coal layer with six horizontal bedding planes is assumed. Each bedding plane (laminae) is cut by minor vertical cleats that is neglected in this analysis. The major cleats has different lay up in each plane for example: (30/-30/0/0/-30/30). To simplify the problem the following assumptions have been adapted:

1. The material is linearly elastic and orthotropic with respect to rectilinear coordinates x, y, z.
2. The coal layer as a laminate is sufficiently thin in the z -direction that σ_z and τ_{xz}, τ_{yz} are neglected.
3. Interfacial friction and distributed normal loading are neglected and only tensile forces due to excavation are considered.

The following formulation consists of exempts from Mechanics of Composite Materials by Robert M. Jones (1972).

The stress strain relations in principal material coordinates for a coal laminae of an orthotropic material under plane stress are

$$\begin{Bmatrix} \sigma_1 \\ \sigma_2 \\ \tau_{12} \end{Bmatrix} = \begin{bmatrix} Q_{11} & Q_{12} & 0 \\ Q_{12} & Q_{22} & 0 \\ 0 & 0 & Q_{66} \end{bmatrix} \begin{Bmatrix} \varepsilon_1 \\ \varepsilon_2 \\ \gamma_{12} \end{Bmatrix} \qquad (1)$$

Q_{ij} are defined in terms of the engineering constants as:

$$Q_{11} = \frac{E_1}{1 - \nu_{12}\nu_{21}}$$

$$Q_{12} = \frac{\nu_{12} E_2}{1 - \nu_{12}\nu_{21}} = \frac{\nu_{21} E_1}{1 - \nu_{12}\nu_{21}}$$

$$Q_{22} = \frac{E_2}{1 - \nu_{12}\nu_{21}}$$

$$Q_{66} = G_{12}$$

In any other coordinate system in the plane of the laminae, the stresses are

$$\begin{Bmatrix} \sigma_x \\ \sigma_y \\ \tau_{xy} \end{Bmatrix} = \begin{bmatrix} \bar{Q}_{11} & \bar{Q}_{12} & \bar{Q}_{16} \\ \bar{Q}_{12} & \bar{Q}_{22} & \bar{Q}_{26} \\ \bar{Q}_{16} & \bar{Q}_{26} & \bar{Q}_{66} \end{bmatrix} \begin{Bmatrix} \varepsilon_x \\ \varepsilon_y \\ \gamma_{xy} \end{Bmatrix} \tag{3}$$

where

$$\begin{aligned}
\bar{Q}_{11} &= Q_{11}\cos^4\theta + 2(Q_{12} + 2Q_{66})\sin^2\theta\cos^2\theta + Q_{22}\sin^4\theta \\
\bar{Q}_{12} &= (Q_{11} + Q_{22} - 4Q_{66})\sin^2\theta\cos^2\theta + Q_{12}(\sin^4\theta + \cos^4\theta) \\
\bar{Q}_{22} &= Q_{11}\sin^4\theta + 2(Q_{12} + 2Q_{66})\sin^2\theta\cos^2\theta + Q_{22}\cos^4\theta \\
\bar{Q}_{16} &= (Q_{11} - Q_{12} - 2Q_{66})\sin\theta\cos^3\theta + \\
&\quad (Q_{12} - Q_{22} + 2Q_{66})\sin^3\theta\cos\theta
\end{aligned} \tag{4}$$

$$\bar{Q}_{26} = (Q_{11} - Q_{12} - 2Q_{66}) \sin^3\theta \cos\theta + \quad (4)$$

$$(Q_{12} - Q_{22} + 2Q_{66}) \sin\theta \cos^3\theta$$

$$\bar{Q}_{66} = (Q_{11} + Q_{22} - 2Q_{12} - 2Q_{66}) \sin^2\theta \cos^2\theta +$$

$$Q_{66} (\sin^4\theta + \cos^4\theta)$$

The resultant forces acting on a coal laminate is obtained by integration of the stresses in each layer or lamina through the laminate thickness

$$N_x = \int_{-t/2}^{t/2} \sigma_x dZ \quad (5)$$

where

N_x is a force per unit length (width) of the cross section of the laminate and t the thicknes of the laminate.

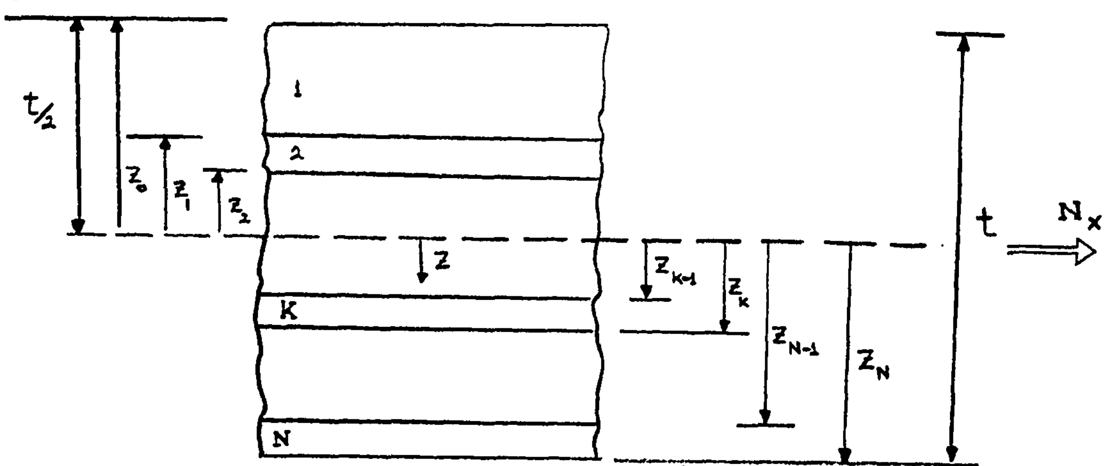

Figure 1-D, Geometry of an n-layered laminate

$$\begin{Bmatrix} N_x \\ N_y \\ N_{xy} \end{Bmatrix} = \begin{bmatrix} A_{11} & A_{12} & A_{16} \\ A_{12} & A_{22} & A_{26} \\ A_{16} & A_{26} & A_{66} \end{bmatrix} \begin{Bmatrix} \varepsilon_x \\ \varepsilon_y \\ \gamma_{xy} \end{Bmatrix} \tag{11}$$

whereupon

$$\begin{Bmatrix} \varepsilon_x^0 \\ \varepsilon_y^0 \\ \gamma_{xy} \end{Bmatrix} = \begin{bmatrix} A_{11} & A_{12} & A_{16} \\ A_{12} & A_{22} & A_{26} \\ A_{16} & A_{26} & A_{66} \end{bmatrix}^{-1} \begin{Bmatrix} N_x \\ N_y \\ N_{xy} \end{Bmatrix} \tag{12}$$

To call the matrix A^{-1} as A' and when $N_x = N_1$ and $N_y = N_{xy} = 0$, the strains are

$$\begin{Bmatrix} \varepsilon_x^0 \\ \varepsilon_y^0 \\ \gamma_{xy} \end{Bmatrix} \cdot \begin{bmatrix} A'_{11} & A'_{12} & A'_{16} \\ A'_{12} & A'_{22} & A'_{26} \\ A'_{16} & A'_{26} & A'_{66} \end{bmatrix} \begin{Bmatrix} N_1 \\ 0 \\ 0 \end{Bmatrix} \tag{13}$$

or more simply

$$\begin{aligned} \varepsilon_x^0 &= A'_{11}N_1 \\ \varepsilon_y^0 &= A'_{12}N_1 \\ \gamma_{xy}^0 &= A'_{16}N_1 \end{aligned} \tag{13-a}$$

The stresses in each layer are obtained by use of the stress-strain relations for a lamina

$$\begin{Bmatrix} \sigma_x \\ \sigma_y \\ \tau_{xy} \end{Bmatrix}_K = \begin{bmatrix} \bar{Q}_{11} & \bar{Q}_{12} & \bar{Q}_{16} \\ \bar{Q}_{12} & \bar{Q}_{22} & \bar{Q}_{26} \\ \bar{Q}_{16} & \bar{Q}_{26} & \bar{Q}_{66} \end{bmatrix} \begin{Bmatrix} A'_{11}N_1 \\ A'_{12}N_1 \\ A'_{16}N_1 \end{Bmatrix} \tag{14}$$

The maximum stress criterion, the maximum strain criterion or the Tsai-Hill criterion can be applied in order to find out the failure occurrence.

Maximum stress theory:

In the maximum stress theory, the stresses in principal material directions must be less than the respective strengths, otherwise fracture is said to have occurred, that is, for tensile stresses,

$$\begin{aligned} \sigma_1 &< x_t \\ \sigma_2 &< y_t \end{aligned} \tag{15}$$

and for compressive stresses

$$\begin{aligned} \sigma_1 &> x_c \\ \sigma_2 &> y_c \end{aligned} \tag{16}$$

or $$\begin{Bmatrix} N_x \\ N_y \\ N_{xy} \end{Bmatrix} = \int_{-t/2}^{t/2} \begin{Bmatrix} \sigma_x \\ \sigma_y \\ \tau_{xy} \end{Bmatrix}_K dz = \sum_{K=1}^{N} \int_{Z_{K-1}}^{Z_K} \begin{Bmatrix} \sigma_x \\ \sigma_y \\ \tau_{xy} \end{Bmatrix} dz \qquad (6)$$

where Z_K and Z_{K-1} are defined in Figure 1.

The integration indicated in (6) can be rearranged to include the fact that the stiffness matrix for a coal laminae is constant within the lamina. Thus the stiffness matrix goes outside the integration over each layer but is within the summation of force resultants for each layer.

The stresses in the K^{th} layer can be expressed in terms of the laminate surface strains and curvature as

$$\begin{Bmatrix} \sigma_x \\ \sigma_y \\ \tau_{xy} \end{Bmatrix} = \begin{bmatrix} \bar{Q}_{11} & \bar{Q}_{12} & \bar{Q}_{16} \\ \bar{Q}_{12} & \bar{Q}_{22} & \bar{Q}_{26} \\ \bar{Q}_{16} & \bar{Q}_{26} & \bar{Q}_{66} \end{bmatrix}_K \left\{ \begin{Bmatrix} \varepsilon_x^0 \\ \varepsilon_y^0 \\ \gamma_{xy}^0 \end{Bmatrix} + Z \begin{Bmatrix} K_x \\ K_y \\ K_{xy} \end{Bmatrix} \right\} \qquad (7)$$

where K's are the middle surface curvatures, now substitute (7) and (6) yields

$$\begin{Bmatrix} N_x \\ N_y \\ N_{xy} \end{Bmatrix} = \sum_{K=1}^{N} \begin{bmatrix} \bar{Q}_{11} & \bar{Q}_{12} & \bar{Q}_{16} \\ \bar{Q}_{12} & \bar{Q}_{22} & \bar{Q}_{26} \\ \bar{Q}_{16} & \bar{Q}_{26} & \bar{Q}_{66} \end{bmatrix} \left\{ \int_{Z_{K-1}}^{Z_K} \begin{Bmatrix} \varepsilon_x^0 \\ \varepsilon_y^0 \\ \gamma_{xy}^0 \end{Bmatrix} dx + \int_{Z_{K-1}}^{Z_K} \begin{Bmatrix} K_x \\ K_y \\ K_{xy} \end{Bmatrix} Zdz \right\} \qquad (8)$$

However, we should now recall that ε_x^0, ε_y^0, γ_{xy}^0, K_x, K_y, and K_{xy} are not functions of Z but are middle surface values and thus can be removed from under the summation. Thus

$$\begin{Bmatrix} N_x \\ N_y \\ N_{xy} \end{Bmatrix} = \begin{bmatrix} A_{11} & A_{12} & A_{16} \\ A_{12} & A_{22} & A_{26} \\ A_{16} & A_{26} & A_{66} \end{bmatrix} \begin{Bmatrix} \varepsilon_x^0 \\ \varepsilon_y^0 \\ \gamma_{xy}^0 \end{Bmatrix} + \begin{bmatrix} B_{11} & B_{12} & B_{16} \\ B_{12} & B_{22} & B_{26} \\ B_{16} & B_{26} & B_{66} \end{bmatrix} \begin{Bmatrix} K_x \\ K_y \\ K_{xy} \end{Bmatrix} \tag{9}$$

where

$$\begin{aligned} A_{ij} &= \sum_{K=1}^{N} (\bar{Q}_{ij})_K \, (Z_k - Z_{K-1}) \\ B_{ij} &= \frac{1}{2}\sum_{K=1}^{N} (\bar{Q}_{ij})_K \, (Z_K^2 - Z_{K-1}^2) \end{aligned} \tag{10}$$

The A_{ij} are called extensional stiffness, the B_{ij} are called coupling stiffnesses. The presence of the B_{ij} implies coupling between bending and extension of a laminate. Thus, it is impossible to pull on a laminate that has B_{ij} terms without at the same time bending and/or twisting the laminate.

If the angle-ply coal laminate is symmetric about its middle surface, there is no coupling between bending and extension. In the case the laminate is subjected to uniaxial tension the force strain relations are where

x_t, y_t, x_c, y_c are strengths in tension and compression in different directions.

The stresses in the principal material directions are obtained by transformation as

$$\sigma_1 = \sigma_x \cos^2\theta$$
$$\sigma_2 = \sigma_x \sin^2\theta \tag{17}$$

Then by inversion of (17) and substitution of equation (5), the maximum uniaxial stress, σ_x, is the smallest of

$$\sigma_x < \frac{x}{\cos^2\theta}$$
$$\sigma_x < \frac{y}{\sin^2\theta} \tag{18}$$

If the inequalities (18) are not satisfied, then the assumption is made that the coal layer has failed by the failure mechanism associated with x_t, x_c, y_t, y_c respectively.

Now to solve a hypothetical problem consider Figure 2. The first step is to calculate all of the components of $[A]$. Because of the symmetry a simple representation of the case is 30/-30/0 and assume the thickness (t) of each coal laminae to be one inch. The following mechanical properties are assummed for the coal layer:

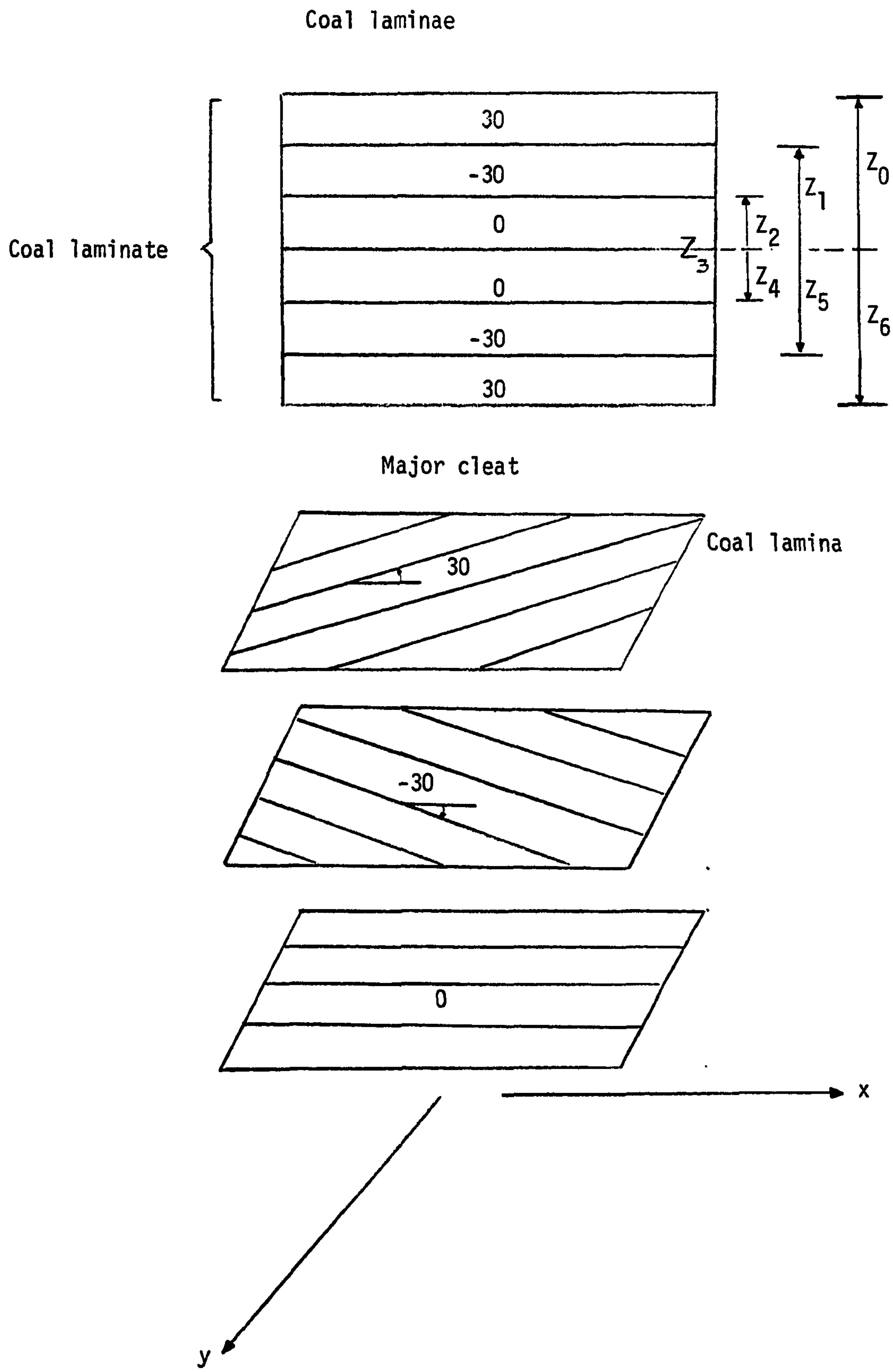

Figure 2-D, An Angle-Ply Coal Laminate

$E_1 = 9.8 \times 10^6$ psi

$E_2 = .18 \times 10^6$ psi

$\nu_{12} = 0.17$

From the reciprocal relations $\frac{\nu_{21}}{E_2} = \frac{\nu_{12}}{E_1}$, $\nu_{21} = .00312$

and from equation 2,

$Q_{11} = 9.805 \times 10^6$ psi

$Q_{12} = 0.0306 \times 10^6$ psi

$Q_{22} = 0.18 \times 10^6$ psi

$Q_{66} = G_{12} = 0.30 \times 10^6$ psi

By equation 4, we can obtain,

$\bar{Q}_{11}|_{30} = 5.65 \times 10^6$ psi

but

$$(\bar{Q}_{ij})_{+\alpha} = -(\bar{Q}_{ij})_{-\alpha}$$

Thus,

$\bar{Q}_{11}|_{30} = 5.65 \times 10^6$ psi

$\bar{Q}_{11}|_{0} = Q_{11} = 9.805 \times 10^6$ psi

$\bar{Q}_{12}|_{30} = 1.66 \times 10^6$ psi

$$\bar{Q}_{12}|_{30} = -\bar{Q}_{12}|_{-30} = -1.66 \times 10^6 \text{ psi}$$

$$\bar{Q}_{12}|_{0} = Q_{12} = 0.0306 \times 10^6 \text{ psi}$$

$$\bar{Q}_{22}|_{30} = 0.92 \times 10^6 \text{ psi}$$

$$\bar{Q}_{22}|_{0} = Q_{22} = 0.18 \times 10^6$$

$$\bar{Q}_{16}|_{30} = 3.03 \times 10^6 \text{ psi}$$

$$\bar{Q}_{16}|_{-30} = -3.03 \times 10^6 \text{ psi}$$

$$Q_{16}|_{0} = 0.0$$

$$\bar{Q}_{26}|_{30} = 1.14 \times 10^6 \text{ psi}$$

$$\bar{Q}_{26}|_{-30} = -1.14 \times 10^6 \text{ psi}$$

$$\bar{Q}_{26}|_{0} = 0.0$$

$$\bar{Q}_{66}|_{30} = 1.93 \times 10^6 \text{ psi}$$

$$\bar{Q}_{66}|_{-30} = -1.93 \times 10^6 \text{ psi}$$

$$\bar{Q}_{66}|_{0} = Q_{66} = 0.3 \times 10^6 \text{ psi}$$

Substitution in equation 10, gives

$$A_{11} = 42.21 \times 10^6 \text{ lb/in}$$

$$A_{12} = 6.70 \times 10^6 \text{ lb/in}$$

$$A_{16} = 0.0$$

$$A_{22} = 4.04 \times 10^6 \text{ lb/in}$$

$$A_{26} = 0.0$$

$$A_{66} = 8.32 \times 10^6 \text{ lb/in}$$

Therefore, the $[A]$ matrix is formed as:

$$[A] = 10^6 \begin{bmatrix} 42.21 & 6.70 & 0.0 \\ 6.70 & 4.04 & 0.0 \\ 0.0 & 0.0 & 8.23 \end{bmatrix} \quad \text{lb/in}$$

Then

$$[A]^{-1} = 10^{-6} \begin{bmatrix} 0.032 & -0.0055 & 0.0 \\ -0.0055 & 0.0055 & 0.0 \\ 0.0 & 0.0 & 0.015 \end{bmatrix} \quad \text{in/lb}$$

Now, from 13-a, strains are

$$\varepsilon_x = 0.0032$$

$$\varepsilon_y = -0.00055$$

$$\gamma_{xy} = 0.0$$

Thus, the stress in the first layer is

$$\begin{Bmatrix} \sigma_x \\ \sigma_y \\ \tau_{xy} \end{Bmatrix} = 10^6 \begin{bmatrix} 5.65 & 1.66 & 3.03 \\ 1.66 & 0.92 & 1.14 \\ 3.03 & 1.14 & 1.93 \end{bmatrix} \begin{Bmatrix} 0.0032 \\ -0.00055 \\ 0.0 \end{Bmatrix}$$

Then,

$$\sigma_x = 17.2 \quad K/in^2$$

$$\sigma_y = 5.0 \quad K/in^2$$

$$\tau_{xy} = 9.0 \quad K/in^2$$

To obtain stresses in other layers, the same approach should be followed.